

**Investigation of MicroRNA's in the
Gastroesophageal Reflux – Barrett's Oesophagus – Adenocarcinoma
Sequence**

Cameron Michael Smith

Submitted in total fulfilment of the requirements of the degree of
Doctor of Philosophy

June 2012

Flinders University
The Department of Surgery,
Flinders Medical Centre

Table of Contents

TABLE OF CONTENTS	II
SUMMARY	VII
DECLARATION	IX
ACKNOWLEDGEMENTS	X
PUBLICATIONS.....	XII
SELECTED CONFERENCE PRESENTATIONS ARISING FROM THIS THESIS..	XIV
ABBREVIATIONS.....	XV
CHAPTER 1	
Introduction.....	1
1.1 THE OESOPHAGUS	2
1.1.1 <i>The oesophageal mucosa</i>	2
1.2 DISEASES OF THE OESOPHAGUS: THE REFLUX-BARRETT'S-ADENOCARCINOMA SEQUENCE	4
1.2.1 <i>Gastroesophageal reflux disease</i>	4
1.2.2 <i>Defining Barrett's oesophagus</i>	6
1.2.3 <i>Models for the Pathogenesis of Barrett's oesophagus</i>	9
1.2.4 <i>Key genes in Barrett's Pathogenesis</i>	14
1.2.5 <i>Barrett's oesophagus and oesophageal adenocarcinoma</i>	15
1.3 MICRORNAS	19
1.3.1 <i>Mammalian miRNA biogenesis</i>	20
1.3.2 <i>Regulation of miRNA expression</i>	22
1.3.3 <i>miRNAs and cancer development</i>	23
1.3.4 <i>miRNAs as biomarkers</i>	24
1.3.5 <i>miRNA target prediction</i>	25
1.4 MIRNAS AND THE REFLUX-BARRETT'S-ADENOCARCINOMA SEQUENCE	29
1.5 THESIS AIMS.....	29
CHAPTER 2	
General Materials and Methods.....	31
2.1 MATERIALS	31
2.1.1 <i>General reagents</i>	31
2.1.2 <i>Buffers and Solutions</i>	31
2.2 METHODS.....	33

2.2.1	<i>RNA isolation and quality control</i>	33
2.2.2	<i>Quantitative real-time polymerase chain reaction (RT-PCR) analysis of miRNA expression</i>	34
2.2.3	<i>Quantitative RT-PCR analysis of mRNA expression</i>	36
2.2.4	<i>Thawing of cells for cell culture</i>	38
2.2.5	<i>Cell culture and miRNA over expression</i>	38
2.2.6	<i>Proliferation and apoptosis assays</i>	41
2.2.7	<i>Statistical analysis and correlations</i>	42
2.2.8	<i>In-situ hybridisation</i>	42
2.2.9	<i>mRNA array analysis</i>	43
2.2.10	<i>Western Blotting and antibody details</i>	44
2.2.11	<i>Ingenuity Pathway Analysis</i>	47

CHAPTER 3

Investigation of miRNA expression in oesophageal squamous epithelia, Barrett's oesophagus and oesophageal adenocarcinoma 48

3.1	INTRODUCTION.....	48
3.2	TISSUE SAMPLES - COLLECTION, HISTOPATHOLOGY AND RNA EXTRACTION	49
3.3	RESULTS: TAQMAN® QUANTITATIVE RT-PCR IDENTIFIES ALTERED MIRNA EXPRESSION IN BARRETT'S OESOPHAGUS AND OESOPHAGEAL ADENOCARCINOMA.....	50
3.4	DISCUSSION: MIRNA EXPRESSION IS ALTERED IN BARRETT'S OESOPHAGUS AND OESOPHAGEAL ADENOCARCINOMA	57
3.4.1	<i>miR-203 and miR-205 are enriched in oesophageal, squamous epithelia compared with columnar epithelia</i>	59
3.4.2	<i>miR-194 and intestinal metaplasia</i>	59
3.4.3	<i>Elevated miR-143 and miR-145 and Barrett's oesophagus development</i>	59
3.4.4	<i>miR-21 expression is up regulated in Barrett's oesophagus and oesophageal adenocarcinoma</i>	60
3.4.5	<i>miR-143, miR-145 and miR-215 are down-regulated in oesophageal adenocarcinoma and may act as tumour suppressor miRNAs</i>	61
3.4.6	<i>Limitations</i>	62
3.4.7	<i>Comparing expression data with other studies</i>	62
3.4.8	<i>Summary</i>	63

CHAPTER 4

Impact of gastroesophageal reflux on microRNA expression, location and function..... 64

4.1	INTRODUCTION.....	64
-----	-------------------	----

4.2	TISSUE SAMPLES - COLLECTION, HISTOPATHOLOGY AND RNA EXTRACTION.....	66
4.3	RESULTS: MIRNA AND MRNA QUANTITATION BY RT-PCR.....	66
4.3.1	<i>Het-1A Cell Culture and miRNA over expression.....</i>	72
4.3.2	<i>Spatial expression of miR-143, miR-145 and miR-205 in oesophageal biopsies.....</i>	76
4.4	DISCUSSION	78
4.4.1	<i>Increased miRNA expression in patients with gastroesophageal reflux disease correlates with mRNA differentiation marker expression.....</i>	78
4.4.2	<i>Increased miRNA expression in patients with gastroesophageal reflux disease may regulate proliferation and apoptosis at the basal layer of the oesophageal epithelium.....</i>	79
4.4.3	<i>Nuclear localisation of miR-143, miR-145 and miR-205.....</i>	80
4.4.4	<i>Limitations.....</i>	80
4.4.5	<i>Summary.....</i>	81

CHAPTER 5

Loss of tumour suppressor miRNAs in Barrett's oesophagus: links with neoplastic progression to oesophageal adenocarcinoma 82

5.1	INTRODUCTION.....	82
5.2	RESULTS: OE-19 CELL CULTURE AND MIRNA OVER-EXPRESSION....	83
5.2.1	<i>Changes in gene expression post miRNA transfection.....</i>	87
5.2.2	<i>Changes in protein expression post miRNA transfection.....</i>	94
5.2.3	<i>miR-143, miR-145 and miR-215 are detected in the crypts of Barrett's oesophagus but are not detected in oesophageal adenocarcinoma.....</i>	103
5.3	DISCUSSION: MIR-143, MIR-145 AND MIR-215 ACT AS TUMOUR SUPPRESSORS IN OESOPHAGEAL ADENOCARCINOMA.....	104
5.3.1	<i>Proliferative and apoptotic effects of restoring miRNA expression in oesophageal adenocarcinoma.....</i>	104
5.3.2	<i>Loss of miRNA function in the crypts of Barrett's oesophagus epithelia may contribute to the development of oesophageal adenocarcinoma.....</i>	105
5.3.3	<i>miRNA directed changes in gene expression may contribute to altered proliferation and apoptosis.....</i>	106
5.3.4	<i>The fold increase in miR-143 post transfection was lower than miR-145 and miR-215.....</i>	109
5.3.5	<i>Robust mRNA array data would streamline the process of identifying miRNA targets.....</i>	110
5.3.6	<i>Summary.....</i>	110

CHAPTER 6

The expression of miR-200 family members is downregulated upon neoplastic progression of Barrett's oesophagus. 111

6.1	INTRODUCTION.....	111
6.2	TISSUE COLLECTION AND PROCESSING.....	114
6.3	RESULTS: QUANTITATIVE RT-PCR ANALYSIS OF MIR-200 FAMILY, ZEB1 AND ZEB2 EXPRESSION	115
6.3.1	<i>Predicted implications of reduced miR-200 family expression in Barrett's oesophagus</i>	118
6.3.2	<i>miR-200, ZEB1 and ZEB2 expression in Barrett's oesophagus and oesophageal adenocarcinoma.....</i>	123
6.3.3	<i>The miR-200 family and the EMT in oesophageal adenocarcinoma</i>	129
6.4	DISCUSSION	131
6.4.1	<i>Decreased miR-141 and miR-200c expression in Barrett's oesophagus</i>	131
6.4.2	<i>Fibronectin is a predicted target of miR-200c.....</i>	132
6.4.3	<i>miR-200c and dysplastic Barrett's oesophagus.....</i>	133
6.4.4	<i>The miR-200 family - ZEB1, ZEB2 feedback loop and and EMT in oesophageal adenocarcinoma.....</i>	134
6.4.5	<i>Clinical Relevance</i>	134
6.4.6	<i>Limitations</i>	135
6.4.7	<i>Summary.....</i>	135
CHAPTER 7		
Summary, conclusions and future studies		136
7.1	SUMMARY AND CONCLUSIONS.....	136
7.1.1	<i>Gastroesophageal reflux disease: Unravelling roles for miRNAs in the oesophagus.....</i>	136
7.1.2	<i>Tumour suppressor miRNAs in oesophageal adenocarcinoma.....</i>	137
7.1.3	<i>The miR-200 family: Involvement in Barrett's oesophagus and oesophageal adenocarcinoma.....</i>	138
7.2	FUTURE DIRECTIONS	139
7.2.1	<i>Global profiling of miRNA expression in Barrett's oesophagus and oesophageal adenocarcioma.....</i>	139
7.2.2	<i>Additional in vitro investigation into the role of miRNAs in the development of Barrett's oesophagus</i>	139
7.2.3	<i>Assessing nuclear localisation of miRNAs.....</i>	141
7.2.4	<i>miRNA expression and invasive oesophageal adenocarcinoma.....</i>	142
7.2.5	<i>Validating bioinformatic predictions or miR-141 and miR-200c function in vitro.....</i>	143
Appendices.....		147
APPENDIX 1: ELEVATED MIR-143 AND MIR-145 IS OBSERVED IN SPECIMENS FROM RESECTED OESOPHAGEAL ADENOCARCINOMA		147

APPENDIX 2: THE TOP 40 GENES FOR EACH MIRNA INDICATED BY
STUDENT-T TEST TO BE SIGNIFICANTLY DOWN REGULATED VIA MRNA
ARRAY..... 151

References..... 154

Publications..... 173

Summary

Gastrointestinal reflux disease can lead to the development of Barrett's oesophagus (conversion of oesophageal squamous epithelium to columnar epithelium with intestinal metaplasia) and oesophageal adenocarcinoma. However, the molecular mechanisms driving the reflux-Barrett's oesophagus-oesophageal adenocarcinoma sequence are not fully understood. MicroRNAs (miRNAs) are a class of small RNA molecules involved in almost every cellular process investigated.

In this study quantitative assessment identified seven differentially expressed miRNAs in Barrett's oesophagus compared with squamous epithelium including: increased expression of miR-21, miR-143, miR-145, miR-194, miR-215 and decreased expression of miR-203 and miR-205. miR-143, miR-145 and miR-205 were also increased in gastroesophageal reflux disease. MiR-143, miR-145 and miR-215 were decreased in oesophageal adenocarcinoma.

Gastroesophageal reflux disease: Unravelling roles for miRNAs in the oesophagus

Subsequent studies were performed to explore the biological consequences of these changes in miRNA expression. Investigation of increased miR-143, miR-145 and miR-205 levels in an oesophageal squamous cell line identified these miRNAs can regulate proliferation and apoptosis. We therefore hypothesized that these miRNAs might act as regulators of oesophageal epithelial restitution in response to reflux. Investigation of miRNA and mRNA expression in tissues identified correlations between miR-143 and both BMP4, a key promoter of columnar specific gene expression and CK8, a marker of a columnar phenotype. This data is consistent with a possible role for miRNA expression in development of Barrett's oesophagus.

Tumour suppressor miRNAs in oesophageal adenocarcinoma

Studies using an oesophageal adenocarcinoma cell line revealed that decreased miR-143, miR-145 and miR-215 expression likely contributes to a reduction in proliferative and apoptotic control in this cancer. Further, this reduction is likely

mediated by a number of miRNA directed changes in gene expression. In-situ hybridisation identified localisation of these miRNAs to the crypts within the Barrett's oesophagus epithelium. Dysplasia is thought to originate from the crypts of the Barrett's oesophagus epithelium, so we hypothesized that miR-143, miR-145 and miR-215 play a role in regulating proliferation and apoptosis in these crypts, with decreased expression promoting the development cancer development in these areas.

The miR-200 family: Involvement in Barrett's oesophagus and oesophageal adenocarcinoma

Decreased expression of miR-141 and miR-200c, members of the miR-200 family was found to distinguish Barrett's oesophagus from related gastric and intestinal epithelia. Bioinformatic analysis provided computational evidence that this decreased miRNA expression might contribute to the abnormal proliferative and apoptotic status of Barrett's oesophagus epithelium.

We observed decreased expression of the miR-200 family (miR-141, miR-200a, miR-200b, miR-200c and miR-429) and increased expression of *ZEB1* and *ZEB2* in oesophageal adenocarcinoma. The miR-200 family regulates the epithelial to mesenchymal transition, a key process in tumour metastasis, by targeting the transcription factors *ZEB1* and *ZEB2*. These results provided the first evidence implicating miRNAs in the epithelial to mesenchymal transition in oesophageal adenocarcinoma.

Moving forward

This study provides an exciting platform to build from, especially for further investigating a miRNA mechanism for the development of both Barrett's oesophagus and oesophageal adenocarcinoma. In addition, this study provides preliminary support for the development of miRNA based tools for (1) assessing the efficacy of reflux control, (2) classifying patients at risk of developing Barrett's oesophagus and oesophageal adenocarcinoma, and (3) therapies targeted towards modulating miRNA expression to reduce oesophageal adenocarcinoma tumour growth.

Declaration

I certify that this thesis does not incorporate without acknowledgment any material previously submitted for a degree or diploma in any university; and that to the best of my knowledge and belief it does not contain any material previously published or written by another person except where due reference is made in the text.

Signed Date

Acknowledgements

I would like to thank my supervisors Dr. Damian Hussey, Dr. Michael Michael and Prof. David Watson for supporting me throughout this project. While you have all helped me complete my project in different ways, your passion for research has been a great motivator for me.

Damian, I am very grateful for the opportunity to study in your laboratory. The friendly and dynamic lab that you have established has provided me with the ability to work in an efficient and relaxed environment. Your friendly, organised and enthusiastic approach has been a constant source of motivation and support.

Michael, your enthusiasm and encouragement has been constant throughout my project and this has helped me to establish new techniques and ask new and exciting questions. I have learnt a lot from your collaborative nature and this has helped me expand the scope of my project to many different areas.

David, the clinical focus that you have brought to this project has been extremely helpful. I have learnt a lot from discussion with you and have also been motivated by your ability to bring together many different sectors of the medical research community.

There are also so many people throughout the Flinders Medical Centre that I would like to acknowledge and thank. Thank you to Mary Leong, George Mayne, Tingting Wang, Stuti Srivastava, Olga Sukocheva, Jakob Kist, Rainer Haberberger, Tim Chataway, Gino Saccone, Ann Schloithe, Dani Dixon, Kim Griggs for your assistance, encouragement and support throughout my project. I would also like to acknowledge and thank Dr Richard Hummel for his friendly motivation and humour which has been of great assistance to me throughout his time in the lab.

I feel a special mention and thank you should go out to the PhD office shared by many on level 3. Lauren Thurgood, you were the first to finish, and showed us all that it could be done. George Barretto and Alison Elder, thank you for all of the

laughs and constructive discussions we shared. You both made the office a fun and enjoyable place to work.

Thank you to the staff in Anatomical Pathology at SA Pathology, Flinders Medical Centre for assistance with tissue processing and staining of tissue slides. I would also like to acknowledge work by Grace Tan, Richard Hummel and Stuti Srivastava. Grace used PCR to assess the expression of *IL6*, *CK14*, *BMP4*, *CK8*, *CK20*, *CDX2*, *HNF1 α* and *GATA4* in samples from patients with ulcerative oesophagitis. Richard performed additional miRNA PCR analysis to allow miRNA expression to be compared between Barrett's oesophagus, tissue control and ulcerative oesophagitis patient groups. Stuti performed transfections, RNA isolations, and PCRs for predicted miRNA targets. In addition, Stuti performed western blot experiments for KRAS, ZEB2, YES, RTKN, DTL, HDAC7 and GAPDH in protein isolate from cells transfected with miR-143, miR-145 or miR-215. I would also like to thank Dr Peter Rabinovitch for kindly providing the Barrett's oesophagus and dysplastic cell lines Qh, Ch and Gi.

This study was funded by a Competing Project Grant from the National Health and Medical Research Council of Australia. I was supported by a Flinders University Research Scholarship and a PROBE-NET PhD scholarship funded by a Strategic research Partnerships Grant from the Cancer Council of New South Wales. These funding sources have allowed this project to be completed in a timely fashion for which I am very grateful.

I would like to thank my parents John and Debbie Smith as well as my sister Allannah. As always, your love and support has been without limits. To all my other family and friends, I thank you for providing both encouragement and laughter, as these have been a great motivator for completing my thesis.

Finally, I would like to thank my wife Siobhan Smith for her love and support that she provides on a daily basis. Thanks for being there for the emotional rollercoaster that comes part and parcel with every PhD project.

Publications

Publications arising directly from this thesis:

Smith CM, Michael MZ, Watson DI and Hussey DJ. microRNA expression in oesophageal adenocarcinoma and proximal gastric adenocarcinoma. *World Journal of Surgery* 2009; **33** (Supp1).

Smith CM, Watson DI, Michael MZ, Hussey DJ. MicroRNAs, development of Barrett's esophagus, and progression to esophageal adenocarcinoma. *World Journal of Gastroenterology* 2010; **16**(5): 531-537.

Wijnhoven BP, Hussey DJ, Watson DI, Tsykin A, **Smith CM**, Michael MZ, and South Australian Oesophageal Research Group. MicroRNA profiling of Barrett's oesophagus and oesophageal adenocarcinoma. *British Journal of Surgery* 2010; **97**(6): 853-861.

Smith CM, Watson DI, Leong MP, Mayne GC, Michael MZ, Wijnhoven BP, Hussey DJ. miR-200 family expression is downregulated upon neoplastic progression of Barrett's esophagus. *World Journal of Gastroenterology* 2011; **17**(8): 1036-1044.

Smith CM, Michael MZ, Watson DI, Tan G, Astill D, Hummel R, Hussey DJ. Impact of gastroesophageal reflux disease on miRNA expression, location and function. Manuscript in preparation for submission to *Digestive Diseases and Sciences*.

Other Publications:

Barreto SG, Bazargan M, Zotti M, Hussey DJ, Sukocheva OA, Peiris H, Leong M, Keating DJ, Schloithe AC, Carati CJ, **Smith CM**, Toouli J, Saccone GT. Galanin receptor 3 - a potential target for acute pancreatitis therapy. *Neurogastroenterology and Motility* 2011; **23**(3): e141-151.

Hummel R, Watson DI, **Smith CM**, Kist J, Michael MZ, Haier J, Hussey DJ. Mir-148a improves response to chemotherapy in sensitive and resistant oesophageal adenocarcinoma and squamous cell carcinoma cells. *Journal of Gastrointestinal Surgery* 2011; **15**(3): 429-438.

Selected conference presentations arising from the thesis

Surgical Research Society of Australasia, Adelaide, SA, November 2008. **Smith CM**, Michael MZ, Watson DI, Bright T, Wijnhoven, BP, Dijckmeester WA, Mayne GC, Astill D and Hussey DJ. miR-143 expression in gastroesophageal reflux disease and Barrett's oesophagus.

The Australian Society for Medical Research, Adelaide, SA, June 2009. **Smith CM**, Michael MZ, Watson DI and Hussey DJ. miRNA expression in gastroesophageal reflux disease and Barrett's oesophagus.

International Surgical Week, Adelaide, SA, November 2009. **Smith CM**, Michael MZ, Watson DI and Hussey DJ. MicroRNA expression in oesophageal adenocarcinoma and proximal gastric adenocarcinoma

Lorne Genome Conference, Lorne, VIC, February 2010. **Smith CM**, Michael MZ, Watson DI and Hussey DJ. Altered microRNA expression in gastroesophageal reflux disease.

Australian Health and Medical Research Congress, Melbourne, VIC, November 2010. **Smith CM**, Tan G, Michael MZ, Watson DI and Hussey DJ. Altered miRNA expression in gastroesophageal reflux disease and miR-143 expression in Barrett's oesophagus.

Keystone Symposia: microRNAs and non-coding RNAs and cancer, Banff, Canada, February 2011. **Smith CM**, Michael MZ, Watson DI and Hussey DJ. Down regulation of miR-143, miR-145 and miR-215 is directly linked with neoplastic hallmarks of oesophageal adenocarcinoma.

Abbreviations

In text abbreviations

GORD	gastroesophageal reflux disease
BE	Barrett's oesophagus
HGD	high grade dysplasia
EAC	oesophageal adenocarcinoma
miRNA	microRNA
IPL	interpapillary basal layer
PBL	papillary basal layer
H&E	hematoxylin and eosin
<i>ABPASD</i>	alcian blue periodic Schiff diastase
Pri-miRNA	primary miRNA
TRBP	trans-activation-responsive RNA-binding protein
miRNP	miRNA-containing ribonucleo-protein particles
RISC	RNA induced silencing complex
HITS-CLIP	high throughput sequencing of RNA's being isolated following immuno-precipitation of RISC complexes
MQ	milliQ
SDS	sodium dodecyl sulfate
EDTA	ethylenediaminetetraacetic acid
cDNA	complementary DNA
Het-1A	cell line derived from oesophageal squamous tissue
Qh	Barrett's oesophagus cell line
Ch, Gi	High grade dysplasia cell lines
OE-19	oesophageal adenocarcinoma cell line
Tris	tris(hydroxymethyl)aminomethane
TBE	tris-borate-EDTA
DMEM	Dulbecco's modified eagle medium
DEPC	diethyl pyrocarbonate
DIG	digoxigenin
LNA	locked nucleic acid

SSC	saline sodium citrate
HCl	hydrochloric acid
NBT	nitro blue tetrazoliumchloride
kDa	kilodalton
ISH	in-situ hybridisation
RT-PCR	real-time polymerase chain reaction
RT	reverse transcription
EMT	epithelial to mesenchymal transition

Gene Names used in text

<i>BMP4</i>	bone morphogenic protein 4
<i>CDX2</i>	caudal type homeobox 2
<i>HNF1α</i>	HNF1 homeobox A
<i>NFKβ</i>	nuclear factor kappa B
<i>GATA4</i>	GATA binding protein 4
<i>RARX</i>	retinoic acid receptor X
<i>PDCD4</i>	programmed cell death 4
<i>CITED2</i>	Cbp/p300-interacting transactivator, with Glu/Asp-rich carboxy-terminal domain, 2
<i>EGR1</i>	early growth response 1
<i>DUSP10</i>	dual specificity phosphatase 10
<i>SLAMF7</i>	SLAM family member 7
<i>GEM</i>	GTP binding protein overexpressed in skeletal muscle
<i>ANKRD1</i>	ankyrin repeat domain 1
<i>CYR61</i>	cysteine-rich, angiogenic inducer, 61
<i>H2AFX</i>	H2A histone family, member X
<i>RTKN</i>	rhotekin
<i>PABPC4</i>	poly(A) binding protein, cytoplasmic 4
<i>NUAK2</i>	NUAK family, SNF1-like kinase, 2
<i>HDAC7</i>	histone deacetylase 7
<i>KRAS</i>	v-Ki-ras2 Kirsten rat sarcoma viral oncogene homolog
<i>YES</i>	v-yes-1 Yamaguchi sarcoma viral oncogene homolog 1

<i>DTL</i>	denticleless homolog (Drosophila)
<i>CXCR2</i>	chemokine (C-X-C motif) receptor 2
<i>TGFβ</i>	transforming growth factor, beta 1
<i>IL6</i>	interleukin 6
<i>CK</i>	cytokeratin
<i>ZEB1</i>	zinc finger E-box binding homeobox 1
<i>ZEB2</i>	zinc finger E-box binding homeobox 2
<i>PRKCE</i>	protein kinase C, epsilon
<i>PI3K</i>	phosphoinositide-3-kinase, catalytic, alpha polypeptide
<i>AKT</i>	v-akt murine thymoma viral oncogene homolog 1
<i>API</i>	jun proto-oncogene
<i>EGR3</i>	early growth response 3
<i>HS3ST1</i>	heparan sulfate (glucosamine) 3-O-sulfotransferase 1
<i>RPS6KB1</i>	ribosomal protein S6 kinase, 70kDa, polypeptide 1
<i>mTOR</i>	mechanistic target of rapamycin
<i>MUC1</i>	mucin 1, cell surface associated
<i>FSCN1</i>	fascin homolog 1, actin-bundling protein (Strongylocentrotus purpuratus)
<i>JAMA</i>	F11 receptor
<i>TSPAN8</i>	tetraspanin 8
<i>MAPK</i>	mitogen activated protein kinase 1
<i>ERK</i>	mitogen activated protein kinase 1
<i>JNK</i>	mitogen activated protein kinase 8
<i>P38</i>	mitogen activated protein kinase 14

Chapter 1

Introduction

Gastrointestinal reflux disease is a common condition that can lead to the development of Barrett's oesophagus and oesophageal adenocarcinoma. However, the molecular mechanisms driving the reflux-Barrett's-oesophageal adenocarcinoma sequence are not fully understood. microRNAs (miRNAs) are a class of small RNA molecules involved in almost every cellular process investigated. miRNAs are often referred to as master regulators for their ability to regulate hundreds of different genes. Altered miRNA expression has been linked with key cellular processes known to be aberrantly regulated or dysfunctional in patients with reflux, Barrett's oesophagus and oesophageal adenocarcinoma.

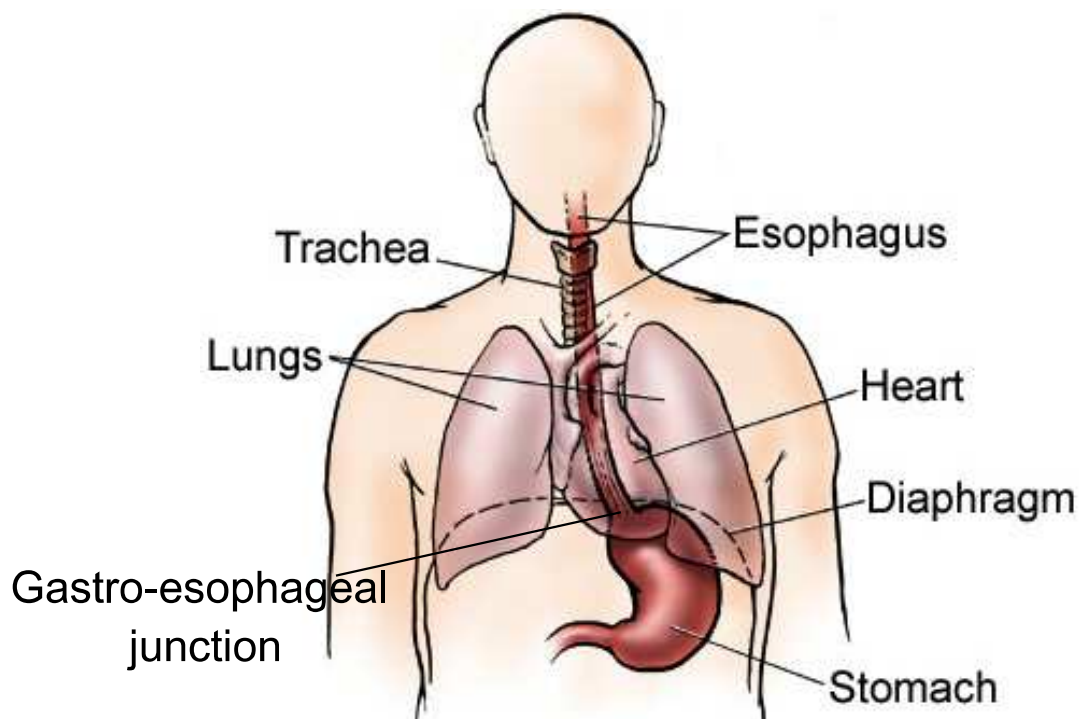
The role of miRNAs in the reflux-Barrett's-oesophageal adenocarcinoma sequence is not clear. As specific miRNA contributions to cellular processes and disease pathologies are unravelled we can expect the identification of new targets for therapeutic intervention leading to increased efficacy in patient care. This thesis aims to identify changes in miRNA expression across the reflux-Barrett's-oesophageal adenocarcinoma sequence and investigate how these miRNA changes may contribute to aberrant regulation of cellular processes, pathological development and disease progression.

This chapter provides an introduction to gastrointestinal pathologies including chronic reflux disease, Barrett's oesophagus and oesophageal adenocarcinoma. It also introduces miRNAs and their role as both crucial mediators of numerous cellular processes and biomarkers of specific tissues in greater detail.

1.1 The Oesophagus

The oesophagus acts as a transport mechanism from the pharynx to the stomach. It consists of a muscular tube stretching approximately 20cm in length, beginning at the cricoid cartilage and extending caudally behind the heart to join the cardia of the stomach, forming the gastroesophageal junction¹ (Figure 1.1).

Figure 1.1: Identifies the key features of the upper gastrointestinal tract including the oesophagus, gastroesophageal junction and stomach. Surrounding visceral organs are also labelled.



(Reproduced from: The society of thoracic surgeons, 2010)²

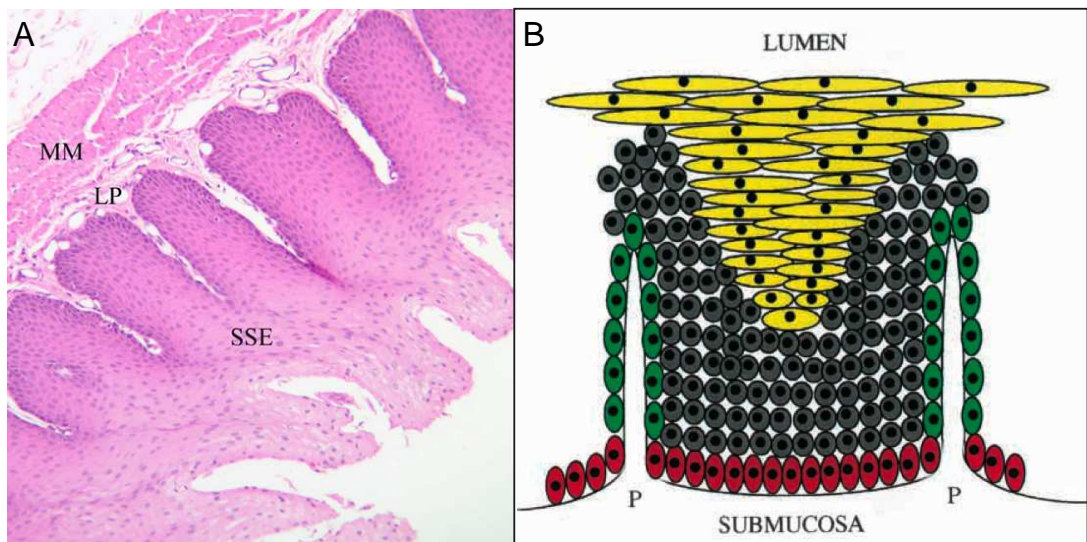
1.1.1 The oesophageal mucosa

In adults, a mucous membrane lines the surface of the oesophagus. The mucosal lining is comprised of a stratified squamous epithelium that is continually invaginated by mucosal glands (Figure 1.2A). These mucosal glands project into the mucosa or submucosa, acting to secrete mucus to line the oesophagus. The squamous epithelium lining the luminal surface is comprised of terminally differentiated cells that are non-keratinizing, and possess an elongated, flat morphology. Beneath the

basal mucosal boundary there is an additional layer known as the lamina propria, consisting mainly of connective tissue. Invaginations in the lamina propria produce papillary structures that project perpendicular to the luminal surface. These invaginations tend to occur more frequently in the distal oesophagus forming linear rows of protrusions into the epithelium³.

The squamous lining of the oesophagus undergoes continual renewal as epithelial cells break away over time. This regeneration is provided from the basal layer of the oesophageal mucosa⁴. The basal mucosal layer is separated into sections created by papillae from the lamina propria. These include the interpapillary basal layer (IPL) and the papillary basal layer (PBL)⁴ (Figure 1.2B). For epithelium renewal, cell division is confined to the basal and epi-basal layers of the mucosa. The IPL is hypothesised to be lined with infrequently dividing stem cells⁵. Cell division at the IPL can have two possible outcomes. Firstly cell division can result in the production of a migratory daughter cell and a replacement cell at the basement layer. The migratory daughter cell enters the epi-basal layer and undergoes several rounds of cell division on its path to the luminal surface. Before reaching the surface, this daughter cell undergoes terminal squamous differentiation. Alternatively, cells from the IPL can produce two daughter cells that remain on the basement membrane. This option occurs with less frequency but is thought to replenish cells on the PBL, pushing cells sideways along the basal surface⁵ (Figure 1.2B). The division of cells lining the PBL contributes to maintaining an oesophageal epithelium and these cells divide at a rate 4 times faster than cells lining the IPL⁴.

Figure 1.2: (A) Shows an H&E stain of a section of the oesophagus. SSE marks the stratified squamous epithelium consisting of fully differentiated squamous cells that is continually invaginated by papillae. LP marks the lamina propria and MM marks the muscularis mucosa. (B) Represents the different cellular layers of the oesophageal epithelium. Yellow marks the differentiated cell layer, consisting of fully differentiated squamous cells. Grey, marks the regenerative epi-basal zone, cells from this region undergo squamous differentiation and renew the oesophageal epithelium. The green papillary basal layer (PBL) and red intra-papillary basal layer (IBL) are thought to be oesophageal stem cells that divide to either replenish cell numbers in the epi-basal layer or increase cell numbers at the basal layer.



(Reproductions from: Pistorio 2007⁶, Seery J, 2002⁴)

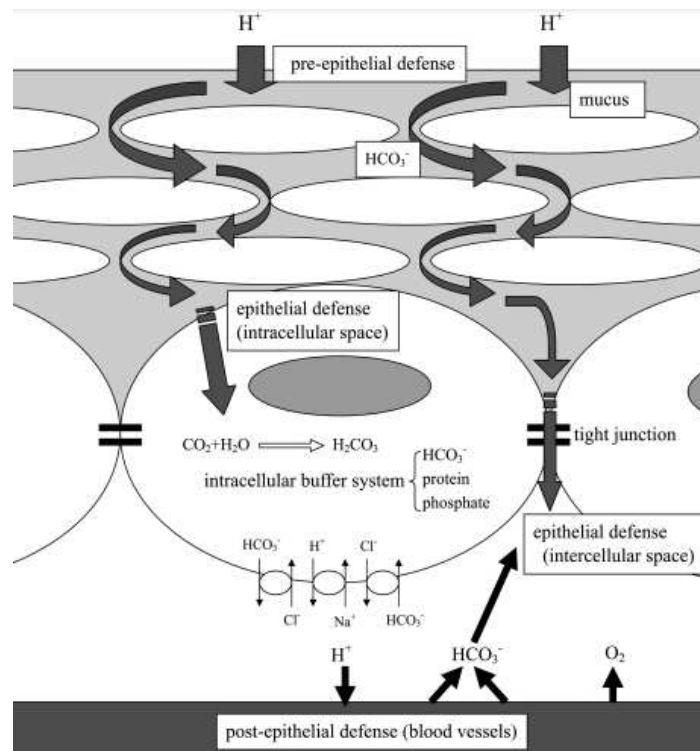
1.2 Diseases of the oesophagus: The reflux-Barrett's-adenocarcinoma sequence

1.2.1 Gastroesophageal reflux disease

Gastroesophageal reflux disease is a chronic condition affecting up to 50% of Western populations⁷, with 30% suffering from at least one reflux episode per month⁸. Chronic gastroesophageal reflux disease results from continual oesophageal exposure to excessive quantities of gastric (acid) and/or duodenal (bile) contents and generally occurs due to transient relaxation of the lower oesophageal sphincter⁸. While intestinal physiology offers protection from acid and bile, the oesophageal

lumen remains largely unprotected from reflux as it lacks a viscous adherent mucous barrier⁹. Intracellular production and blood vessel mediated intercellular supply of bicarbonate acts to buffer temporary acidosis¹⁰ (Figure 1.3), however, these mechanisms fail to cope with continual reflux exposure and as a result the oesophageal epithelium becomes damaged.

Figure 1.3: Hydrogen ions from noxious acidic content must penetrate through three defensive layers. Firstly, the pre-epithelial defence mechanism involves mucous secretion attempting to block or reduce exposure of epithelial cells to damaging acidic content. Secondly, epithelial defence involves an intracellular bicarbonate buffering system to combat acidosis where carbon dioxide and water react to produce bicarbonate ions; these ions take up free hydrogen ions and increase pH. Thirdly, once the noxious acid penetrates the epithelial defence it breaks down tight junctions and then penetrates deeper into the oesophagus where post-epithelial defence mechanisms release bicarbonate ions from the blood stream to assist in the uptake of free hydrogen ions.



(Reproduced from: Yoshida, 2007¹⁰)

Oesophageal damage caused by reflux exposure occurs on two fronts. Firstly, there is rapid lymphocytic infiltration in the sub mucosal layer that progresses to the mucosal

layer of the oesophagus¹¹. Neutrophil infiltration then follows some time after. The initial inflammatory response is thought to signal cytokine release from squamous cells in the oesophageal mucosa attracting immune cells, leading to epithelial damage¹¹. Secondly, at the luminal surface, refluxate exposure causes squamous cells to slough from the epithelium, as well as tight junction destruction, allowing noxious contents to penetrate deeper into the oesophageal epithelium^{12, 13}. Both the acid and bile components of reflux likely play a role in gastroesophageal reflux disease pathogenesis and progression to other pathologies¹⁴. Gastric acid exposure alone is linked with neoplastic development as it leads to intracellular acidification, DNA hydrolysis and genomic instability^{14, 15}. Bile constituents are also linked with neoplastic development as they can induce cellular proliferation¹⁶, a major hallmark of chronic gastroesophageal reflux disease¹⁷. Increased cellular proliferation in the oesophageal epithelium is observed as basal cell hyperplasia¹⁸ and this occurs to replenish the oesophageal epithelium. Bile constituents can also induce reactive oxygen species production, a process significant because of its association with increased DNA damage and therefore increased potential for cancer development^{15, 19}. Increased apoptosis is also observed in gastroesophageal reflux disease and is likely caused by the increase in both genomic instability and DNA damage caused by acid and bile²⁰.

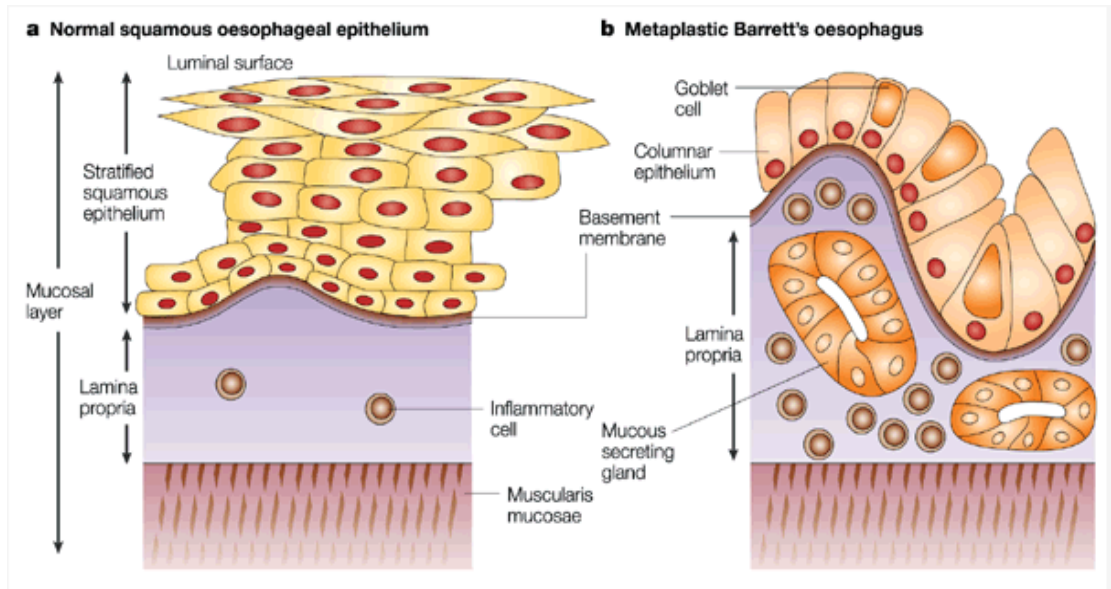
Clinically, reflux induced, epithelial cell damage presents macroscopically as an ulcerated oesophageal mucosa. In most cases ulcerated mucosae can heal via replacement with additional squamous cells. In some cases, more serious complications such as Barrett's oesophagus or oesophageal adenocarcinoma can arise.

1.2.2 Defining Barrett's oesophagus

Barrett's oesophagus is characterised by the replacement of the normal, stratified squamous, oesophageal epithelium with a metaplastic, columnar epithelium (Figure 1.4). The development of Barrett's oesophagus is described as metaplastic, as it involves the reversible replacement of one differentiated cell type with another differentiated cell type. Histological features include a glandular phenotype with the

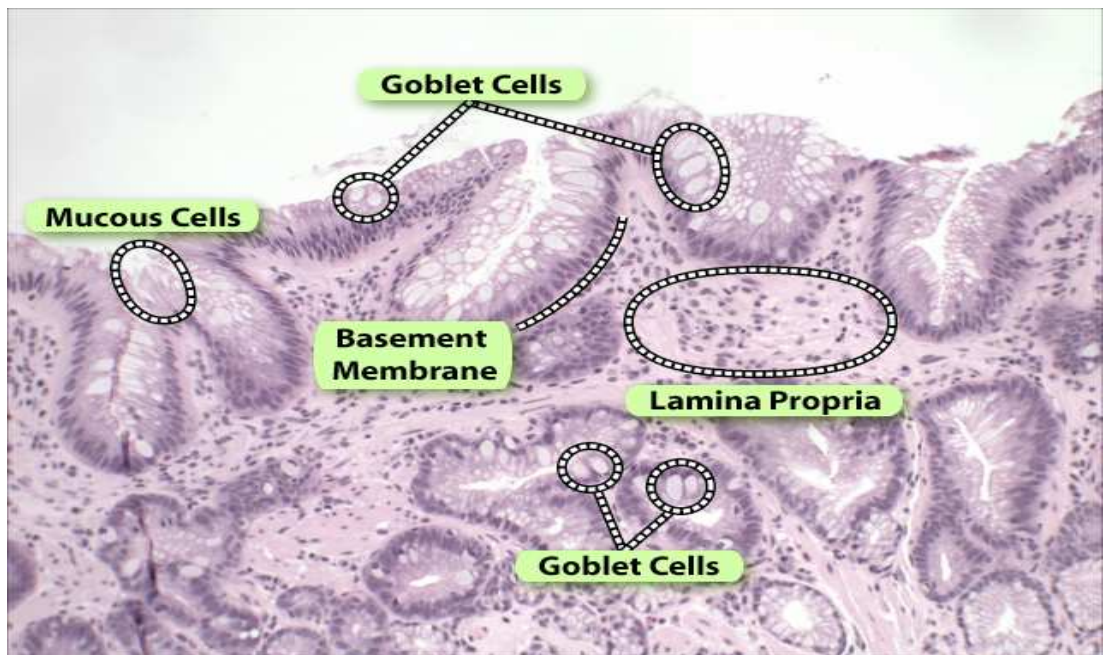
presence of mucin secreting goblet cells (Figure 1.5). Barrett's oesophagus metaplasia is probably an adaptive response to the insult from exposure of the oesophageal epithelium to gastric acid and/or duodenal bile salts²¹. The Barrett's oesophagus epithelium possesses secretory and absorptive cell types, and these closely resemble those found in normal gastric and intestinal epithelia^{22, 23}. However, the epithelium of Barrett's oesophagus has a molecular profile that distinguishes it from oesophageal, gastric and duodenal epithelia²⁴. The gastric and intestinal features of Barrett's oesophagus likely allow the epithelium to resist noxious acid and bile exposure better than the normal oesophageal epithelium^{21, 25}. For example, the Barrett's epithelium secretes heavily glycosylated, gel forming proteins called mucins that form a major component of a continuous protective mucous layer^{21, 25}. The Barrett's epithelium also produces proteins thought to provide improved reflux resistance by increasing early stage mucosal healing and repair capabilities and decreasing reflux permeability through alternate extracellular matrix and tight junction formation^{21, 25}. Also, patients with Barrett's oesophagus usually have diminished reflux symptoms²⁶. However, Barrett's oesophagus is not completely resistant to acid and bile induced DNA damage as bile and acid exposure has been shown to increase DNA damage in Barrett's oesophagus biopsies and cells through increased intracellular acidification and reactive oxygen species production¹⁴.

Figure 1.4: (a) depicts the normal, squamous, oesophageal epithelium. (b) depicts the metaplastic Barrett's oesophagus epithelium. Key changes to differentiation features compared with (a) include the presence of a columnar phenotype with goblet cells (intestinal metaplasia). There is also a marked increase in the number of inflammatory cells.



(Reproduced from: Wild & Hardie, 2003²⁷)

Figure 1.5: Depicts a H&E stain of a section of Barrett's oesophagus. Mucous secreting, columnar cells as well as intestinal goblet cells are present. The lamina propria is circled to highlight the dense infiltrate of inflammatory cells.



(Reproduced from: Ozode, R 2008²⁸)

1.2.3 Models for the Pathogenesis of Barrett's oesophagus

Current Hypotheses

The origin of the characteristic columnar epithelium with intestinal metaplasia of Barrett's oesophagus is unknown. Barrett's oesophagus was initially hypothesised to form when columnar cells from the proximal stomach migrated into the oesophagus to repair the reflux-damaged, oesophageal epithelium²⁹. This hypothesis is no longer supported; firstly, it does not account for the presence of intestinal metaplasia (goblet cells), and secondly, studies show cases where the Barrett's oesophagus epithelium is not connected to the gastroesophageal junction³⁰. Currently, there are two main hypotheses for the formation of Barrett's oesophagus. The first hypothesis involves trans-differentiation of mature squamous, oesophageal cells into columnar cells. The second hypothesis involves altered differentiation of oesophageal stem cells^{12, 29}, with alternate differentiation driven either by reflux exposure or, stromal based signals directing oesophageal stem cells towards columnar, epithelial differentiation and/or intestinal metaplasia³¹⁻³³. In addition to these two main hypotheses, there is

some very preliminary evidence to suggest that stromal cells may undergo mesenchymal to epithelial transition, followed by differentiation to a columnar cell phenotype in the oesophagus^{12, 34}.

Hypothesis 1: Barrett's oesophagus development; trans-differentiation of mature squamous cells into columnar cells with intestinal metaplasia

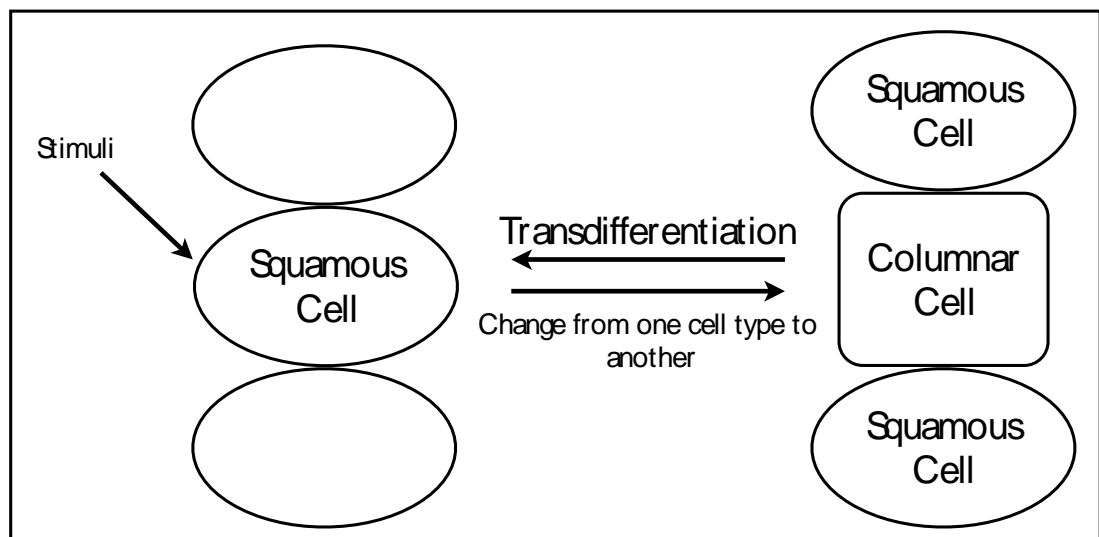
Trans-differentiation involves a change from one differentiated cell type to another, occurring as metaplasia, resulting in a change in cell fate or a switch in phenotype³⁵. Support for the trans-differentiation hypothesis for Barrett's oesophagus development considers how the normal oesophagus develops and how a reversal of this developmental mechanism may allow for the pathogenesis of Barrett's oesophagus.

The oesophagus begins to form during week four of embryonic development, with the formation of the foregut³⁶. However, it is not until week five that the foregut can be visually divided into oesophagus, stomach and duodenum³⁷. Development of the oesophageal lumen begins in developmental weeks seven and eight, when the epithelium begins to proliferate. By week ten the lumen is enclosed and lined with a ciliated columnar epithelium^{36, 38, 39}. It is not until the fourth month of gestation that a columnar-squamous transition is observed as the ciliated columnar epithelium begins to be replaced by a squamous epithelium. This transition does not remove all columnar cells, residual islands of columnar epithelia remain, and these give rise to oesophageal glands³⁶.

The columnar-squamous transition that occurs in the developing oesophagus is thought to arise via a trans-differentiation event, as it is not dependent on cell division. In addition, some epithelial cells express both squamous and columnar markers during the transition period⁴⁰. Although these two criteria are not requirements for trans-differentiation, they do suggest that the epithelium is not being replaced with new epigenetically distinct cells and highlight the interchangeable differentiation profile of oesophageal cells.

Hypothesis 1 suggests that a reversal of normal, oesophageal developmental mechanisms may occur in the formation of Barrett's oesophagus. In this scenario, a squamous-columnar transition would be observed, leading to the development of a columnar epithelium with intestinal metaplasia in the squamous lined oesophagus (Figure 1.6). Recent studies support trans-differentiation, showing that exposure of oesophageal organ cultures to retinoic acid leads to columnar differentiation independent of cell proliferation¹². Retinoic acid is a powerful differentiation agent, and it is interesting that nuclear retinoic acid receptors can be actively bound by a component of bile called lithocholic acid⁴¹. This points to a possible reflux associated, bile acid induced mechanism for trans-differentiation of squamous to columnar cells, as occurs in Barrett's oesophagus development.

Figure 1.6: Hypothesis one; trans-differentiation of post mitotic mature, squamous cells. Normal squamous cells of the oesophageal epithelium in the presence of a reflux mediated stimulus transdifferentiate from a squamous cell phenotype to a columnar cell phenotype. This trans-differentiation event leads to the development of a columnar cell population inside the normal population of squamous cells.



Hypothesis 2: Barrett's oesophagus development; alternate differentiation of oesophageal stem cells

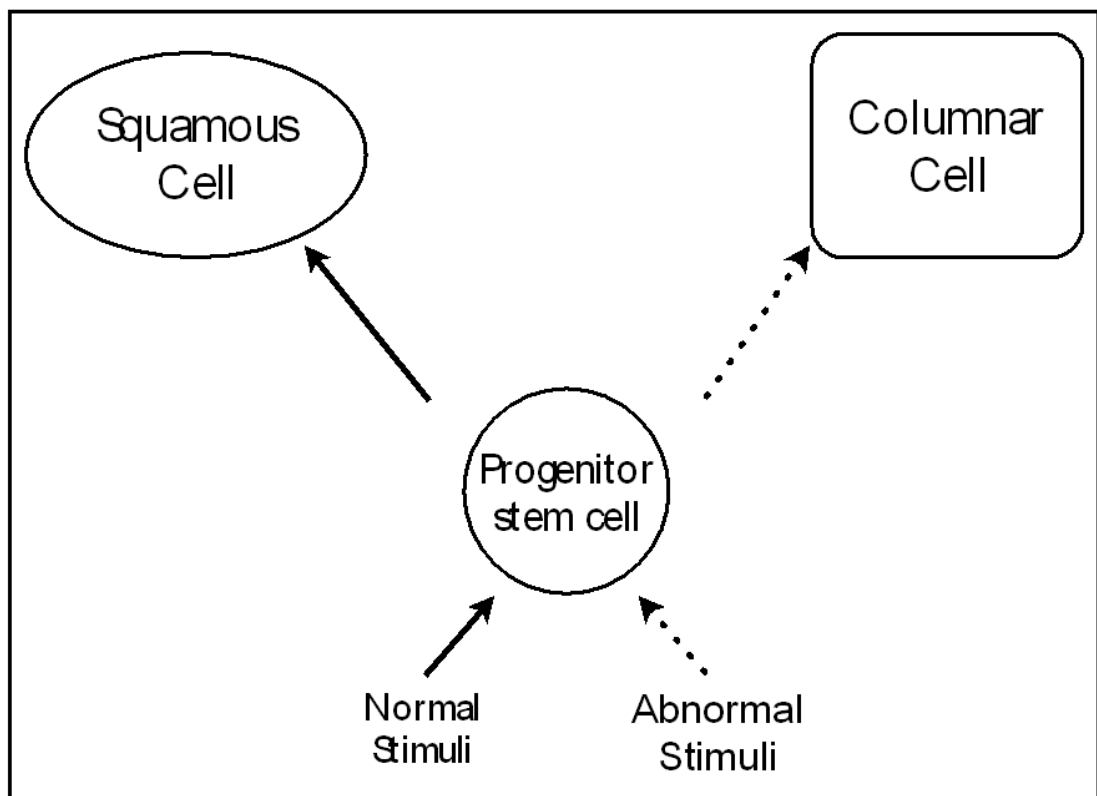
The hypothesis of altered stem cell differentiation giving rise to Barrett's oesophagus concerns undifferentiated stem cells located in either the basal layer of the oesophageal mucosal epithelium or in oesophageal sub-mucosal glands^{5, 42}. It is hypothesized that stem cells of the oesophageal epithelium, in response to specific direct or indirect stimuli have the ability to differentiate into either squamous or columnar/intestinal phenotypes, with a squamous differentiation program occurring in the oesophagus, under normal conditions (Figure 1.7). Stimuli hypothesised to direct stem cell differentiation from a squamous, to a columnar phenotype with intestinal metaplasia vary. However, as gastroesophageal reflux disease is the underlying precursor pathology associated with the development of a columnar epithelium with intestinal metaplasia (Barrett's oesophagus), it is likely that this pathology provides the stimuli to drive columnar differentiation and intestinal metaplasia in the oesophagus.

Prolonged reflux exposure can lead to epithelial injury and the development of erosive oesophagitis. Studies show this reflux induced epithelial injury allows damaging refluxate to penetrate deep into the oesophagus exposing basal and sub-mucosal gland stem cells⁴³. As reflux exposure to the oesophageal epithelium has been shown to increase the expression of a number of genes known to direct gastric and intestinal differentiation (See key genes in Barrett's pathogenesis, discussed below) gastroesophageal reflux exposure to oesophageal stem cells could directly stimulate alternate differentiation of these stem cells, leading to the development of a columnar cell with intestinal metaplasia in the squamous oesophageal epithelium. Alternatively, recent evidence suggests that reflux induced epithelial damage might make way for the colonisation of the basal layer by residual embryonic cell populations capable of differentiating into metaplastic columnar cells³³.

Also, preliminary evidence suggests that signals arising from the stroma of the oesophageal epithelium could act on oesophageal stem cells to promote columnar and intestinal differentiation. For example, reflux leads to the development of a pro-inflammatory or 'reactive stroma' where increases in cytokines and other regulatory

signals implicated in gastric and/or intestinal differentiation could assist in directing the columnar differentiation of oesophageal stem cells. For example, acid and bile has been shown to increase stromal bone morphogenic protein 4 (*BMP4*) expression *in vivo* (See discussion of *BMP4* below), with this increased stromal *BMP4* expression directing intestinal type changes in the oesophageal epithelium³¹. Although there is preliminary evidence that stromal signals may have a role to play in initiating a columnar/ intestinal phenotype in the oesophagus there is no direct evidence showing stromal signals acting on oesophageal stem cells.

Figure 1.7: Hypothesis 2; alternate differentiation of oesophageal stem cells. Normal differentiation mechanisms are altered due to reflux mediated stimuli resulting in a change in the progenitor cell differentiation profile from a squamous to a columnar phenotype.



For now, the debate over whether Barrett's oesophagus arises from fully differentiated squamous cells or undifferentiated stem cells continues. Similar to the cell of origin, the genetic mechanisms that drive the pathogenesis of Barrett's oesophagus are unknown.

1.2.4 Key genes in Barrett's Pathogenesis

Candidate genes thought to play crucial roles in the development of Barrett's oesophagus include caudal type homeobox 2 (*CDX2*), HNF1 homeobox A (*HNF1a*), *BMP4*, nuclear factor kappa-beta (*NFKB*), and GATA binding protein 4 (*GATA4*). All of these genes are induced in Barrett's oesophagus compared with normal squamous epithelia⁴⁴⁻⁴⁶. However, it appears individual changes in the expression of these genes is not sufficient to drive the development of Barrett's oesophagus, suggesting a multi-step differentiation process^{47, 48}. Although there are many studies linking these genes with gastric and intestinal development their mechanistic involvement in the development of Barrett's oesophagus remains speculative.

Studies in developmental biology highlight the importance of *CDX2*, *HNF1a* and *GATA4* in the development of Barrett's oesophagus. *CDX2*, *HNF1a* and *GATA4* are all transcription factors that localise to the nucleus and control the expression of numerous gastric and intestinal specific genes. Expression of *CDX2* is crucial for normal intestinal development. *CDX2* null mice are embryonic lethal and heterozygous *CDX2* mice develop intestinal polyps containing squamous, gastric and parietal cell mixtures^{49, 50}. *HNF1a* is required for normal gastric development as knockout mice show defective gastric differentiation⁵¹. *GATA4* is important for both gastric and intestinal development^{52, 53}. Recent evidence suggests that these transcription factors work cooperatively in inducing intestinal differentiation, with *CDX2* and *HNF1a* thought to induce genes required for intestinal differentiation and *GATA4* thought to induce morphological changes⁵⁴. In a study by Benoit et al.⁵⁴ an undifferentiated human intestinal crypt cell line was used. Individual ectopic expression of *CDX2* or *HNF1a* was shown to reduce cell proliferation through cyclin D1 and p27 and induce expression of the late stage intestinal enterocyte differentiation marker sucrase-isomaltase⁵⁵. Also, ectopic expression of *HNF1a* and

GATA4 induced cell polarisation and microvilli formation. These studies highlight that different features of fully differentiated intestinal epithelial cells are induced by different combinations of transcription factors, and that individual changes to these transcription factors is not sufficient for complete intestinal differentiation. This is in keeping with the multiple genetic changes hypothesised to be required for the development of Barrett's oesophagus.

Direct or indirect responses to reflux have the ability to induce the expression of *CDX2* and *GATA4*, while studies have not addressed the impact of reflux on *HNF1a* induction. Direct receptor interaction of the bile constituent lithocholic acid with retinoic acid receptor X (*RARX*) leads to the transcription of *CDX2*¹². Also, indirect gene induction in response to reflux could occur through *NFKB* or *BMP4*. *NFKB* is a transcription factor that can induce *CDX2* expression⁵⁶ and *BMP4* is a growth factor that can induce *GATA4* and *CDX2* expression⁵⁶⁻⁵⁸. Both *NFKB* and *BMP4* are expressed as a result of the pro-inflammatory phenotype that develops in response to continual reflux exposure^{59, 60}.

Taken together these studies support a hypothetical model where the oesophagus, in response to gastroesophageal reflux may initiate an inflammatory response where *BMP4* and *NFKB* expression levels are elevated. Chemical components of reflux and/or bile, *BMP4*, *NFKB* and other reflux induced genes could then act on the Barrett's cell of origin to increase the levels of *CDX2*, *GATA4* and *HNF1a*. Increased *CDX2*, *GATA4* and *HNF1a* levels could then act cooperatively to initiate intestinal and gastric differentiation and drive morphological change leading to the development of a columnar phenotype with intestinal metaplasia.

1.2.5 Barrett's oesophagus and oesophageal adenocarcinoma

The metaplasia to Barrett's oesophagus may be of benefit in resisting damage from reflux. However, the molecular profile of the Barrett's oesophagus epithelium is considered premalignant as it can progress through varying grades of dysplasia to oesophageal adenocarcinoma.

Dysplasia in Barrett’s oesophagus is categorised as either low or high-grade dysplasia. A low grade dysplasia diagnosis generally includes the atypical presence of enlarged, crowded, hyperchromatic, stratified nuclei as well as increased atypical mitosis and nucleoli^{61, 62} (Table 1.1). Dysplastic cells can also show reduced mucin levels and goblet cell numbers as well as an increased nuclear to cytoplasmic ratio⁶² (Table 1.1). Progression to a diagnosis of high-grade dysplasia or non-invasive adenocarcinoma generally results from a marked increase in the prevalence of abnormalities described above. Also, an increase in architectural complexity such as marked crowding of crypts, crypt budding or crypt branching is seen in high-grade dysplasia⁶² (Table 1.1).

Table 1.1: Cytological and architectural hallmarks of dysplasia in Barrett’s oesophagus.

Feature	Low Grade	High Grade
Cytology		
↑ N/C ratio	+	++
Loss of cell polarity	–	+
Mitosis	+	++
Atypical mitosis	+/-	+
Full-thickness nuclear stratification	–	+
Decreased goblet cells (+/- dystrophic)	+	++
Hyperchromasia	+	++
Multiple nucleoli	+/-	+/-
Large irregular (prominent) nucleoli	–	+/-
Irregular nuclear contour	+	++
Nuclear pleomorphism	–	+
Architecture		
Villiform change	–	+/-
Crypt budding/branching	+/-	++
Crowded (back-to-back) crypts	+/-	++
Irregular crypt shapes	+/-	+
Intraluminal papilla/ridges	–	+/-
Lamina propria between glands	+	+/-

N/C, nuclear/cytoplasmic ratio; –, absent; +/-, may be present; +, usually present.

(Reproduced from: Odze, RD 2006⁶²)

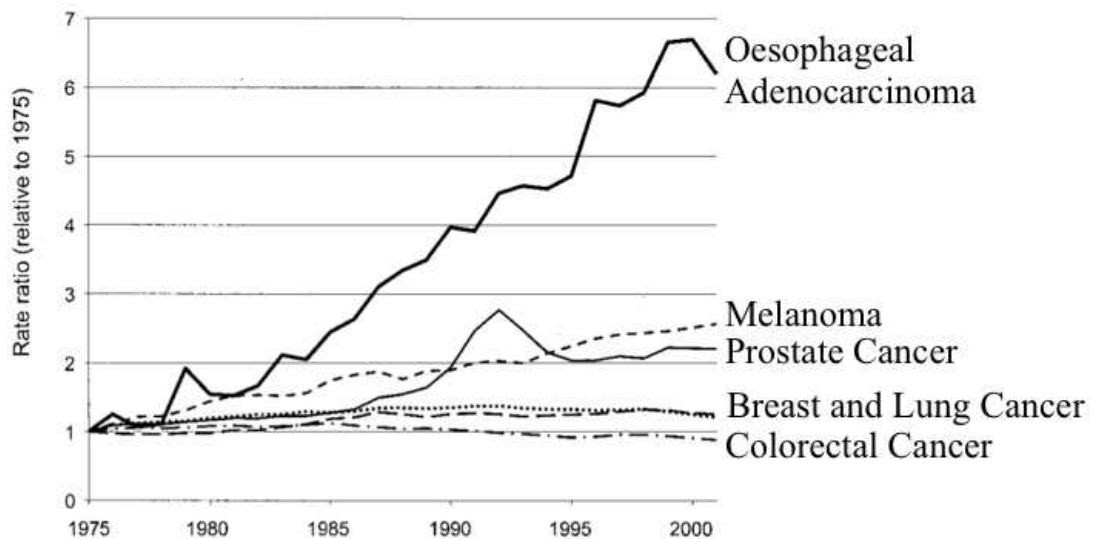
Due to the large number of characteristics that are considered for the diagnosis of dysplasia there is a significant amount of variability in diagnosis amongst pathologists^{62, 63}. This is particularly true for diagnosing and differentiating low grade dysplasia from tissue regeneration in Barrett's epithelium^{62, 64}. In order to reduce the variability seen amongst pathologists, effective tissue biomarkers are required to assist in confirming a diagnosis. Some preliminary evidence suggests that miR-196a may be an effective classifier of low and high-grade dysplasia⁶⁵ in Barrett's oesophagus, however further work is required to conclusively prove this.

The cancer risk associated with Barrett's oesophagus and dysplasia has led to the development of different treatment regimes⁶⁶. As acid reflux is thought to play a major role in the development of oesophageal adenocarcinoma treatment, regimes generally prioritise the control of reflux using medication or anti-reflux surgery⁶⁷. Treatment offered for Barrett's oesophagus and low grade dysplasia can include either endoscopic surveillance with mucosal biopsy or ablation of the columnar mucosa to allow the regeneration of a new 'neo-squamous' epithelium⁶⁶. Many forms of ablation are available but all share a similar concept, releasing a controlled, high energy emission to destroy the columnar lined epithelium in the oesophagus⁶⁸. Treatment offered for high-grade dysplasia can include 1) ablation, 2) endoscopic mucosal resection, where an endoscope attachment is used to excise regions thought to be neoplastic or 3) oesophagectomy, where the entire neoplastic segment of the oesophagus is removed and a remaining, healthy oesophagus is joined to the stomach⁶⁹. The management of Barrett's oesophagus and dysplasia is heavily debated. This debate stems from the varied cost, level of invasiveness associated with each treatment, treatment prognosis and complications as well as risk for future development of high-grade dysplasia or adenocarcinoma^{66, 68, 70}. While the management of Barrett's oesophagus is debated, the risk for oesophageal adenocarcinoma development means there is great interest in understanding the mechanisms driving progression of Barrett's oesophagus to oesophageal adenocarcinoma.

Oesophageal adenocarcinoma is a malignancy with extremely poor prognosis. The five-year mortality rate of this cancer exceeds 80%^{71, 72}. The poor prognosis of oesophageal adenocarcinoma can be attributed to its common diagnosis as a late

stage metastatic tumour. The lack of patient symptoms and appropriate diagnostic markers probably contribute to the high mortality rate. Furthermore, an alarming trend is emerging with an increase in the prevalence of oesophageal adenocarcinoma being observed in Western countries^{72, 73}. Studies show the rate of increase in oesophageal adenocarcinoma diagnosis is exceeding that of all other solid tumours (Figure 1.8)⁷⁴. While the number of oesophageal adenocarcinoma's being diagnosed is still significantly lower than more frequently diagnosed cancers, such as colon and breast cancer, it is clear that increased oesophageal adenocarcinoma incidence will be placing additional pressure on the health care system in the future.

Figure 1.8: The rate of oesophageal adenocarcinoma diagnosis is increasing faster than that of any other solid tumour.



(Reproduced from: Pohl & Welch 2005⁷⁴)

Interestingly, with early diagnosis five-year survival rates for oesophageal adenocarcinoma exceed 90% thus highlighting the importance of early detection mechanisms⁷⁵. The only identifiable pre-cursor to oesophageal adenocarcinoma is Barrett's oesophagus. Therefore, Barrett's oesophagus has been under the spotlight, with researchers looking to this precursor lesion to identify either the mechanisms driving adenocarcinoma development or potential biomarkers for early diagnosis.

However, the rate of progression from Barrett's oesophagus to oesophageal adenocarcinoma is quite low. A Dutch longitudinal study of 42,207 patients with

Barrett's oesophagus identified a cumulative risk of 0.4% per annum⁷⁶, while, a UK based, longitudinal study identified an overall risk of 4.1%⁷⁷. Furthermore, an increased risk of Barrett's oesophagus progressing to adenocarcinoma is associated with males, individuals with uncontrolled gastroesophageal reflux disease, and individuals who are obese or smokers⁷⁸. However, not all oesophageal adenocarcinoma patients are diagnosed with Barrett's oesophagus. Regardless of these statistics, great interest surrounds the identification of early molecular changes that contribute to the pathogenesis of Barrett's oesophagus, as these may present opportunities for therapeutic development, or new strategies for the prevention or early diagnosis of oesophageal adenocarcinoma. They might also be useful for risk stratification and therefore decision making on patient surveillance. Of particular interest is a class of molecules known as microRNAs, and the potential roles they may play in the development of Barrett's oesophagus and adenocarcinoma. miRNAs are ~22 nucleotide long, non-coding segments of RNA that act to regulate gene expression⁷⁹.

1.3 MicroRNAs

Since the initial discovery of miRNAs in *Caenorhabditis elegans* in 1993 an enormous body of research has been published, implicating miRNAs in almost every cellular process investigated^{79, 80}. These small RNA molecules use complementary base pairing to target and inhibit expression of specific genes⁸⁰. Each miRNA has the ability to repress the expression of numerous genes and therefore miRNAs are often referred to as master regulators of gene networks⁸¹. Investigation of miRNA involvement in the regulation of cellular processes, as well as differentiation, highlights the importance of these molecules in maintaining normal cellular function with loss of expression leading to abnormal regulation of cellular processes, poor differentiation or neoplastic development⁸².

1.3.1 Mammalian miRNA biogenesis

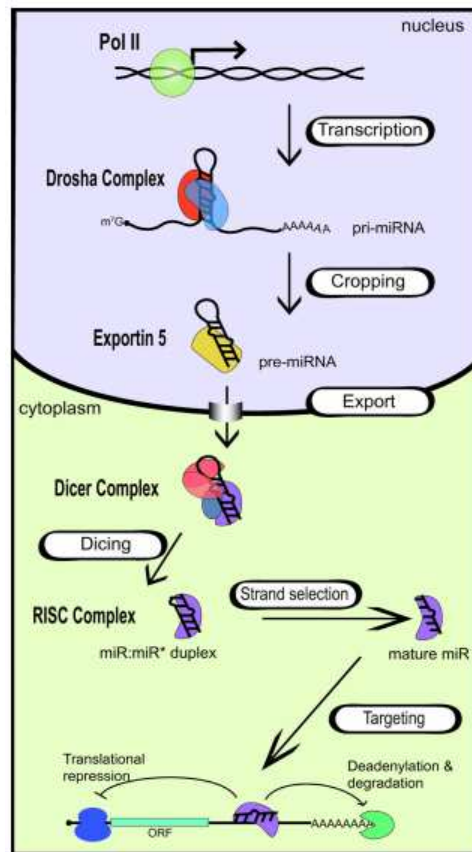
The nucleus

miRNAs are within non-coding RNA, or within introns of protein coding genes⁸³. miRNA biogenesis begins with primary miRNAs (pri-miRs, inactive form), which are either transcribed by RNA polymerase II or RNA polymerase III, or excised from portions of intronic sequence contained in precursor mRNA molecules⁸⁴⁻⁸⁶. Pri-miRs are processed in the nucleus by Drosha, an RNaseIII enzyme that complexes with the RNA binding domain protein DGCR8 to cleave out a 60-100nt hairpin section from the pri-miR sequence (pre-miR)^{83, 87}. Pre-miR hairpins then complex with exportin-5 and Ran-GTP for export from the nucleus to the cytoplasm^{84, 85, 88}.

The cytoplasm

In the cytoplasm, the RNaseIII enzyme Dicer, in coordination with the trans-activation-responsive RNA-binding protein (TRBP) cleaves the pre-miR hairpin to produce a 22nt double stranded complex, comprised of the mature miRNA guide strand and a miRNA* passenger strand^{83, 89}. The mature miRNA strand is determined by thermodynamic asymmetry and this concept acts to allow cytoplasmic accumulation of only the mature miRNA guide strand⁹⁰. In short, the asymmetry rule states that the 5' end of the mature miRNA guide strand is located at the end of the duplex that has the lowest thermodynamic energy⁹⁰. The miRNA guide strand complexes with miRNA-containing ribonucleo-protein particles (miRNPs) forming an RNA induced silencing complex (RISC), while the passenger strand is usually degraded⁹¹. At the core of miRNPs are the highly conserved argonaute proteins. Here a single mature miRNA guide strand complexes with an argonaute protein⁹². There are four different human argonaute proteins (Argonaute 1-4), however only argonaute 2 has the ability to cleave mRNA with its 'slicer' activity⁹³. Although the selection criteria for miRNA-argonaute pairing is unknown recent deep sequencing suggests that most miRNAs associate with Argonaute 1-3 in relatively even quantities⁹⁴. Following assembly of the miRNP, the miRNA directs targeting of mRNA transcripts through base pairing, acting to repress translation⁸³. Mammalian miRNA biogenesis is summarised in Figure 1.9.

Figure 1.9: Shows the basic stages of miRNA biogenesis. Biogenesis begins in the nucleus where pri-miRNAs are transcribed. Pri-miRNAs then fold and are cleaved by DROSHA to form a stem loop pre-miR. The pre-miRNA exits the nucleus and enters the cytoplasm via exportin 5. The pre-miRNA is processed in the cytoplasm by DICER producing a double stranded molecule. The mature RNA strand then complexes with miRNPs to produce a RISC complex. The risk complex then targets mRNA transcripts to inhibit translation.



(Reproduced from: Davis & Hata, 2009⁹⁵)

miRNA targeting

Mammalian miRNAs target mRNA transcripts for translational repression based on their seed sequence. The seed sequence of a miRNA includes nucleotides 2-8 at the 5' end⁹⁰. Complementarity between the miRNA seed sequence and regions of the mRNA transcript's non-coding 3' untranslated region or coding 5' region is required for translational repression⁹⁶. The extent of the seed sequence-target complementarity determines the mechanism of translational repression. Perfect complementarity inhibits translation by directing transcript cleavage, an event more

common in plants than in mammals^{97, 98}. Imperfect complementarity is thought to direct translational inhibition by blocking access to translational machinery or directing the target mRNA to cytoplasmic processing bodies where mRNA degradation occurs via de-adenylation and de-capping^{81, 99, 100}. Both the degradation and direct translational inhibition mechanisms can cause detectable decreases in mRNA levels and act to repress protein levels¹⁰¹.

1.3.2 Regulation of miRNA expression

miRNA expression needs to be tightly regulated as aberrant expression leads to dysfunctional control of cellular processes. For example, by knocking out Drosha or Dicer functionality, increased invasive capacity is observed in lung adenocarcinoma cells¹⁰² and increased tumour development is observed in a v-Ki-ras2 Kirsten rat sarcoma viral oncogene (*KRAS*) induced model of lung cancer¹⁰². Several studies have investigated the regulatory processes involved in maintaining tight regulation of miRNA biogenesis and these studies show regulation of miRNA biogenesis can occur through a number of mechanisms⁹⁵.

miRNAs are transcribed from genomic DNA by the same mechanism as protein coding genes. Therefore, standard mechanisms of epigenetic control that apply to mRNA transcription likely apply to miRNA transcription⁹⁵. For example, numerous miRNAs have been shown to be repressed by methylation and this has been linked to cancer metastasis¹⁰³. Further, histone de-acetylase inhibition has been shown to induce miRNA expression¹⁰⁴.

Control of miRNA biogenesis can be regulated in the nucleus as Drosha activity can be regulated by a number of mechanisms. For example, the dead-box RNA helicases *p68* and *p72* in cooperation with signal transducing Smad proteins have the ability to promote Drosha processing of specific miRNAs^{88, 105}. Also, proteins have the ability to bind Drosha and increase miRNA abundance by increasing Drosha activity. For example the transcription factor p53 has the ability to bind Drosha and increase Drosha processing¹⁰⁶. Interestingly, *p53* expression is induced in response to DNA damage, acting to increase Drosha mediated pri-miRNA processing which results in

increased mature miRNA expression. Also, *p53* dysfunction has been shown to increase tumourigenesis through repression of miRNA expression¹⁰⁶. Mutations in *p53* have been described in Barrett's oesophagus and oesophageal adenocarcinoma¹⁰⁷, however, it is not known if these mutations impact on miRNA biogenesis in these pathologies. Furthermore, the expression of Droscha requires tight regulation, as evidenced by the correlation between increased expression of Droscha with poor prognosis in oesophageal adenocarcinoma patients¹⁰⁸.

Regulation of Dicer activity and expression can also influence miRNA activity. For example mature levels of miR-143 and miR-145 are decreased in tumour tissues but pre-miR-143 and pre-miR-145 levels are unchanged indicating dysfunctional processing by Dicer¹⁰⁹⁻¹¹¹. Aberrant regulation of Dicer expression is linked with increased tumorigenesis. Reduced Dicer expression is observed in small-cell-lung cancer, correlating with poor patient prognosis¹¹². Also, reduced Dicer expression enhances cell proliferation and invasion in an *in vivo* xenograph model of breast cancer¹¹³.

1.3.3 miRNAs and cancer development

Aberrant miRNA expression has been linked with the development and progression of almost all cancers studied to date. Through the use of miRNA array technology rapid advances in global miRNA profiling have mapped up and down-regulation of miRNAs in many tumours¹¹⁴. Key hallmarks of cancer include unrestricted growth, apoptotic resistance and immortalization, as well as the development of angiogenic, migratory and invasive capability⁸². Functional assessment of aberrant miRNA expression has implicated these molecules in regulating these key hallmarks of cancer¹¹⁵⁻¹¹⁷. Early miRNA studies identified miRNAs acting as both oncogenes (eg. miR-17-92 cluster) and tumour suppressors (eg let-7)¹¹⁸⁻¹²⁰. Forced expression of the miR-17-92 cluster in mice leads to the accelerated development of B-cell lymphoma¹¹⁹. Also, the miR-17-92 cluster is over expressed in lung cancer, and this is associated with an increase in cellular proliferation^{119, 121}. Let-7 acts as a tumour suppressor through suppression of Ras^{118, 120}. In lung cancer decreased let-7 expression results in increased cellular proliferation¹²⁰. Also, increased let-7

expression *in vivo* has been shown to inhibit lung cancer xenograft growth in mice¹²². More recent evidence shows aberrant miRNA expression can promote cancer development through numerous cellular processes. For example the miR-17-92 polycistron paralogue, the miR-106b-25 polycistron acts as an oncogene in oesophageal adenocarcinoma. Increased expression of this polycistron *in vitro* causes increased proliferative capacity, apoptotic resistance and promotion of cell cycle progression¹¹⁵. In addition, miR-200a, one of the five miRNA members of the miR-200 family has a validated role in regulating the epithelial to mesenchymal transition, a key process in tumour invasion and acts as a tumour suppressor in nasopharyngeal carcinoma with decreased expression leading to increases in cell growth, migration and invasion¹²³. At the beginning of this doctoral study there were no reports of the functional roles of miRNAs in oesophageal adenocarcinoma. Given, the increasing evidence implicating miRNA in cancer development, there are a number of interesting questions regarding the role of miRNAs in oesophageal adenocarcinoma development and progression.

1.3.4 miRNAs as biomarkers

Biomarkers have the ability to classify specific biological states. The uses for biomarkers are quite broad as they can classify everything from response, to treatment regimes, to specific tissue phenotypes or disease states. A good biomarker should show strong, stable expression in the group it classifies, it should be easy to detect and its level of expression needs to be quantifiable. Expression of miRNAs satisfy all of these criteria and therefore these molecules are presenting as promising candidates for classifying a number of different tissue phenotypes and disease pathologies. Interestingly, miRNA profiling can be used to effectively classify different tumour types where mRNA profiling had failed¹²⁴. This study by Lu et al. 2005¹²⁴, showed that while miRNA expression profiling could be used to classify poorly differentiated breast, colon, lung and ovary tumours, mRNA expression profiling was unsuccessful. 2-4% of cancer diagnoses are unable to identify the cellular origin of the tumour¹²⁵. Accordingly, this study¹²⁴ highlights the potential of miRNA biomarkers in providing additional diagnostic certainty by assisting in confirming the tumours tissue of origin.

miRNA expression is often enriched in particular tissues and cell phenotypes. For example, miR-1 is enriched in muscle¹²⁶ and miR-134 is expressed exclusively in the brain¹²⁷. miRNAs have already proven to be useful biomarkers for tumour classification as well as predicting patient prognosis and therapeutic response¹²⁸. Advances in the ability to profile different aspects of tumourigenesis have led to the rapid identification of differentially expressed miRNAs in cancer¹¹⁴. Different miRNA expression profiles are observed for normal and tumourigenic tissues¹¹⁴, where miRNA expression is generally down-regulated in tumour compared with normal samples¹²⁴. Studies into miRNA expression in cancer have identified miRNA tumour profiles which can be used to classify different tumour subtypes^{124, 129}, some of which are now commercially available for use as clinical diagnostics¹³⁰. Studies have also constructed miRNA expression profiles that can identify tumour origin¹²⁴. This is particularly useful in the classification of poorly differentiated tumours.

There is promise for the clinical implementation of miRNA biomarkers in reflux pathology, Barrett's oesophagus and oesophageal adenocarcinoma diagnosis. By identifying changes in miRNA expression we may have the ability to use miRNA expression patterns to assist in diagnosis and prognosis prediction in upper gastrointestinal pathologies^{124, 131}.

1.3.5 miRNA target prediction

While the involvement of miRNAs in translational regulation has been studied extensively few mRNA targets of miRNAs have been validated experimentally. This is likely because of the lengthy target validation process¹³². In order to increase the throughput speed for miRNA target validation numerous target prediction algorithms have been established, predicting miRNA:mRNA interactions. These prediction algorithms take into account a number of critical requirements for miRNA targeting, and weight these features in order of importance. It is generally accepted that the most important requirement for translational repression is sequence complementarity between the miRNA 7-8 nucleotide seed region and the mRNA transcript^{133, 134}. Most commonly used prediction programs incorporate other features into their

prediction algorithms. For example, accounting for evolutionary sequence conservation has been shown to provide marked improvement in an algorithm's predictive power, while the location and number of the miRNA target binding sites in the 3'UTR, 5' UTR and coding region is also important^{134, 135}. Also, incorporating miRNA accessibility due to mRNA folding and negative correlations between miRNA and mRNA abundance into prediction algorithms have been shown to improve target prediction efficacy¹³³⁻¹³⁵. In addition, high throughput sequencing of RNAs being isolated following immuno-precipitation of RISC complexes (HITS-CLIP)¹³⁶ is now being combined with prediction algorithms to reduce false positive rates. A recent review by Bartel¹³⁴ gives an overview of the key features of some commonly used prediction algorithms (Figure 1.10) selecting TargetScan as the prediction algorithm of choice due to its requirement for stringent seed sequence pairing and seed sequence accessibility following RNA folding post transcription.

Figure 1.10: Comparison of commonly used prediction algorithms and the key features accounted for in predicting miRNA:mRNA interactions.

Table 1. Tools for Predicting Metazoan miRNA Targets				
Tool*	Clades*	Criteria for Prediction and Ranking	Website URL	Recent Reference
Site Conservation Considered				
TargetScan	m	Stringent seed pairing, site number, site type, site context (which includes factors that influence site accessibility); option of ranking by likelihood of preferential conservation rather than site context	http://targetscan.org	Friedman et al., 2008
TargetScan	f,w	Stringent seed pairing, site number, site type	http://targetscan.org	Ruby et al., 2007; Ruby et al., 2006
EMBL	f	Stringent seed pairing, site number, overall predicted pairing stability	http://russell.embl-heidelberg.de	Stark et al., 2005
PicTar	m,f,w	Stringent seed pairing for at least one of the sites for the miRNA, site number, overall predicted pairing stability	http://pictar.mdc-berlin.de	Lall et al., 2006
EIMMo	m,f,w	Stringent seed pairing, site number, likelihood of preferential conservation	http://www.mirz.unibas.ch/EIMMo2	Gaidatzis et al., 2007
Miranda	m,f,w,+	Moderately stringent seed pairing, site number, pairing to most of the miRNA	http://www.microrna.org	Betel et al., 2008
miRBase Targets	m,f,w,+	Moderately stringent seed pairing, site number, overall pairing	http://microrna.sanger.ac.uk	Griffiths-Jones et al., 2008
PITA Top	m,f,w	Moderately stringent seed pairing, site number, overall predicted pairing stability, predicted site accessibility	http://genie.weizmann.ac.il/pubs/mir07/mir07_data.html	Kertesz et al., 2007
mirWIP	w	Moderately stringent seed pairing, site number, overall predicted pairing stability, predicted site accessibility	http://146.189.76.171/query	Hammell et al., 2008
Site Conservation Not Considered				
TargetScan	m	Stringent seed pairing, site number, site type, site context (which includes factors that influence site accessibility)	http://targetscan.org	Grimson et al., 2007
PITA All	m,f,w	Moderately stringent seed pairing, site number, overall predicted pairing stability, predicted site accessibility	http://genie.weizmann.ac.il/pubs/mir07/mir07_data.html	Kertesz et al., 2007
RNA22	m,f,w	Moderately stringent seed pairing, matches to sequence patterns generated from miRNA set, overall predicted pairing and predicted pairing stability	http://cbcsrv.watson.ibm.com/rna22.html	Miranda et al., 2006

*Tools are listed according to criteria for prediction and ranking, which for those tools assessed with recent proteomics results generally correspond to their overall performance (Baek et al., 2008).

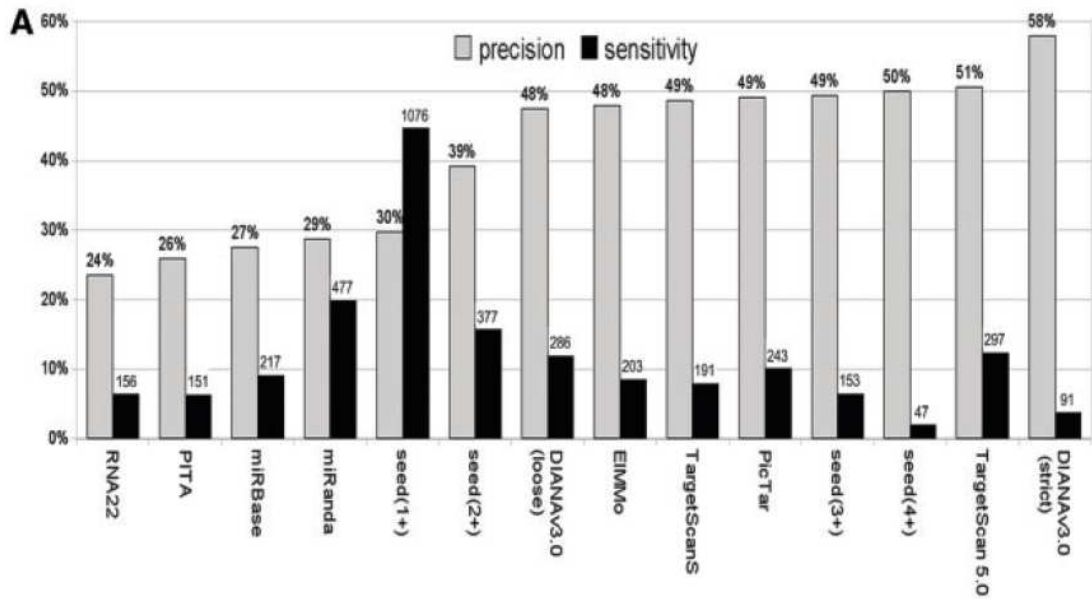
†Letters indicate predictions provided for the mammalian/vertebrate (m), fly (f), worm (w), or additional (+) clades.

(Reproduced from: Bartel et al.¹³⁴)

As a result of the numerous factors that influence miRNA:mRNA interaction, target prediction programs often provide conflicting results. A recent study by Alexiou et al.¹³⁵ compared experimental data of protein expression changes¹³⁷ after increasing or decreasing miRNA levels with predicted targets for the miRNAs of interest. The study measured an algorithm's precision, or ability to identify the experimentally validated targets of a miRNA, as well as measure sensitivity as a function of the number of false positive miRNA targets identified. The study by Alexiou et al.¹³⁵ found that five target prediction programs achieved approximately 50% precision, i.e. approximately 50% of the total number of predicted targets matched the experimentally determined targets (Figure 1.11). These prediction programs included DIANA-microT 3.0, TargetScan 5.0, TargetScanS, Pictar and EIMMo. Of these 5 programs, DIANA-microT 3.0 has the highest precision, while TargetScan 5.0 had

the highest sensitivity (ie 12% of the experimentally determined targets were predicted by TargetScan). Therefore, either DIANA microT 3.0 or TargetScan 5.0 present as the current search algorithms of choice.

Figure 1.11: When considering the top 5 miRNA target prediction programs, results from TargetScan 5.0 give the highest sensitivity while results from DIANA microT 3.0 give the highest precision.



Reproduced from: Alexiou et. al.¹³⁵

1.4 miRNAs and the reflux-Barrett's-adenocarcinoma sequence

Numerous cellular processes are differentially regulated during the reflux-Barrett's-adenocarcinoma sequence^{29, 138-140}. Reflux pathology associated with gastroesophageal reflux disease includes chronic inflammation, basal cell hyperplasia and increased levels of apoptosis.

In Barrett's oesophagus the epithelium is hyper-proliferative, displays abnormal crypt proliferation and is resistant to apoptosis¹⁴¹⁻¹⁴⁴. Barrett's oesophagus development is thought to require either transdifferentiation or induction of alternate oesophageal stem cell differentiation. Cellular processes of interest in oesophageal adenocarcinoma, like all cancers, include cell proliferation, apoptosis and invasion. miRNAs have been shown to play roles in the biological processes that are relevant to the development of Barrett's oesophagus and its neoplastic conversion. Therefore, there is great scope for studying alterations in miRNA expression along the reflux-Barrett's oesophagus - oesophageal adenocarcinoma pathway and exploring the biological roles of miRNAs in this setting.

Prior to the start of this thesis a miRNA array was carried out, assessing global miRNA expression in squamous oesophageal epithelia, Barrett's oesophagus and oesophageal adenocarcinoma¹¹⁰. The array identified a number of differentially expressed miRNAs and provided the preliminary data for this thesis.

1.5 Thesis aims

- 1) Determine and quantify differences in the miRNA expression profile of oesophageal squamous epithelium, Barrett's epithelium and oesophageal adenocarcinoma.
- 2) Determine whether the miRNAs that are differentially expressed in Barrett's epithelium, compared to squamous epithelium are also differentially expressed in squamous epithelium from patients with oesophagitis caused by gastroesophageal reflux disease.

3) Assess the location of miRNAs differentially expressed in gastroesophageal reflux disease and use a cell line derived from oesophageal squamous tissue (Het-1A) to assess their ability to regulate cellular processes regulated in gastroesophageal reflux disease i.e. apoptosis and proliferation

4) Identify tumour suppressor functions of miRNAs that are down-regulated in oesophageal adenocarcinoma by:

A) Assessing the location of miRNAs in Barrett's oesophagus, high-grade dysplasia and oesophageal adenocarcinoma.

B) Assessing the effects on proliferation and apoptosis after increasing the levels of miRNAs down regulated in oesophageal adenocarcinoma in an oesophageal adenocarcinoma cell line.

5) Investigate whether changes in miR-200 family expression may contribute to abnormal cellular processes in Barrett's oesophagus and/or epithelial to mesenchymal transition in oesophageal adenocarcinoma by:

A) Assessing the expression of the miR-200 family in Barrett's oesophagus.

B) Assessing the expression of the miR-200 family and its transcription factor targets zinc finger E-box binding homeobox 1 (ZEB1) and zinc finger E-box binding homeobox 2 (ZEB2) in oesophageal adenocarcinoma.

Chapter 2

General Materials and Methods

2.1 *Materials*

2.1.1 General reagents

All chemicals, cell culture media and supplements were of analytical grade and were used without further purification.

2.1.2 Buffers and Solutions

All general solutions and buffers were either purchased direct from the manufacturer or made up with double deionised MilliQ (MQ) water to the required concentration. All solutions and buffers used for PCR were certified DNase and RNase free.

10X PBS

NaCl	80 g
KCl	2 g
Na ₂ HPO ₄ · 2H ₂ O	18.05 g
KH ₂ PO ₄	2.4 g
MQ	1 L

TBE buffer

NaOH	0.5 g
Tris Base	54 g
H ₃ BO ₃	27.5 g
EDTA	3.7 g
MQ	1 L

Cell Lysis Buffer for protein isolation

1M Trisma hydrochloride	10 ml
1% Tween 20	2 ml
5M NaCl	6 ml
100mM Na ₄ P ₂ O ₇	20 ml
100mM NaVO ₄	2 ml
1:500 w/v NaN ₃ in H ₂ O	400ul
MQ	114 ml

1 Protease inhibitor cocktail tablet (added fresh) (Roche, Dee Why, NSW #11836153001)

Roche protease inhibitor cocktail tablet contains:

Pancreas extract	0.02 mg/ml
Pronase	0.005 mg/ml
Thermolysin	0.0005 mg/ml
Chymotrypsin	0.0015 mg/ml
Papain	0.33 mg/ml

10x Running Buffer for gel electrophoresis

Tris Base	30.3 g
Glycine	144 g
SDS	10 g
MQ	800 ml

Adjust to pH 8.3

MQ to 1 L

1x Transfer Buffer for protein transfer from gel to PVDF membrane

Tris base	12.12 g
Glycine	57.6 g
MQ	3 L
Methanol	800 ml

Add MQ to 4 L

PBS-T

PBS

1% Tween-20

Blocking Buffer

5% Non-fat dried milk in PBS-T

5x Sample Buffer (SDS reducing)

MQ	4 ml
500mM Tris-HCl pH 6.8	1 ml
Glycerol	0.8 ml
10% SDS	1.6 ml
0.05% Bromophenol Blue	0.2 ml
2-β-Mercaptoethanol	0.4 ml

AnnexinV Binding Buffer

10mM HEPES/NaOH, pH 7.4

140mM NaCl

2.5mM CaCl₂

2.2 *Methods*

2.2.1 RNA isolation and quality control

All RNA used in the experiments comprising this thesis was extracted using TRIzol[®] (Invitrogen, Carlsbad, CA) following the manufacturer's protocol with some variations.

RNA was extracted from cell lines and human tissue. RNA extraction from cell lines began with a wash with serum free medium before adding 500 µl of TRIzol[®] directly to attached cells. For RNA extraction from human tissue, 250 µl of TRIzol[®] was added to tissue inside an Eppendorf tube before homogenising the tissue with a plastic pestle, followed by further addition of 250 µl of TRIzol[®].

Samples in TRIzol[®] were then heated to 37 °C for 5 min, pulse centrifuged for 5 sec, and 100 µl of chloroform was added to each sample. Samples were then vortexed for 15 sec, and then incubated at room temperature for 5 min. Samples were then centrifuged at 12,000 x g for 15 min at 4 °C. 300 µl of isopropanol was added to fresh eppendorf tubes. After centrifugation the aqueous phase was removed and placed into the new eppendorf tube containing isopropanol, incubated at room temperature for 10 min and then centrifuged at 12,000 x g for 30 min at 4 °C. After centrifugation the isopropanol was removed and 500 µl of ethanol was added before vortexing. Samples were then centrifuged at 7,600 x g for 5 min at 4 °C before removing the ethanol. Samples were centrifuged again at 7,600 x g for 1 min and any excess ethanol was removed. To dissolve the RNA pellet 22 µl of ultra pure water (Fisher Biotec, Subiaco, WA) was added before incubating samples at 60 °C for 10 min, followed by a pulse centrifuge, then a further incubation for 5 min at 60 °C. The RNA concentration of each sample was measured using a Biophotometer (Eppendorf, North Ryde, NSW). RNA quality was determined by gel electrophoresis (1% gel, 3 g of agarose in 300 ml of TBE buffer). Ethidium bromide staining (40 µl of 10 mg/ml ethidium bromide in 800 ml MQ) for 30minutes and UV illumination was used to visualise and photograph intact 18 and 28S rRNA bands.

2.2.2 Quantitative real-time polymerase chain reaction (RT-PCR) analysis of miRNA expression

Expression of selected miRNAs were assessed using individual TaqMan[®] miRNA Assays (Applied Biosystems, Foster City, CA, USA). 5ng of total RNA was reverse transcribed into complementary DNA (cDNA) using gene-specific primers (primer details Table 2.1) and the TaqMan[®] miRNA reverse transcription kit (#4366597, Applied Biosystems) following the manufacturers protocol. After reverse transcription miRNA expression was assessed by real-time PCR, using the Applied Biosystems, TaqMan[®] Universal PCR Master Mix, No AmpErase[®] UNG (#4324018) and individual miRNA TaqMan[®] assays. Individual miRNA TaqMan[®] assay details are shown in Table 2.1.

Table 2.1: Individual TaqMan[®] miRNA assay details including the assessed mature miRNA sequence.

miRNA	Assay ID	Mature miRNA sequence
hsa-miR-21	000397	UAGCUUAUCAGACUGAUGUUGA
hsa-miR-141	000463	U AACACUGUCUGGUA AAGAUGG
hsa-miR-143	002249	UGAGAUGAAGCACUGUAGCUC
hsa-miR-145	002278	GUCCAGUUUCCCCAGGAAUCCCU
hsa-miR-194	000493	UGUAACAGCAACUCCAUGUGGA
hsa-miR-200a	000502	U AACACUGUCUGGUA ACGAUGU
hsa-miR-200b	002251	UAAUACUGCCUGGUA AUGAUGA
hsa-miR-200c	002300	UAAUACUGCCGGGUA AUGAUGGA
hsa-miR-215	000518	AUGACCUAUGAAUUGACAGAC
hsa-miR-429	001024	UAAUACUGUCUGGUA A AACC GU
hsa-RNU44	001094	CCTGGATGATGATAGCAAATGCTG ACTGAACATGAAGGTCTTAATTAG CTCTAACTGACT

Reverse transcriptase (RT) reactions contained 5 ng of RNA sample, 100 nM stem-loop RT primer, 100mM of dNTPs, 50U/ μ L Multiscribe reverse transcriptase, 20 U/ μ L RNase inhibitor, 1.5 μ L 10 x RT Buffer (all from Applied Biosystems) and ultra pure water. The 15 μ L reactions were incubated in a Thermocycler (Eppendorf, North Ryde, NSW, Australia) for 30 min at 16°C, 30 min at 42°C, 5 min at 85°C and then held at 4°C. After reverse transcription the RT product (cDNA) was diluted with 41.25 μ l of ultra pure water.

Real-time PCR was performed using a Rotor-Gene 6000 (Corbett Life Science, Sydney, NSW, Australia). The 20 μ L PCR reaction included 5 μ L of diluted RT product, 1 μ L of primers, 10 μ L TaqMan[®] Universal PCR Master Mix, No AmpErase[®] UNG (#4324018, Applied Biosystems) and 4 μ L of ultra pure water. Triplicate reactions were performed on all samples. The data was quantitatively analysed using Q-Gene software¹⁴⁵ and then prepared for presentation with KaleidaGraph software (Synergy Software, PA). MiRNA expression data were normalized for levels of RNU44 (assay detail, Table 2.1).

2.2.3 Quantitative RT-PCR analysis of mRNA expression

Expression of selected mRNAs compared were assessed using a QuantiTect® Reverse Transcription kit (#205313, Qiagen, Valencia, CA) and either the QuantiTect® SYBRGreen mastermix (#204145, Qiagen) or TaqMan® Gene Expression Mastermix (#4369016, Applied Biosystems) for PCR following the manufacturers protocol. Primer details for Quantitect® SYBRGreen PCRs are shown in Table 2.2. Primer details for TaqMan® gene expression assays are shown in Table 2.3.

Genomic DNA was removed from 336 ng of total RNA by treating with gDNA wipeout buffer. The 336 ng RNA sample was then reverse transcribed into cDNA using a mixture of oligo-dT and random hexamer primers. After reverse transcription mRNA expression was assessed by real-time PCR, using the Quantitect® SYBRGreen and gene specific primers. PCR was carried out in a Rotor-Gene 6000 (Corbett Life Science).

Reverse transcription reactions were at a final volume of 20 µl and contained 336 ng of RNA sample in 5 µl of ultra pure water, 2 µl of gDNA wipeout buffer, 1 µl of reverse transcriptase, 4µl of 5x RT buffer and 1µl of RT primer mix (all from Qiagen) and 7 µl of ultra pure water. The 20 µl reverse transcription reaction was carried out in a thermocycler (Eppendorf, North Ryde, NSW) for 30 min at 42°C, 3 min at 95°C and then held at 4°C. After reverse transcription the RT product (cDNA) was diluted with 150 µl of ultra pure water.

Real-time PCR was performed using a Rotorgene 6000 thermocycler (Corbett Life Science). Both methods of PCR consisted of a 20 µL PCR reaction including 5µL of reverse transcribed cDNA product. The Quantitect® SYBRGreen system required 1µL each of 5 µM forward and reverse primers (Gene works, Thebarton, SA), 10 µL Quantitect® SYBRGreen (Qiagen) and 3 µL of ultra pure water. The TaqMan® gene expression assay required 1 µl of primer, 10 µl of TaqMan® universal master mix (all from Applied Biosystems) and 4 µl of ultra pure water. Triplicate reactions were performed on all samples. The data was quantitatively analysed using Q-Gene

software²⁴ and then prepared for presentation with KaleidaGraph software (Synergy Software, PA). mRNA expression data were normalized for levels of a reference ‘house keeper’ gene.

Table 2.2: Primer details for Quantitect® SYBRGreen PCR

Gene Name	Forward Sequence	Reverse Sequence
18S	CCGCGCTGGTTGG	GTCGGCATCGTTTATGGTC
β-actin	TTGCCGACAGGATGCAGAAG	GCCGATCCACACGGAGTACT
BMP4	CATCCACTCACCCACACACT	TGGTCAAAACATTTGCACGTA
CDX2	CAGCTAAGATAGAAAGCTGGACTG	CACCCTGTGCATACACCAGCCAAG
CK8	AGCGTACAGAGATGGAGAAC	TGAGGAAGTTGATCTCGTCG
CK14	ACGATGGCAAGGTGGTGT	GGGATCTTCCAGTGGGATCT
GATA4	TCTTGGAACAGCCTGGTCTT	GGCCTCCTTCTTTGCTATCC
HNF1α	TTGTTTGGGGCAGGAGTAGC	CCTGGGGTCACCTCTTTCTT
IL6	GCAATAACCACCCCTGACC	TAAAGCTGCGCAGAATGAGA
ZEB1	TCGATCTGGCATTGTTTATC	GCGGATTTAGCATATGTTTACCA
ZEB2	GTTCAGCCAAGACAGATGTAGACG	CAGGATTAGTCTCTGAACCACAC

Table 2.3: TaqMan® gene expression assay details.

Gene ID	Assay ID
PC	Hs00559398_m1*
NUAK2	Hs00388292_m1*
PABPC4	Hs00906354_m1*
MECP2	Hs00172845_m1*
H2AFX	Hs00266783_s1*
RTKN	Hs00895015_m1*
GEM	Hs00738924_m1*
DUSP10	Hs00200527_m1*
EGR1	Hs00152928_m1*
CITED2	Hs01897804_s1*
SLAMF7	Hs00900280_m1*
ANKRD1	Hs00173317_m1*
CYR61	Hs00155479_m1*

2.2.4 Thawing of cells for cell culture

A cryo-tube of the required cell line was rapidly thawed under lukewarm water before being transferred into a 10 ml centrifuge tube. 7 ml of culture medium was added to the centrifuge tube before centrifugation at 400 x *g*. The supernatant was removed and a further 7 ml of cell culture medium was added followed by additional centrifugation at 400 x *g*. The supernatant was again discarded and cells were resuspended in 1 ml of cell culture medium. Cells were then aliquoted into a 75 ml culture flask and incubated at 37°C with 5% CO₂.

2.2.5 Cell culture and miRNA over expression

Het-1A¹⁴⁶ and OE-19¹⁴⁷ cells were cultured and transfected with miRNA mimics to elevate miRNA expression (miRNA mimic and negative control details are shown in Table 2.4). Het-1A cells were cultured using LHC-9 medium (Invitrogen, Mulgrave, VIC) supplemented with 0.2 µg/ml penicillin-streptomycin (Invitrogen) and 0.1mg/ml, Normocin (Invivo-Gen, San Diego, CA). Het-1A cells were transfected with miR-143, miR-145 or miR-205 mimics or a negative control duplex. Plasticware used for Het-1A cell culture was coated with a coating media prepared from LHC-9 medium by adding 0.01 mg/ml fibronectin (Sigma, Castle Hill, NSW), 2.3 µg/ml Collagen (BD biosciences, North Ryde, NSW) and 0.1 mg/ml bovine serum albumin (Sigma). Once the coating media was prepared it was added to cell culture plasticware and incubated overnight at 37°C. The following day the coating media was removed and the plastic ware was left to dry thoroughly.

OE-19 cells were cultured using Dulbecco's modified eagle medium (DMEM) supplemented with 10% fetal bovine serum (Invitrogen), 1% (weight/volume) penicillin-streptomycin (Invitrogen) and 0.06% (volume/volume) Normocin (Invivo-Gen). OE-19 cells were transfected with either miR-143, miR-145 or miR-215 mimics or a negative control duplex.

miRNA levels were increased by transfecting Het-1A cells with miR-143, miR-145 or miR-205 mimics and OE-19 cells with miR-143, miR-145 or miR-215 mimics

using the Lipofectamine™ 2000 system (Invitrogen) as per the manufacturer's protocol. miRNA mimic and negative control duplexes were supplied lyophilized and were dissolved in ultra pure water to achieve a concentration of 150 μM for storage. Cells were exposed to miRNA duplexes for 24 hr then the transfection cell culture media was replaced with fresh media. Cells were transfected using miRNA mimic or negative control duplexes at 33 nM concentration (GenePharma, Shanghai, China) (Table 2.4). RNA was extracted from transfected cells using TRIzol®, and miRNA over expression was confirmed by using the PCR methods described in section 2.2.2 to assess RNA obtained from transfected cell lines 24 and 48 hr after the cells were exposed to the miRNA duplexes.

Table 2.4: Sequence details and product numbers for mimic and negative control duplexes used for cell line transfection experiments. miRNA mimic and negative control probes were obtained from GenePharma.

miR-143 (#2988) sequence:
5'- UGAGAUGAAGCACUGUAGCUC -3' 5'- GCUACAGUGCUUCAUCUCAU -3'
miR-145 (#8480) sequence:
5'- GUCCAGUUUCCCAGGAAUCCCU -3' 5'- GGAUUCCUGGGAAAACUGGACUU -3'
miR-205 (#3391) sequence:
5'- UCCUUCAUUCACCGGAGUCUG -3' 5'- GACUCCGGUGGAAUGAAGGAUU -3'
miR-215 (#3895) sequence:
5'- AUGACCUAUGAAUUGACAGAC -3' 5'- CUGUCAAUUCAUAGGUCAUUU -3'
Negative control duplex (#1733)
5'- UUCUCCGAACGUGUCACGUTT -3' 5'- ACGUGACACGUUCGGAGAATT -3'

2.2.6 Proliferation and apoptosis assays

In Het-1A (chapter 4) and OE-19 (chapter 5) transfection experiments, cell proliferation and apoptosis were assayed 24 and 48h post transfection (n=2 experimental replicates). Experiments measuring proliferation were conducted using 96 well plates. 3000 cells were plated per well and 10 wells were used for each experimental and control group. Cell proliferation levels were measured by assessing cell numbers using the MTS assay system (Promega, Alexandria, NSW) as per the manufacturers protocol. For each cell line the MTS assay was first used to calculate a standard curve from absorbance readings of known cell numbers at 490 nm. To assess cell numbers 20 μ l of MTS solution was added to each well of the 96 well plate that contained attached cells and 100 μ l of cell culture media. After adding the MTS solution 96 well plates were incubated at 37°C for two hours before an absorbance reading at 490 nm was obtained from each well using a scanning plate reader (Bio-Rad, Gladesville, NSW). Absorbance readings and the standard curve were used to calculate cell numbers. Cell numbers at each time point were assessed, comparing cell groups transfected with a miRNA mimic with cells transfected with the negative control duplex. Differences in cell numbers were assessed for statistical significance using the Mann-Whitney test.

Experiments measuring apoptosis levels were conducted using 24 well plates. 50,000 cells were plated per well and 8 wells were used for each experimental and control group. Apoptosis was measured by assessing the numbers of pre-apoptotic cells. Post transfection cells floating cells were removed and placed in a centrifuge tube. Attached cells were detached using trypsin, 0.05% (1X) with EDTA 4Na (Invitrogen) and pooled with floating cells, twice centrifuged at 400 x *g* and washed with PBS + 0.05% Na azide then resuspended in 200 μ l of annexinV binding buffer (BD biosciences). 5 μ l of the annexinV antibody (BD Biosciences) was added to cells with 5 μ l of propidium iodide (Sigma) as per the manufacturers protocol to stain viable, pre-apoptotic and non-viable cells 24 and 48 hr post-transfection. Propidium iodide indicative cell viability and positive AnnexinV, pre-apoptotic staining was measured using flow cytometry (BD FACSCANTO II from BD Biosciences) and the BD FACSDiva software package.

2.2.7 Statistical analysis and correlations

miRNA and mRNA PCR data were processed using Q-Gene software to produce relative quantification data¹⁴⁵. Differences in miRNA expression between the three tissue groups were assessed for statistical significance using GraphPad PRISM software to perform Kruskal-Wallis tests and post hoc testing using the Holm-Bonferroni method. Spearman rank order correlation tests between miRNA vs. mRNA expression were determined on-line (<http://www.wessa.net/rankcorr.wasp>). Statistical analysis of miRNA and mRNA expression was performed using GraphPad Prism software (GraphPad Software, Inc. La Jolla, CA, USA). Apparent differences in proliferation and apoptosis were assessed using the Mann-Whitney test.

2.2.8 In-situ hybridisation

To localise miRNA activity in-situ hybridization was performed, probing against miRNAs of interest. Flinders Medical Centre, Anatomical Pathology staff performed standard hematoxylin and eosin staining on a slide from each tissue biopsy to confirm the tissue type. In-situ hybridization was performed on serial 4 µm sections of 4% formalin fixed, paraffin embedded oesophageal tissue biopsies from controls and individuals with ulcerative oesophagitis. The in-situ hybridization protocol was based on a protocol published by Pena and colleagues¹⁴⁸ with the following changes. All buffers were purchased direct from the manufacturer or prepared with diethyl pyrocarbonate (DEPC) (Sigma) treated water and sterilised via autoclave unless otherwise stated. Sections were deparaffinised in Histo-Clear (National Diagnostics, Atlanta, Georgia) and rehydrated through an ethanol dilution series (100-25%). Slides were then washed for 5 min in water treated with DEPC followed by 13 min in 2 µg/ml proteinase K treatment (Roche Diagnostics, Mannheim, Germany). Tissue sections were acetylated¹⁴⁸ for 10 min and then washed twice, for five minutes in PBS. Sections were framed with a wax pen (Vector Laboratories, Burlingame, California), covered with 40 µl of pre-hybridisation buffer¹⁴⁸ and incubated at room temperature for four hours. Pre-hybridisation buffer was tipped from the slides and replaced with 40 µl of either the digoxigenin (DIG)-labeled, Locked Nucleic Acid (LNA)-miRNA probe or LNA-scramble probe (Exiqon, Vedbaek, Denmark) diluted

to 250 nM with denaturing hybridization buffer (0.25% CHAPS detergent (Amresco, Solon #0465-5g), 0.1% Tween-20 (Sigma, #P1379). Slides were then incubated at 55 °C overnight. The LNA-probes used include miR-143 (#38515-15), miR-145 (#38517-15), miR-205 (#18099-15), miR-215 (#99999-15), U6 (#99002-15) and miR-SCR (#99004-15). The sequence of the miR-SCR duplex, used as a negative control, shared no homology with known miRNAs.

Slides were washed twice with 0.2X saline sodium citrate (SSC) buffer (Sigma) heated to 60 °C and then incubated with 0.2X SSC buffer 60 min at 60 °C. Levamisole (24% weight/volume) (Sigma, #L9756-5G) was used to reduce background alkaline phosphate activity. Slides were submerged in levamisole buffer containing 1M TRIS pH 7.5 and 5M NaCl for 5 min at room temperature. The sections were then incubated with a blocking buffer (1% blocking buffer and 1X maleic acid buffer, DIG Wash and Block Buffer Set, (Roche Diagnostics) for 60 min. 40 µl of anti-DIG antibodies (Roche Diagnostics) diluted 1:2000 using blocking buffer was added to each section and then slides were incubated overnight at 4 °C. The slides were then washed in 1X wash buffer (DIG Wash and Block Buffer Set, Roche Diagnostics) and incubated with the detection buffer (0.08 M Tris-HCl containing 0.17 M NaCl pH 9.5) for 10 min. The slides were then submerged in a 1:500 dilution of nitro blue tetrazolium chloride (NBT) /BCIP (5-bromo-4-chloro-3-indolyl phosphate, toluidine salt) (Roche Diagnostics) until staining was observed. Buffered glycerol was added to each section before cover-slipping. Slides were viewed using an Olympus BX50 microscope and photographed at 10x magnification using the SPOT software package.

2.2.9 mRNA array analysis

Changes in global gene expression were assessed by microarray analysis (Human Gene 1.0 ST Arrays, Affymetrix, Surrey Hills, VIC) using RNA obtained from OE-19 cells (Methods, 2.2.1) 24 hr post transfection with either miRNA mimics of miR-143, miR-145, miR-215 or the negative control scramble probe (Methods 2.2.5). The Human Gene 1.0 ST Arrays from Affymetrix assess 28,869 genes, using 26 probes mapping across each genes transcript. For each miRNA mimic and negative

control n=3 RNA samples were assessed via mRNA array. All mRNA arrays were performed by staff at the Adelaide microarray facility. 300ng of RNA was labelled using the Affymetrix WT Sense Target labelling assay (#701880, Affymetrix) and then hybridised to Human Gene 1.0 ST Arrays (Affymetrix). Analysis of the array data was performed using the Partek Genomics suite 6.4 (Partek, Missouri, USA). RMA background correction, GC content correction and mean probe summarization was performed in the Partek software package, followed by assessing differences in gene expression for statistical significance via ANOVA with Benjamini-Hochberg p-value adjustment¹⁴⁹.

2.2.10 Western Blotting and antibody details

Protein for western blotting was isolated from OE-19 cells 24 hr post transfection using cell lysis buffer. Cells were washed with PBS and cell lysis buffer was added (500 µl: confluent T75 flask of cells and 200 µl: confluent well in a 6 well plate). Cell lysate was placed on ice and sonicated at 15 Amplitude Microns for 20 seconds (direct probe, Misonix Sonicator 4000, CT, USA) before storage at -20°C.

Protein concentration was quantified using the EZQ® protein quantification kit (Invitrogen, Mulgrave, VIC) following the manufacturer's protocol. 40 µg of each protein sample was required for western blot. Protein samples were diluted to equal volumes, sample buffer was added and then samples were heated to 100°C for 5 min. Samples were then cooled and loaded into 12%, 10% or 7.5% polyacrylamide/bisacrylamide pre-cast gels (Bio-Rad) depending on the protein size. Precision plus dual colour protein standards (Bio-Rad) were also added to one lane of the pre-cast gel as a molecular marker. Gels were loaded into the electrophoresis apparatus (Bio-Rad), submerged in a gel tank filled with running buffer and run at 200 V for ~30 min until the sample buffer reached the lower end of the gel. After electrophoresis gels were placed onto a methanol activated PVDF membrane (membrane soaked in 100% methanol for 30 sec), and prepared for transfer as a blotting sandwich, surrounded by a filter paper layer and a sponge layer. The blotting sandwich was then loaded into a plastic transfer cassette (Bio-Rad). Transfer cassettes were loaded in the gel transfer apparatus (Bio-Rad) and run at 400 mA for 2 hr.

After transfer PVDF membranes were submerged in blocking buffer for 40 min then submerged in the required dilution of primary antibody (Table 2.5) overnight. The following morning membranes were removed from primary antibody, washed with PBS-T and submerged in the required dilution of horseradish peroxidase conjugated secondary antibody for 1 hr (Table 2.5). Membranes were then washed with PBS-T and bands were detected using the Amersham™ ECL Plus Western Blotting Detection Reagent (GE health care, Buckinghamshire, England) following the manufacturer's protocol.

Bands were visualised using a Las-4000 enhanced chemiluminescent exposure imager (Fujifilm Life Science, Holliston, MA) and photographed using MultiGauge version 3.0 image capture software (Fujifilm Life Science). Band intensity for the protein of interest and the loading control protein was quantified using Carestream Image Analysis software (Carestream, Rochester, NY). After Western blotting membranes were re-blotted for the loading control protein GAPDH using the same methods described above. Loading control band intensities were used to normalise protein of interest band intensities. Differences in experimental group and control band intensities were assessed for statistical significance using the Mann-Whitney test.

Table 2.5: Antibody details used in western blot analysis.

miRNA of interest	Protein	Name	Protein Size (kDa)	Company	Product Number	Type	Raised in	1' Dilution
miR-143	KRAS	Harvey rat sarcoma viral oncogene homologue	21	Santa Cruz	F234	Monoclonal	Mouse	PBS 1:1,000
miR-215	ZEB2	Smad interacting protein 1	197, 150, 110, 97	Santa Cruz	SC-48789	Monoclonal	Mouse	PBS 1:200
miR-145	YES	Protein tyrosine kinase 1	58	Cell Signalling	2734	Polyclonal	Rabbit	PBS 1:500
miR-145	RTKN	Rhotekin	62	Abnova	H00006242	Monoclonal	Mouse	PBS 1:1,000
miR-215	DTL	Denticleless homolog	95, 77, 26	Bethyl	A300-948A	Polyclonal	Rabbit	PBS 1:1,500
miR-143	HDAC7	Histone deacetylase 7	102	Sigma	H6663	Monoclonal	Mouse	PBS 1:8,000
House keeper	GAPDH	Glyceraldehyde 3 phosphate dehydrogenase	34	Abcam	ab9484	Monoclonal	Mouse	PBS 1:1,000

2.2.11 Ingenuity Pathway Analysis

A core Ingenuity Pathways Analysis was performed on predicted targets of miR-141 and miR-200c. Ingenuity Pathways parameters were set to assess a knowledge base derived from direct and indirect associations between genes in human experiments and also epithelial cell lines. All interactions identified in the Ingenuity Pathways Core Analysis are based on published experimental data (not predicted interactions). The Ingenuity Pathways Analysis first assessed the input predicted gene targets of miR-141 and miR-200c and built a “biological network” based on validated interactions between the input predicted target genes and any other gene where an interaction had been published. The analysis then grouped the genes in the network according to their validated biological function (eg. proliferation or apoptosis etc.), and then tested the gene interactions and grouping for statistical significance using a Fisher’s exact test. The analysis produced a “biological network” of genes (top five biological networks are listed), with a common biological function, that have been validated in experimental studies to interact with each other, and have been tested for significance to ensure their grouping did not occur by chance. Secondly, the Ingenuity Pathways Analysis grouped the input predicted gene targets of miR-141 and miR-200c according to their validated biological functions and listed the “top molecular and cellular functions” (top five molecular and cellular functions are listed), and again tested each group for statistical significance using a Fisher’s exact test.

Chapter 3

Investigation of miRNA expression in oesophageal squamous epithelia, Barrett's oesophagus and oesophageal adenocarcinoma

3.1 *Introduction*

The mechanisms that drive the development of Barrett's oesophagus and oesophageal adenocarcinoma not fully understood. Although numerous molecular alterations have been identified, there are still a number of interesting, unanswered questions regarding the role of miRNAs in Barrett's oesophagus and oesophageal adenocarcinoma.

Prior to my PhD candidature no study had quantitatively assessed miRNA expression in Barrett's oesophagus and oesophageal adenocarcinoma. Our research group hypothesised that miRNA expression would be altered in Barrett's oesophagus and oesophageal adenocarcinoma and these changes in miRNA expression might contribute to the development of these pathologies. Therefore, as a first step in investigating the role of miRNAs in the development of Barrett's oesophagus and oesophageal adenocarcinoma our laboratory aimed to assess miRNA expression. In our study¹¹⁰ miRNA arrays were used to assess global miRNA expression comparing squamous oesophageal epithelia with both Barrett's oesophagus and oesophageal adenocarcinoma. These arrays identified numerous miRNAs that were potentially differentially expressed in Barrett's oesophagus or oesophageal adenocarcinoma¹¹⁰. An analysis of this microarray data was performed by Dr Anna Tsykin (Adelaide Microarray Centre) prior to commencing my PhD candidature, and this provided the preliminary data for my PhD studies. Prior to the publication of our microarray study¹¹⁰, a study by Feber¹⁵⁰ was published which identified altered miRNA expression in oesophageal adenocarcinoma using miRNA arrays. The study by Feber¹⁵⁰ highlighted that miRNAs were differentially expressed in oesophageal adenocarcinoma. However, miRNA changes were not quantitatively assessed and the

Barrett's oesophagus samples assessed were all from patients with oesophageal adenocarcinoma.

The first step of my PhD project involved using quantitative RT-PCR to validate the results of the miRNA microarray analysis. From the microarray analysis, the most differentially expressed miRNAs, including miR-21, miR-194, miR-203, miR-205 and miR-215 were selected for quantitative validation. Two additional miRNAs, miR-143 and miR-145, were also selected for validation from the list of potentially differentially expressed genes because of previous literature indicating their role in maintenance of columnar gastrointestinal epithelium.¹⁰⁹.

3.2 Tissue samples - collection, histopathology and RNA extraction

Biopsies were collected from patients with either Barrett's oesophagus or oesophageal adenocarcinoma who were undergoing endoscopy assessment at our institution. "Barrett's oesophagus" was defined as columnar lined oesophageal mucosa with intestinal metaplasia. Biopsies were collected according to usual clinical practice and placed in formalin for standard histopathological evaluation by Dr David Astill (Consultant, Division of Surgical Pathology, IMVS). Additional biopsies were collected for research purposes from the tissue of interest (Barrett's oesophagus or cancer), as well as proximally from the squamous oesophageal epithelium (5 cm proximal to the upper margin of the metaplastic epithelium or carcinoma) and distally from the mucosa of the proximal stomach. For the Barrett's oesophagus, specimens were all collected from the oesophagus, 1cm above the gastroesophageal junction, and intestinal metaplasia was confirmed to be present by histopathology in all instances. Gastric tissue was collected as reference columnar epithelia. All biopsies were stored in RNAlater[®] (Ambion, Austin, TX, USA).

In addition, tissue samples (squamous epithelium, intestinal metaplasia, oesophageal adenocarcinoma, and proximal gastric epithelium) were collected from 8 patients who underwent surgical resection of the oesophagus for invasive oesophageal adenocarcinoma at Flinders Medical Centre (South Australia, 2 patients) or Erasmus Medical Centre, Rotterdam (Netherlands, 6 patients). In each case, these patients had

not received neoadjuvant chemo-radiotherapy. The surgical resection specimens were transported on ice to a pathology laboratory, where tissues were sampled and stored in liquid nitrogen for further processing, according to recent published guidelines¹⁵¹. The protocol for this study was approved by the Flinders Clinical Research Ethics Committee.

A small piece of the tissue specimens collected for research, either at endoscopy or surgery, was removed, fixed in formalin and embedded in paraffin for haematoxylin-eosin and Alcian blue periodic Schiff diastase (ABPASD) staining. The remaining tissue was used for gene expression analysis. Histopathology from the formalin fixed portion of these tissues (squamous epithelium, intestinal metaplasia, oesophageal adenocarcinoma, and gastric epithelium groups) confirmed that the samples consisted only of their characteristic epithelium, and had no other detectable epithelia/admixture. Tissue cut-up, RNA extraction and RNA quality control was performed by Dr Damian Hussey and Dr Bas Wijnhoven.

3.3 Results: TaqMan[®] quantitative RT-PCR identifies altered miRNA expression in Barrett's oesophagus and oesophageal adenocarcinoma

miR-21, miR-143, miR-145, miR-194, miR-203, miR-205 and miR-215 were assessed by TaqMan[®] RT-PCR (Methods, chapter 2, section 2.2.2) to quantitatively validate the microarray results across the different tissue samples derived from 32 individuals (normal oesophagus n=29; intestinal metaplasia n=20; proximal gastric epithelium n=24; oesophageal adenocarcinoma n=20).

Expression of miR-21 was significantly higher in all types of columnar epithelia (intestinal metaplasia, gastric epithelium, oesophageal adenocarcinoma) compared to squamous epithelium (Table 3.1 & Figure 3.1). The level of miR-21 expression was not significantly higher in oesophageal adenocarcinoma relative to intestinal metaplasia. miR-143 levels were also significantly higher in intestinal metaplasia and gastric epithelium compared to squamous epithelium (Table 3.1 & Figure 3.2). miR-145 was significantly higher in intestinal metaplasia compared to squamous

epithelium (Table 3.1 & Figure 3.3). miR-145 was also higher in gastric epithelium compared to squamous epithelium, but this did not reach significance with post-hoc testing ($p=0.02$). In oesophageal adenocarcinoma, however, miR-143 and miR-145 expression was significantly less than in Barrett's oesophagus epithelium (Table 3.1, Figure 3.2 & Figure 3.3).

miR-203 and miR-205 expression was significantly higher in squamous epithelium compared to all types of columnar tissues (Table 3.1, Figure 3.4 & 3.5). There were no significant differences in miR-203 expression between the columnar tissue types, whereas miR-205 levels were significantly higher in intestinal metaplasia and oesophageal adenocarcinoma compared to proximal gastric epithelium (Table 3.1 & Figure 3.5).

miR-215 expression was tissue-specific with highest expression in intestinal metaplasia. The level of expression of miR-215 was significantly lower in oesophageal adenocarcinoma, gastric epithelium and squamous epithelium compared to intestinal metaplasia (Table 3.1 & Figure 3.6). Gastric epithelium and oesophageal adenocarcinoma had significantly higher levels of miR-215 than squamous epithelium (Table 3.1 & Figure 3.6). The levels of miR-194 expression were also significantly higher in columnar tissues than squamous tissue (Table 3.1 & Figure 3.7). There were no significant differences in miR-194 expression between the different columnar tissue types (Table 3.1 & Figure 3.7).

Table 3.1: Relative median miRNA expression values validated by TaqMan[®] polymerase chain reaction in squamous mucosa, Barrett’s oesophagus, oesophageal adenocarcinoma and proximal gastric mucosa. A large range in miRNA expression is observed for miR-143 and miR-145 in squamous mucosa. This is discussed in Appendix 1.

	Squamous mucosa	Barrett’s oesophagus	Oesophageal adenocarcinoma	Proximal gastric mucosa	p-value
miR-21	1.145 (0.829, 1.731)	3.161 (2.698, 4.528)	4.810 (3.603, 9.241)	5.104 (4.725, 7.211)	<0.0001 * + ∞ ¥
miR-143	0.0009 (0.0033, 0.0242)	0.0102 (0.0060, 0.0306)	0.0033 (0.0039, 0.0094)	0.0119 (0.0098, 0.0156)	0.0005 * ∞ ◇ #
miR-145	0.0131 (0.0163, 0.122)	0.0450 (0.0333, 0.115)	0.0249 (0.0212, 0.058)	0.0508 (0.0413, 0.0664)	0.0059 * ◇
miR-194	0.00051 (0.00048, 0.0011)	0.0633 (0.0476, 0.107)	0.0446 (0.0325, 0.0945)	0.0705 (0.0100, 0.0660)	<0.0001 * + ∞
miR-215	0.00068 (0.0007, 0.00191)	0.0129 (0.0094, 0.0290)	0.0041 (0.0027, 0.0195)	0.0057 (0.0055, 0.0086)	<0.0001 * + ∞ ¥ ◇
miR-203	0.4730 (0.411, 0.669)	0.0278 (0.0256, 0.106)	0.0204 (0.0153, 0.0475)	0.0273 (0.0253, 0.0360)	<0.0001 * + ∞
miR-205	2.455 (1.975, 3.354)	0.0140 (0.0485, 0.388)	0.0029 (-0.0106, 0.334)	0.00021 (-0.00025, 0.0019)	<0.0001 * + ∞ ¥ #

All figures are median (95% confidence intervals).

The p-value listed is derived from Kruskal-Wallis testing over the 4 tissue groups

Post-hoc testing for pair-wise comparisons is by Holm-Bonferroni method

* Post-test – P<0.05 for squamous mucosa vs Barrett’s metaplasia

+ Post-test – P<0.05 for squamous mucosa vs oesophageal adenocarcinoma

∞ Post-test – P<0.05 for squamous mucosa vs proximal gastric mucosa

¥ Post-test – P<0.05 for Barrett’s metaplasia vs proximal gastric mucosa

◇ Post-test – P<0.05 for Barrett’s metaplasia vs oesophageal adenocarcinoma

Post-test – P<0.05 for oesophageal adenocarcinoma vs proximal gastric mucosa

Figure 3.1: TaqMan[®] analyses of relative miR-21 levels in normal squamous, Barrett's oesophagus, oesophageal adenocarcinoma and gastric tissue. The relative, normalised miR-21 expression level in each tissue sample is presented as an individual symbol.

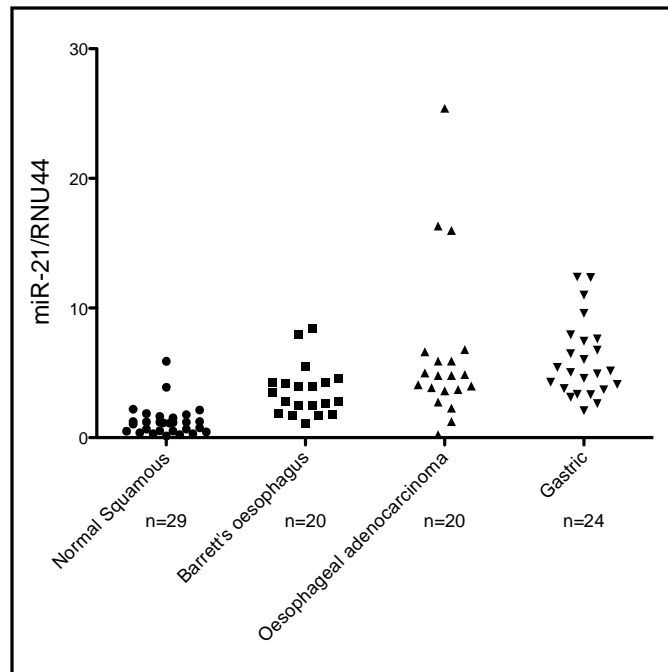


Figure 3.2: TaqMan[®] analyses of relative miR-143 levels in normal squamous, Barrett's oesophagus, oesophageal adenocarcinoma and gastric tissue. The relative, normalised miR-143 expression level in each tissue sample is presented as an individual symbol.

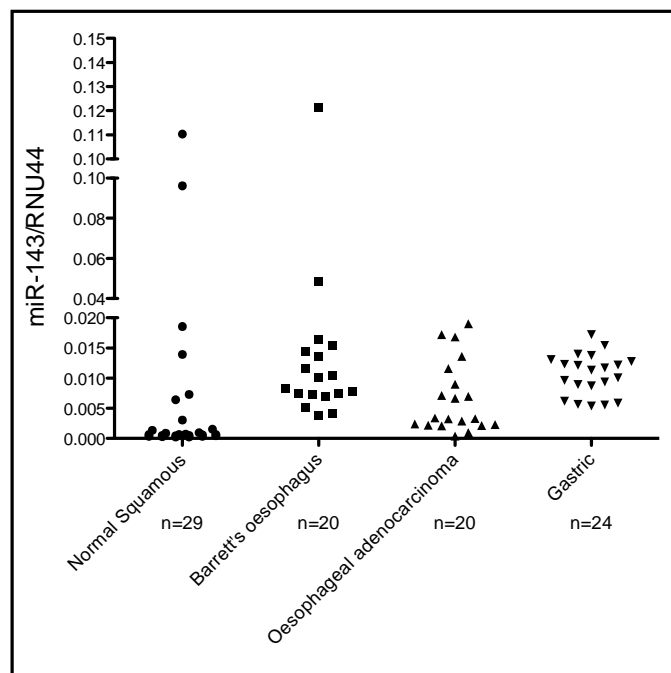


Figure 3.3: TaqMan[®] analyses of relative miR-145 levels in normal squamous, Barrett's oesophagus, oesophageal adenocarcinoma and gastric tissue. The relative, normalised miR-145 expression level in each tissue sample is presented as an individual symbol.

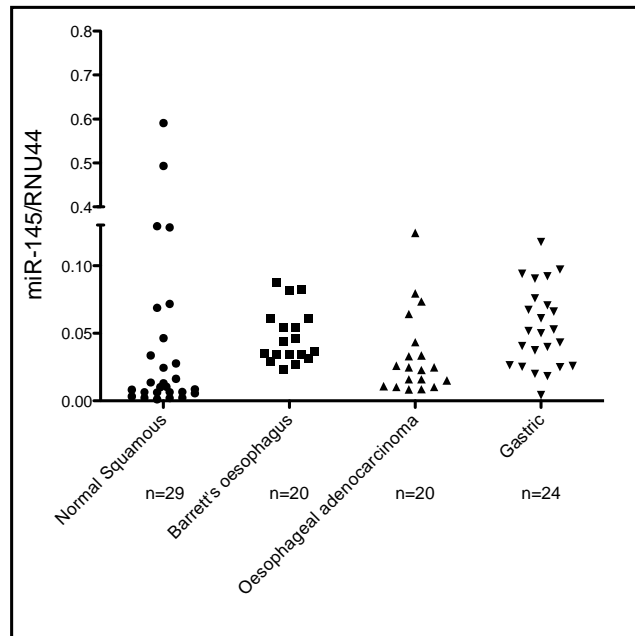


Figure 3.4: TaqMan[®] analyses of relative miR-203 levels in normal squamous, Barrett's oesophagus, oesophageal adenocarcinoma and gastric tissue. The relative, normalised miR-203 expression level in each tissue sample is presented as an individual symbol.

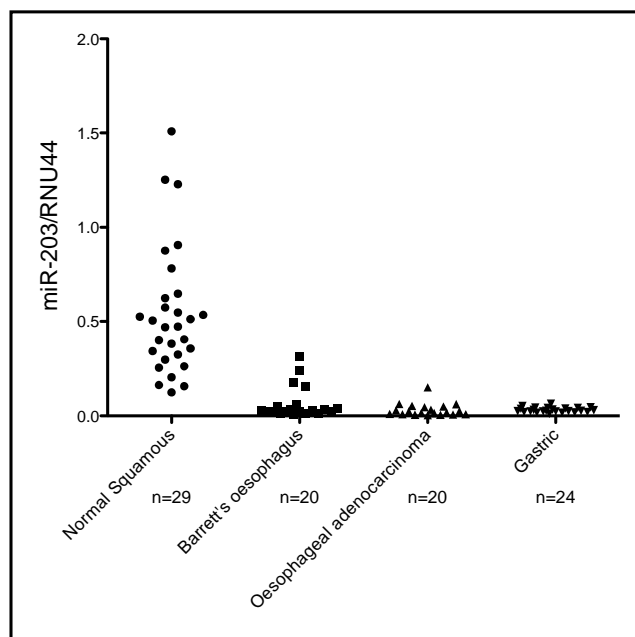


Figure 3.5: TaqMan[®] analyses of relative miR-205 levels in normal squamous, Barrett's oesophagus, oesophageal adenocarcinoma and gastric tissue. The relative, normalised miR-205 expression level in each tissue sample is presented as an individual symbol.

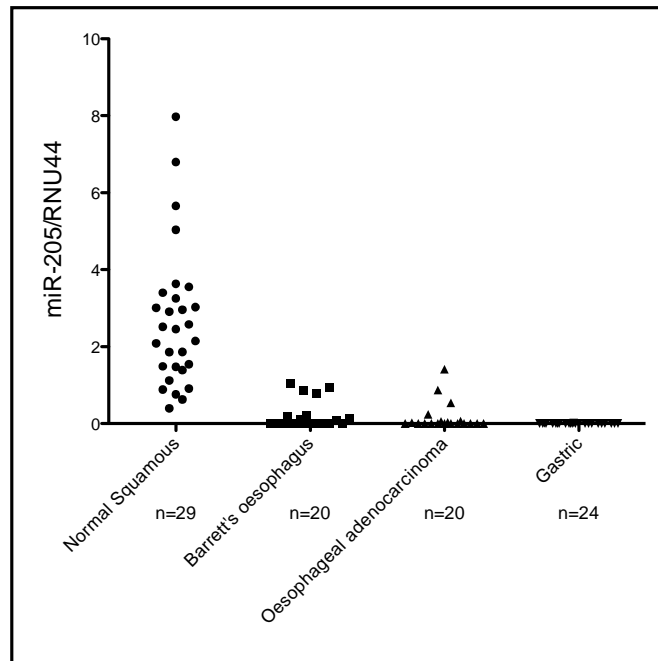


Figure 3.6: TaqMan[®] analyses of relative miR-215 levels in normal squamous, Barrett's oesophagus, oesophageal adenocarcinoma and gastric tissue. The relative, normalised miR-215 expression level in each tissue sample is presented as an individual symbol.

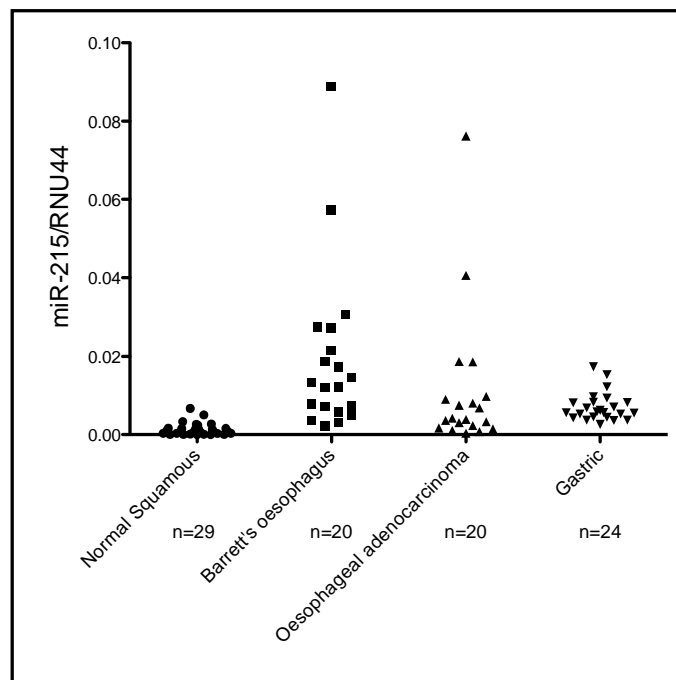
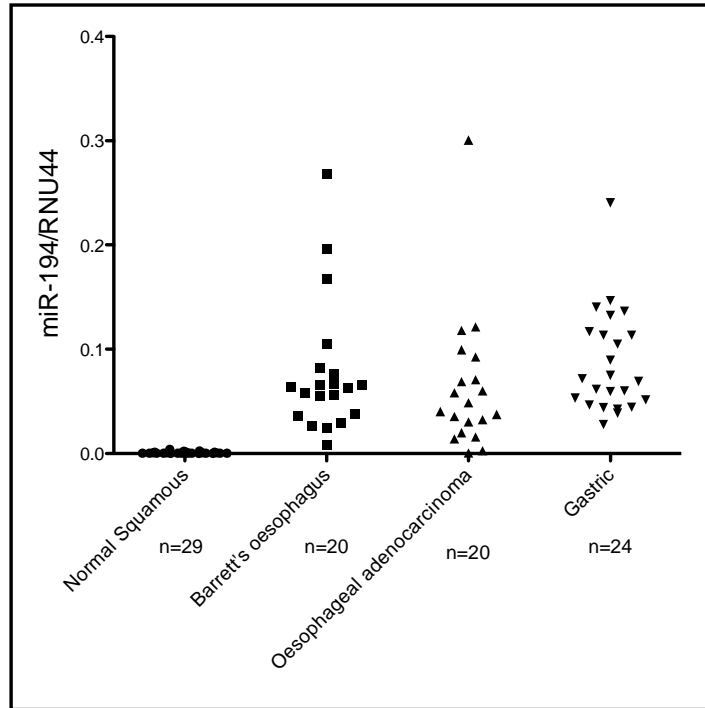


Figure 3.7: TaqMan[®] analyses of relative miR-194 levels in normal squamous, Barrett's oesophagus, oesophageal adenocarcinoma and gastric tissue. The relative, normalised miR-194 expression level in each tissue sample is presented as an individual symbol.



3.4 Discussion: miRNA expression is altered in Barrett's oesophagus and oesophageal adenocarcinoma

Quantitative RT-PCR identified differences in the expression of miR-21, miR-143, miR-145, miR-194, miR-203, miR-205 and miR-215 in Barrett's oesophagus and oesophageal adenocarcinoma compared with squamous oesophageal epithelia. miR-21, miR-143, miR-145, miR-194, miR-203, miR-205 and miR-215 have been implicated in regulating numerous cellular processes by directly targeting specific mRNA transcripts (Table 3.2). The validated targets of these miRNAs, shown in Table 3.2, are involved in regulating cellular processes such as proliferation, apoptosis, cell cycle control, migration and invasion as well as epithelial and stem cell differentiation. Many of these cellular processes are aberrantly regulated in Barrett's oesophagus or oesophageal adenocarcinoma, and dysfunctional regulation of these known miRNA targets (Table 3.2), brought about via alterations in miRNA expression, may contribute to this. No studies have investigated the roles of miR-21, miR-143, miR-145, miR-194, miR-203, miR-205 and miR-215 in Barrett's oesophagus and oesophageal adenocarcinoma. However, these miRNAs have been investigated in other tissues.

Table 3.2: Current knowledge (as of 27/9/11) of direct mRNA targeting by miR-21, miR-143, miR-145, miR-194, miR-203, miR-205 and miR-215. Validated miRNA targets listed in this table were identified via literature review, searching all peer reviewed publications on miR-21, miR-143, miR-145, miR-194, miR-203, miR-205 and miR-215 for validated targets.

microRNA	Validated targets
miR-143	ERK5 ¹⁵² , KRAS ¹⁵³ , ELK1 ¹⁵⁴ , DNMT3A ¹⁵⁵ , FNDC3b ¹⁵⁶ , BCL2 ¹⁵⁷
miR-145	IRS-1 ¹⁵⁸ , c-myc ¹⁵⁹ , RTKN ¹⁶⁰ , FLJ21308 ²⁷ , KLF4 ^{154, 161} , CAMK2- δ ¹⁵⁴ , OCT4 ¹⁶¹ , SOX2 ¹⁶¹ , YES ¹⁶² , STAT1 ¹⁶² , ER-alpha ¹⁶³ , DFF45 ¹⁶⁴ , MUC1 ¹⁶⁵ , FSCN1 ¹⁶⁶ , DFF45 ¹⁵⁹ , PPP3A ¹⁶⁷ , CBF ¹⁶⁷ , CLINT1 ¹⁶⁷
miR-194	Various cell cycle transcripts ¹⁶⁸
miR-215	Various cell cycle transcripts ¹⁶⁸ , DTL ¹⁶⁹ , ZEB2 ¹⁷⁰ , DHFR ¹⁷¹ , TYMS ¹⁷¹
miR-203	p63 ¹⁷² , ABL1 ¹⁷³
miR-205	ZEB1 ¹¹⁶ , SIP1 ¹¹⁶ , SHIP2 ¹⁷⁴ , ErbB3/HER3 ¹⁷⁵ , VEGF-A ¹⁷⁵ , INPPL1 ¹⁷⁴ , MED1 ¹⁷⁶
miR-21	PTEN ¹⁷⁷ , TPM1 ¹⁷⁸ , E2F1, TGFBR2, CDK6 ¹⁷⁹ , TIMP3, PDCD4 ¹⁷⁹ , SERPINB5 ¹⁸⁰ , NFIB ¹⁸¹ , BTG2 ¹⁷⁹ , BMPR2 ¹⁷⁹ , IL6R ¹⁷⁹ , IL6 ¹⁸² , SOCS5 ¹⁷⁹ , CDC25A ¹⁸³ , RECK ¹⁸⁴ , MTAP ¹⁸⁵ , SOX5 ¹⁸⁵ , JAG1 ¹⁸⁶ , MARCK5 ¹⁸⁷ , LRRFIP1 ¹⁸⁸

3.4.1 miR-203 and miR-205 are enriched in oesophageal, squamous epithelia compared with columnar epithelia

miR-203 and miR-205 were highly expressed in squamous epithelium, compared to columnar epithelia. Previous investigations have also reported high levels of miR-203 expression in other squamous epithelia, such as skin and the upper respiratory tract^{189, 190}. miR-203 has been shown to control stem-cell renewal in stratified epithelia through regulation of *p63* and, possibly, *Zfp281*¹⁹¹. It is possible that similar control of differentiation is lost in columnar-lined oesophageal mucosa.

miR-205 has been reported to be up regulated in head and neck squamous cancer cell lines, bladder cancer, and ovarian cancer^{190, 192, 193}, and down-regulated in breast¹⁹⁴ and prostate cancer¹⁹⁵. Compared to gastric epithelium, miR-205 levels were significantly higher in Barrett's oesophagus and oesophageal adenocarcinoma. Whether this implies a cancer-associated role for miR-205 in columnar epithelia, even at relatively low levels compared to squamous epithelium, however, remains to be shown.

3.4.2 miR-194 and intestinal metaplasia

miR-194 is up regulated in Barrett's oesophagus compared with squamous oesophageal epithelia¹⁹⁶. miR-194 expression is regulated by *HNF-1 α* , a transcription factor induced in Barrett's oesophagus and oesophageal adenocarcinoma¹⁹⁷. A study by Hino et al.¹⁹⁷ also showed that miR-194 expression is induced during intestinal epithelial cell differentiation. Taken together these results could suggest that elevated miR-194 expression may promote intestinal differentiation in Barrett's oesophagus.

3.4.3 Elevated miR-143 and miR-145 and Barrett's oesophagus development

miR-143 and miR-145 are highly expressed in columnar tissues from the upper gastrointestinal tract. Also, miR-143 and miR-145 are expressed in many tissues, but

show high expression in human colonic tissues¹⁰⁹. Evolutionary conservation of strong miR-143 and miR-145 expression in the zebra fish gastrointestinal tract suggests that these miRNAs play important roles in controlling intestinal identity and function¹⁹⁸. In support of this hypothesis miR-145 has been implicated in directing intestinal maturation in zebra fish¹⁹⁹. Furthermore, during the course of my PhD studies I demonstrated that elevated miR-143 and miR-145 expression is observed in gastroesophageal reflux disease, the underlying pathology associated with the development of Barrett's oesophagus (See chapter 4).

3.4.4 miR-21 expression is up regulated in Barrett's oesophagus and oesophageal adenocarcinoma

miR-21 expression is up regulated in gastric tissue, Barrett's oesophagus and oesophageal adenocarcinoma, compared with squamous oesophageal epithelia²⁰⁰. miR-21 has been demonstrated to act as an onco-miR in a number of solid tumours²⁰¹ and appears to be a key requirement for maintaining B-cell lymphoma²⁰². In addition, elevated miR-21 has been implicated in many cellular processes required for neoplastic development and progression. Elevations in miR-21 have been shown to promote survival in myeloma cells²⁰³, confer apoptotic resistance in prostate cancer cells¹⁸⁷, increase cell proliferation, migration and invasion in hepatocellular carcinoma cells²⁰⁴, and increase invasion and metastasis in colorectal cancer cells²⁰⁵.

Although miR-21 is classified as an oncogene its up-regulation in non-malignant Barrett's oesophagus may have an alternate role. Increased miR-21 expression in breast cancer cells has been shown to play an anti-apoptotic role by repressing programmed cell death (PDCD) 4 translation¹⁷⁹, and miR-21-induced suppression of *PDCD4* protects cardiac myocytes from apoptosis induced by oxidative stress²⁰⁶. Reactive oxygen species are known to be produced in Barrett's oesophagus and, when considered with the higher miR-21 expression in Barrett's epithelium compared with squamous mucosa, it is possible that miR-21 also plays a protective role in Barrett's oesophagus epithelium.

3.4.5 miR-143, miR-145 and miR-215 are down-regulated in oesophageal adenocarcinoma and may act as tumour suppressor miRNAs

miR-143, miR-145 and 215 are down-regulated in oesophageal adenocarcinoma¹⁹⁶. Similar alterations are observed in other expression profiling studies, where miR-143, 145 and 215 are all down-regulated in colonic adenocarcinoma^{109, 207}, as well as numerous other solid tumours including lung, breast and prostate cancer^{208, 209}.

Some specific roles for miR-143, 145, and 215 in carcinogenesis have been elucidated. miR-143 has been shown to target the *KRAS* oncogene, suppressing colorectal cancer cell growth via inhibition of *KRAS* translation²¹⁰. Therefore, loss of miR-143 expression in oesophageal adenocarcinoma could result in a loss of *KRAS* regulation contributing to neoplastic development. Also, miR-143 has been shown to directly target *DNMT3A* in colorectal adenocarcinoma¹⁵⁵. *DNMT3A* is implicated in directing specific gene methylation profiles and therefore aberrant regulation of *DNMT3A* in cancer could lead to methylation directed suppression of tumour suppressor genes¹⁵⁵.

In Jurkat T cells miR-143 up-regulation has been linked with the regulation of *FAS* mediated apoptosis²¹¹. miR-145 has also been implicated in regulating apoptosis via a negative feedback loop involving *TP53*, through direct targeting of *STAT1* and *DFF45* in colon cancer cell lines and also via direct targeting of rhotekin (*RTKN*) in breast cancer cell lines^{160, 162-164}. Also, *p53* has been shown to induce miR-145 to repress the apoptotic regulator *c-myc*¹⁵⁹. Therefore, the loss of both miR-143 and miR-145 in the progression of Barrett's oesophagus to oesophageal adenocarcinoma may alter the cells ability to direct appropriate apoptotic responses.

Recent evidence implicates miR-145 with regulating invasion through direct targeting of mucin 1 (*MUC1*), v-yes-1 Yamaguchi sarcoma viral oncogene homolog 1 (*YES*), fascin homolog 1, actin-bundling protein (*Strongylocentrotus purpuratus*) (*FSCN1*) and F11 receptor (*JAMA*)^{162, 165, 166, 212}. Therefore, down-regulation of miR-145 expression may contribute to tumour invasion in oesophageal adenocarcinoma.

miR-215 acts in cooperation with miR-192 to regulate cell cycle events through their

ability to induce cell cycle arrest^{168, 207}. Loss of miR-215 expression causes a reduction in the ability of cells to regulate proliferation, a key neoplastic attribute. It is interesting that the loss of miR-215 expression in oesophageal adenocarcinoma compared to Barrett's oesophagus was not predicted by our microarray results. This highlights the known limitations of micro-array analysis, and the need for separate validation by quantitative PCR based methods²¹³.

It is therefore possible that miR-143, 145 and 215 may act as tumour suppressors in Barrett's oesophagus, with loss of expression contributing to the development of oesophageal adenocarcinoma. Investigation of some of the tumour suppressor properties of miR-143, miR-145 and miR-215 will be presented in chapter 5.

3.4.6 Limitations

A limitation of this study is that the squamous tissue used for analysis was taken from patients with Barrett's oesophagus or oesophageal adenocarcinoma, rather than disease free control subjects. However, the use of control tissue from subjects with oesophageal pathology is still a valid approach, and it is informative of changes in miRNA expression across the range of tissues that represent the transition to oesophageal adenocarcinoma. Another possible criticism of this study was the possibility that outcomes could be influenced by heterogeneity of tissue types within individual segment of Barrett's oesophagus. However, we did address this by splitting individual oesophageal biopsies to ensure matched histopathology was available for all samples used for molecular biology analysis, and this process minimized the possible impact of this problem.

3.4.7 Comparing expression data with other studies

Our finding of lower miR-203 and miR-205, and higher miR-21 in tumour relative to squamous epithelium is in agreement with the results of Feber *et al.*¹⁵⁰. Interestingly, the differences we observed in miR-215, miR-143 and miR-145 between oesophageal squamous epithelium, Barrett's epithelium and oesophageal adenocarcinoma were not reported by this group. The fact that our study includes

Barrett's oesophagus epithelium from patients who did not have malignancy, whereas the study by Feber *et al* used Barrett's oesophagus epithelium only from patients undergoing oesophagectomy for cancer might account for this difference.

After the study presented in this chapter began, other groups have reported differential miRNA expression in either Barrett's oesophagus, dysplasia or oesophageal adenocarcinoma. A study by Fassan *et al.*²¹⁴ reported among other miRNA changes a similar increase in miR-215 and decrease in miR-203 and miR-205 to our reports in Barrett's oesophagus. Mathe *et al.*²¹⁵ compared non-cancerous tissue with oesophageal adenocarcinoma, presenting a similar increase in miR-21 and decrease in miR-203 to our reports in these tissues. Maru *et al.*⁶⁵ and Yang *et al.*²¹⁶ reported miRNA expression changes in Barrett's oesophagus, high-grade dysplasia and oesophageal adenocarcinoma. Maru *et al.*⁶⁵ attempted to use miR-196a levels as a potential marker of Barrett's oesophagus, high-grade dysplasia and oesophageal adenocarcinoma tissues. In assessing these tissue types Maru *et al.*⁶⁵ was able to show step-wise increases in miR-196a levels from Barrett's oesophagus to high-grade dysplasia to oesophageal adenocarcinoma. Yang *et al.*²¹⁶ assessed non-cancerous and cancerous tissues from patients with high-grade dysplasia or oesophageal adenocarcinoma, showing that miRNA expression levels could distinguish non-cancerous from cancerous tissue in these patients.

3.4.8 Summary

Chapter 3 compares miRNA expression in squamous, Barrett's oesophagus and oesophageal adenocarcinoma tissues. The results show that several miRNAs are differentially expressed in these tissues. Given the increasing evidence implicating miRNAs in the regulation of cellular processes discussed above, identifying the consequences of altered miRNA expression may provide a better understanding of the pathogenesis of Barrett's oesophagus and oesophageal adenocarcinoma.

Chapter 4

Impact of gastroesophageal reflux on microRNA expression, location and function

4.1 Introduction

Gastroesophageal reflux disease affects up to 50% of Western populations⁷. As described in chapter 1, section 1.2.1, gastric physiology offers protection from exposure to acid and bile, although the oesophageal lumen is largely unprotected, lacking an adherent mucous barrier⁹. Patients with chronic reflux can present with endoscopically visible mucosal damage, and this manifests as mucosal ulceration (ulcerative oesophagitis)⁷. At the cellular level, ulcerative oesophagitis is associated with increased cell proliferation²¹⁷ and apoptosis²⁰. Increased inflammatory cell infiltrate²¹⁸ and hyper-proliferation of basal cells are typical histopathological changes associated with gastroesophageal reflux^{217, 219}. Additionally, our laboratory has shown previously that increases in interleukin 6 (*IL6*) and cytokeratin (CK) 14 correlate with increased severity of reflux⁷. These are molecular markers of inflammation and basal cell hyperplasia, respectively.

Barrett's oesophagus is associated with a 40 fold increase in oesophageal adenocarcinoma risk²²⁰. Studying gene expression in gastroesophageal reflux might identify changes that promote progression to Barrett's oesophagus and cancer. Previous reports have shown increased expression of genes that determine columnar or intestinal cell phenotype, such as *BMP4* and *CDX2*, in squamous oesophageal epithelium from individuals with ulcerative oesophagitis^{221, 222}. The implications of elevated *BMP4* and *CDX2* are highlighted in chapter 1, section 1.2.4.

Chapter three described miRNAs that are differentially expressed in Barrett's oesophagus compared to oesophageal squamous epithelium¹¹⁰. miR-203 and miR-205 are expressed at higher levels in squamous epithelium, and miR-143, miR-145, miR-194 and miR-215 are expressed at higher levels in Barrett's oesophagus.

Currently, it is not known whether miRNA expression is altered in gastroesophageal reflux in the absence of Barrett's oesophagus. Identifying altered miRNA expression might provide insight into the development of Barrett's oesophagus. In this study we hypothesised that miR-203, 205, 21, 143, 145, 194 and 215 expression might be altered in oesophageal squamous mucosa in response to chronic gastroesophageal reflux.

The aims of the study were to:

- 1) Determine the expression of miRNAs known to be differentially expressed between normal squamous and Barrett's oesophagus mucosa (miR-203, 205, 21, 143, 145, 194 and 215) in oesophageal squamous epithelium from individuals with gastroesophageal reflux disease.
- 2) Assess the location of miRNA activity within the oesophageal epithelium.
- 3) Assess the role of these miRNAs in regulating proliferation and apoptosis, processes that contribute to tissue restoration.

Quantitative RT-PCR was used to compare miRNA expression levels in oesophageal mucosa from individuals with or without gastroesophageal reflux, and individuals with Barrett's oesophagus, and correlations between miRNA expression and known mRNA differentiation markers were determined. mRNA expression levels of *IL6*, *CK14*, *BMP4*, *CK8*, *CK20*, *CDX2*, *HNF1 α* and *GATA4* were assessed by real-time PCR. miRNA regulation of proliferation and apoptosis was evaluated following transfection of a cell line derived from oesophageal squamous tissue (Het-1A) with miR-143, miR-145 or miR-205 mimics. miRNA expression in the oesophageal mucosa in individuals with gastroesophageal reflux was localised using in-situ hybridisation.

4.2 Tissue samples - collection, histopathology and RNA extraction

Oesophageal mucosal fresh tissue biopsies were collected from individuals undergoing upper gastrointestinal endoscopy. Full details of the RNA extraction procedure are described in chapter 2, section 2.2.1. In the current study we used mucosal biopsies collected from the oesophageal squamous mucosa 5 cm above the gastroesophageal junction from individuals who, based on clinical and endoscopic criteria, were determined to not have gastroesophageal reflux disease (Controls, n=13), and from individuals with typical symptoms of gastroesophageal reflux with ulcerative oesophagitis at endoscopy assessment (n=10). Control patients recruited for this study were individuals who at endoscopy had a visibly normal oesophageal mucosa, no other endoscopic indicators of gastroesophageal reflux disease, and no symptoms (or previous history) of gastroesophageal reflux disease⁷. Patients with ulcerative oesophagitis were included in the study if they had typical symptoms of gastroesophageal reflux disease (heartburn and regurgitation), and endoscopically visible mucosal ulceration (ulcerative oesophagitis — Savary Miller grade I to IV)⁷. In addition, the same RNA samples from Barrett's oesophagus mucosal biopsies (n=20) described in chapter 3, section 3.2 were used in this study.

Mucosal biopsy histopathology, storage, RNA extraction and quality control are described in chapter 3, section 3.2. Oesophageal mucosal tissue biopsies, used for in-situ hybridization, were collected adjacent to those used to assess miRNA and mRNA expression by the same collection protocol described in chapter 3, section 3.2. These biopsies were fixed immediately with 10% formalin and subsequently embedded in paraffin.

4.3 Results: miRNA and mRNA quantitation by RT-PCR

The expression of miRNAs miR-21, miR-143, miR-145, miR-194, miR-203, miR-205 and miR-215 and mRNA expression of markers *IL6*, *CK14*, *BMP4*, *CK8*, *CK20*, *CDX2*, *HNF-1 α* and *GATA4* in the different types of oesophageal squamous mucosa was determined by RT-PCR (chapter 2, sections 2.2.2 (miRNA) and 2.2.3 (mRNA)). Due to limited RNA, miR-145 expression was only assessed in ten of the 13 controls. The expression levels of miRNAs were correlated with the mRNA expression level

of squamous epithelial markers of inflammation and basal cell hyperplasia as well as markers of gastric and intestinal differentiation (chapter 2, section 2.2.7). All miRNA expression was normalised to RNU44 levels and mRNA expression was normalised to β -actin levels.

Table 4.1 summarizes the expression of the evaluated miRNA and mRNA markers. The expression of miR-21, miR-143, miR-145, miR-194 and miR-215 was significantly higher and miR-203 and miR-205 expression was significantly lower in Barrett's oesophagus mucosa compared to both types of squamous mucosa. The expression of miR-143 (Figure 4.1), miR-145 (Figure 4.2), and miR-205 (Figure 4.3) were also significantly higher in oesophageal mucosa from subjects with ulcerative oesophagitis compared to control tissues. There were no significant differences seen between the 2 squamous mucosae (with vs without reflux) for the expression of miR-21, miR-194, miR-203 and miR-215.

Table 4.2 summarizes correlations between miRNA and mRNA expression levels in oesophageal mucosal biopsies from individuals with ulcerative oesophagitis . There were significant positive correlations between the expression of miR-143 and *CK8*, miR-143 and *BMP4*, miR-194 and *CK8*, miR-194 and *CK20*, miR-194 and *GATA-4*, miR-194 and *HNF-1 α* , miR-194 and *CDX2*, miR-215 and *CK8*, miR-215 and *IL6*. miR-205 was correlated negatively with *CK14*.

Table 4.1: miRNA expression in oesophageal mucosa from control subjects, individuals with ulcerative gastroesophageal reflux disease or Barrett’s oesophagus. Relative expression values are expressed as median (95% confidence intervals).

	Controls (n=13)	Reflux (n=10)	Barrett’s oesophagus (n=20)	P-value
miR-143	0.000157 (0.000171, 0.000317)	0.000361 (0.000160, 0.00130)	0.0102 (0.00601, 0.0306)	<0.0001
miR-145	0.00846 (0.00458, 0.0101)	0.0177 (0.00956, 0.0363)	0.045 (0.0333, 0.0115)	<0.0001
miR-205	0.6721 (0.481, 1.061)	1.73 (1.31, 2.54)	0.014 (0.0485, 0.388)	<0.0001
miR-21	0.604 (0.304, 0.977)	0.459 (0.233, 1.25)	3.16 (2.70, 4.52)	<0.0001
miR-194	0.000138 (0.000101, 0.000213)	0.000134 (9.77 ⁻⁰⁵ , 0.000238)	0.0633 (0.0476, 0.107)	<0.0001
miR-203	0.169 (0.135, 0.265)	0.27 (0.206, 0.336)	0.0278 (0.0256, 0.106)	<0.0001
miR-215	5.99 ⁻⁰⁵ (-0.000180, 0.000716)	5.45 ⁻⁰⁵ (3.63 ⁻⁵ , 0.000128)	0.0129 (0.00940, 0.0290)	<0.0001

Comparison of 3 tissue types undertaken using the Kruskal-Wallis test. Significant differences were identified by post-hoc testing using the Holm-Bonferroni method. Results of post-hoc testing: Control vs. Reflux - miR-143 (P=0.0101), miR-145 (P=0.0115) & miR-205 (P=0.00260), and Reflux vs. Barrett’s oesophagus - miR-143 (P<0.0001) miR-145 (P=0.0012), miR-205 (P<0.0001), miR-21 (p<0.0001), miR-194 (p<0.0001), miR-203 (p=0.0002) & miR-215 (P<0.0001). The expression data from Barrett’s oesophagus mucosa in this table has been published elsewhere¹⁴ and reported in Chapter 3.

Figure 4.1: TaqMan[®] analyses of relative miR-143 levels in normal squamous tissue, gastroesophageal reflux disease with ulcerative oesophagitis and Barrett's oesophagus. Data presented is median miR-143 expression normalised to RNU44 levels. 95% confidence intervals are shown for each tissue group.

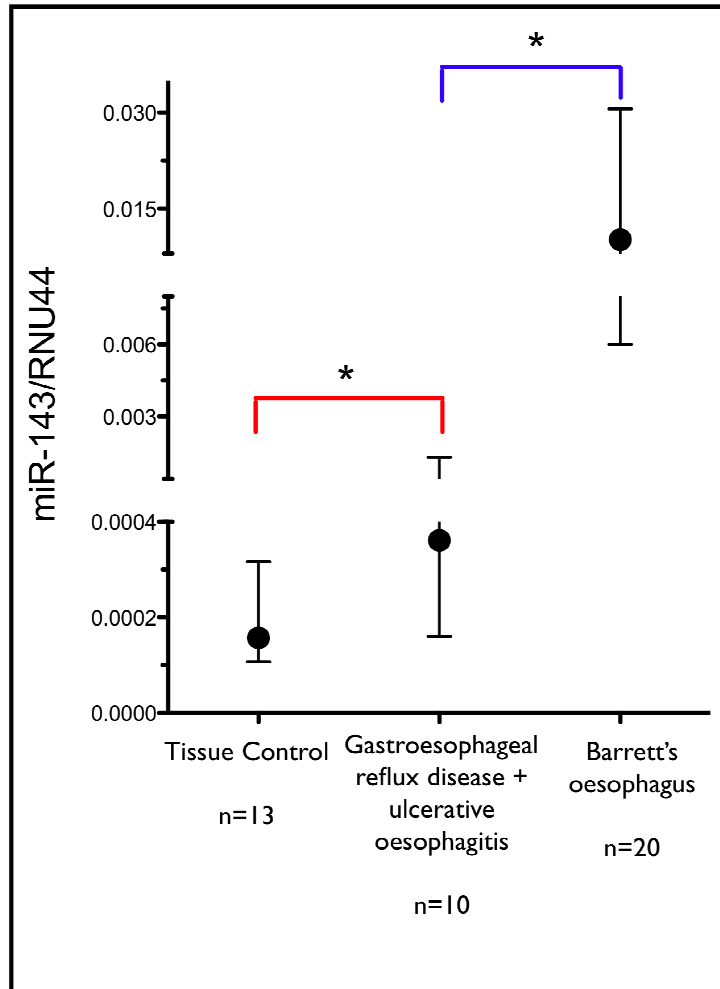


Figure 4.2: TaqMan[®] analyses of relative miR-145 levels in normal squamous tissue, gastroesophageal reflux disease with ulcerative oesophagitis and Barrett's oesophagus. Data presented is median miR-145 expression normalised to RNU44 levels. 95% confidence intervals are shown for each tissue group.

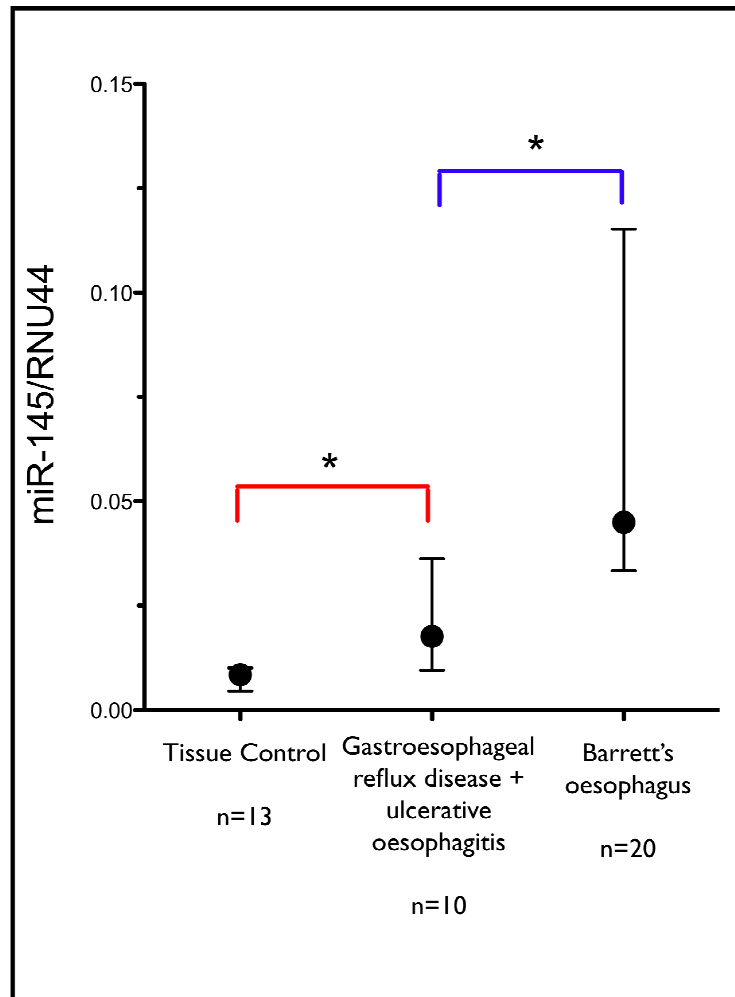


Figure 4.3: TaqMan[®] analyses of relative miR-205 levels in normal squamous tissue, gastroesophageal reflux disease with ulcerative oesophagitis and Barrett's oesophagus. Data presented is median miR-205 expression normalised to RNU44 levels. 95% confidence intervals are shown for each tissue group.

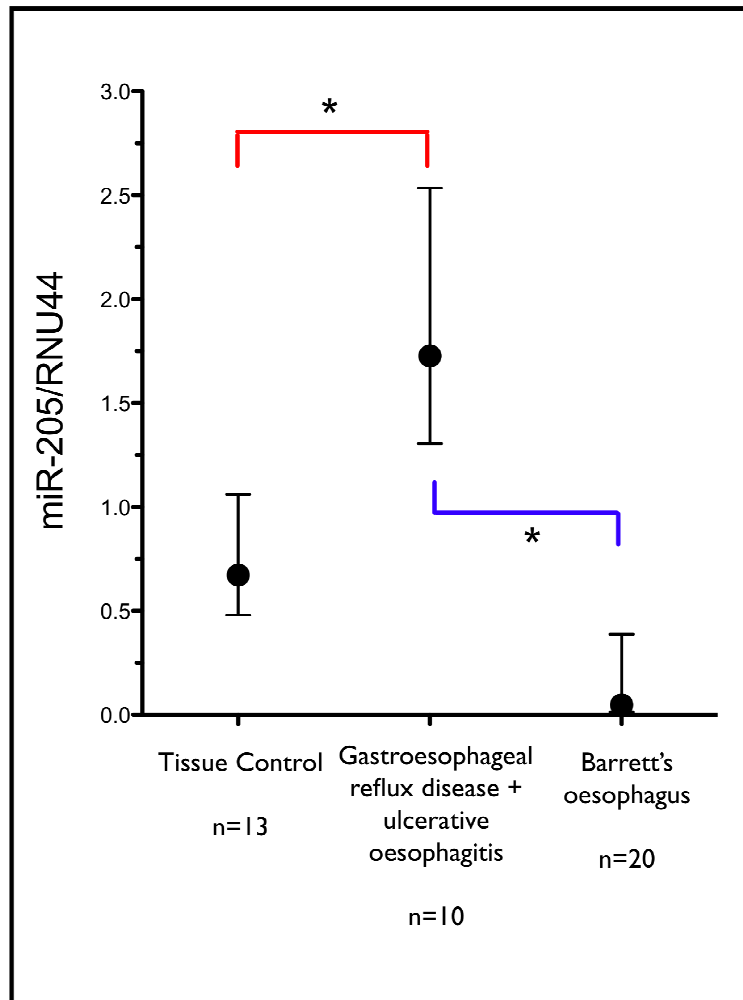


Table 4.2: Correlations between miRNA and mRNA differentiation marker expression levels in oesophageal mucosa from individuals with gastroesophageal reflux and ulcerative oesophagitis.

miRNA	Gene of interest	r value	p-value
miR-143	BMP4	0.802	0.0038
miR-143	CK8	0.591	0.032
miR-194	CK8	0.644	0.0198
miR-194	CK20	0.507	0.0308
miR-194	GATA4	0.785	0.0008
miR-194	HNF1 α	0.619	0.0086
miR-194	CDX2	0.562	0.0168
miR-205	CK14	-0.587	0.034
miR-215	CK8	0.6	0.03
miR-215	IL6	0.697	0.0118

All data are correlation coefficients (Rho = r value) determined using Spearman's test

4.3.1 Het-1A Cell Culture and miRNA over expression

To assess the impact of selected miRNAs on proliferation and apoptosis in oesophageal epithelial cells miR-143, miR-145 or miR-205 mimics were transfected into Het-1A cells (Methods, chapter 2, section 2.2.5), a cell line derived from oesophageal squamous tissue^{7, 146}. Proliferation and apoptosis was measured 24 and 48 hr post transfection and results were compared in cells transfected with miR-143, miR-145 or miR-205 mimics and cells transfected with a negative control probe (Methods, chapter 2, sections 2.2.6 & 2.2.7).

Figure 4.4 summarizes the effect of transfecting miR-143, miR-145 or miR-205 mimics into the cell line. Transfection induced increases in miR-143, miR-145 or miR-205 levels were associated with significantly decreased proliferation and

significantly increased apoptosis ($p < 0.05$, Mann-Whitney test). The median fold increase in miR-143, miR-145 and miR-205 levels, 24 hours after transfection, is presented in Figure 4.5.

Figure 4.4: Cell proliferation (A) and apoptosis (B) levels in Het-1A cells 48h after transfection with miR-143 (A: $p=0.00567$, B: $p=0.00135$), miR-145 (A: $p<0.0001$, B: $p=0.001348$) or miR-205 (A: $p=0.000325$, B: 0.000931). Data are represented as a percentage of the negative control. The mean standard error is shown for each group. Decreased proliferation (A) and increased apoptosis (B) were observed for all miRNAs.

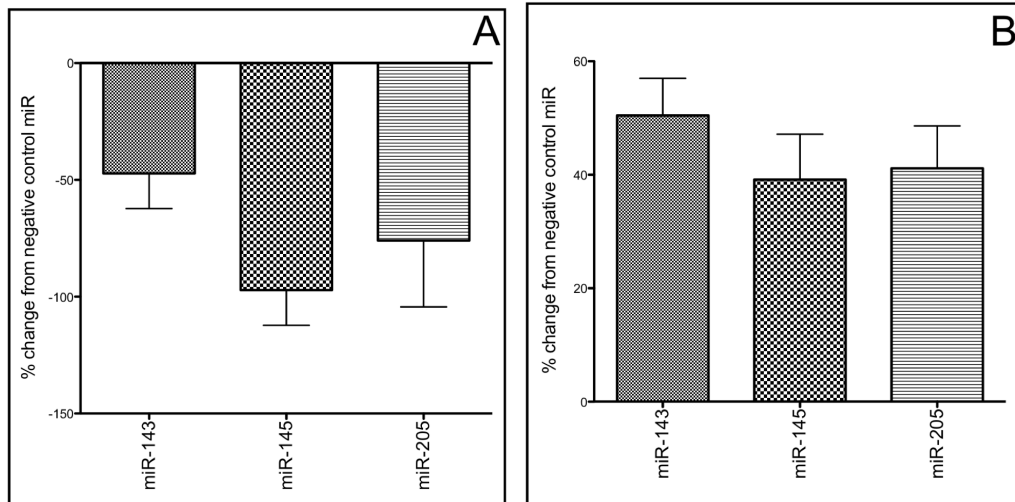
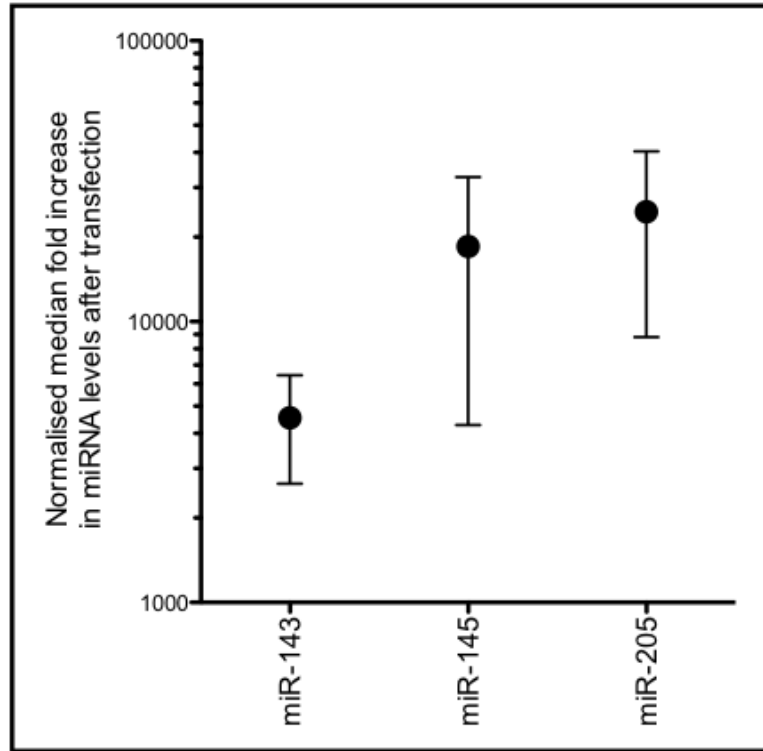


Figure 4.5: A comparison of relative miR-143, miR-145 and miR-205 levels 24 hr after transfection with a miRNA mimic. Relative miRNA levels were normalised to RNU44 expression. Data points represent the fold increase in miRNA levels in miRNA mimic transfected cells compared with cells transfected with the negative control probe. 95% confidence intervals are shown for each group.



4.3.2 Spatial expression of miR-143, miR-145 and miR-205 in oesophageal biopsies

To localise miRNA activity within the oesophageal mucosa in-situ hybridisation was performed, probing against miRNAs elevated in ulcerative oesophagitis (chapter 2, 1.2.7). Prior to in-situ hybridization, standard hematoxylin and eosin staining was performed on a slide from each tissue biopsy to confirm the tissue type. Hematoxylin and eosin stained sections showed elongated papillae and an enlarged basal layer, consistent with known gastroesophageal reflux histopathology (Figure 4.6-A). Staining for miR-143 (Figure 4.6-B), miR-145 (Figure 4.6-C) and miR-205 probes (Figure 4.6-D) revealed similar expression patterns to each other, with the most intense staining seen in the basal layer of the epithelium. Staining of both the cytoplasm and nucleus was seen, with greater staining intensity seen within the nucleus in most cells. No staining was observed with the negative control duplex (Figure 4.6-E).

Figure 4.6: miRNA in-situ hybridization analysis in oesophageal mucosal biopsies from patients with gastroesophageal reflux and ulcerative oesophagitis. A: Staining with hematoxylin and eosin. The basal layer, papillae and differentiated squamous epithelium are clearly visible. B, C, D and E: Hybridization with LNA-probes for miRNAs miR-143 (B), miR-145 (C) and miR-205 (D), and LNA-negative control (E). No hybridization was observed with the LNA-negative control probe. A region from each section has been magnified 100x. In A, rounded nuclei in the oesophageal epithelium are evident. B, C & D depict the cytoplasmic and punctate nuclear staining observed for each miRNA.

4.4 Discussion

miRNA regulation of gene expression has been implicated in most cellular processes²²³, and as discussed in chapter 3 it probably plays a role in the development of Barrett's oesophagus and cancer. If the role of miRNAs in this development can be understood, then miRNA expression patterns might be useful biomarkers for the clinical assessment and management of oesophageal cancer and precursor pathologies. Chapter 3 compares miRNA expression in normal squamous oesophageal epithelium with Barrett's oesophagus and shows increased expression of miR-21, miR-143, miR-145, miR-194 and miR-215, and decreased expression of miR-203 and miR-205 in Barrett's oesophagus. As gastroesophageal reflux predisposes to the development of Barrett's oesophagus, and its subsequent progression to adenocarcinoma, further investigation of these miRNAs in the earlier context of gastroesophageal reflux was undertaken.

4.4.1 Increased miRNA expression in patients with gastroesophageal reflux disease correlates with mRNA differentiation marker expression

Elevated miR-143 and miR-145 levels are observed in the oesophageal mucosa from subjects with gastroesophageal reflux with ulcerative oesophagitis, and this extends the previous observation of elevated miR-143 and miR-145 expression in Barrett's oesophagus epithelium¹¹⁰ (chapter 3, section 3.3) to an earlier stage in the reflux - Barrett's oesophagus - adenocarcinoma sequence. Alterations in miR-143 and miR-145 expression might occur at an early stage in the development of Barrett's oesophagus. In support, positive correlations were observed when comparing the expression of miR-143 and *CK8*, and miR-143 and *BMP4*, in the oesophageal mucosa from individuals with reflux. The *BMP4* pathway is activated in the oesophageal mucosa in both ulcerative oesophagitis and Barrett's oesophagus, and this promotes the expression of columnar gene markers²²¹. Further, *CK8* is a known marker of columnar epithelia²²⁴. Taken together, these correlations with *BMP4* and *CK8* support an association between elevated miR-143 expression and a columnar cell phenotype. Also, miR-143 and miR-145 expression is still significantly higher

in Barrett's oesophagus mucosa compared to all types of squamous mucosa (Table 4.1). Therefore, if these miRNAs have a role in the metaplastic conversion of a squamous to a columnar cells they may need to reach a threshold level before metaplasia develops. Significant correlations were also identified between miR-194 expression and *CK8*, *CDX2*, *GATA4* and *HNF1 α* mRNA levels. As discussed in chapter 1, section 1.2.4, *CDX2*, *GATA4* and *HNF1 α* are key transcription factors that determine the gastric and or intestinal epithelial phenotype and these are enriched in Barrett's oesophagus^{45, 54, 224, 225}. miR-215 levels also correlated with *CK8*, a columnar marker, and *IL6* an inflammatory marker which correlates with reflux severity⁷. However, neither miR-194 or miR-215 displayed significantly elevated expression in gastroesophageal reflux squamous tissue in this study. Accordingly, it is important not to over interpret these correlations.

4.4.2 Increased miRNA expression in patients with gastroesophageal reflux disease may regulate proliferation and apoptosis at the basal layer of the oesophageal epithelium

Two major hallmarks of oesophageal squamous mucosa in the presence of ulcerative oesophagitis include increased proliferation and apoptosis^{7, 20, 217}. Given the known association of miR-143, miR-145 and miR-205 with proliferation and apoptosis their function was assessed in the context of these cellular processes using a non-neoplastic oesophageal cell line¹⁴⁶. Reduced proliferation and increased apoptosis was observed in the cells following transfection with miR-143, miR-145 and miR-205 mimics. Restoring miR-143, miR-145 or miR-205 expression in cancer cell models has also been shown to reduce cell proliferation and increase apoptosis^{175, 195, 209, 211, 226}. This study also used in-situ hybridisation to identify the spatial expression of miR-143, miR-145 and miR-205 and identify where these miRNAs might be active in the oesophageal mucosa. In ulcerative oesophagitis miR-143, miR-145 and miR-205 staining intensity was greatest in the basal layer of the oesophageal epithelium, and it is possible that these miRNAs might direct anti-proliferative and pro-apoptotic effects within this layer. The pro-apoptotic effects of transfection with miR-143, miR-145 or miR-205 mimics may reflect the physiological apoptotic response observed in the oesophagus following reflux exposure. However, the reduction in proliferation suggests otherwise^{20, 217}. It is possible that up-regulation of

miR-143, miR-145 or miR-205, and the associated anti-proliferative effect, might counterbalance hyperplasia in the basal layer of the oesophageal epithelium. In support of this, an inverse correlation was identified between miR-205 and *CK14*, a marker of basal cell hyperplasia and squamous restoration. Taken together, these results suggest that miR-143, miR-145 and miR-205 might suppress proliferation or promote apoptosis in the basal layer of the oesophageal epithelium.

4.4.3 Nuclear localisation of miR-143, miR-145 and miR-205

In-situ hybridization staining for miR-143, miR-145 and miR-205 appeared to be both nuclear and cytoplasmic. Nuclear staining has been reported for miR-145²²⁷ in breast myoepithelium, but this study is the first to show nuclear staining for miR-143, miR-145 and miR-205 in the oesophagus. Nuclear localisation of mature miRNAs is surprising, as they are typically known to exert their effects in the cytoplasm. However, recent studies also describe the nuclear localisation of mature miRNAs^{228, 229} and suggest that nuclear miRNAs can direct biological processes²³⁰. For example, a recent study by Taft et al.²³⁰ sequenced THP-1 cell line RNA obtained from the nucleus and found that the miR-15/16 cluster was enriched in the nucleus when compared with matched cytoplasmic RNA, and hypothesized this cluster may be involved in epigenetic regulation inside the nucleus. Based on our in-situ hybridisation results, miR-143, miR-145 and miR-205 may regulate gene expression in the nucleus of oesophageal epithelial cells.

4.4.4 Limitations

This study has some limitations. Firstly, this study did not compare differences in miRNA expression between genders. Identifying differences in miRNA expression between genders may help explain why males are more likely to develop Barrett's oesophagus than females²³¹. Secondly, only miRNAs shown by Wijnhoven et al.¹¹⁰ to be differentially expressed between normal squamous epithelia and Barrett's oesophagus were assessed. As global miRNA expression changes were not assessed it is possible that the expression of other miRNAs may be altered in response to chronic reflux. Thirdly, a common transfection protocol was used to increase

miRNA levels in Het-1A cells greater than physiological miRNA levels. This may impact on the biological relevance. However, all assay results were compared with Het-1A cells transfected with a negative control duplex at similar levels.

4.4.5 Summary

This study has shown miRNA expression is altered in the oesophageal mucosa from individuals with gastroesophageal reflux and ulcerative oesophagitis. These changes in miR-143, miR-145 and miR-205 expression appear to be most pronounced in the basal layer of the oesophageal epithelium. In the context of gastroesophageal reflux these expression changes might influence proliferation and apoptosis and thereby regulate epithelial restoration. It is reasonable to hypothesize that they could represent early molecular events preceding the development of Barrett's oesophagus, although proving this will require further studies.

Chapter 5

Loss of tumour suppressor miRNAs in Barrett's oesophagus: links with neoplastic progression to oesophageal adenocarcinoma

5.1 Introduction

Oesophageal adenocarcinoma is a malignancy with poor prognosis^{74, 139}. Studying Barrett's oesophagus, a pre-malignant lesion, and the only identifiable precursor to oesophageal adenocarcinoma, provides an opportunity to investigate molecular changes that may contribute to the development of oesophageal adenocarcinoma^{29, 139}.

Although we observed differences in miRNA expression between Barrett's oesophagus and oesophageal adenocarcinoma (Table 3.1) the implications of this altered miRNA expression in oesophageal adenocarcinoma development (if any) are unknown. It is clear that miRNAs play a role in neoplastic development and numerous studies have identified miRNAs acting as tumour suppressors^{82, 139}. In this capacity, they may regulate hallmarks of neoplastic development, such as cellular proliferation and apoptosis²³². Chapter three describes decreased levels of miR-143, miR-145 and miR-215 in oesophageal adenocarcinoma compared with Barrett's oesophagus¹¹⁰. Chapter 3, section 3.4.5 also discusses miR-143 and miR-145 regulation of proliferation and apoptosis and miR-215 regulation of cell cycle progression. These discussions highlight how decreased expression of miR-143, miR-145 or miR-215 might contribute to a decrease in proliferative and apoptotic control.

From the expression data in chapter 3 we hypothesized that miR-143, miR-145 or miR-215 may act as tumour suppressors in Barrett's oesophagus, and that restoring their expression levels in oesophageal adenocarcinoma would reduce proliferation and increase apoptosis. Key points for further study included testing this hypothesis,

and determining the location of miR-143, miR-145 and miR-215 biological activity within Barrett's epithelium.

The aims of this study were to:

- 1) Assess the impact of restoring miR-143, miR-145 or miR-215 on cell proliferation and apoptosis, processes that contribute to oesophageal adenocarcinoma tumorigenesis.
- 2) Assess the location of miRNA activity within Barrett's oesophagus epithelium.
- 3) Investigate the global changes in gene expression that occur in response to restoring miR-143, miR-145 or miR-215 expression in oesophageal adenocarcinoma and quantify protein levels of genes relevant to proliferation and apoptosis.

In this study regulation of proliferation and apoptosis by miRNAs was evaluated following transfection of an oesophageal adenocarcinoma cell line (OE-19) with miR-143, miR-145 or miR-215 mimics. After increasing miR-143, miR-145 or miR-215 levels, global changes in gene expression were assessed at the RNA level by mRNA array and real time PCR, and at the protein level by Western blot. miRNA expression was localised in oesophageal mucosa from individuals with Barrett's oesophagus and oesophageal adenocarcinoma using in-situ hybridisation.

5.2 Results: OE-19 cell culture and miRNA over-expression

To assess the impact of miRNA down regulation in oesophageal adenocarcinoma on proliferation and apoptosis miR-143, miR-145 or miR-215 were over expressed in OE-19 cells (Methods, Chapter 2, section, 2.2.5), an oesophageal adenocarcinoma derived cell line. Three separate transfection experiments (labelled (1), (2) and (3) in Figure 5.1) were performed for each of miR-143, miR-145 and miR-215. In these transfection experiments, varying increases in miRNA levels were observed compared with negative controls (Figure 5.1 A – C). RNA harvested from transfection experiment (1) was used for mRNA array analysis and PCR validation

of mRNA array indicated increases in mRNA expression. Protein harvested from transfection experiment (2) was used for western blot analysis. RNA harvested from transfection experiment (3) was used for PCR validation of mRNA array indicated decreases in mRNA expression. Transfection experiment three (miR-143 (3)) did not appear to increase miR-143 levels when compared with the negative control. In addition, overall transfection of miR-143 resulted in much lower increases in miRNA expression when compared with the increases observed for miR-145 and miR-215 24 hr post transfection. miRNA over expression was associated with significantly decreased proliferation and significantly increased apoptosis (Figure 5.2 A - B).

Figure 5.1 (A – C): A comparison of relative miR-143 levels (A), miR-145 levels (B) and miR-215 levels (C) 24 hr after transfection with a miRNA mimic. Relative miRNA levels were normalised to RNU44 expression. Three separate transfection experiments were performed and varying increases in miRNA levels compared with negative controls were observed. Data points represent the fold increase in miRNA levels in miRNA mimic transfected cells compared with cells transfected with the negative control probe.

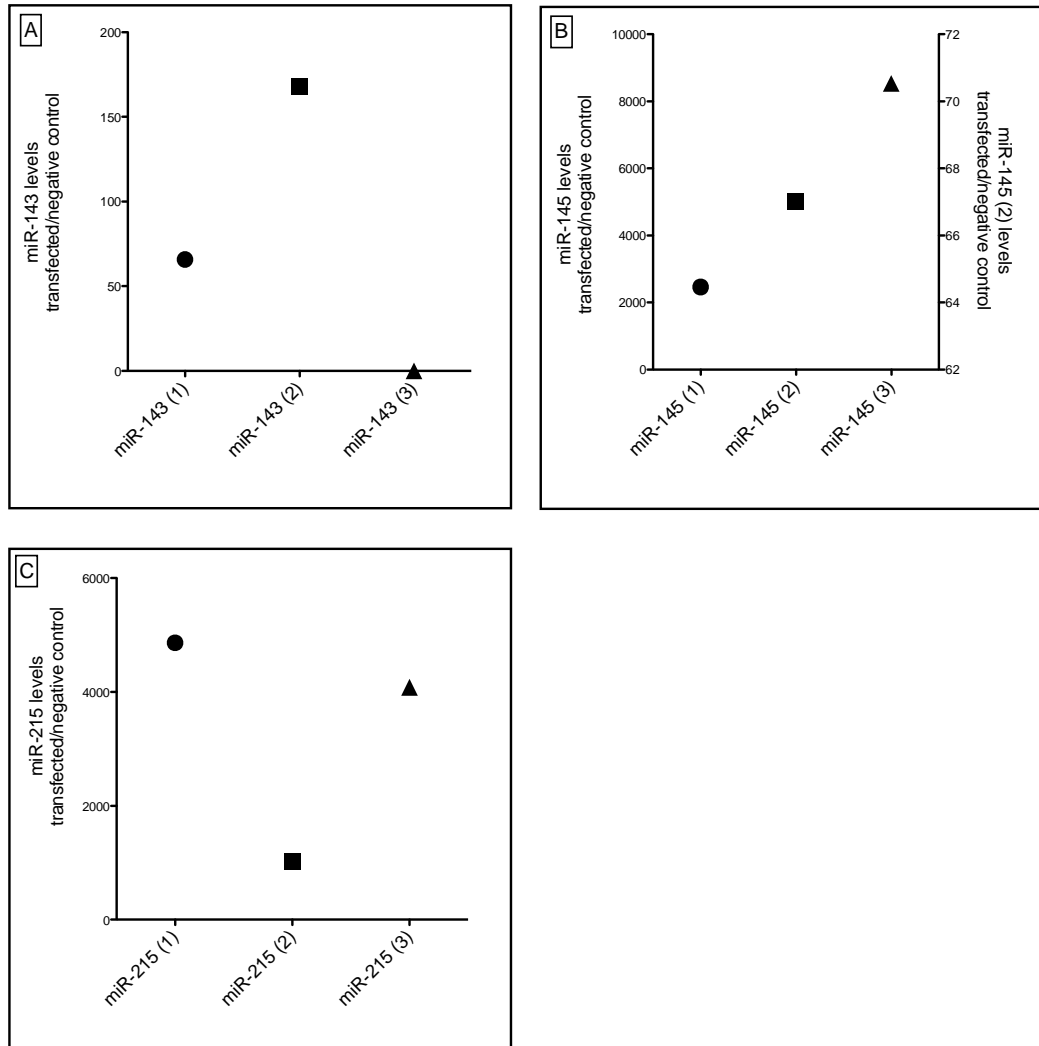
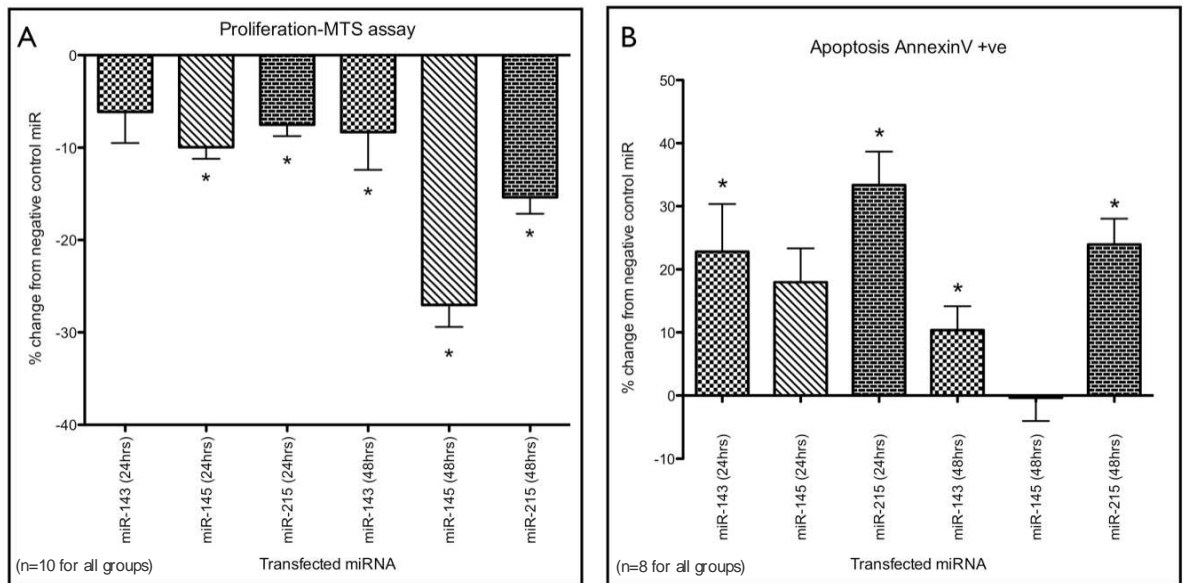


Figure 5.2 (A – B): Cell proliferation (A) and apoptosis (B) levels in OE-19 cells were assessed 24 & 48h after transfection with miR-143, miR-145 or miR-215 (n=8 for each miRNA). Data are represented as a percentage of the negative control. Increased miRNA expression levels were confirmed for each of miR-143, miR-145 and miR-215 and are shown in transfection group (1) of Figure 5.1. Decreased proliferation (A) was observed for miR-143 (24 hr: p=0.164; 48 hr: p=0.0312), miR-145 (24 hr: p=0.0111; 48 hr: p=0.000931) and miR-215 (24 hr: p=0.0262; 48 hr: p=0.000931) while increased apoptosis (B) was observed for miR-143 (24 hr: p=0.00690; 48 hr: p=0.0205) and miR-215 (24 hr: p=0.000155; 48 hr: p=0.00160). All negative control - miRNA mimic comparisons were assessed for significance (p<0.05) using the Mann-Whitney test.



Decreased proliferation and increased apoptosis was confirmed in independent transfection experiments (n=2 experimental replicates). In the second transfection experiment, decreased proliferation was confirmed for miR-143 (24 hr: p=0.185; 48 hr: p=0.0140), miR-145 (24 hr: p<0.0001; 48 hr: p=0.0207) and miR-215 (24 hr: p=0.0316; 48 hr: p=0.0192) while increased apoptosis was confirmed for miR-143 (24 hr: p=0.08213; 48 hr: p<0.0001) and miR-215 (24 hr: p=0.0821; 48 hr: p=0.000445).

5.2.1 Changes in gene expression post miRNA transfection

Changes in global gene expression were assessed 24 hr post transfection by microarray analysis (Methods, chapter 2, section 2.2.9). However, after routine statistical analysis and step-up adjustment (ANOVA with multiple statistical comparisons Benjamini-Hochberg p-value adjustment¹⁴⁹) (Methods, chapter 2, section 2.2.9) no genes were indicated as being differentially expressed.

Changes in mRNA levels in response to targeting from miRNAs can be small in magnitude^{233, 234}. For example, studies by Selbach et al.²³³ and Lim et al.²³⁴ used mRNA arrays to assess mRNA levels in HeLa cells after increasing miRNA levels. Selbach et al.²³³ reported that miRNAs directed numerous small decreases in mRNA levels, in the order of 20-50% (See supplementary Figure S5²³³), while Lim et al.²³⁴ reported decreases in mRNA levels as low as 40% (see supplementary Table 2²³⁴). As the current array experiment only used 3 replicates for each miRNA or negative control mimic, it was hypothesised that small changes in mRNA expression may occur, but due to the limited number of technical replicates in the experiment the changes would fail to produce data robust enough to pass multiple statistical comparisons adjustment.

To further assess the data, student-t statistical analysis (unpaired, two tailed, equal distribution) was performed on the mRNA array data. It was acknowledged that using the student t-test statistical analysis would increase the detection of false positive changes in mRNA expression. However, using student-t statistical testing, preliminary analysis of the mRNA array data identified small but statistically significant ($p < 0.05$) changes in mRNA expression. Therefore, I aimed to use PCR (Methods, chapter 2, section 2.2.3) to quantitatively validate changes in genes that had known roles in regulating proliferation and apoptosis and were indicated as being significantly differentially expressed ($p < 0.05$) in the mRNA array.

In all PCR experiments mRNA levels were assessed using TaqMan[®] gene expression assays (Primer details, chapter, 2.2.3) and compared in RNA from cells transfected with miR-143, miR-145 or miR-215 with RNA from cells transfected with the

negative control. Potential differences in gene expression were assessed for statistical significance via a student-t statistical analysis.

The main aim of the mRNA array analysis was to identify miRNA target genes (i.e. down regulated mRNAs). However, the first PCR validation step involved assessing the expression of genes indicated by the mRNA array as having the greatest change in expression, as these changes were hypothesised to be large enough to be quantitatively validated. For step one of the PCR analysis, a 20% change in gene expression compared with the negative control group was required. This cut-off was chosen because it corresponded to the lower end of the changes in mRNA levels observed in studies by Selbach et al.²³³. Seven genes reached >20% cut-off and had validated roles in either proliferation or apoptosis (Table 5.1). However, all of these genes were indicated by the mRNA array as being up regulated.

Genes up regulated greater than 20% on the array included Cbp/p300-interacting transactivator, with Glu/Asp-rich carboxy-terminal domain, 2 (*CITED2*), early growth response 1 (*EGR1*), dual specificity phosphatase 10 (*DUSP10*), SLAM family member 7 (*SLAMF7*) and GTP binding protein over expressed in skeletal (*GEM*) after transfection with miR-143, *GEM* and *DUSP10* after transfection with miR-145 and *DUSP10*, *GEM*, ankyrin repeat domain 1 (*ANKRD1*) and cysteine-rich, angiogenic inducer, 61 (*CYR61*) after transfection with miR-215 (array indicated increase and p-value shown in Table 5.2).

PCR analysis showed increased expression of *CITED2*, *EGR1*, *DUSP10*, *SLAMF7* and *GEM* after transfection with miR-143, *GEM* after transfection with miR-145 and *DUSP10*, *GEM*, *ANKRD1* and *CYR61* after transfection with miR-215 (PCR validated increase and p-value shown in Table 5.2).

Step one of the PCR analysis demonstrated that the student-t statistical analysis could be used to identify changes in mRNA expression, and these changes could be quantified using PCR. Interestingly, the fold increase in mRNA levels shown via PCR was much greater in magnitude compared with the percentage increase in mRNA levels indicated via the mRNA array (Table 5.2). This result provided confidence that the >20% cut-off may not be required and therefore this cut-off was

removed from the gene selection criteria. In addition, as increasing miR-143, miR-145 or miR-215 levels in OE-19 cells is known to reduce proliferation or increase apoptosis (Figure 5.2) the accuracy of the student-t analysis might have been further increased by only assessing the expression of genes known to be involved in these cellular processes.

Table 5.1: Shows the genes that were both indicated by the mRNA array to be increased >20% and validated to play a role in 1) apoptosis and or 2) proliferation. The biological model used in each study and the reference/s are also provided.

Transfected miRNA	Gene Name	Gene function in proliferation and/or apoptosis	Biological model
miR-143	CITED2	1) ↑ induces apoptosis ²³⁵ . 2) ↑ decreases cell proliferation ²³⁶ .	1) colorectal cancer cells ²³⁵ . 2) colorectal cancer cells ²³⁶ .
miR-143	EGR1	1) ↑ induces apoptosis ²³⁷ .	1) neuroblastoma cells ²³⁷ .
miR-143, miR-145 or miR-215	DUSP10	2) ↑ decreases cell proliferation ²³⁸	2) prostate cancer cells ²³⁸ .
miR-143	SLAMF7	1) ↑ induces apoptosis ²³⁹ .	1) human natural killer cells ²³⁹ .
miR-143, miR-145 or miR-215	GEM	2) ↑ decreases cell proliferation ²⁴⁰	2) human peripheral blood T cells ²⁴⁰ .
miR-215	ANKRD1	1) ↑ induces apoptosis ²⁴¹ .	1) lung carcinoma cells ²⁴¹
miR-215	CYR61	1) ↑ induces apoptosis ²⁴² . 2) ↑ decreases cell proliferation ²⁴³ .	1) human skin fibroblasts ²⁴² . 2) endometrial cancer cells ²⁴³ .

Table 5.2: PCR analysis of gene expression levels 24 hr after transfection with miR-143, miR-145 or miR-215. Mean gene expression values, normalised to 18S are shown for seven genes indicated by mRNA array as being increased after miRNA transfection. The fold increase in gene expression indicated by mRNA array and PCR analysis are also shown.

Transfected miRNA	Gene Name	PCR - Mean Expression (miRNA mimic)	PCR - Mean Expression (negative control)	mRNA array indicated fold increase in mRNA level	PCR indicated fold increase in mRNA level
miR-143	CITED2	7.93x10 ⁻⁶ (-1.07x10 ⁻⁷ , 1.59x10 ⁻⁵)	2.72 x10 ⁻⁶ (1.83 x10 ⁻⁶ , 3.61 x10 ⁻⁶)	0.222 (p=0.0477)	2.91 (p=0.0500)
miR-143	EGR1	5.68 x10 ⁻⁵ (4.88 x10 ⁻⁵ , 6.47 x10 ⁻⁵)	1.60 x10 ⁻⁵ (1.43 x10 ⁻⁵ , 1.85 x10 ⁻⁵)	0.246 (p=0.00312)	3.55 (p<0.0001)
miR-143	DUSP10	5.36 x10 ⁻⁶ (1.82 x10 ⁻⁶ , 8.89 x10 ⁻⁶)	1.56 x10 ⁻⁶ (1.27 x10 ⁻⁶ , 1.86 x10 ⁻⁶)	0.308 (p=0.00207)	3.43 (p=0.0101)
miR-143	SLAMF7	2.13 x10 ⁻⁶ (-3.59 x10 ⁻⁷ , 4.63 x10 ⁻⁶)	6.39 x10 ⁻⁷ (4.50 x10 ⁻⁷ , 8.27 x10 ⁻⁷)	0.204 (p=0.00229)	3.33 (p=0.0618)
miR-143	GEM	3.39 x10 ⁻⁵ (4.00 x10 ⁻⁶ , 6.39 x10 ⁻⁵)	6.90 x10 ⁻⁶ (5.28 x10 ⁻⁶ , 8.52 x10 ⁻⁶)	0.367 (p=0.0001048)	4.91 (p=0.0178)
miR-145	DUSP10	4.42 x10 ⁻⁶ (-1.61 x10 ⁻⁷ , 9.01 x10 ⁻⁶)	1.57 x10 ⁻⁶ (1.28 x10 ⁻⁶ , 1.86 x10 ⁻⁶)	0.587 (p=0.00225)	2.82 (p=0.0556)
miR-145	GEM	2.36 x10 ⁻⁵ (6.32 x10 ⁻⁶ , 4.08 x10 ⁻⁵)	6.89 x10 ⁻⁶ (5.27 x10 ⁻⁶ , 8.51 x10 ⁻⁶)	0.281 (p=0.0235)	3.42 (p=0.0144)
miR-215	DUSP10	2.77 x10 ⁻⁶ (1.80 x10 ⁻⁶ , 3.73 x10 ⁻⁶)	1.57 x10 ⁻⁶ (1.27 x10 ⁻⁶ , 1.86 x10 ⁻⁶)	0.277 (p=0.00137)	1.76 (p=0.0069)
miR-215	GEM	2.02x10 ⁻⁵ (9.77 x10 ⁻⁶ , 3.07 x10 ⁻⁵)	6.90 x10 ⁻⁶ (5.28 x10 ⁻⁶ , 8.52 x10 ⁻⁶)	0.364 (p=0.000146)	2.92 (p=0.0056)
miR-215	ANKRD1	5.84x10 ⁻⁶ (4.70 x10 ⁻⁶ , 6.97 x10 ⁻⁶)	1.29x10 ⁻⁶ (1.11 x10 ⁻⁶ , 1.47 x10 ⁻⁶)	0.336 (p=0.00189)	4.52 (p=<0.0001)
miR-215	CYR61	5.33 x10 ⁻⁶ (4.05 x10 ⁻⁶ , 6.60 x10 ⁻⁶)	2.65 x10 ⁻⁶ (2.18 x10 ⁻⁶ , 3.11 x10 ⁻⁶)	0.220 (p=0.0115)	2.01 (p=0.0011)

Step one of the PCR analyses only assessed increased mRNA expression. In keeping with biological context of miRNA action, step two of the array analysis sought to identify mRNAs that might be repressed by increasing the levels of miR-143, miR-145 or miR-215.

The mRNA array data indicated that the significant decreases in mRNA expression were quite small in magnitude (The top 40 genes indicated by student-t test to be significantly down regulated for each miRNA are shown in Appendix 2, Tables A.2.1 – A.2.3). To provide confidence for assessing these small array indicated decreases in mRNA expression the array data set was searched for significant decreases in the expression level of predicted mRNA targets (miRecords, target prediction search 14 June 2010) of miR-143, miR-145 and miR-215. miRecords was chosen for miRNA target prediction as it incorporates results from the leading target prediction algorithms including DIANA-microT and TargetScanS (Target prediction programs reviewed in chapter 1, section 1.3.5. In total, the miRecords target prediction program incorporates data from 11 target prediction algorithms including, DIANA-microT 3.0, TargetScanS, Micro Inspector, miRanda, Mir Target 2, mi Target, NB miRTar, PicTar, PITA, RNA22, RNA hybrid.

The mRNA levels of a number of predicted targets of miR-143, miR-145 and miR-215 were indicated via array to be significantly decreased (Table 5.3). The predicted targets listed in Table 5.3, were identified by five or more of the prediction algorithms used by miRecords, with all targets being predicted by TargetScanS (www.targetscan.org). These genes (Table 5.3) were selected for PCR analysis in step two. This PCR analysis identified significant decreases in H2A histone family, member X (*H2AFX*), *RTKN* and poly(A) binding protein, cytoplasmic 4 (*PABPC4*) expression (Table 5.4 and Figures 5.3 – 5.5).

Table 5.3: mRNA array data shows decreased mean mRNA expression levels of predicted miRNA targets (target prediction search 14 June 2010) after transfection with miRNA mimics of miR-143, miR-145 or miR-215 compared with the negative control.

Transfected miRNA	Gene Name	Mean Expression (miRNA mimic)	Mean Expression (negative control)	mRNA array indicated fold decrease in mRNA level	p-value
miR-143	NUAK2	3.814	4.084	-7.093	0.0129
miR-143	PC	5.447	5.738	-5.347	0.0309
miR-145	RTKN	6.494	6.749	-3.915	0.0135
miR-145	H2AFX	6.165	6.684	-8.424	0.0150
miR-215	PABPC4	7.077	7.731	-9.238	0.0322
miR-215	MECP2	5.857	6.131	-4.679	0.0212

Table 5.4: PCR analysis of gene expression levels 24 hr after transfection with miR-143, miR-145 or miR-215. Mean gene expression values, normalised to 18S are shown for six genes indicated by mRNA array as being decreased after miRNA transfection. The fold decrease in gene expression quantified by PCR analysis and p-value are shown.

Gene ID	Decreased expression indicated after transfection with:	p-value on array	Mean Expression (miRNA mimic)	Mean Expression (negative control)	p-value from PCR analysis
NUAK2	143	0.0129	0.241 (0.133, 0.350)	0.172 (0.130, 0.214)	0.200
PC	143	0.0309	1.59 (0.924, 2.26)	1.35 (0.992, 1.71)	0.489
RTKN	145	0.0135	2.99 (1.83, 4.15)	6.68 (4.99, 8.37)	0.000700
H2AFX	145	0.0150	10.7 (8.02, 13.4)	22.0 (16.7, 27.4)	0.000400
PABPC4	215	0.0322	6.96 (5.10, 8.83)	16.5 (12.4, 20.6)	<0.0001
MECP2	215	0.0212	0.918 (0.665, 1.17)	1.03 (0.774, 1.29)	0.487

Figure 5.3: TaqMan[®] gene expression analyses of relative H2AFX levels cell lines 24 hr after transfection with either a miRNA mimic or a negative control scramble probe. Data presented is mean H2AFX expression normalised to 18S levels. 95% confidence intervals are shown for each group.

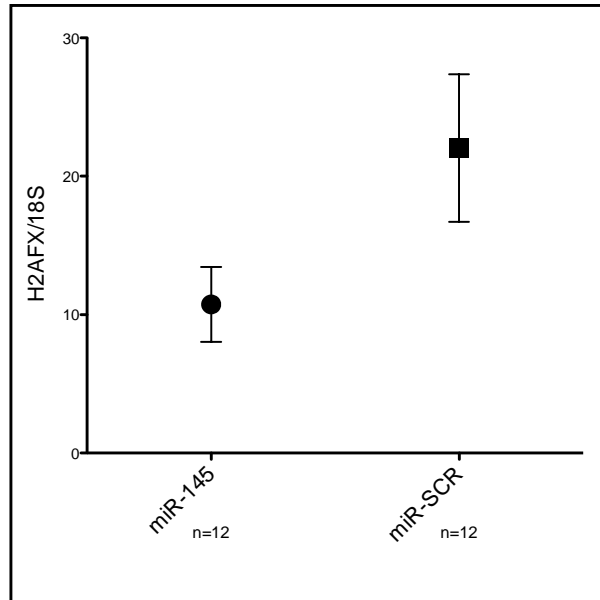


Figure 5.4: TaqMan[®] gene expression analyses of relative RTKN levels cell lines 24 hr after transfection with either a miRNA mimic or a negative control scramble probe. Data presented is mean RTKN expression normalised to 18S levels. 95% confidence intervals are shown for each group.

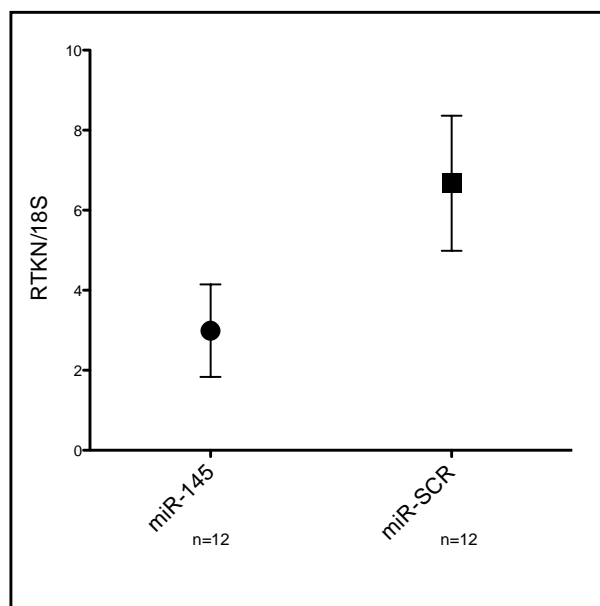
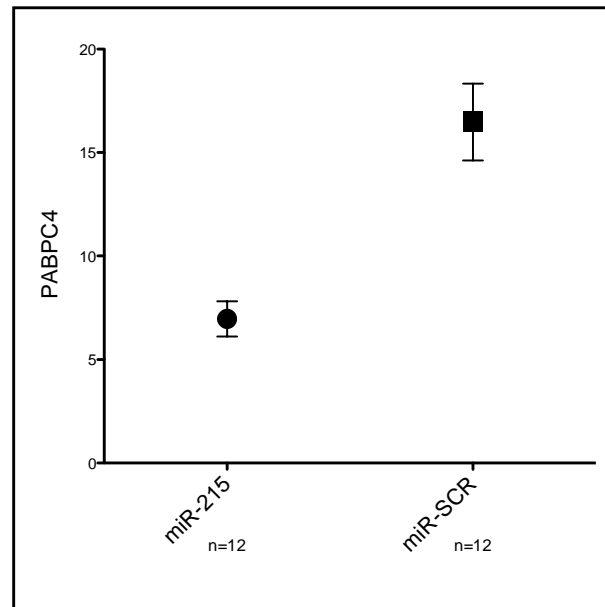


Figure 5.5: TaqMan[®] gene expression analyses of relative PABPC4 levels cell lines 24 hr after transfection with either a miRNA mimic or a negative control scramble probe. Data presented is mean PABPC4 expression normalised to 18S levels. 95% confidence intervals are shown for each group.



5.2.2 Changes in protein expression post miRNA transfection

While attempting to validate the mRNA expression changes presented above I sought independent evidence that biologically relevant miRNA target protein levels were repressed after increasing miRNA expression *in vitro*. Therefore, protein levels of selected validated miR-143, miR-145 or miR-215 targets were assessed by western blot. Western blotting was carried out on protein samples extracted 24 hr post transfection using methods and antibodies described in chapter 2, section 2.2.10. Validated targets of miR-143 (*K-Ras*¹⁵³), miR-145 (*RTKN*¹⁶⁰, *YES*¹⁶²) and miR-215 (denticleless homolog (Drosophila) (*DTL*)¹⁷¹) were chosen for assessment by western blot, as they are known to be involved in either proliferation or apoptosis^{153, 160, 162, 171}.

Western blot analysis also involved assessing one *predicted* target of miR-143, Histone Deacetylase 7 (HDAC7). The rationale for assessing HDAC7 is described as

follows. Increased mRNA expression of the pro apoptotic gene²³⁵ *CITED2* was observed after increasing miR-143 levels (Table 5.2). A review of the literature identified evidence of butyrate mediated histone deacetylase (HDAC) inhibition triggering an increase in *CITED2* expression²³⁶ and, selective inhibition of *HDAC7* inducing apoptosis in cancer cells²⁴⁴. As *HDAC7* was listed as a predicted target of miR-143 in the miRecords search described in section 5.2.2 it was hypothesized that miR-143 might repress *HDAC7* protein expression to direct an increase in apoptosis at least in part through the up regulation of *CITED2* expression. To provide support for this miR-143 mediated mechanism of apoptosis, *HDAC7* protein levels in miR-143 transfected cells were also assessed via western blot 24 hr post miR-143 transfection.

Results of the western blot analysis are shown below in Table 5.5. Of the proteins assessed by western blot *KRAS* showed increased expression, while *HDAC7* and *RTKN* showed decreased expression (Figures 5.6 – 5.8). The results of the western blot analysis of *YES* and *DTL* protein levels are also shown (Figures 5.9 and 5.10)

Table 5.5: Results from the western blot analysis of protein levels 24 hr after transfection with a miRNA mimic or negative control. Results shown are mean normalised band intensity with the band intensity for each protein assessed being normalised to GAPDH band intensity. Potential differences in normalized band intensity were assessed for statistical significance ($p < 0.05$) via student-t statistical analysis.

Protein	Band Size (kDa)	Expression assessed after transfection with:	Mean Expression (miRNA mimic)	Mean Expression (negative control)	p-value from western blot band intensity comparison
KRAS	21	miR-143 (n=8)	0.234 (0.140, 0.328)	0.136 (0.107, 0.166)	0.034
RTKN	62	miR-145 (n=8)	1.022 (0.611, 1.43)	1.52 (1.27, 1.77)	0.046
YES	58	miR-145 (n=12)	0.227 (0.143, 0.310)	0.226 (0.154, 0.299)	0.995
DTL	95	miR-215 (n=12)	0.1445 (0.102, 0.188)	0.170 (0.124, 0.216)	0.367
DTL	77	miR-215 (n=12)	0.145 (0.103, 0.187)	0.164 (0.125, 0.203)	0.468
DTL	28	miR-215 (n=12)	0.610 (0.419, 0.803)	0.689 (0.399, 0.979)	0.235
HDAC7	102	miR-143 (n=8)	0.195 (0.143, 0.247)	0.310 (0.220, 0.401)	0.021

Figure 5.7: Western blot analysis of RTKN (62 kDa¹⁶⁰) protein expression in whole cell lysate 24 hr after transfection with either a miRNA mimic or a negative control scramble probe. Mean RTKN band intensity was normalised to mean GAPDH (34 kDa) band intensity. GAPDH band intensity was obtained after re-blotting of the same membrane used to detect RTKN).

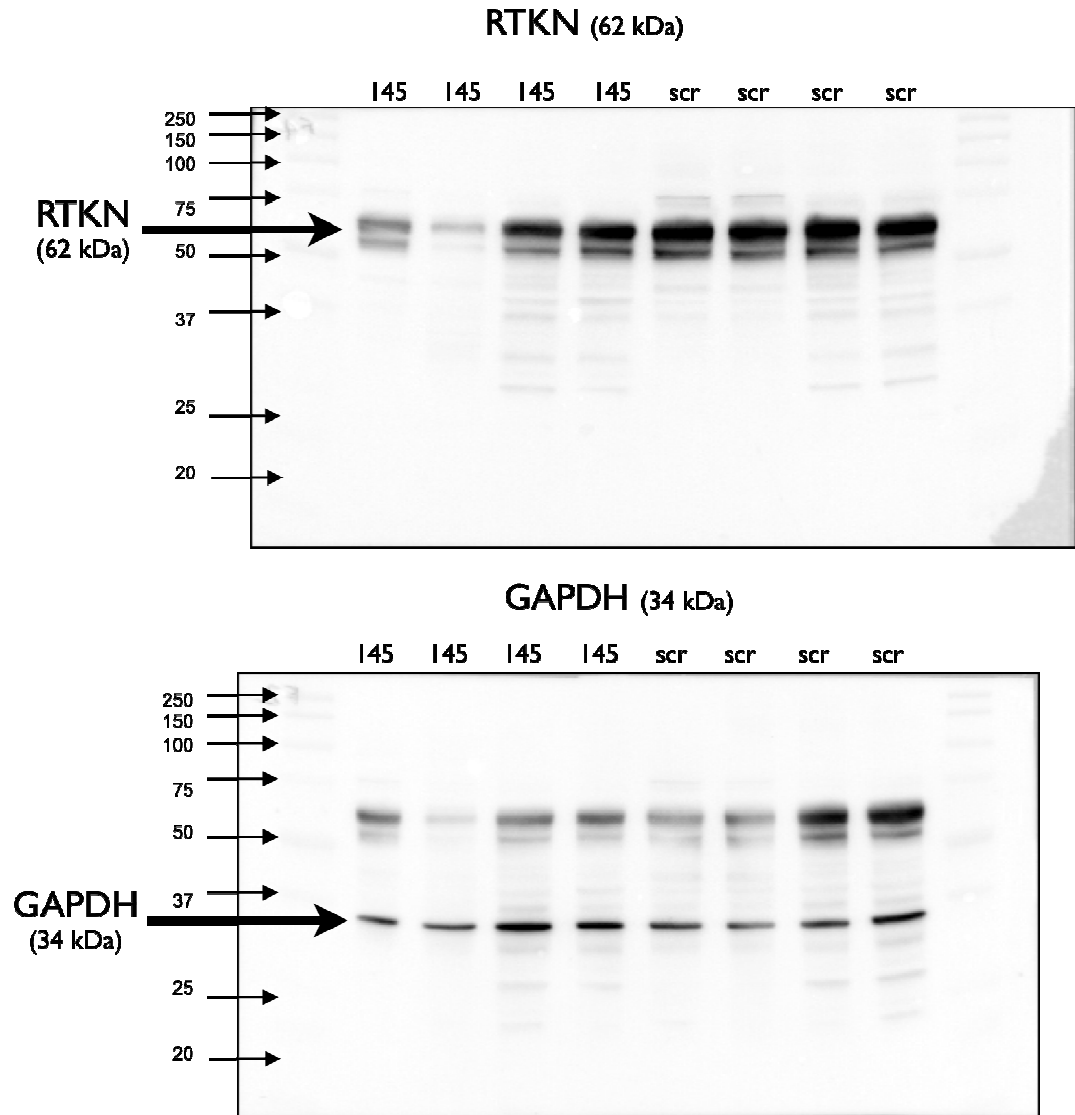


Figure 5.8: Western blot analysis of HDAC7 (102 kDa) protein expression in whole cell lysate 24 hr after transfection with either a miRNA mimic or a negative control scramble probe. Mean HDAC7 band intensity was normalised to mean GAPDH (34 kDa) band intensity. GAPDH band intensity was obtained after re-blotting of the same membrane used to detect HDAC7.

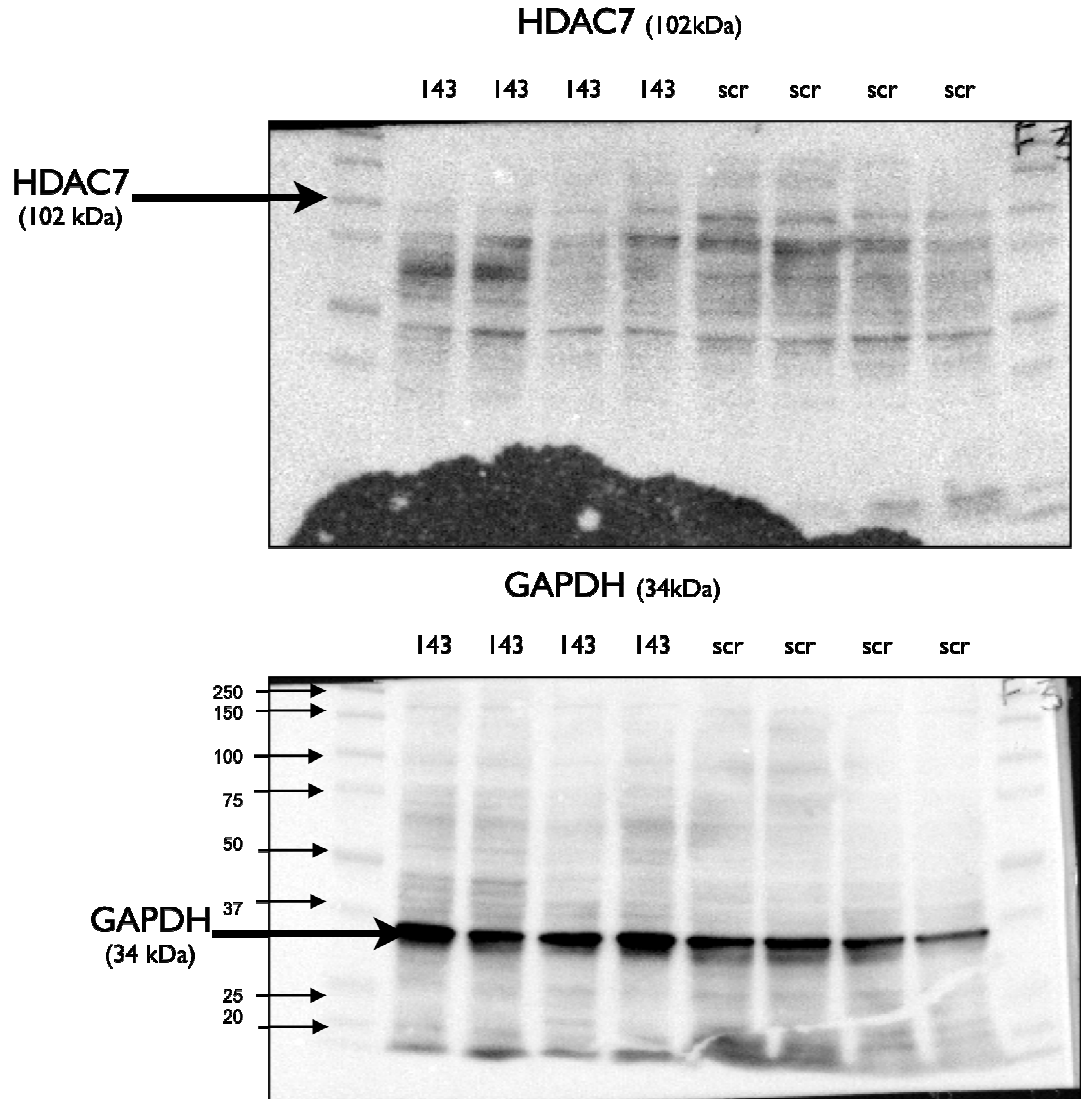


Figure 5.9: Western blot analysis of YES (58 kDa) protein expression in whole cell lysate 24 hr after transfection with either a miRNA mimic or a negative control scramble probe. Mean YES band intensity was normalised to mean GAPDH (34 kDa) band intensity. GAPDH band intensity was obtained after re-blotting of the same membrane used to detect YES.

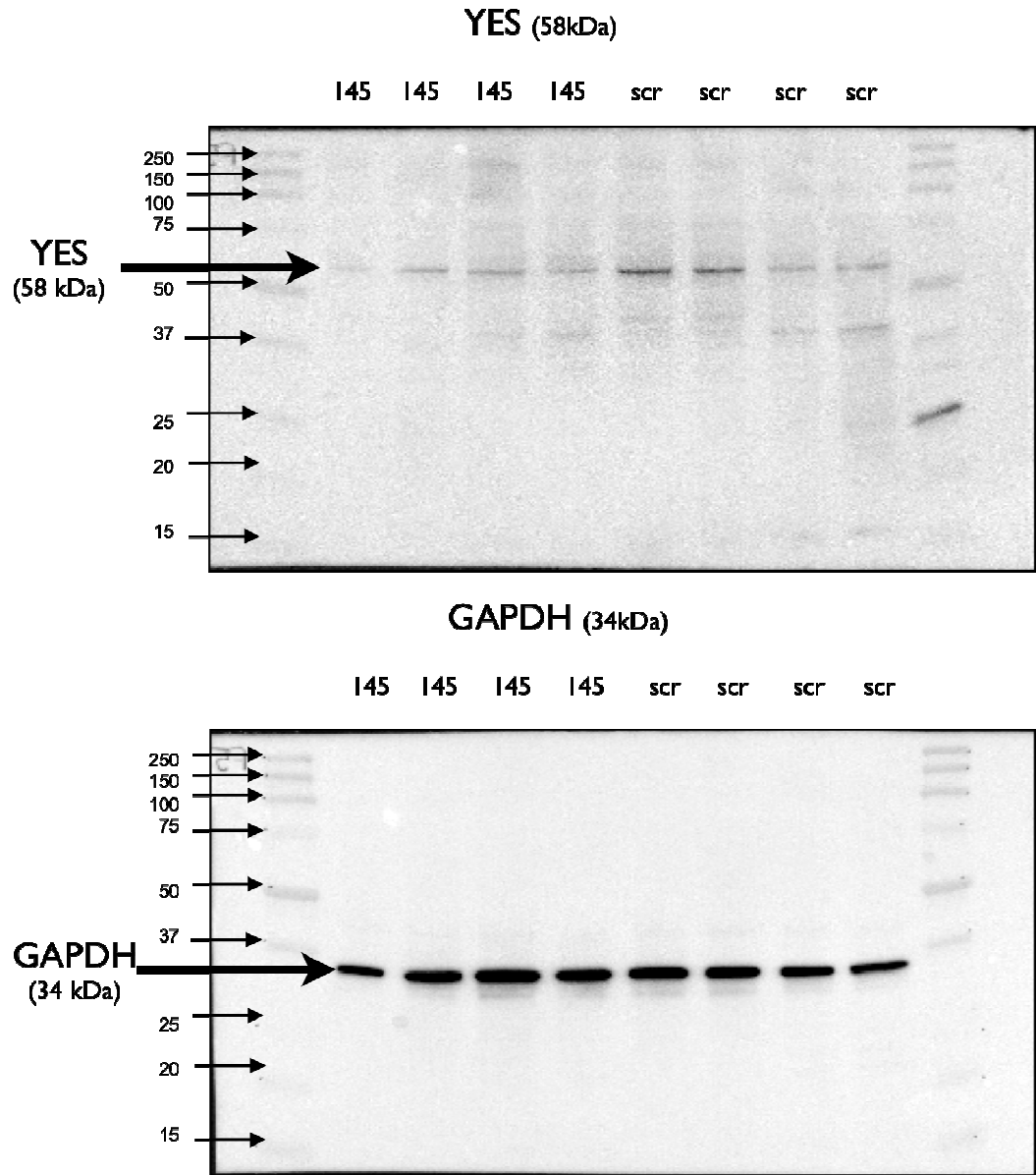


Figure 5.10: Western blot analysis of DTL (95, 77 and 28 kDa) protein expression in whole cell lysate 24 hr after transfection with either a miRNA mimic or a negative control scramble probe. Mean DTL band intensity was normalised to mean GAPDH (34 kDa) band intensity. GAPDH band intensity was obtained after re-blotting of the same membrane used to detect DTL.

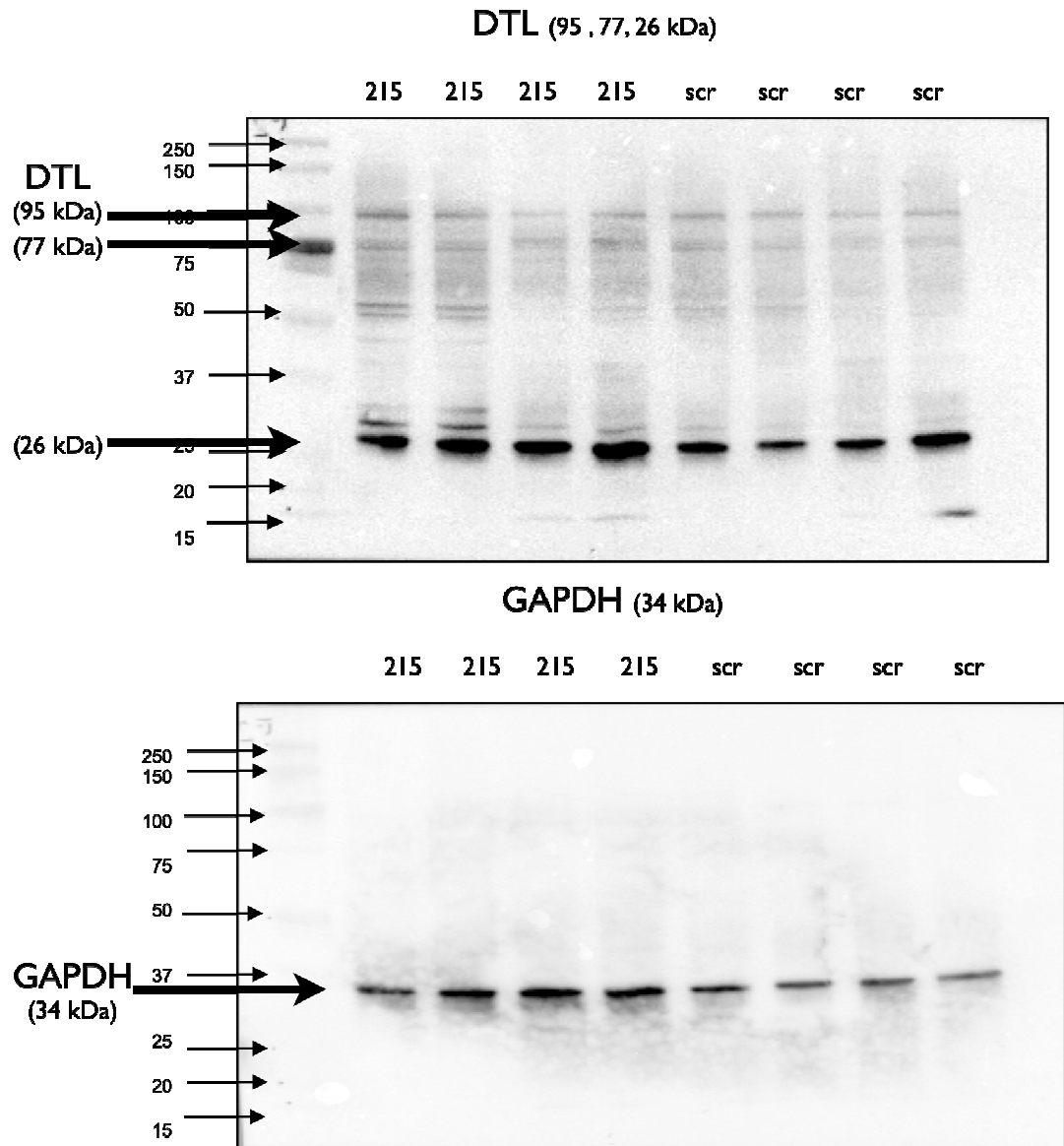


Figure 5.11 – 5.15: miRNA in-situ hybridization analysis in oesophageal mucosal biopsies from patients with Barrett’s oesophagus (A), high grade dysplasia (B) and oesophageal adenocarcinoma (C). Hybridization with LNA-probes for miRNAs miR-143 (Figure 5.11), miR-145 (Figure 5.12), miR-215 (Figure 5.13), LNA-negative control (Figure 5.14) and U6 (Figure 5.15). Intense miR-143, miR-145 and miR-215 staining was observed in Barrett’s oesophagus sections (Figures 5.11 – 5.13 A), while no staining was observed for these miRNAs in high grade dysplasia or oesophageal adenocarcinoma tissue (Figures 5.11 – 5.13 B & C). * is used to mark the presence of muscle tissue in the oesophageal adenocarcinoma sections. These regions stain positive for miR-143 and miR-145 but not miR-215. No hybridization was observed with the LNA-negative control probe (Figure 5.14 A – C). Intense staining for positive control U6 was observed in high grade dysplasia and oesophageal adenocarcinoma sections (Figure 5.15 B & C) showing that these sections are not refractory to staining.

5.2.3 miR-143, miR-145 and miR-215 are detected in the crypts of Barrett's oesophagus but are not detected in oesophageal adenocarcinoma

In situ hybridization analysis (Methods, chapter 2, section 2.2.8) shows miR-143 (Figure 5.11), miR-145 (Figure 5.12) and miR-215 (Figure 5.13) are detected throughout the Barrett's oesophagus epithelium with intense staining in the crypts (Figures 5.11 A, 5.12 A and 5.13 A). Staining for miR-143, miR-145 and miR-215 could not be detected in high grade dysplasia (Figures 5.11 B, 5.12 B and 5.13 B) or oesophageal adenocarcinoma sections (Figures 5.11 C, 5.12 C and 5.13 C) or in the Barrett's oesophagus, high grade dysplasia or oesophageal adenocarcinoma sections probed using the negative control (Figure 5.14 A, B & C). The high grade dysplasia sample used for in-situ hybridisation was defined as carcinoma in-situ as it was obtained from a patient where no invasive cancer was detected. As miR-143, miR-145 and miR-215 were not detectable in high grade dysplasia or oesophageal adenocarcinoma sections, in-situ hybridisation was used to probe for the small RNA housekeeping gene and positive control U6. Intense staining for U6 was observed in both high grade dysplasia and oesophageal adenocarcinoma sections (Figure 5.15 A & B) indicating that these sections were not refractory to staining. U6 staining was not performed on sections of Barrett's oesophagus tissue.

Nuclear localization of miRNAs in Barrett's Oesophagus epithelia

Chapter 4 presented ISH data showing that miR-143, miR-145 localised to nuclei in the oesophageal squamous epithelium. In this study cytoplasmic staining could not be identified for miR-143, miR-145 or miR-215 in ISH carried out on sections from Barrett's oesophagus epithelia. Distinguishing clear nuclear and cytoplasmic staining in Barrett's oesophagus sections was not possible due to the majority of the cell being almost completely filled with mucus. The high mucus content compresses the cytoplasm and nucleus into a small area (Dr David Astill, histopathologist Dept of Anatomical Pathology, personal communication).

5.3 Discussion: miR-143, miR-145 and miR-215 act as tumour suppressors in oesophageal adenocarcinoma

miRNAs have been shown to act as tumour suppressors in many different cancers^{82, 245}. For miRNAs acting as tumour suppressors, decreased miRNA expression leads to loss of regulatory control of many cellular processes required for maintaining tissue homeostasis⁸². Chapter 3 describes decreased expression of miR-143, miR-145 and miR-215 in oesophageal adenocarcinoma compared with Barrett's oesophagus¹¹⁰. Decreased miRNA expression in oesophageal adenocarcinoma might provide an opportunity for biomarker development for use in the clinical assessment and management of oesophageal cancer. Also, investigation into the location of miRNA expression in Barrett's oesophagus and oesophageal adenocarcinoma might help identify where lost miRNA function might contribute to neoplastic progression, and also identify specific regions of the cancerous epithelium to target therapeutically. As Barrett's oesophagus can progress through varying grades of dysplasia to oesophageal adenocarcinoma, and decreased miRNA expression has been shown to contribute to cancer development, this study aimed to assess the consequences of decreased miRNA expression in oesophageal adenocarcinoma.

5.3.1 Proliferative and apoptotic effects of restoring miRNA expression in oesophageal adenocarcinoma

To investigate the effects of increasing the expression of miRNAs known to be down regulated in oesophageal adenocarcinoma, miR-143, miR-145 and miR-215 levels were increased in oesophageal adenocarcinoma cells (OE-19). Decreased proliferation and increased apoptosis is observed early in the progression of Barrett's oesophagus to oesophageal adenocarcinoma^{246, 247}. Given the known association of miR-143, miR-145 and miR-215 with proliferation and apoptosis, their function was assessed in the context of these cellular processes. Reduced proliferation and increased apoptosis was observed in OE-19 cells following over expression of miR-143, miR-145 and miR-215 mimics. These results support studies in other cancer cell models where increased miR-143, miR-145 or miR-215 expression has also been shown to reduce cell proliferation and increase apoptosis^{157, 207, 248-250}. Decreased

miR-143, miR-145 or miR-215 expression likely contributes to the aberrant regulation of proliferation and apoptosis in oesophageal adenocarcinoma and therefore, restoring this decreased miRNA expression may be of therapeutic benefit *in vivo*.

5.3.2 Loss of miRNA function in the crypts of Barrett's oesophagus epithelia may contribute to the development of oesophageal adenocarcinoma

To assess the location of miRNA function in Barrett's oesophagus and identify regions where loss of miRNA function might contribute to abnormal proliferation and apoptosis, in-situ hybridisation was used to probe for miR-143, miR-145 and miR-215. In Barrett's oesophagus miR-143, miR-145 and miR-215 staining intensity was greatest in the crypts of the epithelium. Therefore it is possible that these miRNAs might regulate proliferation or apoptosis within these areas. Dysplasia in Barrett's oesophagus, a key step in adenocarcinoma development, appears to originate from Barrett's oesophagus crypts²⁵¹, and the highest degree of abnormality is generally seen in the deep regions of crypts, apposed to surface epithelia²⁵². It is possible that loss of miR-143, miR-145 or miR-215 expression may occur in dysplastic crypts and this could disrupt the balance between proliferation and apoptosis, contributing to glandular crowding, a key hallmark of dysplasia²⁵¹. When assessing oesophageal sections from areas of high grade dysplasia miR-143, miR-145 and miR-215 staining was not detected suggesting that regulatory control of proliferation or apoptosis by these miRNAs may be lost prior to the development of oesophageal adenocarcinoma. However, while the observed decrease in miR-145 in dysplastic tissue is in keeping with work by Bansal et al.²⁵³, the ISH analysis of dysplastic tissue presented above was obtained from one patient and therefore future studies should assess multiple patients to provide more conclusive data.

5.3.3 miRNA directed changes in gene expression may contribute to altered proliferation and apoptosis

Global gene expression was assessed via mRNA array 24 hr after increasing miR-143, miR-145 or miR-215 levels to identify miRNA induced changes in gene expression that might contribute to the observed reduction in proliferation and/or increase in apoptosis.

Decreased H2AFX levels

Down regulation of H2A histone family, member X (*H2AFX*) mRNA expression was observed after increasing miR-145 levels. *H2AFX* has a role in cellular response to DNA damage²⁵⁴⁻²⁵⁶, and decreased *H2AFX* expression is associated with both increased rates of apoptosis and increased sensitivity to apoptotic induction^{257, 258}. Similarly, miR-145 expression is induced in response to DNA damage¹⁰⁶. Barrett's oesophagus epithelium is associated with high levels of DNA damage²⁵⁴ and miR-145 expression¹¹⁰. Elevated miR-145 expression in Barrett's epithelium may in part be due to exposure to acid and/or bile (See¹⁴ and increased miR-145 expression in patients with gastroesophageal reflux disease, chapter 4, Figure 4.2). Given that reduced *H2AFX* expression is observed after increasing miR-145 levels it is possible that a miR-145 mediated decrease in *H2AFX* levels might be an important contributor to regulating apoptosis after DNA damage caused by acid and/or bile exposure.

Decreased RTKN levels

Decreased RTKN mRNA and protein expression was observed after increasing miR-145 levels. Luciferase reporter assays were not used to confirm direct targeting of RTKN by miR-145 (See Wang et al.¹⁶⁰). However, the western blot analysis of protein expression provides strong support for direct targeting of RTKN by miR-145 in Barrett's oesophagus, with this function likely being lost in oesophageal adenocarcinoma.

Increased *RTKN* levels promote cell survival through *NFKB* dependent down regulation of anti-apoptotic genes²⁵⁹. Increased miR-145 expression has been shown to increase apoptosis and decrease proliferation in breast cancer cells by targeting *RTKN*¹⁶⁰. *RTKN* levels have not previously been studied in Barrett's oesophagus or oesophageal adenocarcinoma. However, *RTKN* levels are increased in gastric cancer promoting cell survival²⁶⁰. Further, miR-145 levels are decreased in this cancer.

The results of the current study did not provide support for miR-145 directing increased apoptosis. However, given the results by Wang et al.¹⁶⁰, they do indicate that increased miR-145 expression in oesophageal adenocarcinoma may contribute to the observed decrease in cell proliferation, at least in part through targeted repression of *RTKN*. ISH results suggest that the function of miR-145 is lost in high grade dysplasia (See²⁵³ and Figure 5.10B). Therefore, decreased miR-145 expression in dysplasia could result in a loss of regulatory control over *RTKN* and this may contribute to the abnormal levels of proliferation seen in dysplastic epithelia.

Decreased PABPC4 levels

Decreased poly(A) binding protein, cytoplasmic 4 (*PABPC4*) mRNA expression was observed after increasing miR-215 levels. Decreased *PABPC4* expression has been shown to direct reduced cell growth in E6 oncoprotein immortalized keratinocytes²⁶¹, at least in part by reducing telomerase reverse transcriptase (*hTERT*) activity. While *PABPC4* levels have not been assessed in dysplasia and oesophageal adenocarcinoma, *hTERT* activity is up regulated in these tissue types²⁶². Given that miR-215 has been shown by others to regulate cell proliferation²⁰⁷, decreased miR-215 expression in high grade dysplasia and oesophageal adenocarcinoma might lead to increases in *PABPC4* and *hTERT* expression, contributing to an increase proliferation.

miR-143 mediated apoptosis, links with CITED2 and HDAC7

Increased *CITED2* mRNA expression and decreased *HDAC7* protein expression was observed after increasing miR-143 levels. Decreased *CITED2* expression is associated with increased proliferation and invasive capacity in colon cancer²³⁶,

while increased *CITED2* expression promotes apoptosis in ulcerative colitis²³⁵. Therefore, targeted suppression of *CITED2* in oesophageal adenocarcinoma may be of therapeutic benefit.

Further, studies show that butyrate mediated HDAC inhibition triggers increased *CITED2* expression²³⁶. Also, selective inhibition of *HDAC7* alone induces apoptosis in uterine sarcoma²⁴⁴. Therefore, the decreased *HDAC7* levels seen after increasing miR-143 levels provide support for an apoptotic mechanism mediated by miR-143. This mechanism involves increased miR-143 expression, directing decreased *HDAC7* expression, which in turn increases *CITED2* expression to promote apoptosis. While this mechanism has not been linked with Barrett's oesophagus, studies by Gonzalez et al.²⁶³ have linked decreased *CITED2* expression with increased apoptosis in response to DNA damage, a hallmark of reflux exposure and a likely contributor to the development of Barrett's oesophagus^{14, 15, 254}. Therefore, this miR-143/*HDAC7*/*CITED2* mechanism of apoptosis might be an important regulator of apoptosis in Barrett's oesophagus. This mechanism may be inactivated due to decreased miR-143 expression in oesophageal adenocarcinoma, promoting apoptotic resistance and invasion.

KRAS and miR-143 mediated apoptosis

Western blot analysis identified increased *KRAS* protein levels. These results are not in keeping with those of others showing decreased *KRAS* expression after increasing miR-143 levels^{153, 245, 248}.

While it is unknown whether *KRAS* expression fluctuates in proliferating cell populations, we speculated that at the time of transfection, some cell populations might have expressed *KRAS* at higher levels than others. In light of this speculation, we hypothesized that these increased *KRAS* levels might confer a selective advantage.

Studies by Wislez et al.²⁶⁴ show that chemokine (C-X-C motif) receptor 2 (*CXCR2*) is induced in alveolar epithelial cells by *KRAS*. Interestingly, *CXCR2* expression has been shown to inhibit apoptosis in ovarian cancer²⁶⁵, and also protect against

apoptotic induction from interferon-gamma in mouse oligodendrocyte progenitor cells²⁶⁶. While *CXCR2* levels have not been studied in oesophageal adenocarcinoma, increased expression is observed in gastric cancer²⁶⁷. Taken together, the links between *KRAS* induced *CXCR2* expression, *CXCR2* mediated protection against apoptosis, and *CXCR2* over expression in gastric cancer, provide support for a mechanism where transfected cells with the highest levels of *KRAS* expression might be protected against miR-143 mediated apoptotic induction, at least in part via a *KRAS* mediated increase in *CXCR2* expression. While speculative, this mechanism of apoptotic protection could select for a population of cells with increased *KRAS* expression and account for the increase in *KRAS* protein expression observed after miR-143 transfection.

5.3.4 The fold increase in miR-143 post transfection was lower than miR-145 and miR-215

miR-143 directed repression of genes involved in regulating cell proliferation and apoptosis by miR-143 could not be validated by PCR or western blot analysis. However, in general, the increase in miR-143 levels after transfection were small when compared with the increased miRNA levels obtained after transfecting miR-145 or miR-215 (Figure 5.1). Also, miR-143 levels were not significantly increased in the RNA used for these experiments (Figure 5.1, miR-143 (3)).

While the increase in miR-143 levels after transfection was much lower than that of miR-145 or miR-215 a distinct decrease in proliferation and increase in apoptosis was observed. These cellular responses were likely mediated through changes in gene expression mediated by miR-143. The miR-143 directed increase in apoptosis, may contribute to the lower levels of miR-143 observed after transfection. As the first RNA sample was extracted 24 hr after transfection, it is possible that cells with high levels of miR-143 underwent apoptosis, detached from the cell culture plate into the culture media and were removed as the culture media was substituted with TRIzol[®] during RNA extraction (Methods, chapter 2, section 2.2.1). Future experiments should extract RNA at earlier time points post transfection to harvest cells before apoptosis occurs, as these cells likely have the highest levels of miR-143.

5.3.5 Robust mRNA array data would streamline the process of identifying miRNA targets

One aim of this study was to use an mRNA array to identify miRNA directed changes in gene expression that might contribute to reducing proliferation and/or increasing apoptosis. While the data generated from the mRNA array was sufficient to pursue this aim, a series of careful checks and selection criteria were required before changes in gene expression could be quantitatively validated.

A more robust array data set would streamline the processes and the checks required. To produce this data set, future experiments should aim to reduce variability. These experiments could assess larger numbers of experimental replicates (e.g. $n = 6 - 9$ samples) as this will increase the chance of identifying changes in mRNA expression using routine statistical analysis (Methods 2.1.10).

5.3.6 Summary

Results of this study have shown that decreased miRNA expression observed in oesophageal adenocarcinoma contributes to reduced apoptosis and proliferation *in vitro*. This reduction may be mediated through changes in gene expression directed by miR-143, miR-145 or miR-215. Expression of miR-143, miR-145 and miR-215 appeared to be most pronounced in the glands of the Barrett's oesophagus epithelium and expression of these miRNAs appears to be lost prior to the development of oesophageal adenocarcinoma. In the context of oesophageal adenocarcinoma restoring the expression of miR-143, miR-145 or miR-215 may be of therapeutic benefit although the next step in proving this will require analysis of these miRNAs *in vivo*. Further, these results demonstrate the biological significance of miR-143, miR-145 and miR-215 in oesophageal adenocarcinoma development, thereby providing support for the use of these miRNAs as diagnostic biomarkers in the Barrett's oesophagus – dysplasia – adenocarcinoma sequence.

Chapter 6

The expression of miR-200 family members is downregulated upon neoplastic progression of Barrett's oesophagus.

6.1 Introduction

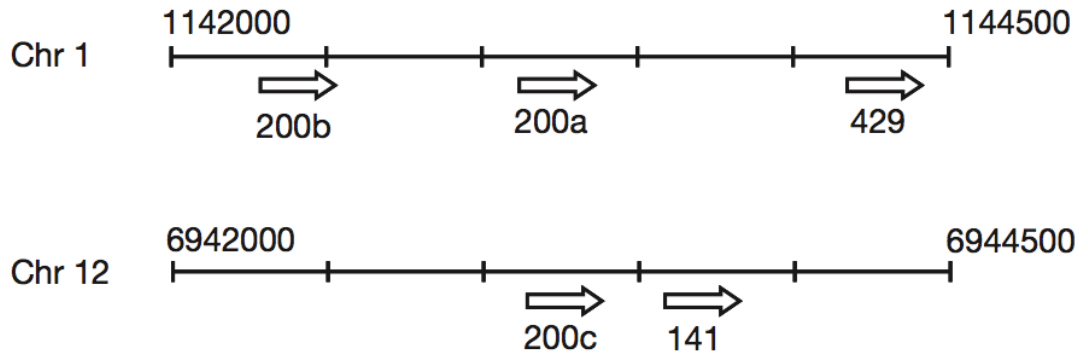
The epithelium associated with Barrett's oesophagus possesses secretory and absorptive cell types, and these closely resemble those found in normal gastric and intestinal epithelia^{22, 23}. mRNA expression profiling studies confirm its similarity to gastric and duodenal epithelia^{24, 268, 269}. However, a specific set of genes is also expressed in Barrett's oesophagus, including genes associated with alterations in cell cycle, proliferation, apoptosis, stress response, and cellular migration pathways, and these distinguish it from all related gastrointestinal mucosae²⁴. Other studies have confirmed unique phenotypic characteristics of Barrett's epithelium that correspond with this specific gene expression profile. For example, unlike gastric and duodenal epithelia, cellular proliferation in Barrett's oesophagus continues along the upper crypt and at the luminal surface, possibly due to abnormal cell cycle entry or exit¹⁴¹. Further, Barrett's oesophagus epithelium expresses unusually high levels of anti-apoptotic proteins²⁷⁰ and can mount a unique anti-apoptotic and proliferative response to reflux^{142-144, 271}.

The progression of Barrett's oesophagus to dysplasia involves increased abnormalities in cell cycle and overall proliferation¹³⁸. Neoplastic progression of Barrett's oesophagus commonly occurs without obvious symptoms, and at the time of diagnosis most patients with oesophageal adenocarcinoma have local invasion or metastases²⁷². A cellular process known as the epithelial to mesenchymal transition (EMT) appears to be a key step in tumour invasion²⁷³. As a result of this process there is a switch in cell phenotype where cells change from an epithelial to an invasive mesenchymal phenotype²⁷³. Several lines of evidence suggest that EMT is required for local invasion and metastasis²⁷⁴. EMT may involve inhibition of E-

cadherin expression and transition from epithelial to a fibroblastic cell type, with associated alterations in cellular adhesion and migration²⁷⁴. Evidence for EMT has been shown in numerous adenocarcinomas including those of the breast, prostate and colon^{273, 275}. In addition, other studies have presented immunohistochemical, gene expression and cell line data that suggest a role for EMT in oesophageal adenocarcinoma^{276, 277}. Initiation of EMT appears to require changes in cell signalling to promote an inflammatory tumour microenvironment²⁷⁸. Inside the tumour microenvironment of invasive cancers, increased expression of transforming growth factor beta (*TGFB*), an inflammatory mediator thought to promote EMT is commonly observed^{276, 279}. *TGFB* is of particular interest in EMT as it is known to mediate decreased expression of key proteins and miRNAs required for maintaining an epithelial phenotype^{276, 279-282}.

The miR-200 family of microRNAs (miR-141, 200a, 200b, 200c and 429) are key regulators/inhibitors of EMT, and act to maintain the epithelial phenotype by targeting the expression of the E-cadherin transcriptional repressors *ZEB1* and *ZEB2*^{116, 280, 283}. Accordingly, the number of studies by others reporting down-regulation of miR-200 family expression in cancer is increasing^{116, 280, 283, 286-289}. In addition, members of the miR-200 family have recently been shown to affect other cell behaviours including proliferation, cell cycle and apoptosis^{284, 290, 291}. MicroRNAs belonging to the miR-200 family are expressed on two separate transcripts, with miR-200a, miR-200b and miR-429 residing on chromosome one and miR-141 and miR-200c residing on chromosome 12 (Figure 6.1). This separate expression may explain why selective miR-200 family member down-regulation has been reported in other studies^{284, 292}. These separate studies observe decreased miR-141 expression in gastric cancer²⁸⁴ and decreased miR-200c expression in ovarian, breast or endometrial carcinoma²⁹². In addition, the miR-200 family share almost complete sequence homology (Figure 6.2), suggesting that there may be redundancy in gene regulation by miR-200 family members.

Figure 6.1: The chromosomal locations of miR-200 family members include miR-200a, miR-200b and miR-429 on a transcript from chromosome one and miR-141 and miR-200c on a transcript from chromosome 12.



(Reproduced from: Gregory et al.¹¹⁶)

Figure 6.2: The miR-200 family members share almost complete sequence homology. A single nucleotide difference (shown red) is observed in the seed region of miR-200a and miR-141.

```

hsa-miR-200b  5' UAAUACUGCCUGGUAAUGAUGAC 3'
hsa-miR-429  5' UAAUACUGUCUGGUAAAACCGU 3'
hsa-miR-200c 5' UAAUACUGCCGGGUAAUGAUGG 3'

hsa-miR-200a 5' UAACACUGUCUGGUAACGAUGU 3'
hsa-miR-141  5' UAACACUGUCUGGUAAGAUGG 3'
  
```

(Reproduced from Gregory et al.¹¹⁶ with nucleotide 'C' coloured red).

This study was designed because of the unique gene expression profile and cellular behaviour in Barrett's oesophagus epithelium, the phenotypic features that characterise its neoplastic progression, and the potential relevance of EMT to oesophageal adenocarcinoma. This study was driven by the hypothesis that Barrett's oesophagus epithelium may possess a miR-200 expression profile different to gastric and duodenal epithelia, and that down regulation of miR-200 family expression may occur upon progression to oesophageal adenocarcinoma. To investigate this hypothesis, this study aimed to determine the expression of miR-200 family members in gastric, duodenal and Barrett's oesophagus epithelium, and to assess changes in their expression upon neoplastic progression of Barrett's oesophagus.

The aims of the study were to:

- 1) Assess and compare miR-200 family expression in non-cancerous Barrett's oesophagus epithelium with gastric and duodenal epithelium.
- 2) Assess and compare miR-200 family expression in non-cancerous Barrett's oesophagus epithelium with oesophageal adenocarcinoma epithelium, and relate this to the expression of *ZEB1* and *ZEB2*.
- 3) Assess whether changes in miR-200 family expression might occur early in the development of oesophageal adenocarcinoma by assessing miR-200 family expression in two dysplastic cell lines and Barrett's oesophagus biopsies from patients with oesophageal adenocarcinoma.

6.2 Tissue collection and processing

Tissues from patients diagnosed with either Barrett's oesophagus (n=17) or oesophageal adenocarcinoma (n=20) were collected at endoscopy or after surgical resection as described in chapter 3, section 3.2. Details of the collection process, patient clinical details, tissue specimen histology (chapter 3, section 3.2), and RNA isolation from tissues (methods, chapter 2, section 2.2.1) have been described earlier in the thesis. RNA was also extracted from cell lines derived from benign Barrett's

oesophagus (Qh) and high grade dysplastic (Ch and Gi) epithelium²⁹³ using TRIzol[®] (methods, chapter 2, section 2.2.1). Dr George Mayne extracted RNA from the Qh, Ch and Gi cell lines.

6.2.1 Quantitative RT-PCR analysis of miR-200 family, ZEB1 and ZEB2 expression

miR-200 expression was determined using commercially available TaqMan[®] miRNA assays (methods, chapter 2, section 2.2.2). *ZEB1* and *ZEB2* mRNA expression was assessed using the Quantiscript[®] RT kit for reverse transcription and the Quantitect[®] SYBR Green mastermix for PCR (methods, chapter 2, section 2.2.3). Statistical analysis and correlation methods are described in methods, chapter 2, section 2.2.7. In addition to miR-200 expression, we also tested miR-215 because decreased expression of this microRNA was observed in oesophageal adenocarcinoma (chapter 3, Table 3.1) and it was also recently shown to directly target *ZEB2*¹⁷⁰.

6.3 Results: miR-200 family expression in Barrett's oesophagus, gastric and duodenal epithelia

Quantitative RT-PCR showed levels of miR-141 and 200c were significantly lower in Barrett's oesophagus epithelium compared with gastric and duodenal epithelia (Table 6.1, Figures 6.3 - 6.4). miR-200a and miR-200b expression was significantly lower in Barrett's oesophagus epithelium than in gastric epithelium, but did not differ in expression between Barrett's oesophagus and duodenal epithelia (Table 6.1). The expression level of miR-429 was not significantly different across these three epithelial types (Table 6.1).

Table 6.1: TaqMan[®] analysis of relative miR-200 family member levels in Barrett's oesophagus, gastric and duodenal epithelia.

Relative expression for each epithelial tissue type				
miRNA	Duodenal (n=10)	Barrett's oesophagus (n=17)	Gastric (n=15)	p-value (Kruskal- Wallis Test)
miR-141	0.076 (0.039,0.167)	0.026 (0.023, 0.036)	0.051 (0.042, 0.092)	0.0002 ^{*#}
miR-200a	0.148 (0.067, 0.340)	0.148 (0.126, 0.177)	0.247 (0.154, 0.509)	0.0314 [#]
miR-200b	0.796 (0.606, 1.276)	0.833 (0.750, 0.993)	1.233 (1.089, 1.963)	0.0011 [#]
miR-200c	2.700 (1.890, 3.511)	1.049 (0.929, 1.170)	2.335 (1.792, 2.773)	<0.0001 ^{*#}
miR-429	0.095 (0.042, 0.070)	0.070 (0.061, 0.087)	0.078 (0.072, 0.153)	0.259

Relative expression values are median (95% confidence intervals). The group p-value is the result of a Kruskal-Wallis test across the three tissue groups. Significant differences were identified by post-hoc testing by Holm-Bonferroni method for: ^{*}Duodenal vs Barrett's oesophagus mucosa - miR-141 (p=0.0008) & miR-200c (p<0.0001), and [#]Gastric vs Barrett's oesophagus mucosa - miR-141 (p=0.0004) miR-200a (p=0.0078), miR-200b (p=0.0001), & miR-200c (p<0.0001).

Figure 6.3: TaqMan[®] analysis of relative miR-141 levels in Barrett's oesophagus, gastric and duodenal epithelia. Data presented is median miR-141 expression normalised to RNU44 levels. 95% confidence intervals are shown for each tissue group.

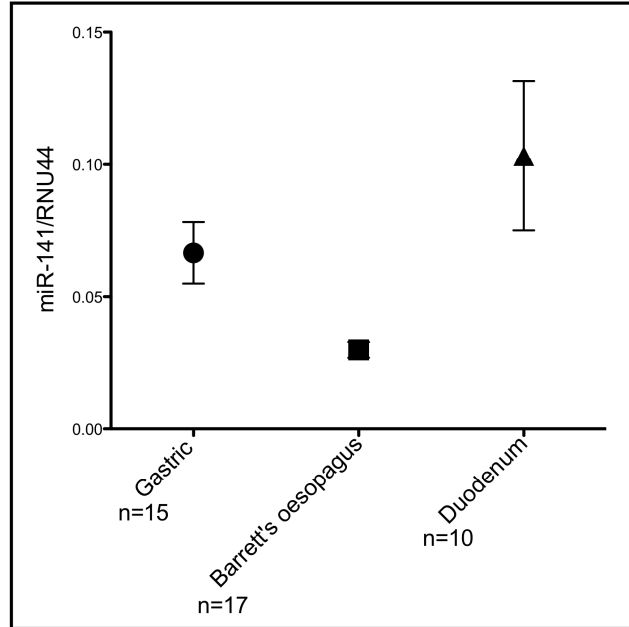
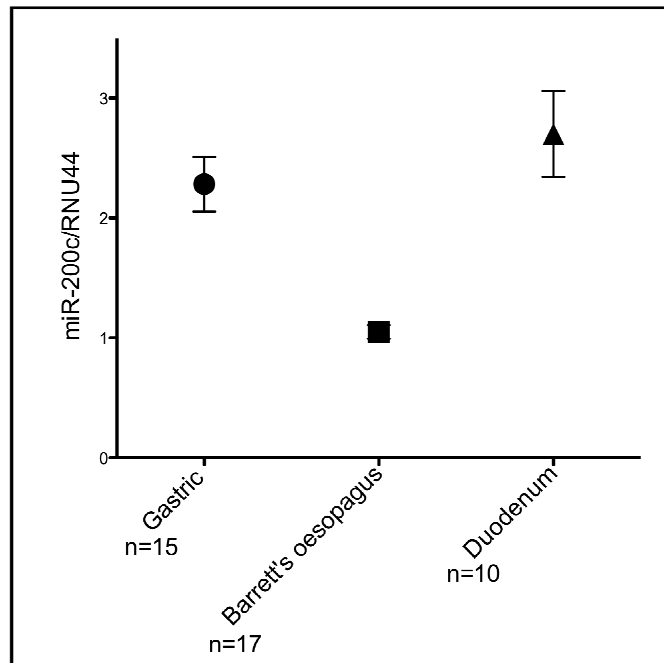


Figure 6.4: TaqMan[®] analysis of relative miR-200c levels in Barrett's oesophagus, gastric and duodenal epithelia. Data presented is median miR-200c expression normalised to RNU44 levels. 95% confidence intervals are shown for each tissue group.



6.3.1 Predicted implications of reduced miR-200 family expression in Barrett's oesophagus

Core Ingenuity Pathway Analysis (Methods, chapter 2, section 2.2.11) on predicted targets of miR-141 and miR-200c were performed to determine likely biological effects of the reduced miRNA expression. Target prediction using miRecords, selecting predictions that were confirmed by five or more prediction algorithms identified 272 potential gene targets for miR-141 and 429 potential gene targets for miR-200c. Ingenuity Pathways Analysis matched a number of the predicted targets for miR-141 or miR-200c to known biological networks and ranked based on their statistical power. The top biological networks for these targets are illustrated in Figures 6.5 and 6.6, and the top molecular and cellular functions associated with these targets are listed in Table 6.2. Of the targets listed in Figures 6.5 and 6.6, nine show increased expression in Barrett's oesophagus^{16, 24, 142, 294, 295} and are predicted targets (direct or indirect/downstream genes) of miR-141 and/or miR-200c (Table 6.3).

Ingenuity Pathway Analysis predicted that the top associated network functions for miR-141 (Figure 6.5) were gene expression, cell death and cell cycle ($p=1 \times 10^{-35}$). The top associated biological network functions for miR-200c (Figure 6.6) were cell morphology, cellular assembly and organisation, as well as cellular function and maintenance ($p=1 \times 10^{-38}$). The p-values are derived from a Right-tailed Fisher's exact test to calculate the probability that each predicted miRNA target matches the ascribed network function due to chance alone.

Figure 6.6: Shows the top associated biological network function for miR-200c (cell morphology, cellular assembly and organisation). Predicted targets of miR-200c are highlighted in grey. Uncoloured entries represent molecules that are associated with the pathway but are not predicted miR-200c.

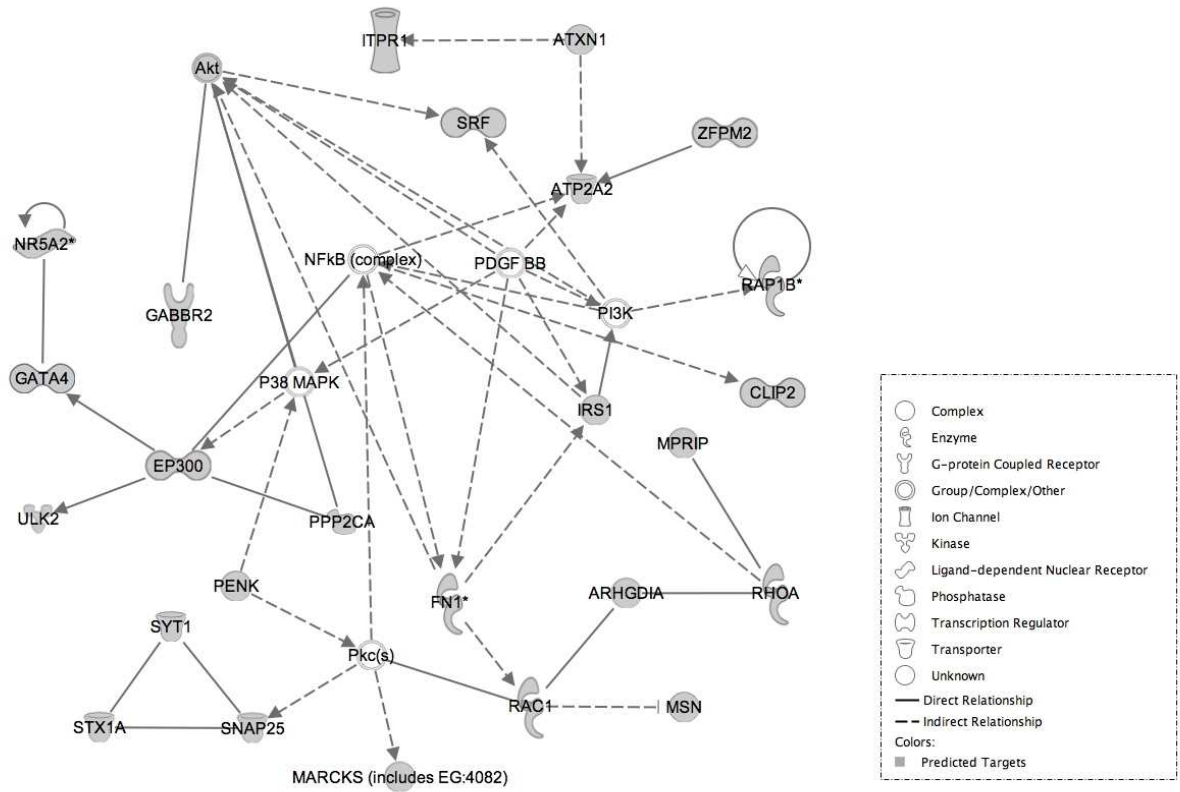


Table 6.2: Top molecular and cellular functions of predicted miR-141 and miR-200c gene targets generated from an Ingenuity Pathways Core Analysis. Predicted targets for miR-141 and miR-200c are grouped according to their known molecular and cellular function. All molecules grouped by molecular and cellular function were tested for statistical significance using a Fisher's exact test and the resulting p-value is shown below.

miRNA	Molecular and Cellular Functions	Molecules Involved	p-value
miR-141	Cell Cycle	41	1.90E-07 - 2.82E-02
	Gene Expression	53	4.94E-07 - 2.82E-02
	Cellular Movement	39	2.45E-05 - 2.82E-02
	Cellular Assembly and Organisation	61	2.88E-04 - 2.82E-02
	Cellular Growth and Proliferation	68	2.88E-04 - 2.28E-02
miR-200c	Gene Expression	84	1.37E-09 - 2.32E-02
	Cellular Growth and Proliferation	108	5.65E-05 - 2.32E-02
	Cell Cycle	53	9.17E-05 - 2.32E-02
	Cell Death	95	9.62E-05 - 2.32E-02
	Cellular Assembly and Organisation	55	1.19E-04 - 2.32E-02

The top five functions associated with the predicted targets of miR-141 and miR-200c, as determined by Ingenuity Pathway Analysis, are shown. For each miRNA the molecular and cellular functions are ranked according to their p-value.

Table 6.3: Lists the genes predicted by the Ingenuity Pathway Analysis to both be, up regulated in response to decreased miR-141 or miR-200c expression and are known to be up regulated in Barrett’s oesophagus. In addition, this table highlights whether these genes are predicted by miRecords to be direct targets of miR-141 or miR-200c, or whether Ingenuity Pathways Analysis predicted indirect/downstream targeting.

Gene Name	Gene Symbol	miRecords Predicted target of	IPA predicted indirect/downstream target
Mitogen Activated Protein Kinase 1	ERK	-	miR-141
Mitogen Activated Protein Kinase 14	p38	-	miR-141/miR-200c
Mitogen Activated Protein Kinase 8	JNK	miR-141	-
Protein Kinase C	PRKCE	miR-141	-
Phosphoinositide 3-kinase	PI3K	-	miR-141/miR-200c
v-akt murine thymoma viral oncogene homologue	AKT	miR-200c	-
Nuclear Factor Kappa Beta	NFKB	-	miR-141/miR-200c
Jun proto-oncogene	AP1	miR-141	-
Fibronectin	FN1	miR-200c	-

6.3.2 miR-200, ZEB1 and ZEB2 expression in Barrett's oesophagus and oesophageal adenocarcinoma

Expression of all members of the miR-200 family was significantly lower in oesophageal adenocarcinoma compared with Barrett's oesophagus epithelium (Table 6.4, Figures 6.7 - 6.11). The median expression of all miR-200 family members was lower in Barrett's oesophagus epithelium proximal to oesophageal adenocarcinoma than in Barrett's epithelium from patients without cancer or dysplasia. However, after post-hoc analysis, only the difference in miR-200c expression was statistically significant (Table 6.4, Figure 6.12). To determine whether this could indicate down-regulation of miR-200 expression in dysplasia, prior to the development of adenocarcinoma, miR-200 family expression was further assessed in a non-dysplastic Barrett's oesophagus derived cell line (Qh), and two cell lines derived from Barrett's oesophagus with high-grade dysplasia (Ch, Gi). Figure 6.13 shows that the expression of all miR-200 members was markedly reduced in both dysplastic cell lines compared to expression in the benign Barrett's oesophagus cell line.

Table 6.4: TaqMan[®] analysis of relative miR-200 family member levels in oesophageal adenocarcinoma tissue and Barrett’s oesophagus tissue from patients with and without concurrent cancer.

Relative expression for each tissue type				
miRNA	BE n=17	Adeno- carcinoma n=20	BE_C n=9	p-value (Kruskal- Wallis Test)
miR-141	0.026 (0.023, 0.036)	0.012 (0.011, 0.025)	0.015 (0.01, 0.04)	0.03398*
miR-200a	0.148 (0.126, 0.177)	0.057 (0.013, 0.042)	0.08 (0.017, 0.201)	0.00079*
miR-200b	0.833 (0.75, 0.993)	0.387 (0.316, 0.572)	0.399 (0.258, 1.13)	0.00068*
miR-200c	1.05 (0.929, 1.170)	0.551 (0.461, 0.939)	0.662 (0.438, 0.965)	0.00323* [#]
miR-429	0.07 (0.062, 0.087)	0.039 (0.029, 0.06)	0.042 (0.036, 0.09)	0.01355*

Relative expression values are median (95% confidence intervals). BE = Barrett’s oesophagus epithelium from individuals without cancer, BE_C = Barrett’s epithelium taken proximal to adenocarcinoma and confirmed by histology to be free of invasive cancer. The group p-value is the result of a Kruskal-Wallis test across the three tissue groups. Significant differences were identified by post-hoc testing using the Holm-Bonferroni method for: *Adenocarcinoma vs Barrett’s oesophagus mucosa from individuals without cancer - miR-141 (p=0.0126), miR-200a (p=0.0001), miR-200b (p<0.0001), & miR-200c (p=0.0014) & miR-429 (p=0.0031), and [#]Barrett’s oesophagus mucosa from individuals with or without cancer - miR-200c (p=0.0191).

Figure 6.7: TaqMan[®] analysis of relative miR-141 levels in Barrett's oesophagus and oesophageal adenocarcinoma tissues. Data presented is median miR-141 expression normalised to RNU44 levels. 95% confidence intervals are shown for each tissue group.

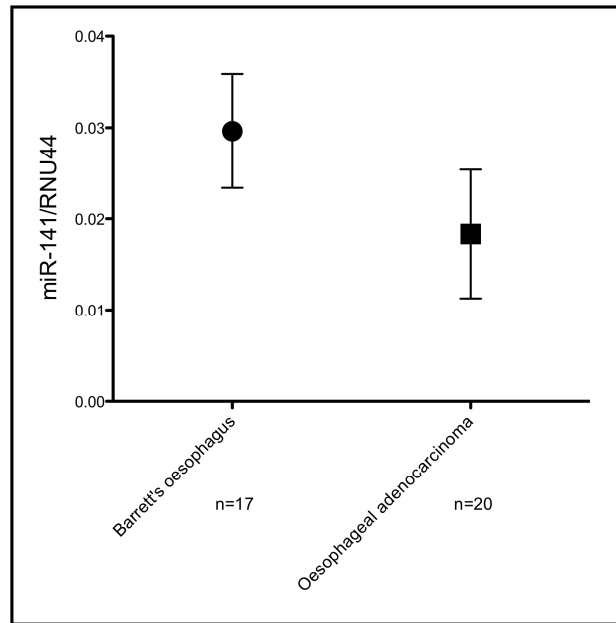


Figure 6.8: TaqMan[®] analysis of relative miR-200a levels in Barrett's oesophagus and oesophageal adenocarcinoma tissues. Data presented is median miR-200a expression normalised to RNU44 levels. 95% confidence intervals are shown for each tissue group.

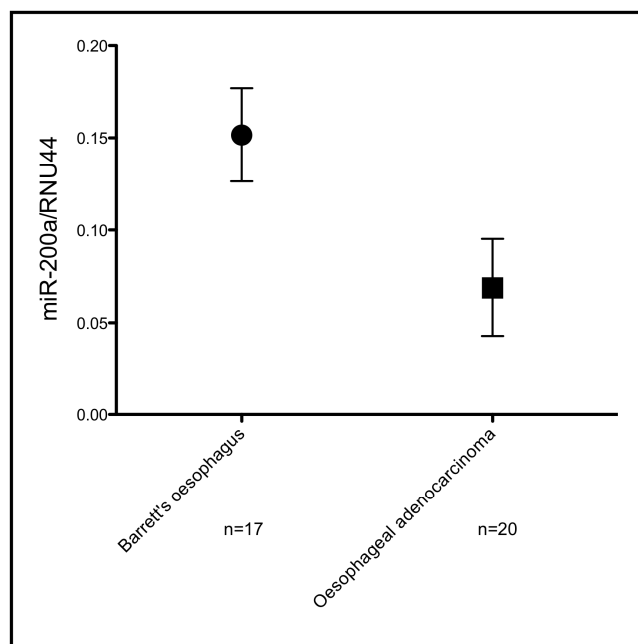


Figure 6.9: TaqMan[®] analysis of relative miR-200b levels in Barrett's oesophagus and oesophageal adenocarcinoma tissues. Data presented is median miR-200b expression normalised to RNU44 levels. 95% confidence intervals are shown for each tissue group.

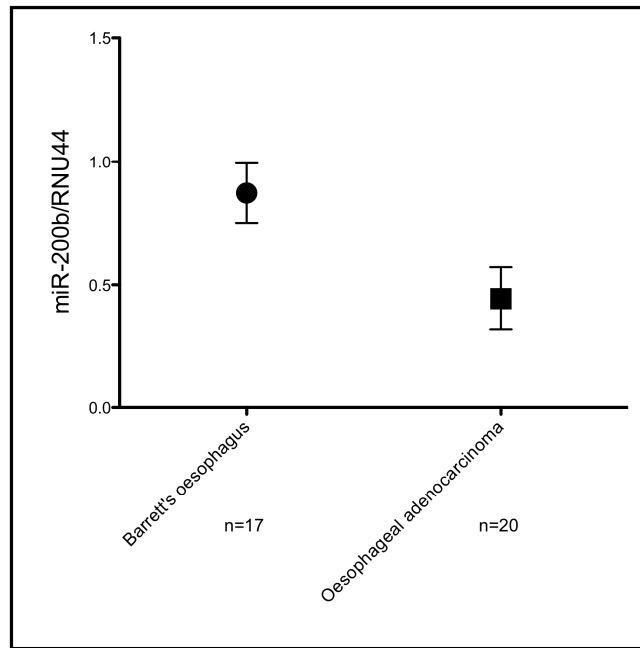


Figure 6.10: TaqMan[®] analysis of relative miR-200c levels in Barrett's oesophagus and oesophageal adenocarcinoma tissues. Data presented is median miR-200c expression normalised to RNU44 levels. 95% confidence intervals are shown for each tissue group.

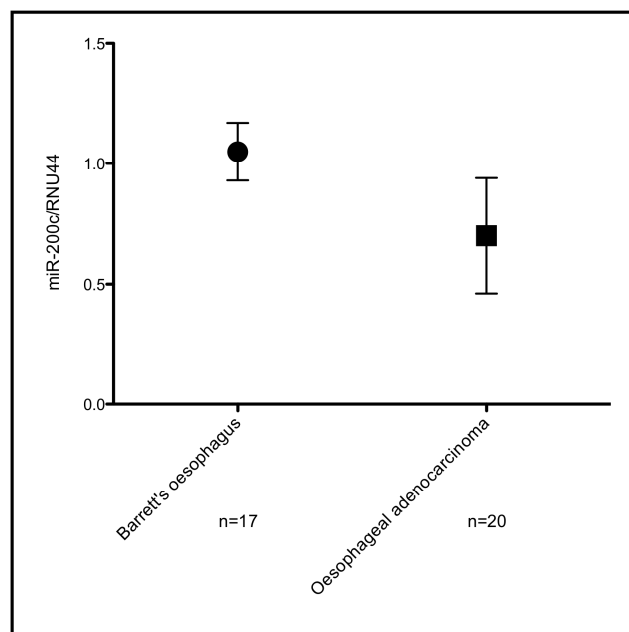


Figure 6.11: TaqMan[®] analysis of relative miR-429 levels in Barrett's oesophagus and oesophageal adenocarcinoma tissues. Data presented is median miR-429 expression normalised to RNU44 levels. 95% confidence intervals are shown for each tissue group.

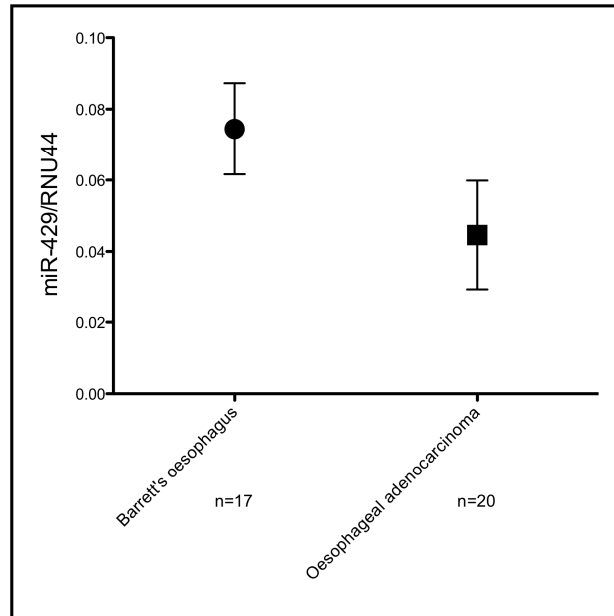


Figure 6.12: TaqMan[®] analysis of relative miR-200c levels in Barrett's oesophagus tissue from patients with (Barrett's oesophagus (EAC)) and without (Barrett's oesophagus) concurrent cancer. Data presented is median miR-200c expression normalised to RNU44 levels. The mean standard error is shown for each tissue group.

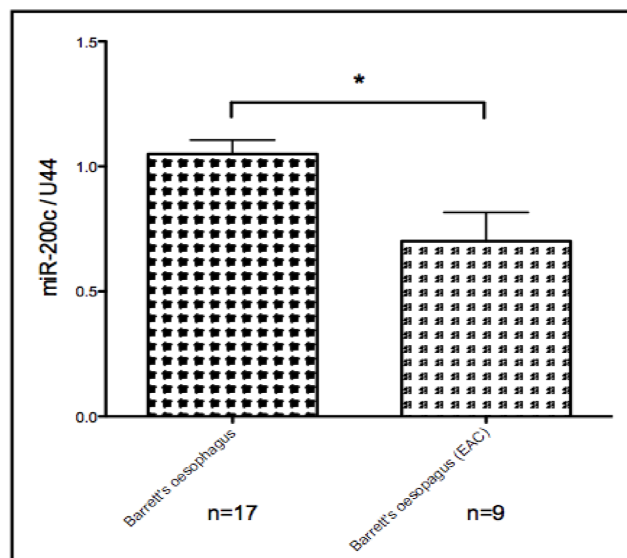
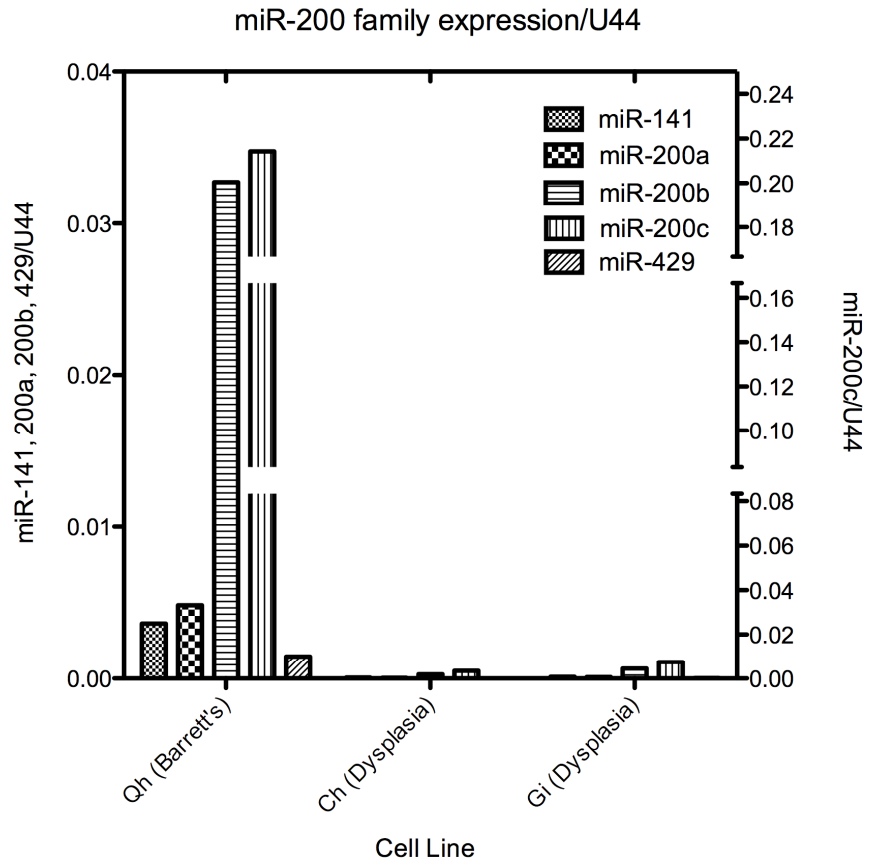


Figure 6.13: TaqMan[®] analysis of relative miR-200 family member levels in benign Barrett's (Qh) and dysplastic cell lines (Ch & Gi). Relative expression of miR-141, miR-200a, miR-200b and miR-429 is shown on the left hand y-axis. Relative expression of miR-200c is shown on the right hand y-axis.



6.3.3 The miR-200 family and the EMT in oesophageal adenocarcinoma

To assess molecular evidence for the miR-200 mediated switch for EMT in oesophageal adenocarcinoma, the mRNA expression of miR-200 targets, *ZEB1* and *ZEB2*, was measured. *ZEB1* and *ZEB2* expression was significantly higher in oesophageal adenocarcinoma compared to Barrett's oesophagus epithelium from patients without cancer or dysplasia (Figures 6.14 and 6.15). There were significant inverse correlations between the expression of *ZEB1/ZEB2* and the expression of some miR-200 members (Table 6.5). miR-215 and *ZEB2* expression were inversely correlated (Table 6.5).

Table 6.5: *ZEB1* and *ZEB2* expression in Barrett's epithelium and oesophageal adenocarcinoma. The fold increase (\uparrow) in median *ZEB1* and *ZEB2* expression in oesophageal adenocarcinoma vs Barrett's oesophagus mucosa from individuals without cancer, and the p-value derived using the Mann-Whitney test are given. Spearman correlations (R= Spearman's rho) between *ZEB1/2* expression and each miR-200 member as well as miR-215, with associated p-values, are also shown.

	Fold \uparrow	miR-141	miR-200a	miR-200b	miR-200c	miR-429	miR-215
ZEB1	2.9 p<0.0001	R= -0.2 p=0.341	R= -0.4 p=0.046	R= -0.5 p=0.009	R= -0.5 p=0.006	R= -0.3 p=0.159	R= -0.3 p=0.152
ZEB2	1.5 p=0.029	R= -0.3 p=0.101	R= -0.3 p=0.085	R= -0.5 p=0.008	R= -0.5 p=0.015	R= -0.4 p=0.067	R= -0.4 p=0.044

Figure 6.14: TaqMan[®] analysis of relative *ZEB1* levels in Barrett's oesophagus and oesophageal adenocarcinoma tissues. Data presented is median *ZEB1* expression normalised to 18S levels. 95% confidence intervals are shown for each tissue group.

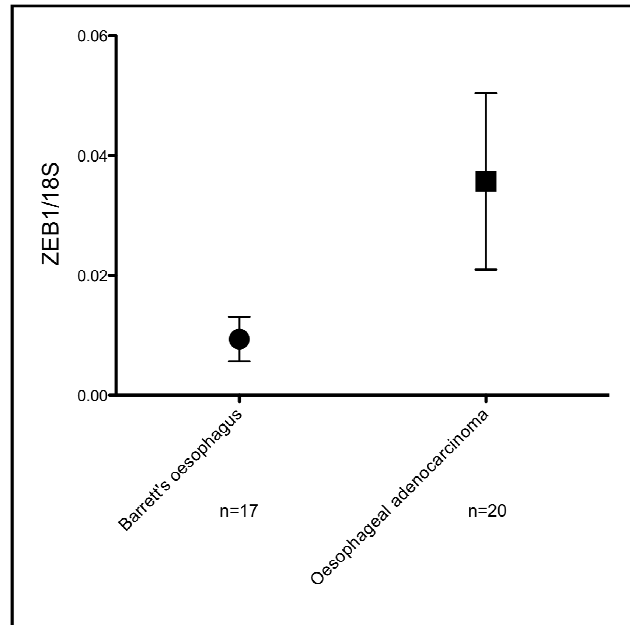
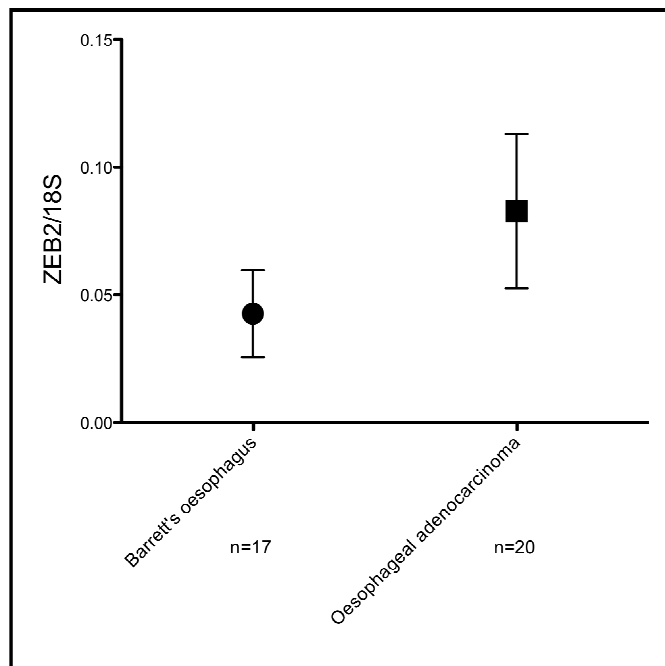


Figure 6.15: TaqMan[®] analysis of relative *ZEB2* levels in Barrett's oesophagus and oesophageal adenocarcinoma tissues. Data presented is median *ZEB2* expression normalised to 18S levels. 95% confidence intervals are shown for each tissue group.



6.4 Discussion

In this study miR-141 and miR-200c were shown to be expressed at lower levels in Barrett's oesophagus epithelium, compared to normal gastric and duodenal epithelia. Bioinformatic analysis indicated this might contribute to the cell cycle, stress response (proliferation, apoptosis), and cellular migration behaviors, which are known to make Barrett's oesophagus epithelium different to gastric and duodenal epithelia^{24, 141-144, 270, 271, 296}. The reduced miR-200 levels that were observed in Barrett's oesophagus epithelium adjacent to adenocarcinoma, and in cell lines derived from Barrett's oesophagus with high-grade dysplasia, suggested an association between down-regulation of miR-200 expression and neoplastic progression in Barrett's oesophagus. The increased expression of *ZEB1* and *ZEB2* in oesophageal adenocarcinoma, and their inverse correlations with miR-200 expression, are consistent with induction of EMT mediated by loss of miR-200 expression. Taken together with the known biological processes that are regulated by the miR-200 family^{284, 290, 291}, our study provides evidence for the influence of these miRNAs in regulating the unique gene expression²⁴ and phenotypic traits^{24, 141-144, 270, 271, 296} characteristic of benign Barrett's oesophagus epithelium, as well as features relevant to neoplastic progression¹³⁸. Further, our data indicate that a microRNA 'switch' for inducing EMT¹¹⁶ might be activated during the development of oesophageal adenocarcinoma.

It is interesting to note in our previous array study that we did not identify significantly reduced miR-200 expression in oesophageal adenocarcinoma. **TAKE section from BJS paper justification for miR-215 not on array but in PCR.**

6.4.1 Decreased miR-141 and miR-200c expression in Barrett's oesophagus

Although the miR-200 family show some redundancy in seed sequence, and therefore the genes they target, they act co-operatively to control the expression of their targets. A change in expression of just one family member is sufficient to alter target transcript levels¹¹⁶. miR-141 and miR-200c are known to modulate apoptosis,

cell cycle, proliferation, and cellular migration through regulation of their target genes^{284, 290, 291}. Several *in vivo* and *in vitro* studies have elucidated the signalling pathways that are activated in Barrett's epithelium and are responsible for its unique anti-apoptotic and proliferative responses to reflux induced stress. These include the three mitogen activated protein kinases (MAPK) *ERK*, *p38* and *JNK*¹⁶; protein kinase C (*PRKCE*)¹⁴³; phosphatidylinositol 3-kinases (*PI3K*) and downstream v-akt murine thymoma viral oncogene homolog 1 (*Akt*)²⁹⁴; as well as transcription factors *NFKappa-B*²⁹⁵ and jun proto-oncogene (*AP-1*)²⁹⁴. Combined target prediction and Ingenuity Pathway Analysis predicted indirect (or direct in the case of *Akt*) targeting of *all* of the aforementioned genes in the top associated network functions of either miR-141 or miR-200c, or both miRNAs. Overall, this suggests that reduced miR-141 and miR-200c expression in Barrett's oesophagus epithelium compared with gastric and duodenal epithelia might activate molecular pathways that are known to promote the specific response of Barrett's oesophagus epithelium to the insult of gastro-oesophageal reflux.

6.4.2 Fibronectin is a predicted target of miR-200c

The Ingenuity Pathways Analysis also predicted *direct* targeting and down-regulation of fibronectin by miR-200c, and this was evident in the top associated network. A recent study showed that fibronectin expression is reduced in cell lines in direct response to miR-200c expression²⁹². Therefore it is reasonable to expect that fibronectin expression should be higher in Barrett's oesophagus epithelium than in gastric and duodenal epithelia, due at least partly to reduced miR-200c expression in Barrett's oesophagus. In agreement with this, fibronectin is in the subset of expressed genes that separates Barrett's oesophagus epithelium from gastric or duodenal epithelium²⁴. Fibronectin has key roles in cellular adhesion and migration²⁹⁷. In the development of Barrett's oesophagus its expression is proposed to help facilitate expansion of epithelial cell populations in order to replace areas of denuded squamous epithelium with metaplastic cells²⁴. Further, fibronectin expression contributes to increased proliferative and anti-apoptotic behaviour through *NFKappa-B* and *PI3K* signalling²⁹⁸. Taken together, these observations lend support to the biological relevance of the bioinformatics based approach, and further

highlight a likely pro-proliferation, anti-apoptotic role for reduced miR-200c expression in Barrett's oesophagus. They provide a strong impetus for experimental validation of these predictions.

6.4.3 miR-200c and dysplastic Barrett's oesophagus

The development of high grade dysplasia significantly increases the risk of progression to oesophageal adenocarcinoma^{299, 300}. Features of dysplastic epithelium, that make it distinct from benign Barrett's oesophagus epithelium, include increased proliferative and anti-apoptotic behaviours¹³⁸. This study shows that miR-200c expression is down-regulated in Barrett's oesophagus sampled from patients with a concurrent oesophageal cancer, and the entire miR-200 family was down-regulated in cell lines derived from patients with high grade dysplasia. The Ingenuity Pathway Analysis indicates this could result in the molecular events known to contribute to the features of dysplastic Barrett's oesophagus, including increased signalling through MAPK pathways³⁰¹, increased activation and expression of *NFKappa-B*^{59, 302}, and increased activation of *Akt*^{301, 303}. Activation of *Akt* is stimulated by interaction of the obesity related hormone leptin and its receptor, and this results in increased proliferation and resistance to apoptosis in Barrett's oesophagus derived cancer cell lines³⁰³. The leptin receptor is down-regulated *in vitro* in response to miR-200c expression²⁹², and our miRecords searches predicted direct targeting of the leptin receptor by miR-200c. Although speculative, reduced miR-200 family expression in dysplasia could be an important mechanism for leptin receptor mediated activation of *Akt*, and this may contribute to the established link between obesity and an increased risk of oesophageal adenocarcinoma⁷⁸. In further support of the relevance of decreased miR-200 expression to the molecular features of neoplastic progression of Barrett's oesophagus, three gene transcripts (early growth response 3 (*EGR3*), heparan sulfate (glucosamine) 3-O-sulfotransferase 1 (*HS3ST1*) and ribosomal protein S6 kinase, 70kDa, polypeptide 1 (*RPS6KB1*)), listed in miRecords to be targets of miR-200c, were present in a panel of 18 transcripts shown to be up regulated in Barrett's epithelium from which cancer had arisen compared with benign Barrett's oesophagus epithelium³⁰⁴.

6.4.4 The miR-200 family - ZEB1, ZEB2 feedback loop and and EMT in oesophageal adenocarcinoma

Down-regulation of E-cadherin expression, via transcriptional repression, is a central mechanism for EMT²⁷⁴. ZEB1 and ZEB2 are amongst a group of transcription factors that repress transcription of E-cadherin²⁷⁴. *ZEB1* and *ZEB2* are targets of the miR-200 family, and an increase in ZEB1 and ZEB2 activity caused by down-regulation of miR-200 expression is sufficient to induce EMT¹¹⁶. EMT promoted by down-regulation of the miR-200 family has now been implicated as an important mechanism for invasion and metastasis in several cancers^{116, 286-289}. Previous epithelial and mesenchymal cell marker studies have provided evidence for the involvement of EMT in the development of oesophageal adenocarcinoma^{276, 277}, but to my knowledge no studies have investigated loss of miR-200 mediated control of *ZEB1* and *ZEB2* expression as a possible mechanism for EMT in this disease. This study has identified down-regulation of the entire miR-200 family and up-regulation of *ZEB1* and *ZEB2* transcription levels upon progression of Barrett's oesophagus to adenocarcinoma. Also, significant inverse correlations were observed between the expression of miR-200 members and *ZEB1/ZEB2* transcripts. miR-215 expression, which I have shown to be down-regulated in neoplastic progression of Barrett's oesophagus, was also inversely correlated with *ZEB2* expression. miR-215 was recently shown to directly target *ZEB2* expression in kidney cells¹⁷⁰ and our results suggest the same in Barrett's oesophagus. Together, these results suggest that the miR-200 family contribute to control of *ZEB1* and *ZEB2* expression in Barrett's oesophagus and this might be important for maintaining the epithelial phenotype. They add to current evidence for the involvement of EMT in oesophageal adenocarcinoma, and indicate down-regulation of miR-200 expression as a potential mechanism for this.

6.4.5 Clinical Relevance

Our current hypothesis is that the miR-200 family might be useful biomarkers for identifying patients with Barrett's oesophagus who are at increased risk of adenocarcinoma. Further studies are required to evaluate this hypothesis. In addition, recent advances in the delivery of small RNAs in a clinical setting³⁰⁵, together with

the demonstrated *in vitro* anti-neoplastic effects of endogenous miR-200 expression^{292, 306}, suggest a possible future role for this family of microRNAs in treating early cancer in Barrett's epithelium.

6.4.6 Limitations

This study has some limitations. First, Barrett's oesophagus epithelium proximal to cancer, and cell lines derived from dysplastic epithelium were used, to generate evidence for reduced miR-200 expression in dysplasia. This study does not demonstrate miR-200 down-regulation in dysplastic epithelium from patients who did not have invasive cancer, and this will be an important area for investigation in future studies. Second, although this study provides support for the effects of miR-200 expression on known gene-expression and phenotypic features of benign and dysplastic Barrett's oesophagus, this support is based on bioinformatic predictions supported by published literature. Future studies should expand on this evidence using functional studies.

6.4.7 Summary

In summary, this study has shown that the miR-200 expression profile in Barrett's oesophagus distinguishes it from gastric and duodenal epithelia, and that down-regulation of miR-200 expression is associated with dysplasia and adenocarcinoma. Further investigation is warranted to evaluate whether changes in the expression of these miRNAs can be used to identify patients with Barrett's oesophagus who are at risk of progression to oesophageal adenocarcinoma.

Chapter 7

Summary, conclusions and future studies

7.1 Summary and conclusions

This study aimed to assess miRNA expression and the role these molecules play in the oesophageal pathologies comprising the reflux-Barrett's oesophagus-oesophageal adenocarcinoma sequence. At the beginning of this PhD project, few changes in miRNA expression had been reported in this sequence, and there were no reports of functional roles for miRNAs in these pathologies.

Quantitative assessment of miRNA expression identified seven differentially expressed miRNAs in Barrett's oesophagus including: increased expression of miR-21, miR-143, miR-145, miR-194, miR-215 and decreased expression of miR-203 and miR-205. Of the miRNAs increased in Barrett's oesophagus, miR-143, miR-145 and miR-205 were also increased in patients with gastroesophageal reflux disease. Further, miR-143, miR-145 and miR-215 were decreased in patients with oesophageal adenocarcinoma.

7.1.1 Gastroesophageal reflux disease: Unravelling roles for miRNAs in the oesophagus

We now know that differential miRNA expression in the oesophageal epithelium is associated with functional consequences. Studies described in this thesis demonstrated increased miR-143, miR-145 and miR-205 levels in gastroesophageal reflux disease and identified that these miRNAs can act to regulate proliferation and apoptosis. From these studies we hypothesized that these miRNAs might act as regulators of oesophageal epithelial restoration in response to gastroesophageal reflux damage.

Of particular interest was whether increased miRNA expression in gastroesophageal

reflux disease might contribute to the development of Barrett's oesophagus. In oesophageal squamous tissue from patients with gastroesophageal reflux disease we observed strong and significant positive correlations between miR-143 and BMP4, a key promoter of columnar specific gene expression, and CK8, a marker of a columnar phenotype. This data is consistent with a possible role for miRNA expression in development of Barrett's oesophagus. However, increasing the levels of miR-143, miR-145 or miR-205 individually in a squamous oesophageal cell line did not lead to the formation of a columnar phenotype with intestinal metaplasia. Given reports by others discussing multiple genetic changes contributing to the development of Barrett's oesophagus it is perhaps ambitious to expect that increasing the level of a single miRNA would drive differentiation to a columnar phenotype. However, as miRNAs can manipulate the levels of hundreds of different genes, it is possible that miRNA transfection in combination (see Future Directions, 7.2.2) might help to identify a miRNA directed mechanism for the development of Barrett's oesophagus.

7.1.2 Tumour suppressor miRNAs in oesophageal adenocarcinoma

Neoplastic development is associated with dysfunctional regulation of numerous cellular processes. Therefore we wanted to investigate the consequences of decreased miRNA expression in oesophageal adenocarcinoma.

These studies identified that decreased miR-143, miR-145 and miR-215 expression in oesophageal adenocarcinoma likely contributes to a reduction in proliferative and apoptotic control in this cancer. mRNA array analysis identified that this loss of control is likely mediated by a number of miRNA directed changes (direct and indirect) in gene expression. Also, in situ hybridisation analysis identified that miR-143, miR-145 and miR-215 localise to the crypts within the Barrett's oesophagus epithelium and are not expressed in dysplastic or cancerous tissue. These studies provide support for a cancer promoting mechanism where decreased miR-143, miR-145 and miR-215 expression in the crypts of the Barrett's oesophagus epithelium leads to dysfunctional regulation of gene expression, directing a decrease in proliferative and apoptotic control and subsequently promoting neoplastic

development from these areas.

Taken together, the assessment of miRNA expression and function in gastroesophageal reflux disease, Barrett's oesophagus and oesophageal adenocarcinoma has identified functional roles for miRNAs in the oesophagus and demonstrated the loss of functional control that could occur when these molecules are aberrantly expressed in these pathologies.

7.1.3 The miR-200 family: Involvement in Barrett's oesophagus and oesophageal adenocarcinoma

Decreased expression of miR-141 and miR-200c was found to distinguish Barrett's oesophagus from related gastric and intestinal epithelia. Bioinformatic analysis of predicted miR-141 and miR-200c targets provided computational evidence that this decreased miRNA expression might contribute to the abnormal proliferative and apoptotic status of Barrett's oesophagus epithelium. These studies demonstrate the ability of computational genetic analysis paired with real time expression data to provide a platform for hypothesis driven research. From these studies we now have a solid foundation from which to investigate functional roles for decreased miR-141 and miR-200c expression in Barrett's oesophagus (see Future Directions 7.2.5).

We observed decreased expression of the miR-200 family (miR-141, miR-200a, miR-200b, miR-200c and miR-429) and increased expression of *ZEB1* and *ZEB2* in oesophageal adenocarcinoma. The miR-200 family regulates the epithelial to mesenchymal transition, a key process in tumour metastasis, by targeting the transcription factors *ZEB1* and *ZEB2*. These results provided the first evidence implicating miRNAs in the epithelial to mesenchymal transition in oesophageal adenocarcinoma. Further investigation of the miR-200 family in oesophageal adenocarcinoma may help to identify an invasive mechanism in oesophageal adenocarcinoma that can be targeted therapeutically.

7.2 *Future directions*

The knowledge gained from this study can be built upon to further understand the role of miRNAs in gastroesophageal reflux disease, Barrett's oesophagus and oesophageal adenocarcinoma.

7.2.1 Global profiling of miRNA expression in Barrett's oesophagus and oesophageal adenocarcinoma

In chapter three, PCR was used to quantitatively validate individual changes in miRNA expression. Since the beginning of this study there have been rapid advances in high throughput, quantitative PCR technology. It is now possible to quantitatively assess global changes in miRNA expression in a relatively short period of time. Although these emerging technologies provide better levels of detection than miRNA arrays, arguably they may not have the power to detect small changes in miRNA expression currently detectable by individual PCR based assays. However, the ability to assess multiple miRNAs simultaneously is appealing. Chapter three focussed on using PCR to quantify the most significant changes in miRNA expression and experiments presented in later chapters assessed the implications of these changes in gastroesophageal reflux pathology (chapter 4) and development of oesophageal adenocarcinoma (chapter 5). Given that a large number of miRNAs were indicated with a significant probability of differential expression by the miRNA array, and some of these miRNAs were further shown to play significant roles in regulating proliferation and apoptosis (Results of chapter 5 and others^{153, 157, 160, 166, 174, 307}), characterising further miRNAs identified in our original miRNA microarray experiments seems warranted.

7.2.2 Additional *in vitro* investigation into the role of miRNAs in the development of Barrett's oesophagus

In chapter 4, increased miR-143, miR-145 and miR-205 expression observed *in vivo* was replicated *in vitro*. These experiments primarily assessed the effects of reflux induced miRNA changes on tissue restoration in the oesophagus. However, a

number of interesting questions remain unanswered regarding the role of increased miRNA expression and the development of Barrett's oesophagus.

As discussed in section chapter 3, section 3.4.3 miR-143 and miR-145 appear to be critical in directing both gastric and intestinal differentiation^{109, 198, 199}. Therefore, these miRNAs are thought to be important in the development of Barrett's oesophagus. Chapter 4, Table 4.1 shows increased miR-143 and miR-145 expression in response to gastroesophageal reflux disease. Further, Table 4.2 shows strong correlations between miR-143 and both BMP4, a key promoter of columnar specific gene expression²²¹ and CK8, a marker of a columnar phenotype²²⁴. Taken together these results indicated a possible link between increased miR-143 and miR-145 expression and a squamous to columnar transition.

No visual changes in squamous cell morphology were observed after increasing miR-143 or miR-145 expression in our squamous oesophageal cell line. This is not necessarily surprising given others have hypothesised that multiple genetic changes are likely required for a transition from a squamous to a columnar phenotype³⁰⁸. In keeping with this hypothesis, assessing the effects of increasing the levels of multiple miRNAs simultaneously in a squamous oesophageal cell line should be the focus of future studies. Combinations of interest include increasing miR-143 and miR-145 levels simultaneously, for reasons discussed above, as well as increasing miR-143, miR-145 and miR-205 levels simultaneously to mimic, *in vitro*, the *in vivo* results reported in chapter 4. Further, as reflux pathology is associated with the development of Barrett's oesophagus, increasing the levels of multiple miRNAs in the presence of acid and/or bile mixtures (similar to those published by others in our lab⁷) also has merit.

The experimental design of chapter 4 utilized a squamous cell line. However, miR-143 and miR-145 expression is hypothesised to be required for maintaining gastric and intestinal differentiation. Therefore, miRNA knockout experiments in a Barrett's oesophagus cell line could provide evidence that these miRNAs are required to maintain a Barrett's oesophagus phenotype *in vitro*.

7.2.3 Assessing nuclear localisation of miRNAs

In-situ hybridisation revealed cytoplasmic and nuclear accumulation of miR-143, miR-145 and miR-205 in oesophageal keratinocytes. As miRNAs are known to regulate translation in the cytoplasm, their localization in the nucleus is somewhat surprising, but not unique, given reports by others^{194, 230, 309}.

Studies reporting both the presence and function of nuclear miRNAs are limited^{194, 230, 309}. However, the potential for miR-143, miR-145 or miR-205 function in the nucleus is intriguing. Of particular interest would be the potential for these miRNAs to regulate transcript levels of transcription factors in the nucleus, especially CDX2, given the multiple studies reporting the importance of this transcription factor in directing intestinal differentiation^{54, 310}.

To confirm the presence of miRNAs in the nucleus, deep sequencing studies could assess small nuclear RNAs from squamous, Barrett's oesophagus and oesophageal adenocarcinoma epithelia. If miRNAs sequences are retrieved from the nucleus, transfection of corresponding fluorescently labelled miRNA mimics, paired with cell microscopy software and real time imaging could be used to characterise the nuclear and cellular distribution of these miRNAs. From this data miRNA levels of accumulation and rates of degradation in the nucleus could also be characterised.

In assessing nuclear miRNA function, studies of interest include investigating whether nuclear localization of miR-143, miR-145 or miR-205 plays a role in reflux pathology or the development of Barrett's oesophagus. Initial studies could include transfecting cells with fluorescently labelled miRNA mimics to characterise the magnitude and stability of nuclear localisation. The development of an expression construct that promotes expression of miR-143, miR-145 or miR-205 transcripts that are tagged for subsequent purification would be required for these studies. Cell samples expressing this construct could be processed using sub cellular fractionation to obtain nuclear and cytoplasmic material. Purification of miRNA complexes from these samples followed by the sequencing bound RNA would assist in identifying if these miRNAs target gene transcripts in the nucleus.

7.2.4 miRNA expression and invasive oesophageal adenocarcinoma

Oesophageal adenocarcinoma is commonly diagnosed with metastasis. A diagnosis of metastasis likely contributes to the poor prognosis associated with this tumour⁷¹. Key processes in tumour metastasis include cell invasion and migration²⁷⁸. Identifying changes in miRNA expression that contribute cell invasion and migration may lead to the development of targeted therapies aiming to reduce metastasis in oesophageal adenocarcinoma. This thesis reports reduced miR-143, miR-145, miR-215 and miR-200 family expression in oesophageal adenocarcinoma (chapter 3, Table 3.1 & chapter 6, Table 6.2). Multiple studies are now reporting associations between decreased expression of these miRNAs and increased cancer cell migration and invasion^{116, 165, 170, 248}. In addition, these studies^{116, 165, 170, 248} show that restoring the expression of these miRNAs *in vitro* can reduce invasive capacity. These reports^{116, 165, 170, 248} paired with the reduced miR-143, miR-145, miR-215 and miR-200 family expression observed in oesophageal adenocarcinoma provide support for investigating the effects of increasing the expression of these miRNAs in oesophageal adenocarcinoma.

Future studies could include assessing invasive capacity by measuring cell invasion and migration after increasing the levels of miRNA expression in an oesophageal adenocarcinoma cell line. miRNAs of interest would include miR-143, miR-145, miR-215 and the miR-200 family. The current system of choice for assessing cell invasion and migration is the xCELLigence platform. The xCELLigence platform is designed to assess migration and invasion in real time, without requiring the removal of cells from incubation. This platform has advantages over other assays such as the scratch or Boyden chamber matrigel assays. For example, the Boyden chamber matrigel assay requires invasion and migration to be assessed at specific time points. This results in an increased risk that key data points could be missed. The scratch assay requires cells to leave the incubator to be taken to a microscope for photography. Removal of cells from incubation introduces variability through continual changes in the cells growth environment.

A number of interesting questions regarding invasion and migration could be

investigated using xCELLigence. Firstly, after increasing miR-143, miR-145, miR-215 or miR-200 family levels in oesophageal adenocarcinoma cells migration and invasion could be assessed. Secondly, increasing miRNA levels in combination could be explored to assess whether synergistic reductions in invasive capacity can be achieved. For example, given that miR-143 and miR-145 are likely expressed on the same transcript^{245, 311} and both are implicated in tumour invasion^{165, 248}, increasing the levels of these miRNAs in combination seems logical. In addition, reports speculate on redundancy across the miR-200 family members^{116, 312} as well as selected miR-200 family members having the ability to individually reduce invasive capacity^{123, 292}. Therefore increasing levels of miR-200 family members in different combinations may identify an optimal synergistic combination to direct a greater reduction in oesophageal adenocarcinoma invasion.

7.2.5 Validating bioinformatic predictions of miR-141 and miR-200c function *in vitro*

The bioinformatic investigation presented in chapter 6 assessed predicted targets of miR-141 and miR-200c and reviewed the literature for published reports on both the functions, as well as any interactions between these predicted targets. This bioinformatic investigation provided an information base for predicting the consequences of decreased miR-141 and miR-200c expression in Barrett's oesophagus (chapter 6, section 6.4.1). For example, miR-141 and miR-200c are known to modulate apoptosis, cell cycle and proliferation^{284, 290, 291} and therefore their decreased expression in Barrett's oesophagus was hypothesised to result in a loss of proliferative and apoptotic control through increased PI3K pathway activity. In addition, chapter 6, section 6.4.1 – 6.4.4 discussed the potential for decreased miR-141 and miR-200c expression increasing the risk of developing dysplastic Barrett's oesophagus.

Based on the hypotheses of chapter 6, understanding the mechanism that leads to decreased miR-141 and miR-200c expression as well as the associated consequences becomes important. This information may assist in the development of therapeutics targeted at reducing the abnormalities in the Barrett's epithelium and potentially reduce the risk of progression to oesophageal adenocarcinoma.

Chapter 6, Figure 6.1 shows that miR-141 and miR-200c are expressed on the same transcript. We hypothesised that this transcript might be down regulated in Barrett's oesophagus. In discussing reduced miR-141 and miR-200c expression epigenetic regulation of miR-141 and miR-200c was considered. However, at the time there was no evidence in the literature to support this and therefore investigation into methylation of these miRNAs was subsequently not pursued. Recently, Vrba et al.³¹³ have shown that decreased miR-141 and miR-200c expression is directed by methylation in breast cancer cells³¹⁴. Therefore, the focus of future studies should primarily include investigation of epigenetic regulation of miR-141 and miR-200c in Barrett's oesophagus. Using the same panel of tissue samples described in section 6.2 the methylation status of transcription sites upstream of pre-miR-141/miR-200c could be assessed in gastric, duodenal and Barrett's oesophagus tissues. In identifying a methylated pre-miR-141/200c promoter region Vrba et al.³¹³ assessed regions 115 – 343 base pairs upstream of pre-miR-141/miR-200c (chromosome 12, 6942000 - 6944500). These methods described by Vrba et al.³¹³ provide a logical starting point for this proposed methylation analysis. Methylation could be further assessed *in vitro* by treating a Barrett's oesophagus cell line (Qh) with an inhibitor of methylation known as 5-aza-Cytidine (DNA methyltransferase inhibitor) and using PCR to assess whether miR-141 or miR-200c expression is increased.

In assessing the consequences of decreased miR-141 and miR-200c expression in Barrett's oesophagus, preliminary *in vitro* studies should include transfecting miRNA mimic oligonucleotides to increase the levels of these miRNAs in a Barrett's oesophagus (Qh) or dysplastic (Ch and/or Gi) cell lines. After increasing miR-141 and/or miR-200c levels, hypotheses generated through the bioinformatic analysis discussed in chapter 6 could be explored.

Firstly, preliminary studies should focus on identifying whether reduced miR-141 or miR-200c expression contributes to the abnormal cellular processes associated with Barrett's oesophagus. Therefore, proliferation and apoptosis could be assessed after increasing miR-141 and/or miR-200c levels *in vitro*. Identifying a role for these miRNAs in proliferative and apoptotic control in Barrett's oesophagus will provide support for these molecules as potential therapeutic targets that may assist in reducing the abnormalities associated with Barrett's oesophagus.

If altered proliferation and/or apoptosis is observed in response to increased miR-141 or miR-200c expression, a potential mechanism should be investigated. Chapter 6, section 6.4.1 highlights that increased activity of the PI3K pathway is observed in response to gastroesophageal reflux. Given that this pathway is associated with the unique anti-apoptotic and proliferative response associated with the Barrett's epithelium reducing this pathway's activity may be of benefit. The mammalian target of rapamycin (*mTOR*) is a key protein in the PI3K pathway. *mTOR* is activated by *Akt* (predicted target of miR-200c) which is in turn activated by *PI3K* (predicted indirect/downstream target of miR-141 and miR-200c) to inhibit apoptosis and promote proliferation. An inhibitor of the PI3K signaling pathway is now available in the form of an mTOR inhibitor known as rapamycin. Exposure of a Barrett's oesophagus cell line (Qh) to Rapamycin alone or in combination with increasing miR-141 and/or miR-200c levels may be useful in assessing whether the PI3K pathway (specifically *mTOR*) is involved in directing abnormal proliferation and apoptosis in Barrett's oesophagus.

Chapter 6, Table 6.2 presents decreased miR-200c expression in Barrett's oesophagus sampled from patients with a concurrent oesophageal cancer. Bioinformatic analysis provided support for a potential role for this reduced miR-200c expression in contributing to the features of dysplastic Barrett's oesophagus. As discussed in chapter 6, section 6.4.3, *Akt* is stimulated by leptin and its receptor, and this results in increased proliferation and resistance to apoptosis in Barrett's oesophagus derived cancer cell lines³⁰³. Based on this, investigation of reduced miR-200 family expression (beginning with miR-200c) in dysplasia may identify a mechanism for leptin receptor mediated activation of *Akt* in Barrett's oesophagus, and this may provide support for a link between obesity and an increased risk of

oesophageal adenocarcinoma⁷⁸. In assessing these questions miR-200 family, *Akt* and leptin expression should be assessed in dysplastic Barrett's oesophagus tissue samples. Secondly, in dysplastic cell lines (Ch and Gi) leptin and Akt activity as well as proliferation, apoptosis and invasion could be assessed after increasing the expression of miR-200 family members (beginning with miR-200c). Results from these studies may provide evidence of miR-200 family member regulation of *Akt* and/or leptin as well as identify any functional effects associated with this regulation.

Appendices

Appendix 1: Elevated miR-143 and miR-145 is observed in specimens from resected oesophageal adenocarcinoma

In assessing miRNA expression in oesophageal mucosal specimens obtained either via endoscopic biopsy or from mucosal sampling of surgically resected tissue, highly elevated miR-143 (130 fold increase above median) and miR-145 (45 fold increase above median) was observed in some specimens. Careful analysis of the data indicated that the elevated expression was only present in some of the mucosal samples from surgically resected tissue, and not in the endoscopic biopsies. As miR-143 and miR-145 are enriched in columnar tissues compared with squamous mucosa (chapter 3, Table 3.1), and oesophageal sub-mucosal glands contain columnar cells, it was initially hypothesised that miR-143 and miR-145 levels may be enriched in sub-mucosal glands and the presence of these glands in resection specimens could account for the increased miR-143 and miR-145 levels. I aimed to test this hypothesis by localising the expression of miR-143 and miR-145 in resected oesophageal specimens that contained oesophageal sub-mucosal glands using ISH.

During the time spent developing the ISH protocol, work by Cordes et al.¹⁵⁴ was published showing tissue specific expression of miR-143 and miR-145 in cardiac smooth muscle tissue. H&E staining of oesophageal resection specimen slides shows that the muscularis mucosae was located closer to the luminal surface of the oesophageal epithelium than oesophageal sub-mucosal glands. Therefore, we also hypothesised that the presence of muscle in resection specimens may account for the elevation in miR-143 and miR-145 levels. To test these hypotheses I aimed to identify the site of increased miR-143 and miR-145 expression observed in some oesophageal resection specimens by performing ISH on oesophageal resection material.

ISH staining showed miR-143 and miR-145 to be significantly enriched in the muscle layers of the oesophagus (marked by arrow heads) and in sub-mucosal glands

(marked by *), (miR-143 - Figure A.1.1-B and miR-145 - Figure A.1.1-C) compared with the scramble probe (Figure A.1.1-D). The muscularis mucosae is closest to the luminal surface of the oesophageal epithelium and shows the greatest intensity for miR-143 and miR-145 staining.

Due to the close proximity of the muscularis mucosae to the basal layer of the oesophageal epithelium (Figure A.1.1-A) and results published by others showing high miR-143 and miR-145 levels in muscle tissue, the favoured hypothesis was that the presence of muscle was causing detection of high levels of miR-143 and miR-145 expression in oesophageal resection specimens compared with oesophageal biopsies. To test this hypothesis I assessed oesophageal mucosal biopsy and resection material for the presence of muscle, and observed a significant amount of muscle in resection specimens with the highest miR-143 and miR-145 expression as determined by quantitative RT-PCR (Figure A.1.2-A). Conversely, biopsy specimens that did not display elevated miR-143 and miR-145 expression and were negative for the presence of muscle (Figure A.1.2-B). No oesophageal sub-mucosal glands were present in the sections I assessed; suggesting miR-143 and miR-145 expression in these glands was not contributing to the increased expression observed in the resection specimens.

Therefore, it is likely that the presence of muscle in resected tissue specimens was the reason RT-PCR detected higher levels of miR-143 and miR-145 in resection specimens compared to biopsies.

Figure A.1.1: The muscularis mucosae and muscularis externa can be identified by the arrow heads in each figure. These layers show the greatest staining intensity for miR-143 (B) and miR-145 (C). No staining is observed when using the negative control probe (D).

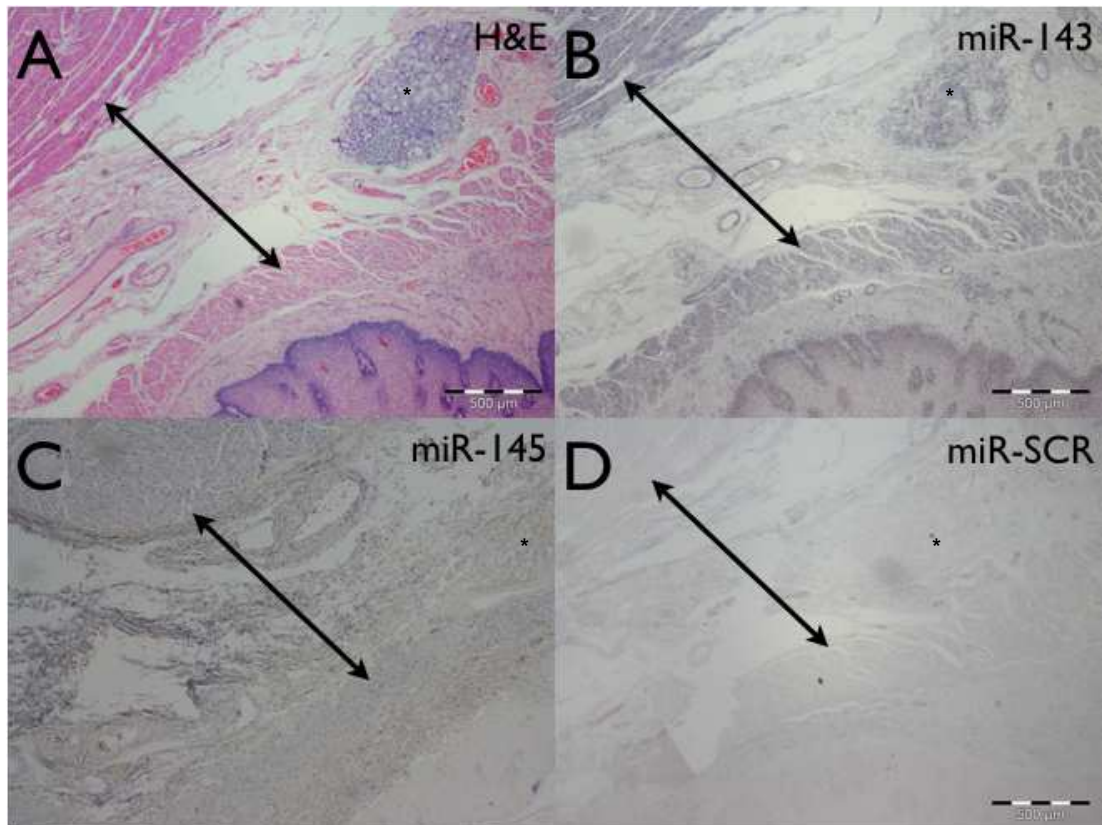
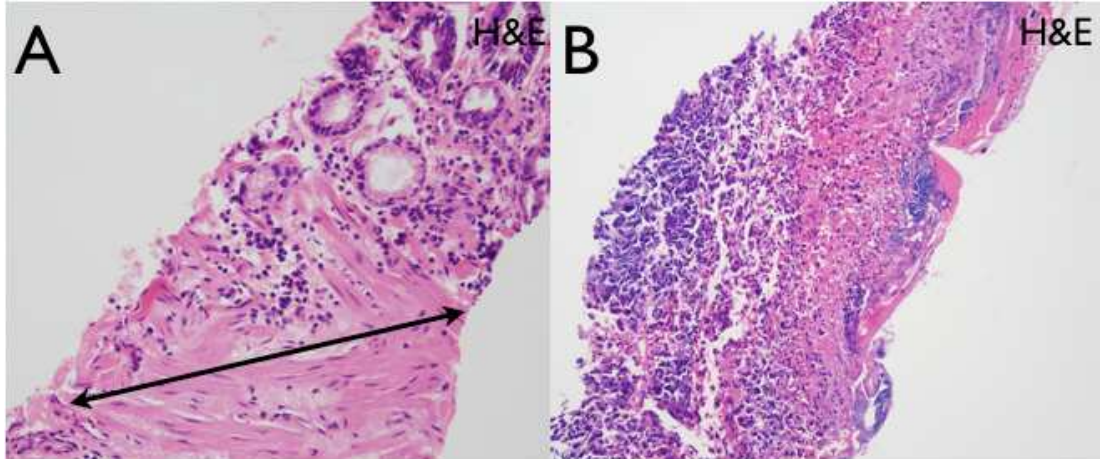


Figure A.1.2: (A) Highlights the presence of muscle in a resection specimen with elevated miR-143 and miR-145 expression. Muscle tissue spans between the arrowheads. No muscle can be identified biopsy specimen (B) and no elevation in miR-143 and miR-145 expression was observed.



Appendix 2: The top 40 genes for each miRNA indicated by student-t test to be significantly down regulated via mRNA array

Table A.2.1: The top 40 genes indicated by student-t test to be significantly down regulated ($p < 0.05$) 24 hr after miR-143 over expression in OE-19 cells.

No	ID	Gene Symbol	RefSeq	Average Expression (143)	Average Expression (NC)	p-value 143vNC (2 SIDED, equal variance)	Decrease in Fold Change
1	7950086	NUMA1	NM_006185	7.88464	8.08086	0.00034	-0.02428
2	8110362	GRK6	NM_001004106	6.01828	6.27716	0.00038	-0.04124
3	7949873	ACY3	NM_080658	5.16523	5.69160	0.00054	-0.09248
4	8171148	ARSD	NM_001669	4.99356	5.15224	0.00073	-0.03080
5	8081036	CADM2	NM_153184	3.42417	3.77338	0.00084	-0.09254
6	8018975	LGALS3BP	NM_005567	7.93729	8.49359	0.00092	-0.06550
7	8091446	PFN2	NM_053024	3.20920	3.51686	0.00115	-0.08748
8	8004804	PFAS	NM_012393	5.14110	5.48338	0.00128	-0.06242
9	8177101	TTY7	NR_001534	3.07699	3.17186	0.00133	-0.02991
10	8176435	TTY7	NR_001534	3.07699	3.17186	0.00133	-0.02991
11	8087119	SLC26A6	NM_022911	5.00564	5.29230	0.00158	-0.05417
12	8043480	IGKV1OR15-118	ENST00000405516	3.10822	3.36693	0.00180	-0.07684
13	8167165	ARAF	NM_001654	6.07030	6.39480	0.00205	-0.05074
14	8137675	PRKAR1B	NM_002735	5.24836	5.68678	0.00206	-0.07709
15	7937518	TSPAN4	NM_001025237	5.66677	6.13631	0.00218	-0.07652
16	8012450	SLC25A35	NM_201520	3.99942	4.27413	0.00297	-0.06427
17	8076962	MAPK12	NM_002969	4.68374	4.84814	0.00305	-0.03391
18	7942453	PLEKHB1	NM_021200	5.89070	6.51510	0.00310	-0.09584
19	8038347	TEAD2	NM_003598	5.64003	5.86988	0.00335	-0.03916
20	7981494	AKT1	NM_001014432	7.08479	7.32238	0.00341	-0.03245
21	8003322	CYBA	NM_000101	5.56350	6.16934	0.00365	-0.09820
22	8090162	ITGB5	NM_002213	6.64270	6.81580	0.00406	-0.02540
23	8050766	ADCY3	NM_004036	6.71629	6.93709	0.00445	-0.03183
24	7913644	E2F2	NM_004091	5.21448	5.53968	0.00455	-0.05870
25	7900159	DNALI1	NM_003462	3.41242	3.59696	0.00479	-0.05131
26	8025382	LASS4	NM_024552	3.28611	3.53447	0.00507	-0.07027
27	8074388	SLC25A1	NM_005984	6.57238	6.94591	0.00547	-0.05378
28	8140504	MAGI2	NM_012301	3.06788	3.26218	0.00591	-0.05956
29	8059097	C2orf24	NM_015680	4.67569	4.83624	0.00593	-0.03320
30	8048995	ITM2C	NM_030926	6.73871	7.17369	0.00607	-0.06064
31	8015575	GHDC	NM_032484	4.65350	4.83663	0.00611	-0.03786
32	7944042	PAFAH1B2	NM_002572	7.47324	7.65311	0.00618	-0.02350
33	8019376	DUS1L	NM_022156	6.67715	6.94727	0.00670	-0.03888
34	8065738	AHCY	NM_000687	7.99248	8.37522	0.00693	-0.04570
35	8157270	SLC31A1	NM_001859	8.09731	8.33596	0.00725	-0.02863
36	8072847	SH3BP1	NM_018957	4.28968	4.53881	0.00742	-0.05489
37	8076690	C2orf9	NM_001009880	5.57089	5.89700	0.00784	-0.05530
38	7932109	SEPHS1	NM_012247	6.40912	6.94145	0.00790	-0.07669
39	7939477	ALKBH3	NM_139178	5.23290	5.48063	0.00808	-0.04520
40	8126371	CCND3	NM_001760	7.33650	7.77084	0.00812	-0.05589

Table A.2.2: The top 40 genes indicated by student-t test to be significantly down regulated 24 hr after miR-145 over expression in OE-19 cells.

No	ID	Gene Symbol	RefSeq	Average Expression (NC)	Average Expression (145)	p-value 145vNC (2 SIDED, equal variance)	Decrease in Fold Change
1	7946061	HBE1	NM_005330	3.17823	2.97757	0.00041	-0.063136753
2	8012598	RCVRN	NM_002903	3.13188	3.05458	0.00053	-0.024683763
3	7924884	HIST3H3	NM_003493	3.73863	3.34907	0.00063	-0.104199488
4	8118556	HLA-DQA1	NM_002122	3.74450	3.41188	0.00083	-0.08882887
5	8149638	DOK2	NM_003974	3.38185	3.20346	0.00102	-0.052748301
6	8031013	DPRX	NM_001012728	3.37299	3.18159	0.00113	-0.056742985
7	8034379	ZNF442	NM_030824	3.54752	3.30738	0.00124	-0.06769236
8	8122966	CLDN20	NM_001001346	3.31487	3.03768	0.00173	-0.083621094
9	8149324	FAM167A	NM_053279	3.59002	3.39344	0.00228	-0.054757406
10	7922804	APOBEC4	NM_203454	3.15543	2.87864	0.00252	-0.087717575
11	8080911	KBTBD8	NM_032505	3.93223	3.47099	0.00255	-0.117298058
12	7943729	C11orf53	BC039669	3.19201	3.08646	0.00265	-0.033066939
13	7944185	CD3G	NM_000073	3.44871	3.31689	0.00284	-0.038223917
14	8125527	PPP1R2P1	AF275684	4.47759	4.27613	0.00286	-0.044994409
15	8178882	PPP1R2P1	AF275684	4.47759	4.27613	0.00286	-0.044994409
16	8180076	PPP1R2P1	AF275684	4.47759	4.27613	0.00286	-0.044994409
17	8109120	AFAP1L1	NM_152406	3.39733	3.18469	0.00310	-0.06259039
18	7948328	OR5B12	NM_001004733	3.42560	3.29268	0.00313	-0.038800053
19	7948316	OR10W1	NM_207374	3.51086	3.29706	0.00400	-0.060895811
20	8050113	LOC100129581	AK125905	3.39061	3.13239	0.00403	-0.076155496
21	8117382	HIST1H2BD	NM_021063	6.00170	5.63688	0.00411	-0.060786666
22	7911532	AURKAIP1	NM_017900	6.95960	6.37375	0.00421	-0.084178209
23	8014169	C17orf102	NM_207454	3.31672	3.08078	0.00433	-0.071138483
24	8102875	RPL14P3	XR_038338	3.77043	3.48143	0.00445	-0.076648266
25	7936833	RPS26P39	XM_001718952	4.70167	4.19837	0.00494	-0.107047704
26	7950003	MRGPRD	NM_198923	2.99823	2.71643	0.00506	-0.093987779
27	8123910	GCM2	NM_004752	3.01112	2.78704	0.00568	-0.0744186
28	7905088	HIST2H2AC	NM_003517	9.62737	8.97847	0.00643	-0.067401239
29	8147543	C8orf47	BC062359	3.66825	3.47950	0.00659	-0.051455962
30	8132387	POU6F2	NM_007252	3.58496	3.39724	0.00666	-0.052365017
31	8039923	AURKAIP1	NM_017900	7.45071	6.83994	0.00672	-0.081974291
32	8170393	CXorf40A	NM_178124	4.75995	4.53436	0.00679	-0.047391988
33	8002344	EXOSC6	NM_058219	5.31662	4.98212	0.00703	-0.062915913
34	8034512	SNORD41	NR_002751	5.96137	5.04524	0.00711	-0.153677762
35	7995813	MT1DP	NR_003658	4.61331	4.44711	0.00737	-0.036027613
36	8124524	HIST1H2AK	NM_003510	7.24545	6.04051	0.00772	-0.166303067
37	8171392	ASB9	NM_024087	3.25351	2.89563	0.00786	-0.109998238
38	7915896	CYP4Z2P	NR_002788	2.72993	2.51093	0.00806	-0.080224181
39	8124430	HIST1H1D	NM_005320	4.40426	3.91621	0.00868	-0.110811737
40	8155754	MAMDC2	NM_153267	3.45450	3.27488	0.00877	-0.051994068

Table A.2.3: The top 40 genes indicated by student-t test to be significantly down regulated 24 hr after miR-215 over expression in OE-19 cells.

No.	ID	Gene Symbol	RefSeq	Average Expression (NC)	Average Expression (215)	p-value 215vNC (2 SIDED, equal variance)	Decrease in Fold Change
1	8141843	IGFBP2	NM_000597	5.65625	5.26762	0.00039	-0.068708107
2	7932864	TNNI2	NM_001145829	3.73298	3.28080	0.00045	-0.121130999
3	7952810	SLC35C1	NM_018389	6.58870	6.20083	0.00074	-0.058868943
4	8139160	VPS26B	NM_052875	6.71253	6.45290	0.00096	-0.038678412
5	7964757	RNH1	NM_002939	7.16052	6.75401	0.00102	-0.056770112
6	8160163	ABC6	NM_005689	6.44524	6.01964	0.00115	-0.066033193
7	8126095	OR5B12	NM_001004733	3.42560	3.18954	0.00122	-0.068908677
8	7937728	PLEKHG3	NM_015549	4.91157	4.69653	0.00126	-0.043781685
9	8034901	GRIA2	NM_001083619	3.18067	2.98640	0.00174	-0.06107839
10	8025382	FRAP1	NM_004958	7.52877	7.34433	0.00174	-0.024498036
11	7945371	XKR8	NM_018053	4.39044	4.11728	0.00190	-0.062216952
12	8168781	SKIV2L	NM_006929	5.50976	4.97430	0.00202	-0.097184511
13	7979721	SLC22A18	NM_002555	5.65559	5.31448	0.00219	-0.060313224
14	8097753	RAB1B	NM_030981	8.80443	8.30767	0.00219	-0.056421597
15	8034512	CAD	NM_004341	7.05228	6.61855	0.00229	-0.061502067
16	8067185	GSTM5	NM_000851	3.44536	3.25727	0.00240	-0.05459221
17	8107847	SPINK6	NM_205841	3.05937	2.91122	0.00243	-0.04842495
18	7933442	MPRIP	NM_201274	6.98422	6.59084	0.00244	-0.056324564
19	8011331	SKIV2L	NM_006929	5.39994	4.89325	0.00251	-0.093831907
20	7958377	SKIV2L	NM_006929	5.39994	4.89325	0.00251	-0.093831907
21	8016476	CD151	NM_004357	8.34611	7.79541	0.00271	-0.065983208
22	8179364	ATP4B	NM_000705	3.43920	3.22869	0.00296	-0.061208943
23	8028194	LOC645339	BC014600	3.10044	2.91335	0.00296	-0.060342983
24	7970595	CTSD	AK022293	6.95208	6.48211	0.00312	-0.067601319
25	8118367	EIF2C1	NM_012199	7.86838	7.52245	0.00320	-0.043965001
26	8178136	LPAR2	NM_004720	5.74627	5.35622	0.00326	-0.067877695
27	7953733	GPS1	NM_212492	7.42943	7.06395	0.00348	-0.049193972
28	7998136	HBE1	NM_005330	3.17823	3.07084	0.00362	-0.033790261
29	8012928	ATP13A5	NM_198505	2.91525	2.78353	0.00380	-0.045185324
30	8027398	ARRDC1	NM_152285	6.77190	6.49068	0.00414	-0.041526525
31	8009639	FAM123B	NM_152424	5.58419	5.34012	0.00434	-0.043708491
32	8165319	C9orf142	BC002613	6.59116	6.34198	0.00441	-0.037804676
33	8082916	GLT8D4	NM_001080393	3.27797	3.08178	0.00456	-0.059850049
34	8015798	C14orf83	NM_182526	2.73887	2.44504	0.00525	-0.107279167
35	8131143	OR3A2	NM_002551	3.21854	2.88719	0.00537	-0.10294937
36	8122982	SLC8A3	NM_033262	2.87734	2.75189	0.00537	-0.043598138
37	8148917	PPM1F	NM_014634	4.93065	4.63691	0.00559	-0.05957366
38	8013157	YIPF3	NM_015388	8.15938	7.90432	0.00584	-0.031259715
39	7936115	MST150	NM_032947	4.68742	4.54499	0.00591	-0.030386275
40	7897132	KIAA0100	NM_014680	8.64300	8.42938	0.00595	-0.024715955

References

1. Heuman DM, Mills, A.S., McGuire, H.H., . *Gastroenterology* W.B. Saunders Company: Philadelphia, 1997.
2. Esophageal Cancer. <http://www.sts.org/patient-information/esophageal-surgery/esophageal-cancer> [Accessed on 7-4-11.
3. Geboes K, Desmet, V., . Histology of the oesophagus *Front Gastrointest Res* 1978;**3**: 1-17.
4. Seery J. Stem cells of the oesophageal epithelium *Journal of Cell Science* 2002;**115**: 1783-1789.
5. Seery JP. Stem cells of the oesophageal epithelium. *J Cell Sci* 2002;**115**(Pt 9): 1783-1789.
6. Laboratory Atlas for the Study of Medical Histology. <http://www.medicalhistology.us/twiki/bin/view/Main/EsophagusAndGastrointestinalAtlas12> [7/4/11.
7. van Roon AH, Mayne GC, Wijnhoven BP, Watson DI, Leong MP, Neijman GE, Michael MZ, McKay AR, Astill D, Hussey DJ. Impact of gastro-esophageal reflux on mucin mRNA expression in the esophageal mucosa. *J Gastrointest Surg* 2008;**12**(8): 1331-1340.
8. Isomoto H, Nishi, Y., Kanazawa, Y., Saburo, S., Mizuta, Y., Inoue, K., Kohno, S., Immune and Inflammatory Responses in GERD and Lansoprazole. *J Clin Biochem Nutr* 2007;**41**: 84-91.
9. Dixon J, Strugala V, Griffin SM, Welfare MR, Dettmar PW, Allen A, Pearson JP. Esophageal mucin: an adherent mucus gel barrier is absent in the normal esophagus but present in columnar-lined Barrett's esophagus. *The American journal of gastroenterology* 2001;**96**(9): 2575-2583.
10. Yoshida N. Inflammation and oxidative stress in gastroesophageal reflux disease. *Journal of clinical biochemistry and nutrition* 2007;**40**(1): 13-23.
11. Souza RF, Huo X, Mittal V, Schuler CM, Carmack SW, Zhang HY, Zhang X, Yu C, Hormi-Carver K, Genta RM, Spechler SJ. Gastroesophageal reflux might cause esophagitis through a cytokine-mediated mechanism rather than caustic acid injury. *Gastroenterology* 2009;**137**(5): 1776-1784.
12. Chang C, Lao-Sirieix P, Save V, De La Cueva Mendez G, Laskey R, Fitzgerald R. Retinoic acid-induced glandular differentiation of the oesophagus. *Gut* 2007;**56**(7): 906-917.
13. Stein HJ, Kauer WK, Feussner H, Siewert JR. Bile acids as components of the duodenogastric refluxate: detection, relationship to bilirubin, mechanism of injury, and clinical relevance. *Hepatogastroenterology* 1999;**46**(25): 66-73.
14. Goldman A, Shahidullah M, Goldman D, Khailova L, Watts G, Delamere N, Dvorak K. A novel mechanism of acid and bile acid-induced DNA damage involving Na⁺/H⁺ exchanger: implication for Barrett's oesophagus. *Gut* 2010;**59**(12): 1606-1616.
15. Jolly AJ, Wild CP, Hardie LJ. Acid and bile salts induce DNA damage in human oesophageal cell lines. *Mutagenesis* 2004;**19**(4): 319-324.
16. Jaiswal K, Lopez-Guzman C, Souza RF, Spechler SJ, Sarosi GA, Jr. Bile salt exposure increases proliferation through p38 and ERK MAPK pathways in a non-neoplastic Barrett's cell line. *Am J Physiol Gastrointest Liver Physiol* 2006;**290**(2):

G335-342.

17. Binato M, Gurski RR, Fagundes RB, Meurer L, Edelweiss MI. P53 and Ki-67 overexpression in gastroesophageal reflux disease--Barrett's esophagus and adenocarcinoma sequence. *Dis Esophagus* 2009;**22**(7): 588-595.
18. Livstone EM, Sheahan DG, Behar J. Studies of esophageal epithelial cell proliferation in patients with reflux esophagitis. *Gastroenterology* 1977;**73**(6): 1315-1319.
19. Jolly AJ, Wild CP, Hardie LJ. Sodium deoxycholate causes nitric oxide mediated DNA damage in oesophageal cells. *Free radical research* 2009;**43**(3): 234-240.
20. Wetscher GJ, Schwelberger H, Unger A, Offner FA, Profanter C, Glaser K, Klingler A, Gadenstaetter M, Klinger P. Reflux-induced apoptosis of the esophageal mucosa is inhibited in Barrett's epithelium. *American journal of surgery* 1998;**176**(6): 569-573.
21. Orlando RC. *Mucosal Defense in Barrett's Esophagus*. In *Barrett's Esophagus and Esophageal Adenocarcinoma*. Blackwell Publishing: Oxford, Uk, 2006.
22. Zwas F, Shields HM, Doos WG, Antonioli DA, Goldman H, Ransil BJ, Spechler SJ. Scanning electron microscopy of Barrett's epithelium and its correlation with light microscopy and mucin stains. *Gastroenterology* 1986;**90**(6): 1932-1941.
23. Levine DS, Rubin CE, Reid BJ, Haggitt RC. Specialized metaplastic columnar epithelium in Barrett's esophagus. A comparative transmission electron microscopic study. *Lab Invest* 1989;**60**(3): 418-432.
24. Barrett MT, Yeung KY, Ruzzo WL, Hsu L, Blount PL, Sullivan R, Zarbl H, Delrow J, Rabinovitch PS, Reid BJ. Transcriptional analyses of Barrett's metaplasia and normal upper GI mucosae. *Neoplasia* 2002;**4**(2): 121-128.
25. Ostrowski J, Mikula M, Karczmariski J, Rubel T, Wyrwicz LS, Bragoszewski P, Gaj P, Dadlez M, Butruk E, Regula J. Molecular defense mechanisms of Barrett's metaplasia estimated by an integrative genomics. *J Mol Med* 2007;**85**(7): 733-743.
26. Cameron AJ, Zinsmeister AR, Ballard DJ, Carney JA. Prevalence of columnar-lined (Barrett's) esophagus. Comparison of population-based clinical and autopsy findings. *Gastroenterology* 1990;**99**(4): 918-922.
27. Wild CP, Hardie LJ. Reflux, Barrett's oesophagus and adenocarcinoma: burning questions. *Nature reviews* 2003;**3**(9): 676-684.
28. What is Dysplasia?
http://www.barrettsinfo.com/content/3c_what_is_dysplasia.cfm [Accessed on 7/4/11.
29. Souza RF, Krishnan K, Spechler SJ. Acid, bile, and CDX: the ABCs of making Barrett's metaplasia. *Am J Physiol Gastrointest Liver Physiol* 2008;**295**(2): G211-218.
30. Bremner CG, Lynch VP, Ellis FH, Jr. Barrett's esophagus: congenital or acquired? An experimental study of esophageal mucosal regeneration in the dog. *Surgery* 1970;**68**(1): 209-216.
31. Wang DH, Clemons NJ, Miyashita T, Dupuy AJ, Zhang W, Szczepny A, Corcoran-Schwartz IM, Wilburn DL, Montgomery EA, Wang JS, Jenkins NA, Copeland NA, Harmon JW, Phillips WA, Watkins DN. Aberrant epithelial-mesenchymal Hedgehog signaling characterizes Barrett's metaplasia. *Gastroenterology* 2010;**138**(5): 1810-1822.
32. Kosinski C, Stange DE, Xu C, Chan AS, Ho C, Yuen ST, Mifflin RC, Powell DW, Clevers H, Leung SY, Chen X. Indian hedgehog regulates intestinal stem cell fate through epithelial-mesenchymal interactions during development. *Gastroenterology* 2010;**139**(3): 893-903.
33. Wang X, Ouyang H, Yamamoto Y, Kumar PA, Wei TS, Dagher R, Vincent M,

- Lu X, Bellizzi AM, Ho KY, Crum CP, Xian W, McKeon F. Residual Embryonic Cells as Precursors of a Barrett's-like Metaplasia. *Cell* 2011;**145**(7): 1023-1035.
34. Phillips WA, Lord RV, Nancarrow DJ, Whiteman DC. Barrett's esophagus. *J Gastroenterol Hepatol* 2011;**26**(4): 639-648.
35. Slack JMW. Metaplasia and transdifferentiation: from pure biology to the clinic. *Nat Rev Mol Cell Biol* 2007;**8**(5): 369-378.
36. Kuo B, Urma D. Esophagus - anatomy and development. In: *Goyal and Shaker's GI Motility Online* Goyal R, Shaker R (eds). Nature Publishing Group: New York, 2006; <http://www.nature.com/gimo/contents/pt1/full/gimo6.html>.
37. Larsen WJ. Development of the Gastrointestinal Tract. In: *Human Embryology*, Sherman LS, Potter SS, Scott WJ (eds). Churchill Livingstone: Philadelphia, Pennsylvania, 2001; 235-263.
38. Guillem PG. How to Make a Barrett Esophagus: Pathophysiology of Columnar Metaplasia of the Esophagus. *Dig Dis Sci* 2005;**50**(3): 415-424.
39. Johns BA. Developmental changes in the oesophageal epithelium in man. *J Anat* 1952;**86**(4): 431-442.
40. Yu WY, Slack JM, Tosh D. Conversion of columnar to stratified squamous epithelium in the developing mouse oesophagus. *Dev Biol* 2005;**284**(1): 157-170.
41. Radomska-Pandya A, Chen G. Photoaffinity labeling of human retinoid X receptor beta (RXRbeta) with 9-cis-retinoic acid: identification of phytanic acid, docosahexaenoic acid, and lithocholic acid as ligands for RXRbeta. *Biochemistry* 2002;**41**(15): 4883-4890.
42. Pera M, Pera, M.,. Experimental Barrett's Oesophagus and the origin of intestinal metaplasia. *Chest Surgery Clinics of North America* 2002;**12**(1): 25-37.
43. Tobey NA, Hosseini SS, Argote CM, Dobrucali AM, Awayda MS, Orlando RC. Dilated intercellular spaces and shunt permeability in nonerosive acid-damaged esophageal epithelium. *The American journal of gastroenterology* 2004;**99**(1): 13-22.
44. Wang J, Qin R, Ma Y, Wu H, Peters H, Tyska M, Shaheen NJ, Chen X. Differential gene expression in normal esophagus and Barrett's esophagus. *J Gastroenterol* 2009;**44**(9): 897-911.
45. Haveri H, Westerholm-Ormio M, Lindfors K, Mäki M, Savilahti E, Andersson LC, Heikinheimo M. Transcription factors GATA-4 and GATA-6 in normal and neoplastic human gastrointestinal mucosa. *BMC Gastroenterol* 2008;**8**: 9.
46. Colleypriest BJ, Ward SG, Tosh D. How does inflammation cause Barrett's metaplasia? *Curr Opin Pharmacol* 2009;**9**(6): 721-726.
47. Kong J, Nakagawa H, Isariyawongse BK, Funakoshi S, Silberg DG, Rustgi AK, Lynch JP. Induction of intestinalization in human esophageal keratinocytes is a multistep process. *Carcinogenesis* 2009;**30**(1): 122-130.
48. Liu T, Zhang X, So CK, Wang S, Wang P, Yan L, Myers R, Chen Z, Patterson AP, Yang C, Chen X. Regulation of Cdx2 expression by promoter methylation, and effects of Cdx2 transfection on morphology and gene expression of human esophageal epithelial cells. *Carcinogenesis* 2007;**28**(2): 488-496.
49. Beck F, Chawengsaksophak K, Waring P, Playford RJ, Furness JB. Reprogramming of intestinal differentiation and intercalary regeneration in Cdx2 mutant mice. *Proceedings of the National Academy of Sciences of the United States of America* 1999;**96**(13): 7318-7323.
50. Tamai Y, Nakajima R, Ishikawa T, Takaku K, Seldin MF, Taketo MM. Colonic hamartoma development by anomalous duplication in Cdx2 knockout mice. *Cancer Res* 1999;**59**(12): 2965-2970.
51. D'Angelo A, Bluteau O, Garcia-Gonzalez MA, Gresh L, Doyen A, Garbay S,

- Robine S, Pontoglio M. Hepatocyte nuclear factor 1alpha and beta control terminal differentiation and cell fate commitment in the gut epithelium. *Development*; **137**(9): 1573-1582.
52. Gao X, Sedgwick T, Shi YB, Evans T. Distinct functions are implicated for the GATA-4, -5, and -6 transcription factors in the regulation of intestine epithelial cell differentiation. *Mol Cell Biol* 1998;**18**(5): 2901-2911.
53. Jacobsen CM, Narita N, Bielinska M, Syder AJ, Gordon JI, Wilson DB. Genetic mosaic analysis reveals that GATA-4 is required for proper differentiation of mouse gastric epithelium. *Dev Biol* 2002;**241**(1): 34-46.
54. Benoit YD, Pare F, Francoeur C, Jean D, Tremblay E, Boudreau F, Escaffit F, Beaulieu JF. Cooperation between HNF-1alpha, Cdx2, and GATA-4 in initiating an enterocytic differentiation program in a normal human intestinal epithelial progenitor cell line. *Am J Physiol Gastrointest Liver Physiol* 2010;**298**(4): G504-517.
55. Lorenzsonn V, Korsmo H, Olsen WA. Localization of sucrase-isomaltase in the rat enterocyte. *Gastroenterology* 1987;**92**(1): 98-105.
56. Kazumori H. Bile acids directly augment caudal related homeobox gene Cdx2 expression in oesophageal keratinocytes in Barrett's epithelium. *Gut* 2006;**55**(1): 16-25.
57. Kobayashi M, Takada T, Takahashi K, Noda Y, Torii R. BMP4 induces primitive endoderm but not trophectoderm in monkey embryonic stem cells. *Cloning and stem cells* 2008;**10**(4): 495-502.
58. Zhou G, Sun YG, Wang HB, Wang WQ, Wang XW, Fang DC. Acid and bile salt up-regulate BMP4 expression in human esophageal epithelium cells. *Scandinavian Journal of Gastroenterology* 2009: 1-7.
59. O'riordan J, Abdel-Latif M, Ravi N, Mcnamara D, Byrne P, McDonald G, Keeling P, Kelleher D, Reynolds J. Proinflammatory Cytokine and Nuclear Factor Kappa-B Expression along the Inflammation-Metaplasia-Dysplasia-Adenocarcinoma Sequence in the Esophagus. *Am J Gastroenterology* 2005;**100**(6): 1257-1264.
60. Krishnath KK. Novel findings in the pathogenesis of esophageal columnar metaplasia or Barrett's esophagus. *Curr Opin Gastroenterol* 2007;**23**(4): 440-445.
61. Goldblum JR. Barrett's esophagus and Barrett's-related dysplasia. *Mod Pathol* 2003;**16**(4): 316-324.
62. Odze RD. Diagnosis and grading of dysplasia in Barrett's oesophagus. *J Clin Pathol* 2006;**59**(10): 1029-1038.
63. Reid BJ, Haggitt RC, Rubin CE, Roth G, Surawicz CM, Van Belle G, Lewin K, Weinstein WM, Antonioli DA, Goldman H, et al. Observer variation in the diagnosis of dysplasia in Barrett's esophagus. *Hum Pathol* 1988;**19**(2): 166-178.
64. Schlemper RJ, Riddell RH, Kato Y, Borchard F, Cooper HS, Dawsey SM, Dixon MF, Fenoglio-Preiser CM, Flejou JF, Geboes K, Hattori T, Hirota T, Itabashi M, Iwafuchi M, Iwashita A, Kim YI, Kirchner T, Klimpfinger M, Koike M, Lauwers GY, Lewin KJ, Oberhuber G, Offner F, Price AB, Rubio CA, Shimizu M, Shimoda T, Sipponen P, Solcia E, Stolte M, Watanabe H, Yamabe H. The Vienna classification of gastrointestinal epithelial neoplasia. *Gut* 2000;**47**(2): 251-255.
65. Maru DM, Singh RR, Hannah C, Albarracin CT, Li YX, Abraham R, Romans AM, Yao H, Luthra MG, Anandasabapathy S, Swisher SG, Hofstetter WL, Rashid A, Luthra R. MicroRNA-196a is a potential marker of progression during Barrett's metaplasia-dysplasia-invasive adenocarcinoma sequence in esophagus. *Am J Pathol* 2009;**174**(5): 1940-1948.
66. American Gastroenterological Association Medical Position Statement on the Management of Barrett's Esophagus. *Gastroenterology*; **140**(3): 1084-1091.

67. Kahrilas PJ, Shaheen NJ, Vaezi MF, Hiltz SW, Black E, Modlin IM, Johnson SP, Allen J, Brill JV. American Gastroenterological Association Medical Position Statement on the management of gastroesophageal reflux disease. *Gastroenterology* 2008;**135**(4): 1383-1391, 1391 e1381-1385.
68. Chennat J, Waxman I. Endoscopic treatment of Barrett's esophagus: From metaplasia to intramucosal carcinoma. *World J Gastroenterol*; **16**(30): 3780-3785.
69. Zehetner J, DeMeester SR, Hagen JA, Ayazi S, Augustin F, Lipham JC, DeMeester TR. Endoscopic resection and ablation versus esophagectomy for high-grade dysplasia and intramucosal adenocarcinoma. *The Journal of thoracic and cardiovascular surgery* 2011;**141**(1): 39-47.
70. Oelschlager BK. Intramucosal esophageal cancer and high-grade dysplasia: which treatment frame the debate. *J Gastrointest Surg* 2009;**13**(7): 1169-1171.
71. Parker SL, Tong T, Bolden S, Wingo PA. Cancer statistics, 1997. *CA: a cancer journal for clinicians* 1997;**47**(1): 5-27.
72. Devesa SS, Blot WJ, Fraumeni JF, Jr. Changing patterns in the incidence of esophageal and gastric carcinoma in the United States. *Cancer* 1998;**83**(10): 2049-2053.
73. Parker SL, Tong T, Bolden S, Wingo PA. Cancer Statistics, 1997. *CA. Cancer J Clin* 1997;**47**: 5-27.
74. Pohl H, Welch HG. The role of overdiagnosis and reclassification in the marked increase of esophageal adenocarcinoma incidence. *Journal of the National Cancer Institute* 2005;**97**(2): 142-146.
75. Wang VS, Hornick JL, Sepulveda JA, Mauer R, Poneris JM. Low prevalence of submucosal invasive carcinoma at esophagectomy for high-grade dysplasia or intramucosal adenocarcinoma in Barrett's esophagus: a 20-year experience. *Gastrointest Endosc* 2009;**69**(4): 777-783.
76. de Jonge PJ, van Blankenstein M, Looman CW, Casparie MK, Meijer GA, Kuipers EJ. Risk of malignant progression in patients with Barrett's oesophagus: a Dutch nationwide cohort study. *Gut* 2010;**59**(8): 1030-1036.
77. Solaymani-Dodaran M, Logan RF, West J, Card T, Coupland C. Risk of oesophageal cancer in Barrett's oesophagus and gastro-oesophageal reflux. *Gut* 2004;**53**(8): 1070-1074.
78. Whiteman DC, Sadeghi S, Pandeya N, Smithers BM, Gotley DC, Bain CJ, Webb PM, Green AC. Combined effects of obesity, acid reflux and smoking on the risk of adenocarcinomas of the oesophagus. *Gut* 2008;**57**(2): 173-180.
79. Pillai RS, Bhattacharyya SN, Filipowicz W. Repression of protein synthesis by miRNAs: how many mechanisms? *Trends Cell Biol* 2007;**17**(3): 118-126.
80. Lee RC, Feinbaum RL, Ambrost VA. The *C. elegans* heterochronic gene *lin-4* encodes small RNAs with antisense complementarity to *lin-14*. *Cell* 1993;**75**(5): 843-854.
81. Pillai RS, Bhattacharyya, S.N., Filipowicz, W., . Repression of protein synthesis by miRNAs: how many mechanisms? *Trends in Cell Biology* 2008;**17**(3): 118-126.
82. Sotiropoulou G, Pampalakis G, Lianidou E, Mourelatos Z. Emerging roles of microRNAs as molecular switches in the integrated circuit of the cancer cell. *RNA* 2009;**15**(8): 1443-1461.
83. Pillai RS. MicroRNA function: Multiple mechanisms for a tiny RNA? *RNA* 2005;**11**(12): 1753-1761.
84. Filipowicz W, Bhattacharyya SN, Sonenberg N. Mechanisms of post-transcriptional regulation by microRNAs: are the answers in sight? *Nat Rev Genet* 2008;**9**: 102-114.

85. Wijnhoven BP, Michael MZ, Watson DI. MicroRNAs and cancer. *Br J surgery* 2007;**94**(1): 23-30.
86. Ruby JG, Jan CH, Bartel DP. Intronic microRNA precursors that bypass Drosha processing. *Nature* 2007;**448**(7149): 83-86.
87. Tomari Y, Zamore PD. MicroRNA biogenesis: drosha can't cut it without a partner. *Curr Biol* 2005;**15**(2): R61-64.
88. Davis BN, Hilyard AC, Lagna G, Hata A. SMAD proteins control DROSHA-mediated microRNA maturation. *Nature* 2008;**454**(7200): 56-61.
89. Chendrimada TP, Gregory RI, Kumaraswamy E, Norman J, Cooch N, Nishikura K, Shiekhattar R. TRBP recruits the Dicer complex to Ago2 for microRNA processing and gene silencing. *Nature* 2005;**436**(7051): 740-744.
90. Tomari Y, Zamore PD. Perspective: machines for RNAi. *Genes Dev* 2005;**19**: 517-529.
91. Gregory RI, Chendrimada TP, Cooch N, Shiekhattar R. Human RISC couples microRNA biogenesis and posttranscriptional gene silencing. *Cell* 2005;**123**(4): 631-640.
92. Carmell MA, Xuan Z, Zhang MQ, Hannon GJ. The Argonaute family: tentacles that reach into RNAi, developmental control, stem cell maintenance, and tumorigenesis. *Genes Dev* 2002;**16**(21): 2733-2742.
93. Liu J, Carmell MA, Rivas FV, Marsden CG, Thomson JM, Song JJ, Hammond SM, Joshua-Tor L, Hannon GJ. Argonaute2 is the catalytic engine of mammalian RNAi. *Science* 2004;**305**(5689): 1437-1441.
94. Burroughs AM, Ando Y, Hoon ML, Tomaru Y, Suzuki H, Hayashizaki Y, Daub CO. Deep-sequencing of human Argonaute-associated small RNAs provides insight into miRNA sorting and reveals Argonaute association with RNA fragments of diverse origin. *RNA Biol* 2011;**8**(1).
95. Davis BN, Hata A. Regulation of MicroRNA Biogenesis: A miRiad of mechanisms. *Cell Commun Signal* 2009;**7**: 18.
96. Kloosterman WP, Wienholds E, Ketting RF, Plasterk RH. Substrate requirements for let-7 function in the developing zebrafish embryo. *Nucleic Acids Res* 2004;**32**(21): 6284-6291.
97. Hutvagner G, Zamore PD. A microRNA in a multiple-turnover RNAi enzyme complex. *Science* 2002;**297**(5589): 2056-2060.
98. Jones-Rhoades MW, Bartel DP, Bartel B. MicroRNAs and their regulatory roles in plants. *Annual review of plant biology* 2006;**57**: 19-53.
99. Parker R, Song H. The enzymes and control of eukaryotic mRNA turnover. *Nature structural & molecular biology* 2004;**11**(2): 121-127.
100. Winter J, Jung S, Keller S, Gregory RI, Diederichs S. Many roads to maturity: microRNA biogenesis pathways and their regulation. *Nat Cell Biol* 2009;**11**(3): 228-234.
101. Guo H, Ingolia NT, Weissman JS, Bartel DP. Mammalian microRNAs predominantly act to decrease target mRNA levels. *Nature* 2010;**466**(7308): 835-840.
102. Kumar MS, Lu J, Mercer KL, Golub TR, Jacks T. Impaired microRNA processing enhances cellular transformation and tumorigenesis. *Nat Genet* 2007;**39**(5): 673-677.
103. Lujambio A, Calin GA, Villanueva A, Ropero S, Sanchez-Cespedes M, Blanco D, Montuenga LM, Rossi S, Nicoloso MS, Faller WJ, Gallagher WM, Eccles SA, Croce CM, Esteller M. A microRNA DNA methylation signature for human cancer metastasis. *Proceedings of the National Academy of Sciences of the United*

States of America 2008;**105**(36): 13556-13561.

104. Saito Y, Liang G, Egger G, Friedman JM, Chuang JC, Coetzee GA, Jones PA. Specific activation of microRNA-127 with downregulation of the proto-oncogene BCL6 by chromatin-modifying drugs in human cancer cells. *Cancer Cell* 2006;**9**(6): 435-443.

105. Fukuda T, Yamagata K, Fujiyama S, Matsumoto T, Koshida I, Yoshimura K, Mihara M, Naitou M, Endoh H, Nakamura T, Akimoto C, Yamamoto Y, Katagiri T, Foulds C, Takezawa S, Kitagawa H, Takeyama K, O'Malley BW, Kato S. DEAD-box RNA helicase subunits of the Drosha complex are required for processing of rRNA and a subset of microRNAs. *Nat Cell Biol* 2007;**9**(5): 604-611.

106. Suzuki HI, Yamagata K, Sugimoto K, Iwamoto T, Kato S, Miyazono K. Modulation of microRNA processing by p53. *Nature* 2009;**460**(7254): 529-533.

107. Keswani RN, Noffsinger A, Waxman I, Bissonnette M. Clinical use of p53 in Barrett's esophagus. *Cancer Epidemiol Biomarkers Prev* 2006;**15**(7): 1243-1249.

108. Sugito N, Ishiguro H, Kuwabara Y, Kimura M, Mitsui A, Kurehara H, Ando T, Mori R, Takashima N, Ogawa R, Fujii Y. RNASEN regulates cell proliferation and affects survival in esophageal cancer patients. *Clin Cancer Res* 2006;**12**(24): 7322-7328.

109. Michael MZ, O' Connor SM, van Holst Pellekaan NG, Young GP, James RJ. Reduced accumulation of specific microRNAs in colorectal neoplasia. *Mol Cancer Res* 2003;**1**(12): 882-891.

110. Wijnhoven BP, Hussey DJ, Watson DI, Tsykin A, Smith CM, Michael MZ, . SAORG. MicroRNA profiling of Barrett's oesophagus and oesophageal adenocarcinoma. *Br J Surg* 2010;**97**(6): 853-861.

111. Akao Y, Nakagawa Y, Kitade Y, Kinoshita T, Naoe T. Downregulation of microRNAs-143 and -145 in B-cell malignancies. *Cancer Sci* 2007;**98**(12): 1914-1920.

112. Karube Y, Tanaka H, Osada H, Tomida S, Tatematsu Y, Yanagisawa K, Yatabe Y, Takamizawa J, Miyoshi S, Mitsudomi T, Takahashi T. Reduced expression of Dicer associated with poor prognosis in lung cancer patients. *Cancer Sci* 2005;**96**(2): 111-115.

113. Han L, Zhang A, Zhou X, Xu P, Wang G, Pu P, Kang C. Downregulation of Dicer enhances tumour cell proliferation and invasion. *Int J Oncol* 2010;**37**(2): 299-305.

114. Volinia S, Calin GA, Liu CG, Ambs S, Cimmino A, Petrocca F, Visone R, Iorio M, Roldo C, Ferracin M, Prueitt RL, Yanaihara N, Lanza G, Scarpa A, Vecchione A, Negrini M, Harris CC, Croce CM. A microRNA expression signature of human solid tumors defines cancer gene targets. *Proc Natl Acad Sci USA* 2006;**103**(7): 2257-2261.

115. Kan T, Sato F, Ito T, Matsumura N, David S, Cheng Y, Agarwal R, Paun B, Jin Z, Oлару A, Selaru F, Hamilton J, Yang J, Abraham J, Mori Y, Meltzer S. The miR-106b-25 Polycistron, Activated by Genomic Amplification, Functions as an Oncogene by Suppressing p21 and Bim. *YGASt* 2009;**136**(5): 1689-1700.

116. Gregory PA, Bert AG, Paterson EL, Barry SC, Tsykin A, Farshid G, Vadas MA, Khew-Goodall Y, Goodall GJ. The miR-200 family and miR-205 regulate epithelial to mesenchymal transition by targeting ZEB1 and SIP1. *Nat Cell Biol* 2008;**10**(5): 593-601.

117. Dews M, Homayouni A, Yu D, Murphy D, Seignani C, Wentzel E, Furth EE, Lee WM, Enders GH, Mendell JT, Thomas-Tikhonenko A. Augmentation of tumor angiogenesis by a Myc-activated microRNA cluster. *Nat Genet* 2006;**38**(9):

1060-1065.

118. Bos JL. ras oncogenes in human cancer: a review. *Cancer Res* 1989;**49**(17): 4682-4689.
119. He L, Thomson J, Hemann M, Hernando-Monge E, Mu D, Goodson S, Powers S, Cordon-Cardo C, Lowe SW, Hannon G, Hammond SM. A microRNA polycistron as a potential human oncogene. *Nature* 2005;**435**(7043): 828-833.
120. Johnson SM, Grosshans H, Shingara J, Byrom M, Jarvis R, Cheng A, Labourier E, Reinert KL, Brown D, Slack FJ. RAS is regulated by the let-7 microRNA family. *Cell* 2005;**120**(5): 635-647.
121. Hayashita Y, Osada, H., Tatematsu, Y., Yamada, H., Yanagisawa, K., Tomida, S., Yatabe, Y., Kawahara, K., Sekido, Y., Takahashi, T. A polycistronic microRNA cluster, miR-17-92, is overexpressed in human lung cancers and enhances cell proliferation. *Cancer Res* 2005;**65**(21): 9828-9832.
122. Esquela-Kerscher A, Trang P, Wiggins J, Patrawala L, Cheng A, Ford L, Weidhaas J, Brown D, Bader A, Slack F. The let-7 microRNA reduces tumor growth in mouse models of lung cancer. *Cell Cycle* 2008;**7**(6): 759-764.
123. Xia H, Ng SS, Jiang S, Cheung WK, Sze J, Bian XW, Kung HF, Lin MC. miR-200a-mediated downregulation of ZEB2 and CTNNB1 differentially inhibits nasopharyngeal carcinoma cell growth, migration and invasion. *Biochem Biophys Res Commun* 2010;**391**(1): 535-541.
124. Lu J, Getz G, Miska EA, Alvarez-Saavedra E, Lamb J, Peck D, Sweet-Cordero A, Ebert BL, Mak RH, Ferrando AA, Downing JR, Jacks T, Horvitz HR, Golub TR. MicroRNA expression profiles classify human cancers. *Nature* 2005;**435**(7043): 834-838.
125. Pavlidis N, Briasoulis E, Hainsworth J, Greco FA. Diagnostic and therapeutic management of cancer of an unknown primary. *Eur J Cancer* 2003;**39**(14): 1990-2005.
126. Yang B, Lin H, Xiao J, Lu Y, Luo X, Li B, Zhang Y, Xu C, Bai Y, Wang H, Chen G, Wang Z. The muscle-specific microRNA miR-1 regulates cardiac arrhythmogenic potential by targeting GJA1 and KCNJ2. *Nat Med* 2007;**13**(4): 486-491.
127. Schratt GM, Tuebing F, Nigh EA, Kane CG, Sabatini ME, Kiebler M, Greenberg ME. A brain-specific microRNA regulates dendritic spine development. *Nature* 2006;**439**(7074): 283-289.
128. Schepeler T, Reinert JT, Ostensfeld MS, Christensen LL, Silahatoglu AN, Dyrskjot L, Wiuf C, Sorensen FJ, Kruhoffer M, Laurberg S, Kauppinen S, Orntoft TF, Andersen CL. Diagnostic and prognostic microRNAs in stage II colon cancer. *Cancer Res* 2008;**68**(15): 6416-6424.
129. Papagiannakopoulos T, Kosik KS. MicroRNAs: regulators of oncogenesis and stemness. *BMC Med* 2008;**6**: 15.
130. Rosetta Genomics. www.rosettagenomics.com/ [7/4/11].
131. Caldas C, Brenton JD. Sizing up miRNAs as cancer genes. *Nat Med* 2005;**11**(7): 712-714.
132. Lai EC. Predicting and validating microRNA targets. *Genome Biol* 2004;**5**(9): 115.
133. Saito T, Saetrom P. MicroRNAs--targeting and target prediction. *N Biotechnol* 2010;**27**(3): 243-249.
134. Bartel D. MicroRNAs: Target Recognition and Regulatory Functions. *Cell* 2009;**136**(2): 215-233.
135. Alexiou P, Maragkakis M, Papadopoulos GL, Reczko M, Hatzigeorgiou AG.

- Lost in translation: an assessment and perspective for computational microRNA target identification. *Bioinformatics* 2009;**25**(23): 3049-3055.
136. Neame E. MicroRNAs: HITS-CLIP hits the microRNA target. *Nature reviews genetics* 2009;**10**: 510-511.
137. Baek D, Villén J, Shin C, Camargo FD, Gygi SP, Bartel DP. The impact of microRNAs on protein output. *Nature* 2008.
138. Reid B, Li X, Galipeau P, Vaughan T. Barrett's oesophagus and oesophageal adenocarcinoma: time for a new synthesis. *Nature reviews* 2010;**10**(2): 87-101.
139. Smith CM, Watson DI, Michael MZ, Hussey DJ. MicroRNAs, development of Barrett's esophagus, and progression to esophageal adenocarcinoma. *World J Gastroenterol* 2010;**16**(5): 531-537.
140. Jankowski JA, Wright NA, Meltzer SJ, Triadafilopoulos G, Geboes K, Casson AG, Kerr D, Young LS. Molecular evolution of the metaplasia-dysplasia-adenocarcinoma sequence in the esophagus. *Am J Pathol* 1999;**154**(4): 965-973.
141. Lao-Sirieix P, Brais R, Lovat L, Coleman N, Fitzgerald RC. Cell cycle phase abnormalities do not account for disordered proliferation in Barrett's carcinogenesis. *Neoplasia* 2004;**6**(6): 751-760.
142. Kaur BS, Ouatu-Lascar R, Omary MB, Triadafilopoulos G. Bile salts induce or blunt cell proliferation in Barrett's esophagus in an acid-dependent fashion. *Am J Physiol Gastrointest Liver Physiol* 2000;**278**(6): G1000-1009.
143. Kaur BS, Triadafilopoulos G. Acid- and bile-induced PGE(2) release and hyperproliferation in Barrett's esophagus are COX-2 and PKC-epsilon dependent. *Am J Physiol Gastrointest Liver Physiol* 2002;**283**(2): G327-334.
144. Dvorakova K, Payne CM, Ramsey L, Bernstein H, Holubec H, Chavarria M, Bernstein C, Sampliner RE, Riley C, Prasad A, Garewal H. Apoptosis resistance in Barrett's esophagus: ex vivo bioassay of live stressed tissues. *The American journal of gastroenterology* 2005;**100**(2): 424-431.
145. Simon P. Q-Gene: processing quantitative real-time RT-PCR data. *Bioinformatics* 2003;**19**(11): 1439-1440.
146. Stoner GD, Kaighn ME, Reddel RR, Resau JH, Bowman D, Naito Z, Matsukura N, You M, Galati AJ, Harris CC. Establishment and characterization of SV40 T-antigen immortalized human esophageal epithelial cells. *Cancer Res* 1991;**51**(1): 365-371.
147. Rockett JC, Larkin K, Darnton SJ, Morris AG, Matthews HR. Five newly established oesophageal carcinoma cell lines: phenotypic and immunological characterization. *Br J Cancer* 1997;**75**(2): 258-263.
148. Pena JTG, Sohn-Lee C, Rouhanifard SH, Ludwig J, Hafner M, Mihailovic A, Lim C, Holoch D, Berninger P, Zavolan M, Tuschl T. miRNA in situ hybridization in formaldehyde and EDC-fixed tissues. *Nat Methods* 2009;**6**(2): 139-141.
149. Benjamini Y, Hochberg H. Controlling the False Discovery Rate: a Practical and Powerful Approach to Multiple Testing. *J R Statist Soc* 1995;**57**(1): 289-300.
150. Feber A, Xi L, Luketich JD, Pennathur A, Landreneau RJ, Wu M, Swanson SJ, Godfrey TE, Litle VR. MicroRNA expression profiles of esophageal cancer. *The Journal of thoracic and cardiovascular surgery* 2008;**135**(2): 255-260; discussion 260.
151. Mager SR, Oomen MH, Morente MM, Ratcliffe C, Knox K, Kerr DJ, Pezzella F, Riegman PH. Standard operating procedure for the collection of fresh frozen tissue samples. *Eur J Cancer* 2007;**43**(5): 828-834.
152. Clapé C, Fritz V, Henriquet C, Apparailly F, Fernandez PL, Iborra F, Avancès C, Villalba M, Culine S, Fajas L. miR-143 interferes with ERK5 signaling,

- and abrogates prostate cancer progression in mice. *PLoS ONE* 2009;**4**(10): e7542.
153. Chen X, Guo X, Zhang H, Xiang Y, Chen J, Yin Y, Cai X, Wang K, Wang G, Ba Y, Zhu L, Wang J, Yang R, Zhang Y, Ren Z, Zen K, Zhang J, Zhang CY. Role of miR-143 targeting KRAS in colorectal tumorigenesis. *Oncogene* 2009;**28**(10): 1385-1392.
154. Cordes KR, Sheehy NT, White MP, Berry EC, Morton SU, Muth AN, Lee TH, Miano JM, Ivey KN, Srivastava D. miR-145 and miR-143 regulate smooth muscle cell fate and plasticity. *Nature* 2009;**460**(7256): 705-710.
155. Ng EK, Tsang WP, Ng SS, Jin HC, Yu J, Li JJ, Röcken C, Ebert MP, Kwok TT, Sung JJ. MicroRNA-143 targets DNA methyltransferases 3A in colorectal cancer. *Br J Cancer* 2009.
156. Zhang X, Liu S, Hu T, He Y, Sun S. Up-regulated microRNA-143 transcribed by nuclear factor kappa B enhances hepatocarcinoma metastasis by repressing fibronectin expression. *Hepatology (Baltimore, Md)* 2009;**50**(2): 490-499.
157. Zhang H, Cai X, Wang Y, Tang H, Tong D, Ji F. microRNA-143, down-regulated in osteosarcoma, promotes apoptosis and suppresses tumorigenicity by targeting Bcl-2. *Oncol Rep* 2011;**24**(5): 1363-1369.
158. Shi B, Sepp-Lorenzino L, Prisco M, Linsley P, Deangelis T, Baserga R. Micro RNA 145 Targets the Insulin Receptor Substrate-1 and Inhibits the Growth of Colon Cancer Cells. *Journal of Biological Chemistry* 2007;**282**(45): 32582-32590.
159. Sachdeva M, Zhu S, Wu F, Wu H, Walia V, Kumar S, Elble R, Watabe K, Mo YY. p53 represses c-Myc through induction of the tumor suppressor miR-145. *Proc Natl Acad Sci USA* 2009;**106**(9): 3207-3212.
160. Wang S, Bian C, Yang Z, Bo Y, Li J, Zeng L, Zhou H, Zhao RC. miR-145 inhibits breast cancer cell growth through RTKN. *Int J Oncol* 2009;**34**(5): 1461-1466.
161. Xu N, Papagiannakopoulos T, Pan G, Thomson JA, Kosik KS. MicroRNA-145 regulates OCT4, SOX2, and KLF4 and represses pluripotency in human embryonic stem cells. *Cell* 2009;**137**(4): 647-658.
162. Gregersen LH, Jacobsen AB, Frankel LB, Wen J, Krogh A, Lund AH. MicroRNA-145 targets YES and STAT1 in colon cancer cells. *PLoS One*; **5**(1): e8836.
163. Spizzo R, Nicoloso MS, Lupini L, Lu Y, Fogarty J, Rossi S, Zagatti B, Fabbri M, Veronese A, Liu X, Davuluri R, Croce CM, Mills G, Negrini M, Calin GA. miR-145 participates with TP53 in a death-promoting regulatory loop and targets estrogen receptor-alpha in human breast cancer cells. *Cell Death Differ* 2009;**Epub**
164. Zhang J, Guo H, Qian G, Ge S, Ji H, Hu X, Chen W. MiR-145, a new regulator of the DNA Fragmentation Factor-45 (DFF45)-mediated apoptotic network. *Mol Cancer*; **9**(1): 211.
165. Sachdeva M, Mo YY. MicroRNA-145 suppresses cell invasion and metastasis by directly targeting mucin 1. *Cancer Res* 2010;**70**(1): 378-387.
166. Kano M, Seki N, Kikkawa N, Fujimura L, Hoshino I, Akutsu Y, Chiyomaru T, Enokida H, Nakagawa M, Matsubara H. miR-145, miR-133a and miR-133b: Tumor suppressive miRNAs target FSCN1 in esophageal squamous cell carcinoma. *Int J Cancer*.
167. Ostefeld MS, Bramsen JB, Lamy P, Villadsen SB, Fristrup N, Sorensen KD, Ulhøi B, Borre M, Kjems J, Dyrskjot L, Orntoft TF. miR-145 induces caspase-dependent and -independent cell death in urothelial cancer cell lines with targeting of an expression signature present in Ta bladder tumors. *Oncogene* 2010;**29**(7): 1073-1084.

168. Georges SA, Biery MC, Kim S-Y, Schelter JM, Guo J, Chang AN, Jackson AL, Carleton MO, Linsley PS, Cleary MA, Chau BN. Coordinated Regulation of Cell Cycle Transcripts by p53-Inducible microRNAs, miR-192 and miR-215. *Cancer Res* 2008;**68**(24): 10105-10112.
169. Song B, Wang Y, Titmus MA, Botchkina G, Formentini A, Kornmann M, Ju J. Molecular mechanism of chemoresistance by miR-215 in osteosarcoma and colon cancer cells. *Mol Cancer*;**9**: 96.
170. Wang B, Herman-Edelstein M, Koh P, Burns W, Jandeleit-Dahm K, Watson A, Saleem M, Goodall GJ, Twigg SM, Cooper ME, Kantharidis P. E-cadherin expression is regulated by miR-192/215 by a mechanism that is independent of the profibrotic effects of transforming growth factor-beta. *Diabetes* 2010;**59**(7): 1794-1802.
171. Song B, Wang Y, Titmus MA, Botchkina G, Formentini A, Kornmann M, Ju J. Molecular mechanism of chemoresistance by miR-215 in osteosarcoma and colon cancer cells. *Mol Cancer* 2010;**9**(1): 96.
172. Lena AM, Shalom-Feuerstein R, Di Val Cervo PR, Aberdam D, Knight RA, Melino G, Candi E. miR-203 represses 'stemness' by repressing $\Delta Np63$. *Cell Death Differ* 2008;**15**(7): 1187-1195.
173. Bueno MJ, Pérez de Castro I, Gómez de Cedrón M, Santos J, Calin GA, Cigudosa JC, Croce CM, Fernández-Piqueras J, Malumbres M. Genetic and epigenetic silencing of microRNA-203 enhances ABL1 and BCR-ABL1 oncogene expression. *Cancer Cell* 2008;**13**(6): 496-506.
174. Yu J, Ryan DG, Getsios S, Oliveira-Fernandes M, Fatima A, Lavker RM. MicroRNA-184 antagonizes microRNA-205 to maintain SHIP2 levels in epithelia. *Proceedings of the National Academy of Sciences of the United States of America* 2008;**105**(49): 19300-19305.
175. Wu H, Zhu S, Mo YY. Suppression of cell growth and invasion by miR-205 in breast cancer. *Cell Res* 2009;**19**(4): 439-448.
176. Mouillet JF, Chu T, Nelson DM, Mishima T, Sadovsky Y. MiR-205 silences MED1 in hypoxic primary human trophoblasts. *Faseb J*;**24**(6): 2030-2039.
177. Lou Y, Yang X, Wang F, Cui Z, Huang Y. MicroRNA-21 promotes the cell proliferation, invasion and migration abilities in ovarian epithelial carcinomas through inhibiting the expression of PTEN protein. *Int J Mol Med*;**26**(6): 819-827.
178. Zhu S, Si M-L, Wu H, Mo Y-Y. MicroRNA-21 targets the tumor suppressor gene tropomyosin 1 (TPM1). *J Biol Chem* 2007;**282**(19): 14328-14336.
179. Frankel LB, Christoffersen NR, Jacobsen A, Lindow M, Krogh A, Lund AH. Programmed cell death 4 (PDCD4) is an important functional target of the microRNA miR-21 in breast cancer cells. *J Biol Chem* 2008;**283**(2): 1026-1033.
180. Zhu S, Wu H, Wu F, Nie D, Sheng S, Mo Y-Y. MicroRNA-21 targets tumor suppressor genes in invasion and metastasis. *Cell Res* 2008;**18**(3): 350-359.
181. Fujita S, Ito T, Mizutani T, Minoguchi S, Yamamichi N, Sakurai K, Iba H. miR-21 Gene expression triggered by AP-1 is sustained through a double-negative feedback mechanism. *J Mol Biol* 2008;**378**(3): 492-504.
182. Iliopoulos D, Jaeger SA, Hirsch HA, Bulyk ML, Struhl K. STAT3 activation of miR-21 and miR-181b-1 via PTEN and CYLD are part of the epigenetic switch linking inflammation to cancer. *Mol Cell* 2010;**39**(4): 493-506.
183. Wang P, Zou F, Zhang X, Li H, Dulak A, Tomko RJ, Jr., Lazo JS, Wang Z, Zhang L, Yu J. microRNA-21 negatively regulates Cdc25A and cell cycle progression in colon cancer cells. *Cancer Res* 2009;**69**(20): 8157-8165.
184. Zhang Z, Li Z, Gao C, Chen P, Chen J, Liu W, Xiao S, Lu H. miR-21 plays a

- pivotal role in gastric cancer pathogenesis and progression. *Lab Invest* 2008.
185. Chen Y, Liu W, Chao T, Zhang Y, Yan X, Gong Y, Qiang B, Yuan J, Sun M, Peng X. MicroRNA-21 down-regulates the expression of tumor suppressor PDCD4 in human glioblastoma cell T98G. *Cancer Lett* 2008;**272**(2): 197-205.
186. Hashimi ST, Fulcher JA, Chang MH, Gov L, Wang S, Lee B. MicroRNA profiling identifies miR-34a and miR-21 and their target genes JAG1 and WNT1 in the coordinate regulation of dendritic cell differentiation. *Blood* 2009;**114**(2): 404-414.
187. Li T, Li D, Sha J, Sun P, Huang Y. MicroRNA-21 directly targets MARCKS and promotes apoptosis resistance and invasion in prostate cancer cells. *Biochem Biophys Res Commun* 2009;**583**(3): 280-285.
188. Li Y, Li W, Yang Y, Lu Y, He C, Hu G, Liu H, Chen J, He J, Yu H. MicroRNA-21 targets LRRFIP1 and contributes to VM-26 resistance in glioblastoma multiforme. *Brain research* 2009;**1286**: 13-18.
189. Yi R, O'carroll D, Pasolli HA, Zhang Z, Dietrich FS, Tarakhovskiy A, Fuchs E. Morphogenesis in skin is governed by discrete sets of differentially expressed microRNAs. *Nat Genet* 2006;**38**(3): 356-362.
190. Tran N, McLean T, Zhang X, Zhao CJ, Thomson JM, O'Brien C, Rose B. MicroRNA expression profiles in head and neck cancer cell lines. *Biochemical and Biophysical Research Communications* 2007;**358**(1): 12-17.
191. Yi R, Poy MN, Stoffel M, Fuchs E. A skin microRNA promotes differentiation by repressing 'stemness'. *Nature* 2008;**452**(7184): 225-229.
192. Gottardo F, Liu CG, Ferracin M, Calin GA, Fassan M, Bassi P, Sevignani C, Byrne D, Negrini M, Pagano F, Gomella LG, Croce CM, Baffa R. Micro-RNA profiling in kidney and bladder cancers. *Urol Oncol* 2007;**25**(5): 387-392.
193. Iorio MV, Visone R, Di Leva G, Donati V, Petrocca F, Casalini P, Taccioli C, Volinia S, Liu CG, Alder H, Calin GA, Ménard S, Croce CM. MicroRNA signatures in human ovarian cancer. *Cancer Res* 2007;**67**(18): 8699-8707.
194. Sempere LF, Christensen M, Silahatoglu A, Bak M, Heath CV, Schwartz G, Wells W, Kauppinen S, Cole CN. Altered MicroRNA expression confined to specific epithelial cell subpopulations in breast cancer. *Cancer Res* 2007;**67**(24): 11612-11620.
195. Majid S, Dar AA, Saini S, Yamamura S, Hirata H, Tanaka Y, Deng G, Dahiya R. MicroRNA-205-directed transcriptional activation of tumor suppressor genes in prostate cancer. *Cancer* 2010.
196. Watson DI, Wijnhoven BPL, Michael MZ, Mayne GC, Hussey DJ. MicroRNA expression profiles in Barrett's Oesophagus. *ANZ Journal of Surgery* 2007;**77**(Supplement 1): A-45.
197. Hino K, Tsuchiya K, Fukao T, Kiga K, Okamoto R, Kanai T, Watanabe M. Inducible expression of microRNA-194 is regulated by HNF-1 during intestinal epithelial cell differentiation. *RNA* 2008;**14**(7): 1433-1442.
198. Wienholds E. MicroRNA Expression in Zebrafish Embryonic Development. *Science* 2005;**309**(5732): 310-311.
199. Zeng L, Carter AD, Childs SJ. miR-145 directs intestinal maturation in zebrafish. *Proc Natl Acad Sci USA* 2009.
200. Wijnhoven BP, Hussey DJ, Watson DI, Tsykin A, Smith CM, Michael MZ, Group ftSAOR. MicroRNA profiling of Barrett's oesophagus and oesophageal adenocarcinoma. *The British journal of surgery* 2010.
201. Selcuklu SD, Donoghue MT, Spillane C. miR-21 as a key regulator of oncogenic processes. *Biochem Soc Trans* 2009;**37**(Pt 4): 918-925.

202. Medina PP, Nolde M, Slack FJ. OncomiR addiction in an in vivo model of microRNA-21-induced pre-B-cell lymphoma. *Nature* 2010;**467**(7311): 86-90.
203. Löffler D, Brocke-Heidrich K, Pfeifer G, Stocsits C, Hackermüller J, Kretzschmar AK, Burger R, Gramatzki M, Blumert C, Bauer K, Cvijic H, Ullmann AK, Stadler PF, Horn F. Interleukin-6 dependent survival of multiple myeloma cells involves the Stat3-mediated induction of microRNA-21 through a highly conserved enhancer. *Blood* 2007;**110**(4): 1330-1333.
204. Meng F, Henson R, Wehbe-Janek H, Ghoshal K, Jacob ST, Patel T. MicroRNA-21 regulates expression of the PTEN tumor suppressor gene in human hepatocellular cancer. *Gastroenterology* 2007;**133**(2): 647-658.
205. Asangani IA, Rasheed SA, Nikolova DA, Leupold JH, Colburn NH, Post S, Allgayer H. MicroRNA-21 (miR-21) post-transcriptionally downregulates tumor suppressor Pcd4 and stimulates invasion, intravasation and metastasis in colorectal cancer. *Oncogene* 2008;**27**(15): 2128-2136.
206. Cheng Y, Liu X, Zhang S, Lin Y, Yang J, Zhang C. MicroRNA-21 protects against the H₂O₂-induced injury on cardiac myocytes via its target gene PDCD4. *Journal of Molecular and Cellular Cardiology* 2009: 1-10.
207. Braun CJ, Zhang X, Savelyeva I, Wolff S, Moll UM, Schepeler T, Orntoft TF, Andersen CL, Dobbstein M. p53-Responsive MicroRNAs 192 and 215 Are Capable of Inducing Cell Cycle Arrest. *Cancer Res* 2008;**68**(24): 10094-10104.
208. Volinia S, Galasso M, Costinean S, Tagliavini L, Gamberoni G, Drusco A, Marchesini J, Mascellani N, Sana ME, Abu Jarour R, Despots C, Teitell M, Baffa R, Aqeilan R, Iorio MV, Taccioli C, Garzon R, Di Leva G, Fabbri M, Catozzi M, Previati M, Ambs S, Palumbo T, Garofalo M, Veronese A, Bottoni A, Gasparini P, Harris CC, Visone R, Pekarsky Y, de la Chapelle A, Bloomston M, Dillhoff M, Rassenti LZ, Kipps TJ, Huebner K, Pichiorri F, Lenze D, Cairo S, Buendia MA, Pineau P, Dejean A, Zanesi N, Rossi S, Calin GA, Liu CG, Palatini J, Negrini M, Vecchione A, Rosenberg A, Croce CM. Reprogramming of miRNA networks in cancer and leukemia. *Genome Res* 2010;**20**(5): 589-599.
209. Takagi T, Iio A, Nakagawa Y, Naoe T, Tanigawa N, Akao Y. Decreased expression of microRNA-143 and -145 in human gastric cancers. *Oncology* 2009;**77**(1): 12-21.
210. Chen X, Guo X, Zhang H, Xiang Y, Chen J, Yin Y, Cai X, Wang K, Wang G, Ba Y, Zhu L, Wang J, Yang R, Zhang Y, Ren Z, Zen K, Zhang J, Zhang C-Y. Role of miR-143 targeting KRAS in colorectal tumorigenesis. *Oncogene* 2009;**28**(10): 1385-1392.
211. Akao Y, Nakagawa Y, Iio A, Naoe T. Role of microRNA-143 in Fas-mediated apoptosis in human T-cell leukemia Jurkat cells. *Leuk Res* 2009;**33**(11): 1530-1538.
212. Gotte M, Mohr C, Koo CY, Stock C, Vaske AK, Viola M, Ibrahim SA, Peddibhotla S, Teng YH, Low JY, Ebnet K, Kiesel L, Yip GW. miR-145-dependent targeting of Junctional Adhesion Molecule A and modulation of fascin expression are associated with reduced breast cancer cell motility and invasiveness. *Oncogene*.
213. Wang Y, Barbacioru C, Hyland F, Xiao W, Hunkapiller KL, Blake J, Chan F, Gonzalez C, Zhang L, Samaha RR. Large scale real-time PCR validation on gene expression measurements from two commercial long-oligonucleotide microarrays. *BMC Genomics* 2006;**7**: 59.
214. Fassan M, Volinia S, Palatini J, Pizzi M, Baffa R, De Bernard M, Battaglia G, Parente P, Croce CM, Zaninotto G, Ancona E, Rugge M. MicroRNA expression profiling in human Barrett's carcinogenesis. *Int J Cancer*.

215. Mathé EA, Nguyen GH, Bowman ED, Zhao Y, Budhu A, Schetter AJ, Braun R, Reimers M, Kumamoto K, Hughes D, Altorki NK, Casson AG, Liu CG, Wang XW, Yanaihara N, Hagiwara N, Dannenberg AJ, Miyashita M, Croce CM, Harris CC. MicroRNA expression in squamous cell carcinoma and adenocarcinoma of the esophagus: associations with survival. *Clin Cancer Res* 2009;**15**(19): 6192-6200.
216. Yang H, Gu J, Wang K, Zhang W, Xing J, Chen Z, Ajani JA, Wu X. MicroRNA Expression Signatures in Barrett's Esophagus and Esophageal Adenocarcinoma. *Clin Cancer Res* 2009.
217. Mulder DJ, Pacheco I, Hurlbut DJ, Mak N, Furuta GT, MacLeod RJ, Justinich CJ. FGF9-induced proliferative response to eosinophilic inflammation in oesophagitis. *Gut* 2009;**58**(2): 166-173.
218. Moons LMG, Kusters JG, Van Delft JHM, Kuipers EJ, Gottschalk R, Geldof H, Bode WA, Stoof J, Van Vliet AHM, Ketelslegers HB, Kleinjans JCS, Siersema PD. A pro-inflammatory genotype predisposes to Barrett's esophagus. *Carcinogenesis* 2008;**29**(5): 926-931.
219. Binato M, Fagundes R, Gurski R, Meurer L, Edelweiss MI. Immunohistochemical overexpression of the p53 protein and Ki-67 (MIB-1) antigen in patients with GERD and chronic esophagitis. *Appl Immunohistochem Mol Morphol* 2010;**18**(3): 236-243.
220. Pera M, Cameron AJ, Trastek VF, Carpenter HA, Zinsmeister AR. Increasing incidence of adenocarcinoma of the esophagus and esophagogastric junction. *Gastroenterology* 1993;**104**(2): 510-513.
221. Milano F, van Baal JW, Buttar N, Rygiel AM, de Kort F, DeMars CJ, Rosmolen WD, Bergman JJ, Van Marle J, Wang K, Peppelenbosch MP, Krishnadath KK. Bone morphogenetic protein 4 expressed in esophagitis induces a columnar phenotype in esophageal squamous cells. *Gastroenterology* 2007;**132**(7): 2412-2421.
222. Eda A, Osawa H, Satoh K, Yanaka I, Kihira K, Ishino Y, Mutoh H, Sugano K. Aberrant expression of CDX2 in Barrett's epithelium and inflammatory esophageal mucosa. *J Gastroenterol* 2003;**38**(1): 14-22.
223. Pillai R, Bhattacharyya S, Filipowicz W. Repression of protein synthesis by miRNAs: how many mechanisms? *Trends in Cell Biology* 2007;**17**(3): 118-126.
224. van Baal JW, Bozikas A, Pronk R, Ten Kate FJ, Milano F, Rygiel AM, Rosmolen WD, Peppelenbosch MP, Bergman JJ, Krishnadath KK. Cytokeratin and CDX-2 expression in Barrett's esophagus. *Scand J Gastroenterol* 2008;**43**(2): 132-140.
225. Piessen G, Jonckheere N, Vincent A, Hemon B, Ducourouble MP, Copin MC, Mariette C, Van Seuning I. Regulation of the human mucin MUC4 by taurodeoxycholic and taurochenodeoxycholic bile acids in oesophageal cancer cells is mediated by hepatocyte nuclear factor 1alpha. *Biochem J* 2007;**402**(1): 81-91.
226. Zaman MS, Chen Y, Deng G, Shahryari V, Suh SO, Saini S, Majid S, Liu J, Khatri G, Tanaka Y, Dahiya R. The functional significance of microRNA-145 in prostate cancer. *Br J Cancer* 2010;**103**(2): 256-264.
227. Sempere L, Christensen M, Silahatoglu A, Bak M, Heath C, Schwartz G, Wells W, Kauppinen S, Cole C. Altered MicroRNA Expression Confined to Specific Epithelial Cell Subpopulations in Breast Cancer. *Cancer Res* 2007;**67**(24): 11612-11620.
228. Hwang HW, Wentzel EA, Mendell JT. A hexanucleotide element directs microRNA nuclear import. *Science* 2007;**315**(5808): 97-100.
229. Liao JY, Ma LM, Guo YH, Zhang YC, Zhou H, Shao P, Chen YQ, Qu LH.

- Deep sequencing of human nuclear and cytoplasmic small RNAs reveals an unexpectedly complex subcellular distribution of miRNAs and tRNA 3' trailers. *PLoS One*;5(5): e10563.
230. Taft RJ, Simons C, Nahkuri S, Oey H, Korbie DJ, Mercer TR, Holst J, Ritchie W, Wong JJ, Rasko JE, Rokhsar DS, Degan BM, Mattick JS. Nuclear-localized tiny RNAs are associated with transcription initiation and splice sites in metazoans. *Nature structural & molecular biology* 2010.
231. Caygill CP, Reed PI, Johnston BJ, Hill MJ, Ali MH, Levi S. A single centre's 20 years' experience of columnar-lined (Barrett's) oesophagus diagnosis. *European journal of gastroenterology & hepatology* 1999;11(12): 1355-1358.
232. Hwang HW, Mendell JT. MicroRNAs in cell proliferation, cell death, and tumorigenesis. *Br J Cancer* 2006;94(6): 776-780.
233. Selbach M, Schwanhäusser B, Thierfelder N, Fang Z, Khanin R, Rajewsky N. Widespread changes in protein synthesis induced by microRNAs. *Nature* 2008.
234. Lim LP, Lau NC, Garrett-Engele P, Grimson A, Schelter JM, Castle J, Bartel DP, Linsley PS, Johnson JM. Microarray analysis shows that some microRNAs downregulate large numbers of target mRNAs. *Nature* 2005;433(7027): 769-773.
235. Yoshida T, Sekine T, Aisaki K, Mikami T, Kanno J, Okayasu I. CITED2 is activated in ulcerative colitis and induces p53 dependent apoptosis in response to butyric acid. *J Gastroenterol* 2011;46(3): 339-349.
236. Bai L, Merchant JL. A role for CITED2, a CBP/p300 interacting protein, in colon cancer cell invasion. *FEBS letters* 2007;581(30): 5904-5910.
237. Xie B, Wang C, Zheng Z, Song B, Ma C, Thiel G, Li M. Egr-1 transactivates Bim gene expression to promote neuronal apoptosis. *J Neurosci* 2011;31(13): 5032-5044.
238. Krishnan AV, Moreno J, Nonn L, Malloy P, Swami S, Peng L, Peehl DM, Feldman D. Novel pathways that contribute to the anti-proliferative and chemopreventive activities of calcitriol in prostate cancer. *The Journal of steroid biochemistry and molecular biology* 2007;103(3-5): 694-702.
239. Stark S, Watzl C. 2B4 (CD244), NTB-A and CRACC (CS1) stimulate cytotoxicity but no proliferation in human NK cells. *International immunology* 2006;18(2): 241-247.
240. Maguire J, Santoro T, Jensen P, Siebenlist U, Yewdell J, Kelly K. Gem: an induced, immediate early protein belonging to the Ras family. *Science* 1994;265(5169): 241-244.
241. Liu B, Liu Y, Chen J, Wei Z, Yu H, Zhen Y, Lu L, Hui R. CARP is a novel caspase recruitment domain containing pro-apoptotic protein. *Biochem Biophys Res Commun* 2002;293(5): 1396-1404.
242. Todorovic V, Chen CC, Hay N, Lau LF. The matrix protein CCN1 (CYR61) induces apoptosis in fibroblasts. *The Journal of cell biology* 2005;171(3): 559-568.
243. Chien W, Kumagai T, Miller CW, Desmond JC, Frank JM, Said JW, Koeffler HP. Cyr61 suppresses growth of human endometrial cancer cells. *J Biol Chem* 2004;279(51): 53087-53096.
244. Hrzenjak A, Moinfar F, Kremser ML, Strohmeier B, Petru E, Zatloukal K, Denk H. Histone deacetylase inhibitor vorinostat suppresses the growth of uterine sarcomas in vitro and in vivo. *Mol Cancer*;9: 49.
245. Kent OA, Chivukula RR, Mullendore M, Wentzel EA, Feldmann G, Lee KH, Liu S, Leach SD, Maitra A, Mendell JT. Repression of the miR-143/145 cluster by oncogenic Ras initiates a tumor-promoting feed-forward pathway. *Genes Dev* 2010;24(24): 2754-2759.

246. Olvera M, Wickramasinghe K, Brynes R, Bu X, Ma Y, Chandrasoma P. Ki67 expression in different epithelial types in columnar lined oesophagus indicates varying levels of expanded and aberrant proliferative patterns. *Histopathology* 2005;**47**(2): 132-140.
247. Katada N, Hinder RA, Smyrk TC, Hirabayashi N, Perdakis G, Lund RJ, Woodward T, Klingler PJ. Apoptosis is inhibited early in the dysplasia-carcinoma sequence of Barrett esophagus. *Arch Surg* 1997;**132**(7): 728-733.
248. Xu B, Niu X, Zhang X, Tao J, Wu D, Wang Z, Li P, Zhang W, Wu H, Feng N, Hua L, Wang X. miR-143 decreases prostate cancer cells proliferation and migration and enhances their sensitivity to docetaxel through suppression of KRAS. *Molecular and cellular biochemistry* 2011.
249. Fuse M, Nohata N, Kojima S, Sakamoto S, Chiyomaru T, Kawakami K, Enokida H, Nakagawa M, Naya Y, Ichikawa T, Seki N. Restoration of miR-145 expression suppresses cell proliferation, migration and invasion in prostate cancer by targeting FSCN1. *Int J Oncol* 2011;**38**(4): 1093-1101.
250. Georges SA, Biery MC, Kim SY, Schelter JM, Guo J, Chang AN, Jackson AL, Carleton MO, Linsley PS, Cleary MA, Chau BN. Coordinated regulation of cell cycle transcripts by p53-Inducible microRNAs, miR-192 and miR-215. *Cancer Res* 2008;**68**(24): 10105-10112.
251. Zhang X, Huang Q, Goyal RK, Odze RD. DNA ploidy abnormalities in basal and superficial regions of the crypts in Barrett's esophagus and associated neoplastic lesions. *Am J Surg Pathol* 2008;**32**(9): 1327-1335.
252. Odze R, Goldblum JR. *Surgical pathology of the GI tract, liver, biliary tract, and pancreas*. Saunders Elsevier: Philadelphia, 2009.
253. Bansal A, Lee IH, Hong X, Anand V, Mathur SC, Gaddam S, Rastogi A, Wani SB, Gupta N, Visvanathan M, Sharma P, Christenson LK. Feasibility of microRNAs as biomarkers for Barrett's Esophagus progression: a pilot cross-sectional, phase 2 biomarker study. *The American journal of gastroenterology* 2011;**106**(6): 1055-1063.
254. Clemons NJ, McColl KE, Fitzgerald RC. Nitric oxide and acid induce double-strand DNA breaks in Barrett's esophagus carcinogenesis via distinct mechanisms. *Gastroenterology* 2007;**133**(4): 1198-1209.
255. Chou SJ, Alawi F. Expression of DNA damage response biomarkers during oral carcinogenesis. *Oral surgery, oral medicine, oral pathology, oral radiology, and endodontics* 2011;**111**(3): 346-353.
256. Jaamaa S, Af Hallstrom TM, Sankila A, Rantanen V, Koistinen H, Stenman UH, Zhang Z, Yang Z, De Marzo AM, Taari K, Ruutu M, Andersson LC, Laiho M. DNA damage recognition via activated ATM and p53 pathway in nonproliferating human prostate tissue. *Cancer Res* 2010;**70**(21): 8630-8641.
257. Srivastava N, Manvati S, Srivastava A, Pal R, Kalaiarasan P, Chattopadhyay S, Gochhait S, Dua R, Bamezai RN. miR-24-2 controls H2AFX expression regardless of gene copy number alteration and induces apoptosis by targeting antiapoptotic gene BCL-2: a potential for therapeutic intervention. *Breast Cancer Res* 2011;**13**(2): R39.
258. Jung EJ, Kim DR. Ectopic expression of H2AX protein promotes TrkA-induced cell death via modulation of TrkA tyrosine-490 phosphorylation and JNK activity upon DNA damage. *Biochem Biophys Res Commun*; **404**(3): 841-847.
259. Liu CA, Wang MJ, Chi CW, Wu CW, Chen JY. Rho/Rhotekin-mediated NF-kappaB activation confers resistance to apoptosis. *Oncogene* 2004;**23**(54): 8731-8742.

260. Liu CA, Wang MJ, Chi CW, Wu CW, Chen JY. Overexpression of rho effector rhotekin confers increased survival in gastric adenocarcinoma. *Journal of biomedical science* 2004;**11**(5): 661-670.
261. Katzenellenbogen RA, Vliet-Gregg P, Xu M, Galloway DA. Cytoplasmic poly(A) binding proteins regulate telomerase activity and cell growth in human papillomavirus type 16 E6-expressing keratinocytes. *J Virol*;**84**(24): 12934-12944.
262. Lord RV, Salonga D, Danenberg KD, Peters JH, DeMeester TR, Park JM, Johansson J, Skinner KA, Chandrasoma P, DeMeester SR, Bremner CG, Tsai PI, Danenberg PV. Telomerase reverse transcriptase expression is increased early in the Barrett's metaplasia, dysplasia, adenocarcinoma sequence. *J Gastrointest Surg* 2000;**4**(2): 135-142.
263. Gonzalez YR, Zhang Y, Behzadpoor D, Cregan S, Bamforth S, Slack RS, Park DS. CITED2 signals through peroxisome proliferator-activated receptor-gamma to regulate death of cortical neurons after DNA damage. *J Neurosci* 2008;**28**(21): 5559-5569.
264. Wislez M, Fujimoto N, Izzo JG, Hanna AE, Cody DD, Langley RR, Tang H, Burdick MD, Sato M, Minna JD, Mao L, Wistuba I, Strieter RM, Kurie JM. High expression of ligands for chemokine receptor CXCR2 in alveolar epithelial neoplasia induced by oncogenic kras. *Cancer Res* 2006;**66**(8): 4198-4207.
265. Yang G, Rosen DG, Liu G, Yang F, Guo X, Xiao X, Xue F, Mercado-Uribe I, Huang J, Lin SH, Mills GB, Liu J. CXCR2 promotes ovarian cancer growth through dysregulated cell cycle, diminished apoptosis, and enhanced angiogenesis. *Clin Cancer Res* 2010;**16**(15): 3875-3886.
266. Tirotta E, Ransohoff RM, Lane TE. CXCR2 signaling protects oligodendrocyte progenitor cells from IFN-gamma/CXCL10-mediated apoptosis. *Glia* 2011;**59**(10): 1518-1528.
267. Cheng WL, Wang CS, Huang YH, Tsai MM, Liang Y, Lin KH. Overexpression of CXCL1 and its receptor CXCR2 promote tumor invasion in gastric cancer. *Ann Oncol* 2011.
268. Vanbaal J, Milano F, Rygiel A, Bergman J, Rosmolen W, Vandeventer S, Wang K, Peppelenbosch M, Krishnadath K. A Comparative Analysis by SAGE of Gene Expression Profiles of Barrett's Esophagus, Normal Squamous Esophagus, and Gastric Cardia. *Gastroenterology* 2005;**129**(4): 1274-1281.
269. Hao Y, Triadafilopoulos G, Sahbaie P, Young H, Omary M, Lowe A. Gene Expression Profiling Reveals Stromal Genes Expressed in Common Between Barrett's Esophagus and Adenocarcinoma. *Gastroenterology* 2006;**131**(3): 925-933.
270. Dvorakova K, Payne CM, Ramsey L, Holubec H, Sampliner R, Dominguez J, Dvorak B, Bernstein H, Bernstein C, Prasad A, Fass R, Cui H, Garewal H. Increased expression and secretion of interleukin-6 in patients with Barrett's esophagus. *Clin Cancer Res* 2004;**10**(6): 2020-2028.
271. Fitzgerald R, Omary MB, Triadafilopoulos G. Dynamic effects of acid on Barrett's esophagus. An ex vivo proliferation and differentiation model. *J Clin Invest* 1996;**98**(9): 2120-2128.
272. Eloubeidi MA, Mason AC, Desmond RA, El-Serag HB. Temporal trends (1973-1997) in survival of patients with esophageal adenocarcinoma in the United States: a glimmer of hope? *The American journal of gastroenterology* 2003;**98**(7): 1627-1633.
273. Hugo H, Ackland ML, Blick T, Lawrence MG, Clements JA, Williams ED, Thompson EW. Epithelial--mesenchymal and mesenchymal--epithelial transitions in carcinoma progression. *J Cell Physiol* 2007;**213**(2): 374-383.

274. Lee JM, Dedhar S, Kalluri R, Thompson EW. The epithelial-mesenchymal transition: new insights in signaling, development, and disease. *The Journal of cell biology* 2006;**172**(7): 973-981.
275. Bates RC, Pursell BM, Mercurio AM. Epithelial-Mesenchymal Transition and Colorectal Cancer: Gaining Insights into Tumour Progression Using LIM1863 Cells. *Cells Tissues Organs* 2007;**185**(1-3): 29-39.
276. Rees JRE, Onwuegbusi BA, Save VE, Alderson D, Fitzgerald RC. In vivo and In vitro Evidence for Transforming Growth Factor-1-Mediated Epithelial to Mesenchymal Transition in Esophageal Adenocarcinoma. *Cancer Res* 2006;**66**(19): 9583-9590.
277. Jethwa P, Naqvi M, Hardy RG, Hotchin NA, Roberts S, Spychal R, Tselepis C. Overexpression of Slug is associated with malignant progression of esophageal adenocarcinoma. *World J Gastroenterol* 2008;**14**(7): 1044-1052.
278. Chaffer CL, Weinberg RA. A Perspective on Cancer Cell Metastasis. *Science* 2011;**331**: 1559-1564.
279. Thiery JP. Epithelial-mesenchymal transitions in tumour progression. *Nature reviews* 2002;**2**(6): 442-454.
280. Bracken CP, Gregory PA, Kolesnikoff N, Bert AG, Wang J, Shannon MF, Goodall GJ. A Double-Negative Feedback Loop between ZEB1-SIP1 and the microRNA-200 Family Regulates Epithelial-Mesenchymal Transition. *Cancer Res* 2008;**68**(19): 7846-7854.
281. Park S-M, Gaur AB, Lengyel E, Peter ME. The miR-200 family determines the epithelial phenotype of cancer cells by targeting the E-cadherin repressors ZEB1 and ZEB2. *Genes Dev* 2008;**22**(7): 894-907.
282. Onwuegbusi BA, Rees JR, Lao-Sirieix P, Fitzgerald RC. Selective loss of TGFbeta Smad-dependent signalling prevents cell cycle arrest and promotes invasion in oesophageal adenocarcinoma cell lines. *PLoS ONE* 2007;**2**(1): e177.
283. Korpala M, Kang Y. The emerging role of miR-200 family of microRNAs in epithelial-mesenchymal transition and cancer metastasis. *RNA Biol* 2008;**5**(3): 115-119.
284. Du Y, Xu Y, Ding L, Yao H, Yu H, Zhou T, Si J. Down-regulation of miR-141 in gastric cancer and its involvement in cell growth. *J Gastroenterol* 2009: 1-6.
285. Wijnhoven BP, Siersema PD, Hop WC, van Dekken H, Tilanus HW. Adenocarcinomas of the distal oesophagus and gastric cardia are one clinical entity. Rotterdam Oesophageal Tumour Study Group. *The British journal of surgery* 1999;**86**(4): 529-535.
286. Dykxhoorn DM, Wu Y, Xie H, Yu F, Lal A, Petrocca F, Martinvalet D, Song E, Lim B, Lieberman J. miR-200 enhances mouse breast cancer cell colonization to form distant metastases. *PLoS One* 2009;**4**(9): e7181.
287. Adam L, Zhong M, Choi W, Qi W, Nicoloso M, Arora A, Calin G, Wang H, Siefker-Radtke A, McConkey D, Bar-Eli M, Dinney C. miR-200 Expression Regulates Epithelial-to-Mesenchymal Transition in Bladder Cancer Cells and Reverses Resistance to Epidermal Growth Factor Receptor Therapy. *Clinical Cancer Research* 2009;**15**(16): 5060-5072.
288. Li Y, VandenBoom TG, 2nd, Kong D, Wang Z, Ali S, Philip PA, Sarkar FH. Up-regulation of miR-200 and let-7 by natural agents leads to the reversal of epithelial-to-mesenchymal transition in gemcitabine-resistant pancreatic cancer cells. *Cancer Res* 2009;**69**(16): 6704-6712.
289. Kong D, Li Y, Wang Z, Banerjee S, Ahmad A, Kim HR, Sarkar FH. miR-200 regulates PDGF-D-mediated epithelial-mesenchymal transition, adhesion, and

- invasion of prostate cancer cells. *Stem Cells* 2009;**27**(8): 1712-1721.
290. Cochrane DR, Howe EN, Spoelstra NS, Richer JK. Loss of miR-200c: A Marker of Aggressiveness and Chemoresistance in Female Reproductive Cancers. *Journal of oncology* 2010;**2010**: 821717.
291. Uhlmann S, Zhang JD, Schwäger A, Mannsperger H, Riazalhosseini Y, Burmester S, Ward A, Korf U, Wiemann S, Sahin O. miR-200bc/429 cluster targets PLCgamma1 and differentially regulates proliferation and EGF-driven invasion than miR-200a/141 in breast cancer. *Oncogene* 2010.
292. Cochrane DR, Spoelstra NS, Howe EN, Nordeen SK, Richer JK. MicroRNA-200c mitigates invasiveness and restores sensitivity to microtubule-targeting chemotherapeutic agents. *Molecular cancer therapeutics* 2009.
293. Palanca-Wessels MC, Klingelhutz A, Reid BJ, Norwood TH, Opheim KE, Paulson TG, Feng Z, Rabinovitch PS. Extended lifespan of Barrett's esophagus epithelium transduced with the human telomerase catalytic subunit: a useful in vitro model. *Carcinogenesis* 2003;**24**(7): 1183-1190.
294. Song S, Guha S, Liu K, Buttar NS, Bresalier RS. COX-2 induction by unconjugated bile acids involves reactive oxygen species-mediated signalling pathways in Barrett's oesophagus and oesophageal adenocarcinoma. *Gut* 2007;**56**(11): 1512-1521.
295. Hormi-Carver K, Zhang X, Zhang HY, Whitehead RH, Terada LS, Spechler SJ, Souza RF. Unlike esophageal squamous cells, Barrett's epithelial cells resist apoptosis by activating the nuclear factor-kappaB pathway. *Cancer Res* 2009;**69**(2): 672-677.
296. Galipeau PC, Prevo LJ, Sanchez CA, Longton GM, Reid BJ. Clonal expansion and loss of heterozygosity at chromosomes 9p and 17p in premalignant esophageal (Barrett's) tissue. *Journal of the National Cancer Institute* 1999;**91**(24): 2087-2095.
297. Pankov R, Yamada KM. Fibronectin at a glance. *Journal of Cell Science* 2002;**115**(Pt 20): 3861-3863.
298. Han SW, Roman J. Fibronectin induces cell proliferation and inhibits apoptosis in human bronchial epithelial cells: pro-oncogenic effects mediated by PI3-kinase and NF-kappa B. *Oncogene* 2006;**25**(31): 4341-4349.
299. Pera M, Trastek VF, Carpenter HA, Allen MS, Deschamps C, Pairolero PC. Barrett's esophagus with high-grade dysplasia: an indication for esophagectomy? *Ann Thorac Surg* 1992;**54**(2): 199-204.
300. Wong T, Tian J, Nagar AB. Barrett's surveillance identifies patients with early esophageal adenocarcinoma. *The American journal of medicine* 2010;**123**(5): 462-467.
301. Ogunwobi O, Mutungi G, Beales IL. Leptin stimulates proliferation and inhibits apoptosis in Barrett's esophageal adenocarcinoma cells by cyclooxygenase-2-dependent, prostaglandin-E2-mediated transactivation of the epidermal growth factor receptor and c-Jun NH2-terminal kinase activation. *Endocrinology* 2006;**147**(9): 4505-4516.
302. Konturek PC, Nikiforuk A, Kania J, Raithel M, Hahn EG, Muhldorfer S. Activation of NFkappaB represents the central event in the neoplastic progression associated with Barrett's esophagus: a possible link to the inflammation and overexpression of COX-2, PPARgamma and growth factors. *Dig Dis Sci* 2004;**49**(7-8): 1075-1083.
303. Beales IL, Ogunwobi O, Cameron E, El-Amin K, Mutungi G, Wilkinson M. Activation of Akt is increased in the dysplasia-carcinoma sequence in Barrett's

- oesophagus and contributes to increased proliferation and inhibition of apoptosis: a histopathological and functional study. *BMC Cancer* 2007;**7**: 97.
304. Helm J, Enkemann SA, Coppola D, Barthel JS, Kelley ST, Yeatman TJ. Dedifferentiation precedes invasion in the progression from Barrett's metaplasia to esophageal adenocarcinoma. *Clin Cancer Res* 2005;**11**(7): 2478-2485.
305. Ashihara E, Kawata E, Maekawa T. Future prospect of RNA interference for cancer therapies. *Current drug targets* 2010;**11**(3): 345-360.
306. Hurteau GJ, Carlson JA, Roos E, Brock GJ. Stable expression of miR-200c alone is sufficient to regulate TCF8 (ZEB1) and restore E-cadherin expression. *Cell Cycle* 2009;**8**(13): 2064-2069.
307. Dar AA, Majid S, de Semir D, Nosrati M, Bezrookove V, Kashani-Sabet M. miRNA-205 suppresses melanoma cell proliferation and induces senescence via regulation of E2F1 protein. *J Biol Chem*; **286**(19): 16606-16614.
308. Liu T, Zhang X, So C-K, Wang S, Wang P, Yan L, Myers R, Chen Z, Patterson AP, Yang CS, Chen X. Regulation of Cdx2 expression by promoter methylation, and effects of Cdx2 transfection on morphology and gene expression of human esophageal epithelial cells. *Carcinogenesis* 2006;**28**(2): 488-496.
309. Hwang H, Wentzel E, Mendell J. A Hexanucleotide Element Directs MicroRNA Nuclear Import. *Science* 2007;**315**(5808): 97-100.
310. Boudreau F, Rings EH, van Wering HM, Kim RK, Swain GP, Krasinski SD, Moffett J, Grand RJ, Suh ER, Traber PG. Hepatocyte nuclear factor-1 alpha, GATA-4, and caudal related homeodomain protein Cdx2 interact functionally to modulate intestinal gene transcription. Implication for the developmental regulation of the sucrase-isomaltase gene. *J Biol Chem* 2002;**277**(35): 31909-31917.
311. Iio A, Nakagawa Y, Hirata I, Naoe T, Akao Y. Identification of non-coding RNAs embracing microRNA-143/145 cluster. *Mol Cancer*; **9**: 136.
312. Smith CM, Watson DI, Leong MP, Mayne GC, Michael MZ, Wijnhoven BP, Hussey DJ. miR-200 family expression is downregulated upon neoplastic progression of Barrett's esophagus. *World J Gastroenterol* 2011;**17**(8): 1036-1044.
313. Vrba L, Jensen TJ, Garbe JC, Heimark RL, Cress AE, Dickinson S, Stampfer MR, Futscher BW. Role for DNA methylation in the regulation of miR-200c and miR-141 expression in normal and cancer cells. *PLoS ONE* 2010;**5**(1): e8697.
314. Neves R, Scheel C, Weinhold S, Honisch E, Iwaniuk KM, Trompeter HI, Niederacher D, Wernet P, Santourlidis S, Uhrberg M. Role of DNA methylation in miR-200c/141 cluster silencing in invasive breast cancer cells. *BMC research notes* 2010;**3**: 219.